Development and Utilisation of Biofunctionalised Scaffolds to Support Neural Stem Cells *in vitro*, in the Intact Brain and during Neural Regeneration

A thesis for the Degree of Doctor of Philosophy

by

Ting Yi Wang

Department of Materials Engineering

Monash University, Victoria, Australia 3800

20th May 2013

Table of Contents

Summary

Currently there is no effective treatment for injuries to the central nervous system. Cell replacement therapy has been investigated for a number of neural injuries/neurodegenerative disease and in some instances led to clinical trials. However, the effectiveness of the treatment, most notably observed in the context of replacing dopamine neurons in Parkinson's disease patients, has been highly variable. In part, this has been attributed to: (i) poor cell survival and (ii) poor integration of the grafted cells into the host tissue. It is likely that the non-conducive environment of the adult brain is partially responsible for these short comings and that providing an improved niche environment, enriched with chemical and physical support for newly implanted cells, could have a significant impact on transplantation outcomes. In this regard, this thesis examines the potential of bio-engineered scaffolds to support neural cells *in vitro* and subsequently provide a stimulating micro-environment to satisfy both physical and biological needs for grafted cells *in vivo*.

Electrospun scaffolds possess many features reminiscent of the brains extracellular matrix and were therefore examined their ability to support of neural cells *in vitro* and *in vivo* (chapter 4, 5 and 6). The scaffolds were additionally chemically modified (with neurotrophic factors) to maximise their bio-functionality. Whilst previous studies have demonstrated the benefits of covalently tethered proteins onto scaffold to prolong exposure, little attention has been paid to the stability and functionality of these proteins. Chapter 4 demonstrates long-term stability of glial-cell derived neurotrophic factor (GDNF), its maintained ability to activate intracellular signalling pathways and, its ability to influence cellular responses (survival, differentiation and neurite growth).

Prior to examining the ability of electrospun scaffolds to support neural transplants, methodologies were established to determine how best to introduce these scaffolds, so as to support the graft (chapter 5). The results showed that cells implanted adjacent to the electrospun scaffold were superior to efforts of implanting scaffolds pre-seeded with neural cells or efforts to implant cells into the cavity of the scaffold *in vivo*. The data illustrated that Poly(ε-caprolactone) (PCL) scaffolds supported graft survival and neurite penetration inside implanted scaffolds.

Subsequently, a more extensive evaluation of the ability of electrospun scaffolds, incorporating tethered GDNF, to support neural cells was performed (Chapter 6). In vitro, PCL with immobilised GDNF (iGDNF) significantly enhanced cell viability and neural stem cell/progenitor proliferation compared to conventional 2-dimensional cultureware. Upon implantation into the intact brain of rats, PCL scaffolds including iGDNF enhanced the survival, proliferation, migration, and neurite growth of transplanted cortical cells, whilst suppressing inflammatory reactive astroglia in the comparison with unmodified PCL scaffolds and cell transplantation alone. The results illustrate the potential of biofunctionalised scaffolds to support neural grafts, findings that could have a significant impact on promoting regeneration in the injured brain.

Finally this thesis examines the potential of scaffolds to support transplanted cells in an animal model of neural injury (a Parkinson's disease model). Whilst chapter 6 explore the potential of electrospun scaffolds for supporting grafts, the final results chapter (Chapter 7) concentrates on developing a more advanced bio-engineered scaffold that is less invasive for implantation. A composite scaffold that could be easily injected into the brain was fabricated

by combining a hydrogel with bio-functionalised electrospun short fibres. The composite scaffolds modified with GDNF were shown to significantly promote cell viability as well as the differentiation and neuritogenesis of dopaminergic neurones (the cell population requiring replacement in Parkinson's disease) in the comparison with other scaffolds. After 28days *in vivo*, the composite scaffolds were demonstrated to maintain the survival and integration of transplanted dopamine neurone. The tethering of GDNF onto the short fibres in the composite scaffolds was shown to also suppress microglia activation when compared to the scaffolds without GDNF.

Collectively, this thesis makes a significant contribution to understanding the potential of biofunctionalised scaffolds to support neural stem cells *in vitro* and *in vivo*, and may have important implications in the future for the development of cell based therapies for the treatment of neural injuries.

Declaration

The work described in this thesis was performed by the author, except where acknowledged, and has not previously submitted for any other degree or diploma.

The thesis is less than 100,000 words in length.

Ting Yi Wang

20th May 2013

Publications

Publications related to this thesis

1. **T.Y. Wang**, C.L. Parish, J.S. Forsythe, D.R. Nisbet. Biofunctionalisation of polymeric scaffolds for neural tissue engineering. *Journal of Biomaterials Application* (2012) Nov;27(4):369-90. DOI: 10.1177/0885328212443297. Impact factor: 2.1 (Chapter 2)

2. **T. Y. Wang**, B. J. Turner., D. R. Nisbet, C. L. Parish. Characterisation of the stability and bio-functionality of tethered proteins on bioengineered scaffolds. *Biomaterials* (submitted). Impact factor: 7.4 (Chapter 4)

3. **T.Y. Wang**, J.S. Forsythe, D.R. Nisbet, C.L. Parish. Promoting engraftment of transplanted neural stem cells/progenitors using biofunctionalised electrospun scaffolds. *Biomaterials* (2012) Dec;33(36):9188-97. Impact factor: 7.4 (Chapter 6)

4. M. Sawawi, **T. Y. Wang**, D. R. Nisbet, G. P. Simon. Scission of electrospun polymer fibres by ultrasonication. Polymer (2013) (accepted). Impact factor: 3.4 (Appendix)

Conference Preceedings

1. **T.Y. Wang**, J.S. Forsythe, D.R. Nisbet, C.L. Parish. Using scaffolds in neural repair: the what, how and why of neural tissue engineering. 5th annual conference of the Florey Postdoctoral Association. Oral presentation. Melbourne, Australia, 2013.

2. **T.Y. Wang**, J. Pettikiriarachchi, J.S. Forsythe, D.R. Nisbet, C.L. Parish, "Biofunctionalized scaffolds and thermogeling polymers promote the survival and integration of transplanted neural stem cells". Poster presentation. Australia Neuroscience Society 34th Annual Meeting, Melbourne, Australia.

3. **T.Y. Wang**, J.S. Forsythe, D.R. Nisbet, C.L. Parish. Promoting engraftment of transplanted neural stem cells/progenitors using biofunctionalised electrospun scaffolds. Oral presentation. Australia Neuroscience Society 34th Annual Meeting, Melbourne, Australia.

4. **T.Y. Wang**, J.S. Forsythe, D.R. Nisbet, C.L. Parish, " Immobilization of neurotrophin GDNF on electrospun scaffolds promotes the survival and integration of transplanted neural stem cells. Poster presentation. Tissue Engineering and Regenerative Medicine World Congress, Vienna, Austria, 2012.

Conference Attendance

1. 5th annual conference of the Florey Postdoctoral Association, Melbourne, Australia 2013

2. Australian Neuroscience Society 34th Annual meeting, Melbourne, Australia 2013

3. 3rd TERMIS world congress**,** Vienna, Austia 2012

4. Electrospinning, Melborune, Australia 2009

Acknowledgments

First of all, I would like to express my gratitude to my supervisors, A/Prof. John Forsythe, A/Prof. Clare Parish and Dr David Nisbet. I would like to thank them for their guidance, funding and advice during my PhD candidature. In particular, to A/Prof. Clare Parish; I have been very fortunate to have worked with Clare as my supervisor. She not only provides constant encouragement, tremendous support, valuable suggestions and specialist knowledge but also acts as my mentor and role model as a scientist. I am always inspired by her passion for scientific research, hardworking attitude as well as her efficiency. I would also deeply like to thank Dr David Nisbet for his encouragement, assurance and great support in every difficult situation I have been in. He has helped me overcome the many hurdles throughout this journey. I admire his enthusiasm, ambition and networking skills towards his research and academic career. I am very fortunate to have completed my PhD in a professional, positive, and friendly research environment provided by my supervisors.

I would like to acknowledge Ms Doris Tomas, Dr. Francesca Ercole and Dr. Kun Zhou for their training, advice and assistance during my PhD. Also great thanks to all my friends for their friendships, company and great memories throughout my candidature; to Ms. Alexandra Rodriguez, Mr. Kelly Tsang, Ms. Jerani Pettikiriarachchi, Mr. Andew Rodda, Ms. Vanalysa Ly, Doc. Fei Liu, Mr. Kenny Jao, Ms. Natalie Sun, Ms. Shu Ying Chen and Mr. Wei Pai Huang.

.

Finally, this PhD thesis is dedicated to my parents as they are the greatest support in my life. I really appreciate my parents for their unconditional love, financial support and life wisdom over all these years; I would not have been able to accomplish my PhD degree without them.

PART A: General Declaration

Monash University

Declaration for thesis based or partially based on conjointly published or unpublished work

General Declaration

In accordance with Monash University Doctorate Regulation 17 Doctor of Philosophy and Research Master's regulations the following declarations are made:

I hereby declare that this thesis contains no material which has been accepted for the award of any other degree or diploma at any university or equivalent institution and that, to the best of my knowledge and belief, this thesis contains no material previously published or written by another person, except where due reference is made in the text of the thesis.

This thesis includes 2 original papers published in peer reviewed journals and 1 submitted publications. The core theme of the thesis is development and utilisation of biofunctionalised scaffolds to support neural stem cells *in vitro*, in the intact brain and during neural regeneration. The ideas, development and writing up of all the papers in the thesis were the principal responsibility of myself, the candidate, working within the tissue engineering group based in the Department of Materials Engineering under the supervision of associate professor John Forsythe.

The inclusion of co-authors reflects the fact that the work came from active collaboration between researchers and acknowledges input into team-based research.

In the case of chapter 2, 4 and 6 my contribution to the work involved the following:

chapter	Publication title	Publication status	Nature and extent of candidate's contribution
2	biofunctionalisation of polymeric scaffolds for neural tissue engineering	published	Planning, researching and writing.
4	characterisation of the stability and bio-functionality of tethered proteins on bioengineered scaffolds	submitted	Experimental design and conduct, writing.
6	promoting engraftment of transplanted neural stem cells/progenitors using biofunctionalised electrospun scaffolds	published	Experimental design and conduct, writing.

I have / have not (circle that which applies) renumbered sections of submitted or published papers in order to generate a consistent presentation within the thesis.

Signed: 

Date: …20.5.2013……

List of Abbreviations

AMP	Amnion-derived multipotent progenitor
BDNF	Brain-derived neurotrophic factor
BMSCs	Bone marrow stromal cells
Chi/ GP	Chitosan/glycerophosphate
CNS	Central nervous system
CPN	Caudate putamen nucleus
DA	Dopaminergic cells
DIV	Day *in vitro*
DRGs	Dorsal root ganglia
E	Embryonic day
ECM	Extracellular matrix
ED	Ethylenediamine
EGF	Epidermal growth factor
ELISA	Enzyme-linked immunosorbent assay
EVAc	Poly(ethylene-*co*-vinyl acetate)
FGF-1	Fibroblast growth factor-1
FN	Fibronectin
GDNF	Glial-cell derived neurotrophic factor
GFAP	Glial fibrillary acidic protein
GFP	Green fluorescent protein
HAc	Hyaluronic acid
HAMC	Hyaluronan methylcellulose

HD	Huntington’s disease
bFGF	Basic fibroblast growth factor
IGF-I	Insulin-like growth factor-I
iGDNF	Immobilised GDNF
LM	Laminin
MAPK	Mitogen-activated protein kinases
MND	Motor neuron disease
NSPC	Neural stem progenitor cells
NT-3	Neurotrophin-3
pERK	Phosphorylation ERK
PCL	Poly(ε-caprolactone)
PD	Parkinson’s disease
PDL	Poly(D-lysine)
PEGDA	Polyethylene glycol diacrylate
PHPMA	Poly[N-(2-hydroxypropyl)-methacrylamide
PLGA	Poly(lactide-*co*-glycolide)
PLLA	Poly-L-lactide
PNS	Peripheral nervous system
SAPS	Self-assembling peptide scaffolds
SCI	Spinal cord injury
SEM	Scanning electron microscopy
SVZ	Subventricular zone
SMCC	Sulfo-succinimidyl 1-(N-maleimidomethyl)-cyclohexane-1-carboxylate
sulfo-SMCC	Sulfo-succinimidyl 1-(N-maleimidomethyl)-cyclohexane-1-carboxylate
TBI	Traumatic brain injury

Trk	Tyrosine kinase
TUJ	Mouse anti-β tubulin
VM	Ventral midbrain
XPS	X-ray photoelectron spectroscopy analysis
6-OHDA	6-hydroxydopamine

Chapter 1

Introduction

Contents

1.1 BACKGROUND

Disease and injuries to the central nervous system (CNS) are one of the most difficult and challenging medical issues, with patients experiencing a range of disabilities decreasing their quality of life. In addition to the devastating physiological consequences to the patient, brain injury also places a large economic burden on society due to the costs from surgeries, medication, physical therapies and intensive care. However, current treatments have not been able to provide an efficient solution to patients who suffer from the consequences of damage to the brain. Additionally an increase in the aging demography will escalate the prevalence of such disabilities highlighting the need to discover new treatments and/or cures for brain disease. Cell replacement therapy has, and continues to be a focus in the development of novel therapies for brain repair. Unfortunately poor survival and integration of transplanted neural cells persist as major stumbling blocks within the field and highlight the necessity for new technologies to support tissue grafts. In this regards more recently, research has been directed towards the development of biomaterials that are capable of instructing cells and exploiting these as platforms that may promote nerve regeneration.

Electrospun polymeric scaffolds have been studied for tissue engineering applications due to their similarity to the extracellular matrix for many types of tissue including neural tissue. In previous studies, electrospun poly(ε-caprolactone) (PCL) scaffolds demonstrated biocompatibility in the brain [1]. PCL scaffolds have the ability to influence the proliferation of neural stem cells and their differentiation into all the main neural cell phenotypes (neurons, astrocytes and oligodendrocytes) *in vitro*; furthermore they are capable of supporting neural cells and their processes following implantation into the brain [1, 2]. The overall objective in

this research was to examine the ability of PCL scaffolds to support grafted primary cells in the brain, and subsequently to investigate the ability of these scaffolds to regenerate damaged neural pathways/ tissue in the brain.

Another principle element in the present research is to improve the biofunctionality of the electrospun scaffolds via chemical modification with neurotrophic factors, in order to enhance the engraftment efficiency of the neural cells in the brain. Therefore another major aim is to reconstruct the injured brain tissue by delivering embryonic primary cortical cells via modified bioengineered scaffolds, which also perform as a long-term delivery system of neurotrophic factors. This research provides a fundamental platform to determine the methodology of combining biologically modified scaffolds and primary cells for a variety of brain injury models including traumatic brain injury (TBI), Parkinson's disease (PD) and Huntington's Disease (HD). To achieve this goal, glial-cell derived neurotrophic factor (GDNF), a neurotrophic factor known to influence the survival, proliferation, differentiation and neurite growth of a number of neural populations, was selected for surface modification to increase the biofunctionality of the scaffolds *in vivo*. This resulted in an increase in survival rate of grafted primary cells, neurite ingrowth and integration between the scaffold and both grafted and host tissue. The later part of the thesis delves further into the, characterisation of the stability and bio-functionality of tethered proteins, again focusing on GDNF as the example molecule.

While the initial studies in this thesis focus on proof of principle for biofunctionalized electrospun scaffolds to support primary neural cells in vitro and upon implantation, the future of such applications will depend on the ability to implant scaffolds with minimal injury

to the brain parenchyma and inflammation. Therefore, to obtain a compromise for provision of support for a lesion and minimising the subsequent injury after implantation, a 3D filling type of polymeric scaffold was considered in the following research. xyloglucan, an injectable hydrogel was applied and combined with short fibres of electrospun poly-L-lactide (PLLA) modified with GDNF for implantation in mouse models of Parkinson's disease. 3-Dimensional xyloglucan hydrogels provide support to the cavity/ lost neural pathway in the brain and acts as a carriage for primary neural cells; the short fibres additionally provide scaffolding for the implanted cells and serve as a delivery system of biological molecules. This research provides a proof of concept for the capacity of implanted advanced bioengineered hybrid scaffolds, containing two different forms of biomaterials (hydrogels and short fibre modified with a biological molecule) to support the survival proliferation and differentiation of neural stem cell grafts, as well as enhance axonal growth and neural circuit restoration in the injured brain.

1.1.1 Neural tissue engineering

Due to the limitation of self-repairing ability in central nervous system, injuries to the brain including disease and trauma are almost incurable. Therefore there is an increasing need for the development of new and novel therapies. Numerous researchers have shown positive results in utilising biomaterials for specific applications in neural tissue engineering. Basic requirements for theses scaffolds in neural tissue engineering include biocompatibility, non-toxicity and controllable mechanical properties [3]. Added to this, the bio-functionality of these scaffolds has been extensively explored in order to induce biological activity of cells in vitro and *in vivo*. The bioengineered scaffolds need to provide a physical support to the lost neural tissue, stimulate neural regeneration, encourage cell differentiation and promote integration between implanted materials and cells with the host tissue [4, 5]. Long term, the

bioengineered scaffolds are required to be biodegradable while slowly being replaced by the new implanted cells, and may release biological cues to enhance neural tissue repair, or even be able to act as a cell carrier to accelerate cell repopulation in the injured site/ lost neural pathway [6-9]. Recently scientists have attempted to developed advanced scaffolds, focusing on specific injuries to the brain; such as stroke, TBI and neurodegenerative diseases including Parkinson's disease.

1.1.1.1 Parkinson's disease

PD results from the progressive neurodegeneration of dopaminergic cells (DA) residing within the ventral midbrain (VM) of the substantia nigra pars compacta [10]. Parkinson's disease affects approximately 1% of the population over the age of 65, and while the majority of cases (>90%) are idiopathic, genetics and exposure to some compounds (namely insecticides) also account for a number of cases [11, 12]. A gradual and progressive death of the midbrain dopaminergic neurons results in changes in basal ganglia output to the motor cortex [13, 14]. Consequently, PD results in multiple motor dysfunctions including resting tremor, bradykinesia (slowness in movement), akinesia (absence of movement), difficulty initiating movement, muscle rigidity and postural instability. Added to this, the majority of patients also progress to be disturbed cognitive and psychiatric characteristics [15].

Currently therapies for PD predominantly focus on pharmaceutical intervention in an effort to increase striatal dopamine. Drugs include the dopamine precursor L-dopa, dopamine agonists and inhibitors of enzymes involved in dopamine degradation. Some patients additionally undergo surgical treatment whereby electrodes are placed in specific areas in the brain (deep brain stimulation) to restore the balance within basal ganglia circuitry and output to the motor

cortex [16]. However, these existing techniques are not able to halt the progressive death of DA neurons and are associated with a number of side-effects and complications. An additional and long term treatment under development for the treatment of PD is cell replacement therapy [13, 17]. A number of clinical trials to date have demonstrated proof of principle that newly implanted dopamine neurons are capable of structurally and functionally integrating into the host brain. Additionally these grafts are able to improve motor impairments in patients. While in principle this technology is feasible, extensive variability is observed among patients. Variable outcomes has largely been attributed to poor survival rate and insufficient integration between host and grafted cells [18, 19]. Therefore novel strategies, focused at improving the physical and chemical niche for implanted cells to survive and integrate may significantly improve cell replacement therapy in the future.

1.1.2 Utilization of transplanted primary cells in neural tissue engineering

Stem cells are well known for the capabilities of self-renewal, differentiation and proliferation [20]. An uncommitted neural stem cell has the ability to divide symmetrically, giving rise to two identical daughter cells that will continue to self-renew, or asymmetrical division, resulting in an identical self-renewing NSC as well as a neural progenitor. Neural progenitors include neuronal progenitors/neuroblasts (giving rise to neurons) and glial progenitors/glioblasts (giving rise to astrocytes and oligodendrocytes), figure 1.1. Combine these cells form neuronal networks with glial cells providing structural and trophic support whilst oligodendrocytes insulate neurons, ensuring rapid electrical conductance. Therefore NSC transplantation has been studied for different applications in neural tissue engineering to efficiently replace the lost neural tissue and reconstruct the injured region for applications including the treatments of Parkinson’s disease [13, 16], traumatic brain injury [21, 22] and ischemic brain injury [23, 24]. Table 1.1 outlines the different neural cell types in embryonic

development, and cell functions and the cell markers used in immunohistochemistry in the thesis [2, 25]. Numerous growth factors including GDNF and BDNF significantly increase the survival rate of grafted neurons, and make cell transplantation a potentially more efficient and promising technique in the clinic [26]. In the present research, transplantation of primary neural cells was applied with implanted bioengineered scaffolds to replace the dead cells in mice with Parkinson's disease. Stem cells present a valuable tool for neural repair however are shrouded by a number of limitations. Pluripotent stem cells, including embryonic stem cells and inducible pluripotent stem cells have the advantage of being an unlimited cell source capable of making any call type in the body. However these advantages also represent their main disadvantages – that is the ability to control their proliferation and prevent tumours or neural overgrowths as well as sufficiently fate restrict these cells along a specific lineage. For this reason, the use of fetal tissue (primary derived neural stem cells and progenitors isolated from the developing embryo) continues to be an attractive cell source for in vivo application. Whilst the use of such tissue also presents concerns, namely a limited cell source and the ethical implications of using aborted fetal tissue, fetal tissue remains the cell of choice for current and ongoing clinical trials. Another possible problem associated with utilization of primary neural cells in neural tissue engineering was the toxicity of bioengineered scaffolds causing cell death *in vitro* and *in vivo*. Therefore the biocompatibility of the scaffolds was one of the primary focuses in the present research, which was improved to overcome poor cell survival.

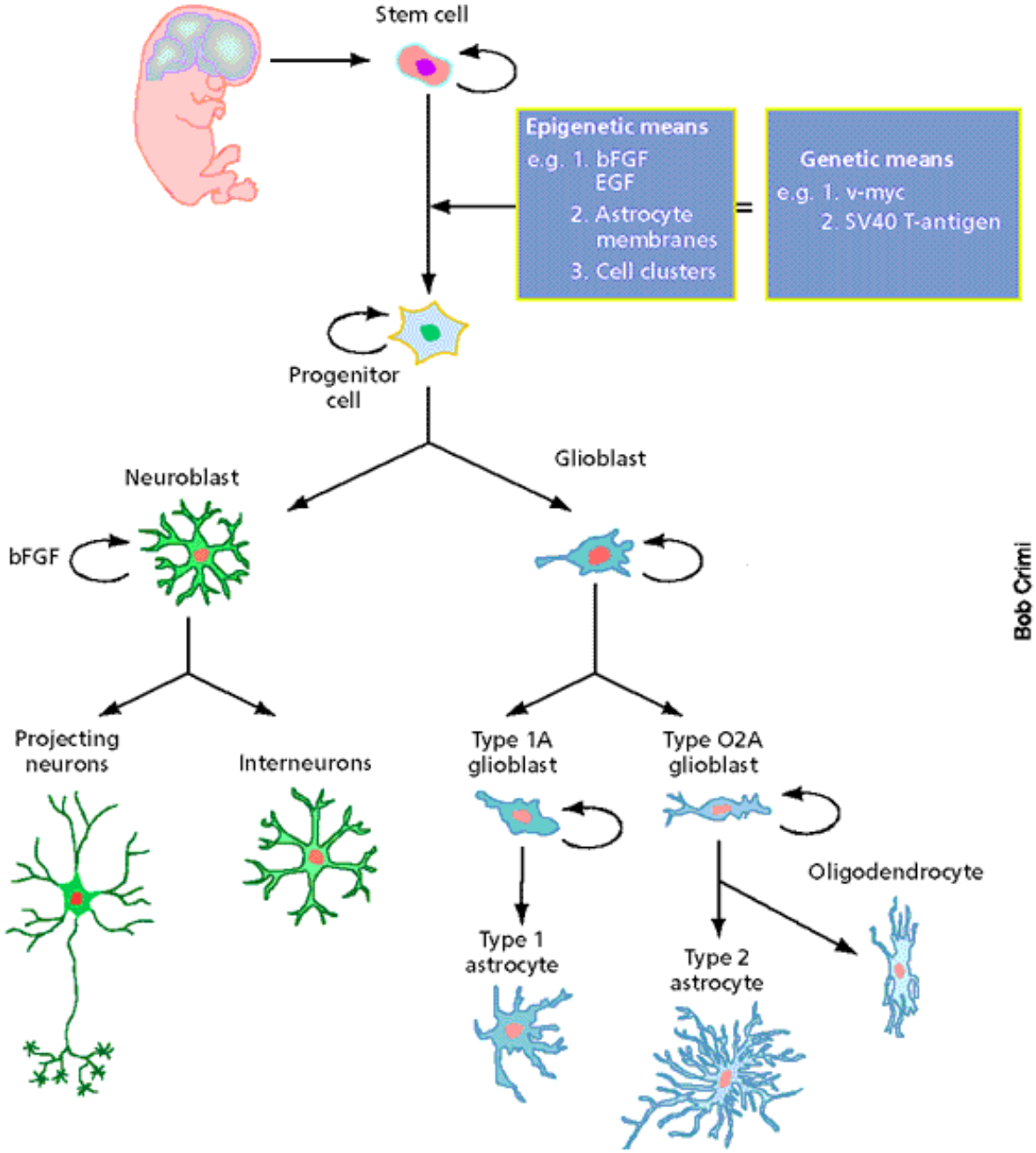

Figure 1.1 The lineage of primary neural cells in embryonic development. Embryonic stem cells can self-renew and generate progenitor cells, which are able to differentiate into neuroblast and glioblast cells. Neuroblast and glioblast can differentiate into neurons, astrocytes and oligodendrocytes. Factors influence cell fate include epigenetic and genetic means as listed in the figure [25].

Table 1.1 The list of different neural cells, roles and cell markers in immunohistochemistry

Neural cells	Role/ Functions	Markers
Neural stem cell	Self-renewing/multipotent neural cells	Nestin
Progenitor	A cell that has a tendency to differentiate into a specific type of cell, but is already more specified than a stem cell e.g. neural progenitors become neurons and glial progenitors become astrocytes and oligodendrocytes	
Neuron	Cells within the nervous system responsible for electrical and biochemical transmission of signals throughout the body	TUJ
Astrocyte	'Support cell' who's functions include secretion of various proteins, neural repair and scarring processes, extracellular matrix, support of brain endothelial cells	GFAP
Oligodendrocyte	support and insulation of axons/ form Myelin sheath	NG2

1.1.2.1 Glia-cell derived neurotrophic factor (GDNF)

GDNF was selected and functionalised to the scaffolds in the PhD research due to the significant biological functions in cell development. Not only GDNF play an important role in survival of dopaminergic neurons following 6-OHDA injection [27], but also major function in cell plasticity during cell development [28]. Upon release from glial cells, GDNF binds to membrane bound receptor GFRa1 on the target cell (the dopamine neuron in the present context). GFRa1 lacks a transmembran and intracellular domain and must therefore interact with a secondary receptor, c-ret, for intracellular signaling. This interaction may activate several intracellular signaling cascades including the mitogen-activated protein kinase–extracellular signal-regulated protein kinase (MAPK/Erk), phosphatidylinositol 3-kinase (PI3-K)/Akt, and phospholipase C (PLC) pathways. Within this thesis the phosphorylation of Erk is used as a readout of activation of intracellular GDNF signalling (Figure 1.2) [29, 30].

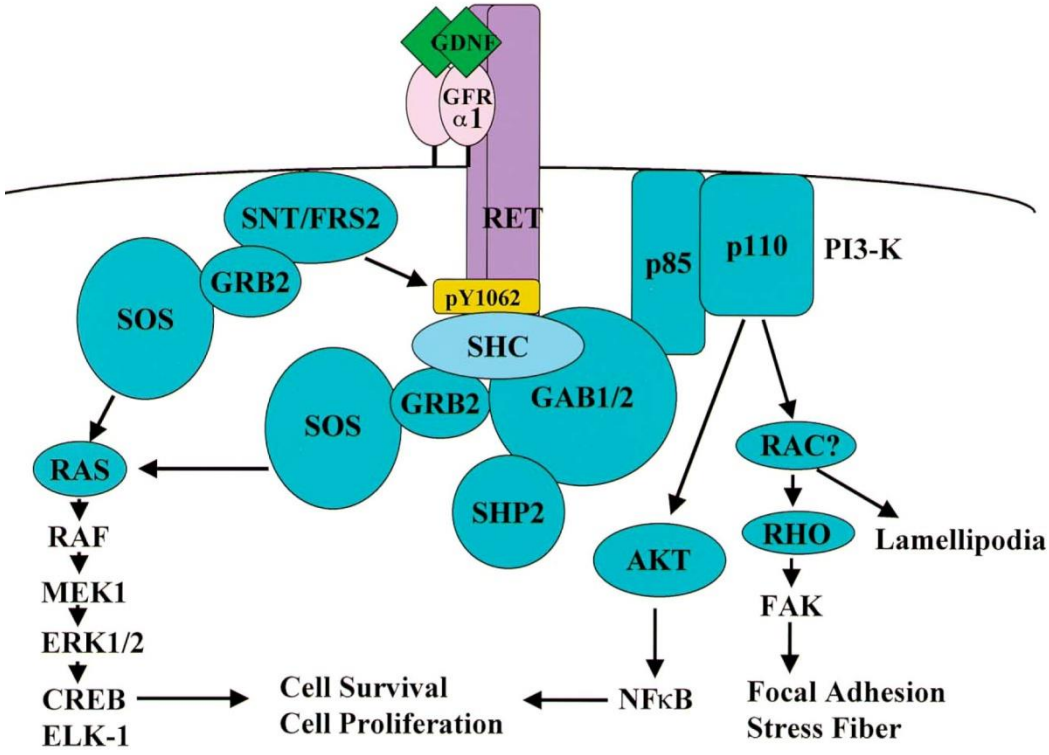

Figure 1.2 An model of intracellular signalling pathways activated by GDNF and the associated biological functions in cell development [30].

1.1.3 Applications of engineered scaffolds in neural tissue engineering

Electrospun polymeric scaffolds have shown significant potential for tissue engineering applications, as they have been employed to mimic some of the essential features of the extracellular matrix (ECM) for many types of tissue. In this research, electrospun poly (ε-caprolactone) (PCL) scaffolds were used because of their proven biodegradability and biocompatibility for regeneration of the CNS. These scaffolds were seeded with primary neural cells (NSCs) and the propensity of the scaffolds to influence proliferate and differentiate were examined. Previous research demonstrated that electrospun PCL scaffolds could influence the proliferation and differentiation capacity of NSCs whilst also encouraging neurite elongation and infiltration. Furthermore, these scaffolds can result in astrocyte activation, important for the secretion of growth factors and supporting neurons in the injured

brain [1, 31]. In addition proteins can be immobilised onto these electrospun PCL scaffolds to further influence cellular responses. In one such example, immobilised brain-derived neurotrophic factor (BDNF) was shown to sustain primary cortical cells, encourage cell proliferation and direct the differentiation towards neurones and oligodendrocytes [2]. In the present project, electrospun scaffolds were optimised specifically for neural stem cell transplantation in order to encourage neural cell proliferation, enhance differentiation of neurons to replace cells lost to disease/ injury and accelerate restoration of lost function following brain injury.

Galactose modified xyloglucan is a thermally sensitive and neutral hydrogel, which has shown to be biocompatible both in vitro and *in vivo* studies [32]. Additionally the interconnective structure of xyloglucan enhances the permeability of oxygen, nutrients and metabolites [33], making them suitable for cell encapsulation in tissue engineering. Injectable hydrogels are ideal for *in vivo* applications due to the less invasive implantation method. Diseases/ injuries to the CNS can often result in the loss of tissue mass and the formation of a spatial/ cystic cavity. Consequently, in these instances, repair requires the replacement of extracellular matrix to enable the support of transplanted cells. In this research (chapter 7) xyloglucan was designed to encapsulate and provide physical support for implanted neural cells. Xyloglucan grafted with PDL was shown to encourage the infiltration of neurite and astrocyte after implantation [32], demonstrating the controllable biofunctionality of the material.

1.2 RESEARCH HYPOTHESIS

A central hypothesis of this work is that electrospun scaffolds immobilised with a neurotrophic factor can support grafted primary neural cells including increased survival, proliferation and innervation *in vivo* in the comparison with cell transplantation alone and unmodified scaffolds. In addition, a hybrid scaffold containing hydrogel and electrospun short fibres tethered with a neurotrophic factor can sustain grafted cells and maintain process development of grafted ventral midbrain cells in an animal model of Parkinson's disease.

In specific terms, the above hypotheses are supported by the following research findings:

A) GDNF can be chemically immobilised onto electrospun PCL scaffolds, which can be a long lasting delivery system without degradation.

B) Tethered GDNF can promote cell viability of ventral midbrain cells and increase the population of dopamine cells in cultures in the comparison with control (2D glass coated with PDL).

C) Biocompatible electrospun scaffolds can be applied to deliver primary neural cells with adequate physical support *in vivo*, which can allow neurite penetration through scaffolds with micro size.

D) Electrospun PCL scaffolds immobilised with GDNF can promote grafted neural stem cell survival and enhance fibre innervation *in vivo* with sufficient physical support and biological stimulus when compared to cell transplantation alone and unmodified scaffolds.

E) Short fibres of electrospun scaffolds immobilised with GNDF can combine with hydrogel, xyloglucan for in vitro and *in vivo* applications.

F) Xyloglucan can be utilised to encapsulate grafted primary neural cells *in vivo*.

G) Incorporation of xyloglucan and tethered GDNF on short fibres can promote the process development *in vivo* in the comparison with the absence of GDNF.

1.3 RESEARCH AIMS

1.3.1 Research aims

This PhD research focuses on the applications of polymeric scaffolds for the support of primary neural cells in vitro and following implantation into the intact and injured brain. The thesis encompasses four main research aims:

1) To characterise the stability, degradation and functionality of immobilised protein on polymeric scaffolds,

2) To develop a methodology for implanting polymeric scaffolds, together with primary neural cells, into the rodent brain.

3) To examine the biological effects of protein tethered scaffolds on primary neural cells and their derivatives *in vitro*, as well as assess the effect of these scaffolds on graft and host-derived neural cells *in vivo*,

4) To utilize easily implantable composite polymeric scaffolds, incorporating biofunctionalized short nanofibres, to enhance the survival and integration of neural transplants into an animal model of PD in the comparison with unmodified scaffolds.

AIM 1

To tether protein (utilizing GDNF to demonstrate proof of principle) onto scaffolds via an optimised crosslinking method. To investigate the stability and degradation of the immobilised protein on polymeric scaffolds in order to assess the amount of amines and proteins tethered onto scaffolds, and release kinetics of the protein and functional activity of the protein over time.

AIM 2

Combining biomaterials and primary neural cells to promote tissue repair relatively to cell transplantation alone in the injured brain is the main focus of this PhD research. Aim 2 will important develop and optimise a method for implanting polymeric scaffolds together with primary neural cells grafts into the rodent brain. The main focus of this aim is to encourage the survival rate of the implanted cells, whilst aim 3 will provide a more detailed assessment of implanted cells based upon optimized methodologies established in aim2.

AIM 3

To assess the biological effects on both graft and host-derived neural cells following implantation together with the GDNF-functionalized electrospun scaffolds. The aim is to demonstrate scaffolds not only provide physical support for implanted primary neural cells but can additionally be utilized for prolonging protein delivery *in vivo*. The main challenge is to enhance the survival of grafted cells, support their proliferation and differentiation and, to encourage the integration between implanted scaffolds, grafted cells and host in the comparison with cell transplantation alone and unmodified scaffolds.

AIM 4

To explore different forms of polymeric scaffolds that can reduce the physical trauma induced upon implantation into the brain. To achieve Aim 4 two different forms of polymeric scaffolds are applied: a hydrogel that can easily injected into the brain and undergoes gelation at physiological temperatures combined with biofunctionalized electrospun short fibres. These composite scaffolds will be implanted into the brains of Parkinsonian mice to assess their ability to support neural tissue grafts.

1.4 RESEARCH STRATEGY

The main research strategy in this PhD is illustrated in figure 1.3. PCL scaffolds were fabricated by electrospinning and immobilised with GDNF. The modified scaffolds were implanted in the brain of rats for 28 days while primary cortical cells transplanted adjacent to the scaffolds. Development of the research lead to the implantation of hybrid scaffolds (xyloglucan gel together with GDNF-functionalized short nanofibres) together with midbrain dopamine cells into animal models of Parkinson’s disease in an effort to promote repair.

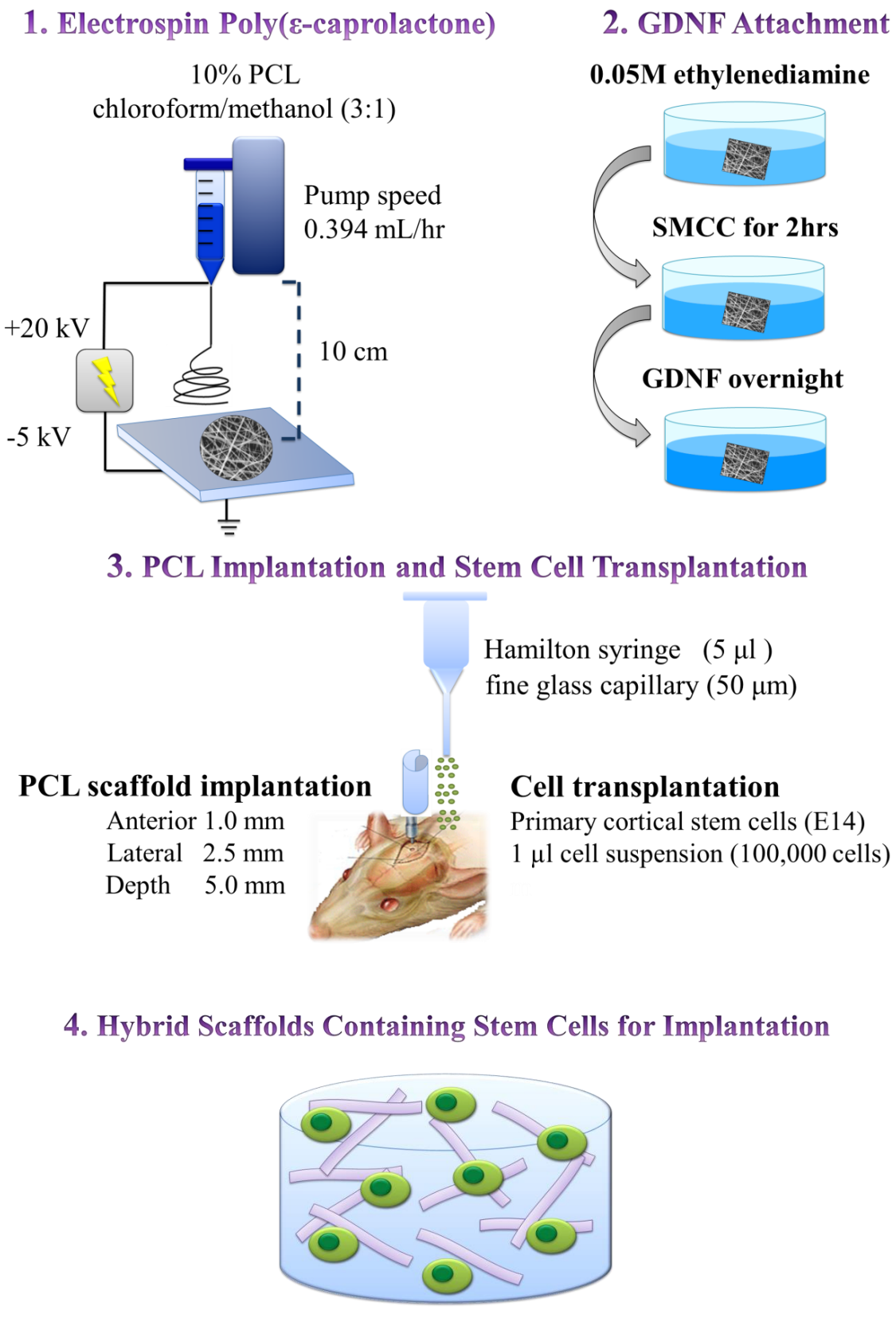

Figure 1.3 The schematic illustration of research strategy

1.5 THESIS OUTLINE

Part1 containing chapters 1-3 concentrates on the different types of polymeric scaffolds and a variety molecules and methods for surface modification in neural tissue engineering. Part2 containing chapter 4 investigates the characterisation of stability, function and degradation of immobilized protein on scaffolds. Part 3 containing chapter 5-7 focuses on the combination of implanting modified electrospun scaffold with transplanting primary neural cells *in vivo,* and utilization of different forms of engineered scaffolds for implantation purpose. Part 4 containing chapter 8 concludes all the research projects conducted during the PhD duration.

This thesis is submitted as a conventional thesis containing three publications and other traditional chapters. Part 1 contains a review article and Part 3 contains a research publications. For the publications in the thesis, the format style and language are specific for each submitted journal, and vary from each other.

1.5.1 Part1- An introduction

Chapter 1

A general introduction and background in neural tissue engineering

This is an introduction chapter giving a brief background of neural tissue engineering, utilization of primary neural cells and biomaterials application in neural tissue engineering, which includes electrospun scaffolds and xyloglucan. And the research hypothesis, aims and an outline of the thesis are detailed.

Chapter 2

Biofunctionalisation of polymeric scaffolds for neural tissue engineering

This is a literature review chapter introducing the current applications of different types of engineered scaffolds, surface modification with molecules and immobilisation methods for neural tissue engineering. A discussion of the potential of bioengineered scaffolds in the field is included.

Chapter 3

Materials and methods

This is a chapter including all the materials and methods applied in this PhD research.

1.5.2 Part2- Characterization of immobilised protein on scaffolds

Chapter 4

Characterisation of the stability and bio-functionality of tethered GDNF on scaffolds

Chapter 4 discusses the characterization of the stability, degradation and biofunction of the immobilized protein on electrospun scaffolds. The chapter details the stability of immobilized protein on the scaffolds over a period of time, the releasing time points and the effects on cultured cells. It gives a better insight of how much proteins can be tethered on to the scaffolds via the crosslinking method, how much leaching off over a period time and the actual releasing time point. Additionally the influence on cell behaviour including survival rate and the population of dopamine cells was detailed in this chapter.

1.5.3 Part3 – Implantation of modified scaffolds with stem cell transplantation

Chapter 5

Optimising implantation of electrospun PCL scaffolds with grafted neural stem cell

Chapter 5 focuses on the combination of scaffolds with primary neural cells together *in vivo*, optimizing an efficient method to deliver both polymeric scaffolds and primary neural cells with significant cell viability. Both in vitro and *in vivo* studies are investigated and discussed in this chapter. It sets the foundation to the following studies.

Chapter 6

Promoting engraftment of transplanted neural stem cells/ progenitors using biofunctionalised electrospun scaffolds

Chapter 6 is a research publication in the journal *Biomaterials*. The study establishes the immobilisation of GDNF on electrospun scaffolds, showing concentration dependency. It shows an increase in survival rate, neurite ingrowth and proliferation of neural stem cells when implanting scaffolds with grafted neural stem cells in the brain for 28 days and integration between implanted scaffolds, transplanted cells and host tissue.

Chapter 7

Composite scaffolds, functionalised with glial derived neurotrophic factor, support dopaminergic neurons in vitro and promote graft integration in an animal model of Parkinson's disease

Chapter 7 is a research publication concentrating on the utilization of bioengineered scaffolds combining hydrogel and short fibres of electrospun scaffolds immobilized with GDNF, with grafted primary neural cells into an animal model of Parkinson's disease.

1.5.4 Part 4- Conclusion and future directions

Chapter 8

Conclusion and future direction

Chapter 8 is a conclusion of the thesis, giving an overview of the research projects and a summary of the results and a discussion of future directions.

1.6 OVERVIEW OF RESEARCH PROJECT SCOPE

Table 1.2 Overview of research project scope

Hypothesis	Aims	Descriptions	Thesis
1) GDNF can be chemically immobilised onto electrospun PCL scaffolds, which can be a long lasting delivery system without degradation. 2) Tethered GDNF can promote cell viability of ventral midbrain cells and increase the population of dopamine cells in cultures when compared to the absence of GDNF.	To investigate the stability and of the immobilised protein on polymeric scaffolds and the bio-functionality.	1) Electrospun PCL scaffolds were fabricated with micron size. 2) The scaffolds were immobilised with GNDF. 3) The stability of tethered GDNF was tested by ELISA. 4) Ventral midbrain cells were cultured on the scaffolds to exam the viability and differentiation.	Chapter 4
Biocompatible electrospun scaffolds can be applied to deliver neural primary neural cells with adequate physical support *in vivo*, which can allow neurite penetration through scaffolds with micro size.	To optimise the method combining implantation of polymeric scaffolds and transplantation of primary neural cells.	1) Primary cortical cells were cultured on PCL scaffolds to test the biocompatibility. 2) Scaffolds with cultured cells were rolled to test the methodology. 3) Scaffolds were implanted while primary neural cells were transplanted *in vivo* and evaluated.	Chapter 5
Electrospun PCL scaffolds immobilised with GDNF can promote grafted neural stem cell survival and enhance fibre innervation *in vivo* with sufficient physical support and biological stimulus when compared to cell transplantation alone and unmodified scaffolds.	To estimate the effects on both grafted and host tissue after implanting the electrospun scaffolds immobilised with a neurotrophic factor.	GDNF immobilisation was confirmed. Primary cortical cells were cultured on modified scaffolds with GDNF. Modified scaffolds were implanted with grafted primary neural cells *in vivo*, and evaluated.	Chapter 6
Xyloglucan can be utilised to encapsulate grafted primary neural cells *in vivo*. Incorporation of tethered GDNF on short fibres can promote the process development *in vivo* in the comparison with the absence of GDNF	To explore different forms of polymeric scaffolds for implantation purpose in order to create a less invasive technique, advance the implanted materials and maximise the survival rate of transplanted cells.	Electrospun scaffolds were sonicated into short fibres. Ventral midbrain cells were cultured on the hybrid scaffolds. Ventral midbrain cells were encapsulated in hybrid scaffolds for implantation *in vivo*.	Chapter 7

1.7 REFERENCES

[1] Nisbet DR, Rodda AE, Horne MK, Forsythe JS, Finkelstein DI. Neurite infiltration and cellular response to electrospun polycaprolactone scaffolds implanted into the brain. Biomaterials. 2009;30:4573-80.
[2] Horne MK, Nisbet DR, Forsythe JS, Parish CL. Three-Dimensional Nanofibrous Scaffolds Incorporating Immobilized BDNF Promote Proliferation and Differentiation of Cortical Neural Stem Cells. Stem Cells Development. 2010;19:843-52.
[3] Willerth SM, Sakiyama-Elbert SE. Approaches to neural tissue engineering using scaffolds for drug delivery. Advanced Drug Delivery Reviews. 2007;59:325-38.
[4] Cao H, Liu T, Chew SY. The application of nanofibrous scaffolds in neural tissue engineering. Advanced Drug Delivery Reviews. 2009;61:1055-64.
[5] Crompton KE, Goud JD, Bellamkonda RV, Gengenbach TR, Finkelstein DI, Horne MK, et al. Polylysine-functionalised thermoresponsive chitosan hydrogel for neural tissue engineering. Biomaterials. 2007;28:441-9.
[6] Nisbet RD, Kylie EC, Malcolm KH, David IF, John SF. Neural tissue engineering of the CNS using hydrogels. Journal of Biomedical Materials Research Part B: Applied Biomaterials. 2008;87B:251-63.
[7] Valmikinathan CM, Wang JP, Smiriglio S, Golwala NG, Yu XJ. Magnetically Induced Protein Gradients on Electrospun Nanofibers. Comb Chem High Throughput Screen. 2009;12:656-63.
[8] Wang TY, Forsythe JS, Parish CL, Nisbet DR. Biofunctionalisation of polymeric scaffolds for neural tissue engineering. J Biomater Appl.
[9] Yu TT, Shoichet MS. Guided cell adhesion and outgrowth in peptide-modified channels for neural tissue engineering. Biomaterials. 2005;26:1507-14.
[10] Jenkinson C, Fitzpatrick R. Cross-cultural evaluation of the short form 8-item Parkinson's Disease Questionnaire (PDQ-8): Results from America, Canada, Japan, Italy and Spain. Parkinsonism & Related Disorders. 2007;13:22-8.
[11] Taylor CA, Saint-Hilaire MH, Cupples LA, Thomas CA, Burchard AE, Feldman RG, et al. Environmental, medical, and family history risk factors for Parkinson's disease: A New England-based case control study. American Journal of Medical Genetics. 1999;88:742-9.
[12] Licker V, Koari E, Hochstrasser DF, Burkhard PR. Proteomics in human Parkinson's disease research. Journal of Proteomics. 2009;73:10-29.
[13] Androutsellis-Theotokis A, Rueger MA, McKay RDG, Jeffrey HK, Mark HT. Stem Cell Therapies for Parkinson's Disease. In: Jeffrey K, Mark T, editors. CNS Regeneration (Second Edition). San Diego: Academic Press; 2008. p. 161-80.
[14] Hagai B, G ther D. Pathophysiology of Parkinson's disease: From clinical neurology to basic neuroscience and back. Movement Disorders. 2002;17:S28-S40.
[15] Alexi T, Borlongan CV, Faull RLM, Williams CE, Clark RG, Gluckman PD, et al. Neuroprotective strategies for basal ganglia degeneration: Parkinson's and Huntington's diseases. Progress in Neurobiology. 2000;60:409-70.
[16] B. Dunnett S, E. Rosser A, Craig H, Dwaine E. Neural Transplantation in Parkinson's Disease. In: Caraig H, dwaine E, editors. Cellular Transplantation. Burlington: Academic Press; 2007. p. 439-54.
[17] Kim H-J. Stem cell potential in Parkinson's disease and molecular factors for the generation of dopamine neurons. Biochimica et Biophysica Acta (BBA) - Molecular Basis of Disease. 2010;In Press, Corrected Proof.

[18] Winkler C, Kirik D, Bjorklund A. Cell transplantation in Parkinson's disease: how can we make it work? Trends in Neurosciences. 2005;28:86-92.
[19] Parish CL, Arenas E. Stem-cell-based strategies for the treatment of Parkinson's disease. Neurodegener Dis 2007;4(4):339-47. 2007.
[20] Gao J, Prough DS, McAdoo DJ, Grady JJ, Parsley MO, Ma L, et al. Transplantation of primed human fetal neural stem cells improves cognitive function in rats after traumatic brain injury. Experimental Neurology. 2006;201:281-92.
[21] Lacza Z, Horvath E, Busija DW. Neural stem cell transplantation in cold lesion: a novel approach for the investigation of brain trauma and repair. Brain Research Protocols. 2003;11:145-54.
[22] Longhi L, Zanier ER, Royo N, Stocchetti N, McIntosh TK. Stem cell transplantation as a therapeutic strategy for traumatic brain injury. Transplant Immunology. 2005;15:143-8.
[23] Honmou O. Transplantation of neural stem cells into ischemic brain. International Congress Series. 2003;1252:477-82.
[24] Kang H-C, Kim D-S, Kim JY, Kim H-S, Lim BY, Kim HD, et al. Behavioral improvement after transplantation of neural precursors derived from embryonic stem cells into the globally ischemic brain of adolescent rats. Brain and Development. 2010;32:658-68.
[25] Zigova T, Sanberg PR. The rising star of neural stem cell research. Nat Biotech. 1998;16:1007-8.
[26] Zawada WM, Zastrow DJ, Clarkson ED, Adams FS, Bell KP, Freed CR. Growth factors improve immediate survival of embryonic dopamine neurons after transplantation into rats. Brain Research. 1998;786:96-103.
[27] Nakajima K, Hida H, Shimano Y, Fujimoto I, Hashitani T, Kumazaki M, et al. GDNF is a major component of trophic activity in DA-depleted striatum for survival and neurite extension of DAergic neurons. Brain Research. 2001;916:76-84.
[28] Pickens CL, Airavaara M, Theberge F, Fanous S, Hope BT, Shaham Y. Neurobiology of the incubation of drug craving. Trends in Neurosciences. 2011;34:411-20.
[29] Uchida M, Enomoto A, Fukuda T, Kurokawa K, Maeda K, Kodama Y, et al. Dok-4 regulates GDNF-dependent neurite outgrowth through downstream activation of Rap1 and mitogen-activated protein kinase. J Cell Sci. 2006;119:3067-77.
[30] Takahashi M. The GDNF/RET signaling pathway and human diseases. Cytokine & Growth Factor Reviews. 2001;12:361-73.
[31] Mahesh VB, Dhandapani KM, Brann DW. Role of astrocytes in reproduction and neuroprotection. Molecular and Cellular Endocrinology. 2006;246:1-9.
[32] Nisbet DR, Rodda AE, Horne MK, Forsythe JS, Finkelstein DI. Implantation of Functionalized Thermally Gelling Xyloglucan Hydrogel Within the Brain: Associated Neurite Infiltration and Inflammatory Response. Tissue Engineering Part A. 2010;16:2833-42.
[33] Nisbet DR, Crompton KE, Hamilton SD, Shirakawa S, Prankerd RJ, Finkelstein DI, et al. Morphology and gelation of thermosensitive xyloglucan hydrogels. Biophysical Chemistry. 2006;121:14-20.

Chapter 2

Literature Review

Contents

Monash University

Declaration for Thesis Chapter 2

Declaration by candidate

In the case of Chapter 2, the nature and extent of my contribution to the work was the following:

Nature of contribution	Extent of contribution (%)
Planning, research and article writing	90%

The following co-authors contributed to the work. Co-authors who are students at Monash University must also indicate the extent of their contribution in percentage terms:

Name	Nature of contribution	Extent of contribution (%) for student co-authors only
John S. Forsythe	Assisted in planning & corrected manuscript	
Clare L. Parish	Assisted in planning & corrected manuscript	
David R. Nisbet	Assisted in planning & corrected manuscript	

Candidate's Signature	[redacted]	**Date** 16.5.2013

Declaration by co-authors

The undersigned hereby certify that:

(1) the above declaration correctly reflects the nature and extent of the candidate's contribution to this work, and the nature of the contribution of each of the co-authors.
(2) they meet the criteria for authorship in that they have participated in the conception, execution, or interpretation, of at least that part of the publication in their field of expertise;
(3) they take public responsibility for their part of the publication, except for the responsible author who accepts overall responsibility for the publication;
(4) there are no other authors of the publication according to these criteria;
(5) potential conflicts of interest have been disclosed to (a) granting bodies, (b) the editor or publisher of journals or other publications, and (c) the head of the responsible academic unit; and
(6) the original data are stored at the following location(s) and will be held for at least five years from the date indicated below:

Location(s)	**Department of Materials Engineering, Monash University**

[Please note that the location(s) must be institutional in nature, and should be indicated here as a department, centre or institute, with specific campus identification where relevant.]

Signature 1	John Forsythe	**Date**
Signature 2	Clare Parish [redacted]	16.5.2013
Signature 3	David Nisbet [redacted]	16.5.2013

Biofunctionalisation of Polymeric Scaffolds for Neural Tissue Engineering

T. Y. WANG and J. S. FORSYTHE

Department of Materials Engineering, Division of Biological Engineering, Monash University, PO Box 69M, Victoria 3800, Australia

C. L. PARISH

Florey Neuroscience Institute and Centre for Neuroscience, The University of Melbourne, Victoria 3010, Australia

D. R. NISBET*

Research School of Engineering, College of Engineering and Computer Science, The Australian National University, Canberra, The Australian Capital Territory 0200, *Australia.*

*Author to whom correspondence should be addressed.
[redacted]

2.1 ABSTRACT

Patients who experience injury to the central or peripheral nervous systems invariably suffer from a range of dysfunctions due to the limited ability for repair and reconstruction of damaged neural tissue. Whilst some treatment strategies can provide symptomatic improvement of motor and cognitive function, they fail to repair the injured circuits and rarely offer long-term disease modification. To this end, biological molecules, used in combination with neural tissue engineering scaffolds, may provide feasible means to repair damaged neural pathways. This review will focus on three promising classes of neural tissue engineering scaffolds, namely hydrogels, electrospun nanofibres and self-assembling peptides. Additionally, the importance and methods for presenting biologically relevant molecules such as, neurotrophins, extracellular matrix proteins and protein-derived sequences that promote neuronal survival, proliferation and neurite outgrowth into the lesion will be discussed.

KEY WORDS

neural tissue engineering, cell transplantation, stem cells, hydrogel, electrospinning, self-assembling peptide, scaffold, biofunctionalisation, neurotrophins.

2.2 INTRODUCTION

In adult mammals, damage to the central nervous system (CNS) is permanent due to a limited ability to restore normal anatomy and function. In many instances regeneration after injury to the peripheral nervous system (PNS) is also limited. As a result, patients with damage and/or neurodegeneration in the CNS or PNS suffer from long-term disabilities which impact on their quality of life. The need for effective/improved treatment strategies has resulted in the emerging field of neural tissue engineering. Within this field a variety of scaffolds have been investigated for their ability to support the regeneration of neural tissue following injury/disease. Many of these materials have been functionalised with biological cues to promote cell attachment, proliferation, differentiation and guided neurite outgrowth. Here, numerous bioengineered scaffolds (including hydrogels, self-assembling peptides and electrospun scaffolds) will be discussed. We will also review the different functionalisation methods that have been employed for each material to provide a neurochemical environment more conducive to neural tissue repair. Finally, we will briefly discuss the current therapies and their limitation, highlighting the challenges and ultimate goals of scaffolds in neural tissue engineering.

2.3 NEURAL TISSUE ENGINEERING SCAFFOLDS

Recent developments in neural tissue engineering are providing an optimistic outlook for improved repair of damaged neural pathways, however further knowledge of disease progression, regenerative processes, cell replacement therapy strategies, coupled with advances in scaffold technology are necessary. Here, we outline some of the current

biomaterials that are employed for the manufacture of neural scaffolds.

Scaffolds can be engineered to promote repair of damaged neural tissues in a variety of manners including: providing physical support for residual neurons around the injury site, delivering trophic factors [1, 2], assisting in the deployment and maintenance of replacement cells [3, 4], contact guidance for directed axonal outgrowth [5, 6] and minimising hostile inflammatory reactions [7, 8]. In order to achieve these, a number of requirements must be satisfied, including biocompatibility, mechanical properties, and possibly biodegradability [9].

Equal weight should be given to materials selection and scaffold morphology, which potentially will be injury and/or disease specific, as both play an important role in controlling neural regeneration. Material type and scaffold architecture go hand in hand in directing and controlling the migration, differentiation and proliferation of neural cells, whether they are transplanted or endogenous [9]. In the following section we will discuss a number of different scaffolds, including their advantages and disadvantages, to support neural repair.

2.3.1 Hydrogels

A hydrogel is a colloidal state of matter consisting of a solid network which retains large amounts of water without dissolution. They can be either natural or synthetic polymers that form a three-dimensional crosslinked network within the dispersant, resulting in a material that can be engineered to have similar mechanical properties to tissue. Hydrogels have been employed as scaffolds for decades in applications including: wound dressings [10], drug delivery [11], cell encapsulation [12], artificial organs [13] and as tissue engineering matrices [14, 15]. Hydrogels can be classified as chemical (where covalent bonding is responsible for

crosslinking) or physical (where secondary bonding between the polymer chains is responsible for network formation) [16]. In addition, the network and chemical composition of hydrogels can also be readily modified to vary the properties of the scaffold, such as degradation rate and mechanical properties.

One of the essential features of tissue engineering scaffolds is that the mechanical and biological properties mimic the local cell environment. Similarities between the scaffold and endogenous tissue can facilitate cell migration and neurite growth into the scaffold, reduce inflammation, as well as encourage proliferation and differentiation [7, 17-19]. Hydrogels also have the advantage of tuneable water uptake (swelling) and diffusion rates that will facilitate oxygen and nutrient flow, mimicking some of the features of endogenous tissue. These features can be utilised to increase neural cell migration, adhesion and ultimately regeneration [14, 18, 20, 21].

Mechanical and structural characteristics of hydrogels can have a dramatic effect on regeneration, altering cellular proliferation, differentiation as well as morphology and neurite extension. This is especially important when considering biodegradable hydrogels where degradation could result in void formation and subsequent tissue collapse. Biodegradation rates can be controlled by chemical or physical crosslinkng during synthesis [19, 22], but it will inadvertently influence the mechanical properties [23] and cellular response. For instance, the elastic modulus of photopolymerisable methacrylamide chitosan (MAC) films affects the proliferation, differentiation and maturation of neural stem progenitor cells (NSPC) [24]. A higher percentage of astrocytes and neurons were observed on hydrogel surfaces when the stiffness was less than 1 kPa; and as the stiffness increased to 7 kPa, the percentage of oligodendrocytes increased to about 70% [24].

Neurite elongation is also sensitive to charge, with positively charged hydrogels such as chitosan-coupled agarose increasing the length of neurites of chick embryonic dorsal root ganglia, while negatively charged materials, such as alginate-coupled agarose hydrogels, decreasing neurite length [25]. We have shown an increase in neurite outgrowth from primary cortical neurons and neurospheres (Figure 2.1) grown on xyloglucan hydrogels when positively charged poly(D-lysine) (PDL) was anchored to the xyloglucan backbone [21]. Similarly, thermally sensitive chitosan/glycerophosphate salt (Chi/ GP) hydrogel scaffolds were also modified with PDL, demonstrating a pronounced effect on cell survival and neurite development within specific doses of PDL, as shown in Figure 2.2 [26]. Furthermore, significant cell migration of astrocytes and neurite in-growth were observed in vivo when xyloglucan hydrogels modified with increased concentrations of PDL (xyloglucan/PDL: 90/10, 50/50 and 100 wt/wt%) were implanted in the brain of adult rats [27]. Interestingly, neurite in-growth corresponded to the concentration of PDL grafted on the hydrogels, which was directly proportional to the number of astrocytes. This neurite growth could be attributed to laminin deposition secreted from astrocytes [27]. Similar results were shown in another study, where neurites and astrocytes were co-localised in poly[N-(2-hydroxypropyl)-methacrylamide] (PHPMA) hydrogels implanted in the brain of rats with fimbria-fornix lesions [28]. These studies highlight the important trophic role astrocytes play in regeneration, discussed later. Table 2.1 summarises a number of studies using various hydrogels with different biomolecular modifications or drug encapsulation for neural tissue engineering.

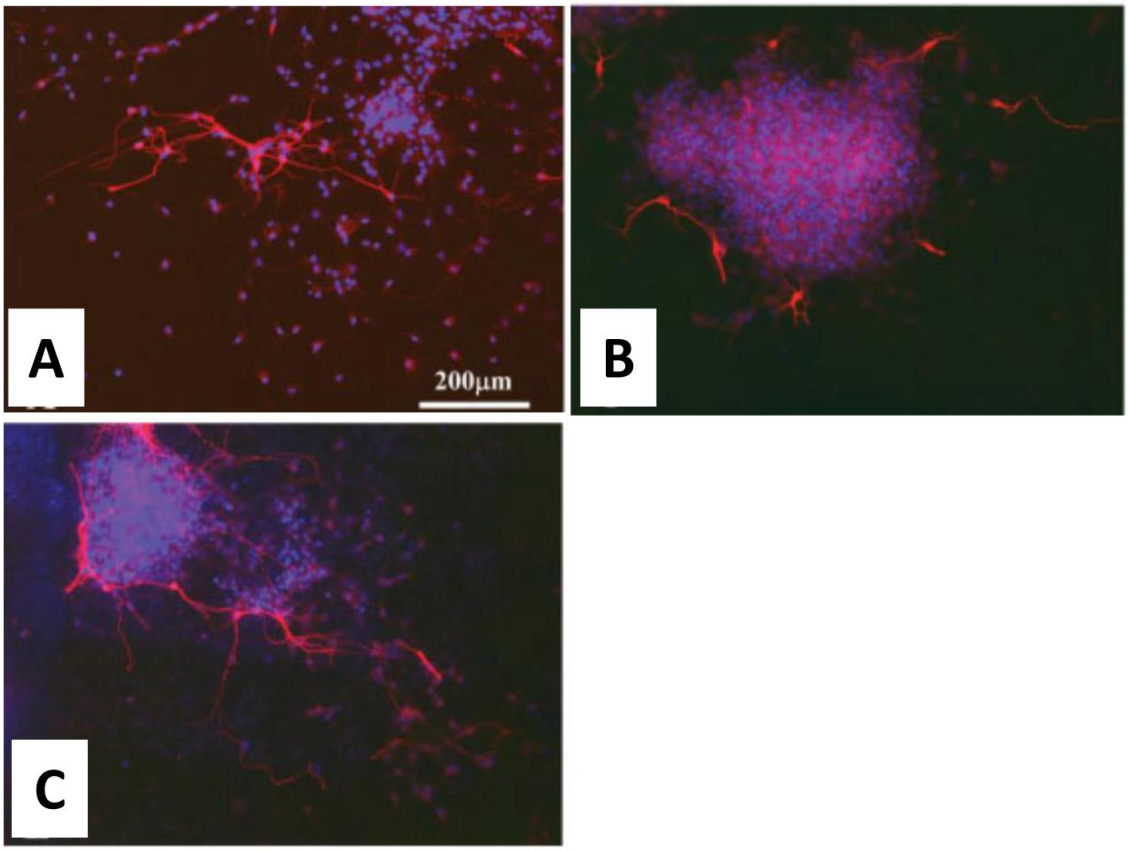

Figure 2.1 The morphology of neurospheres cultured on thermoresponsive xyloglucan blended with different degrees of poly(D-lysine) grafting. Polylysine control (A), 50:50 xyloglucan-graft-PDL (B) and 100% xyloglucan-graft-PDL (C) [21] (the figure has been modified).

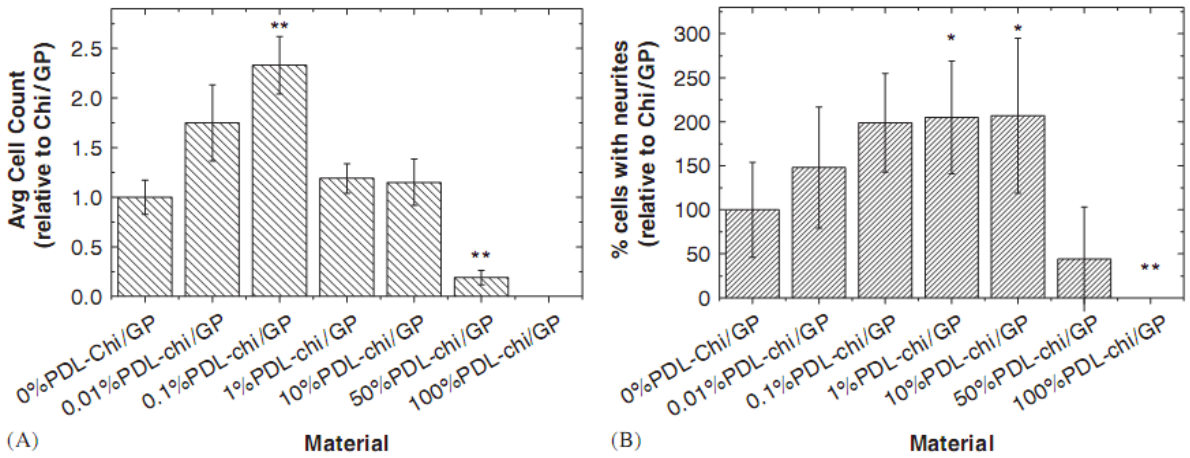

Figure 2.2 Cell viability and neurite outgrowth of foetal mouse cortical cells seeded in 3D chitosan (chi)/ glycerophosphate salt (GP) hydrogels with PDL modification [26].

Table 2.1 Hydrogels, biofunctionalisation and their application in neural tissue engineering

Hydrogel	Biomolecule	Cell type/ location of implantation)	Ref.
Chitosan/glycerophosphate	PDL	Foetal mouse cortical cells	[26]
Polyacrylamide	Fibronectin, laminin, biotin-IKVAV	Rat astroglioma cell, primary rat hippocampal neurons	[29]
Pluronic F127, Matrigel, PuraMatrix		Human fetal NSCs	[30]
Collagen		Rat embryonic hippocampal neurons	[31]
Acrylated PLA-b-PEG-b-PLA	NT-3	Male rat (spinal cord)	[8]
P(HEMA-*co*-MMA)	Collagen, fibrin, FGF-1, NT-3	Female rat (spinal cord)	[32]
Agarose/ alginate		Embryonic rat cortical neurons	[33]
HAc-based hydrogel	BDNF	Rat neurosphere-forming cells	[34]
PHPMA	Arg-Gly-Asp	Female rat (spinal cord)	[35]
HAMC	PLGA (loaded drug)	Female rat (spinal cord)	[36]
Xyloglucan	PDL	Male rat (caudate putamen)	[27]
PHPMA	Glucosamines N-acetyl-glucosamines	Female rat (septum-hippocampus)	[28]

Abbreviations: isolucine-lysine-valine-alanine-valine (IKVAV), neural stem cells (NSCs), poly(2-hydroxyethyl methacrylate-*co*-methyl methacrylate) [P(HEMA-*co*-MMA)], fibroblast growth factor-1 (FGF-1), neurotrophin-3 (NT-3), polyethylene glycol diacrylate (PEGDA), brain-derived neurotrophic factor (BDNF), hyaluronic acid (HAc), poly[*N*-(2-hydroxypropyl)methacrylamide] (PHPMA), hyaluronan methylcellulose (HAMC), poly(lactide-*co*-glycolide) (PLGA).

2.3.2 Electrospun scaffolds

Electrospinning is a common top-down nanofabrication method that is utilised in neural tissue engineering for the production of nanofibrous scaffolds [37-40]. Electrospun scaffolds consist of a nanofibrous mesh formed by uniaxial stretching of a viscoelastic polymer solution under an applied voltage. These nanoscaffolds are attractive, as it is believed that they mimic some of the essential features of the extracellular matrix (ECM, ca. fibrous morphology) [41-45]. In recent years there has been rapid advancements made in the production of these fibrous scaffolds including structural morphology and surface

functionality [46]. During electrospinning, the morphology of the fibrous scaffold can be optimised using a number of different variables, such as the pump speed [47], voltage [48], working distance [49], ambiance (temperature, humidity, atmosphere) [50] solvent type [51], collection device [52] and material properties such as type, concentration, viscosity, molecular weight and conductivity [53-55]. Electrospinning offers flexibility in combining and manipulating these variables to produce the desired product. For more information regarding the electrospinning process and characterisation of electrospun scaffolds, the interested reader is directed to the following reviews [40, 56, 57].

Electrospun scaffolds have three dimensional fibrous architectures, high surface areas and interconnected porosity making them an attractive option for the fabrication of neural tissue engineering scaffolds [5, 58, 59]. Nanofibres influence, and in some cases control neural cell adhesion, infiltration, differentiation, proliferation, and neurite elongation [53, 54, 60, 61]. Electrospun scaffolds can be produced from a range of naturally derived and synthetic polymers for neural tissue engineering (Table 2). Naturally derived polymers generally have superior biocompatibility and biodegradability characteristics compared to synthetic polymers but often at the expense of mechanical properties. However, it is generally more difficult to electrospin naturally derived polymers, with synthetic polymers having the added advantage in that their mechanical properties can be manipulated to a larger degree [60]. Synthetic and natural polymers can be blended to capitalise on the benefits of both types of materials [62]. The materials selection and engineering of electrospun scaffolds is critical to attempt to avoid a chronic inflammatory reaction, whilst also encouraging neural cell adhesion, proliferation, differentiation and infiltration to facilitate long term neural reconstruction [63].

Fibre diameter, orientation and density also influence cell viability, morphology and function [64-67]. Aligned electrospun scaffolds produced from poly(ε-caprolactone) (PCL) have been used to control the neurite orientation of human Schwann cells (hSCs) (Figure 2.3) [68]. While hSCs seeded on PCL films had spread cell morphologies and extend more widely compared to cells cultured on electrospun PCL fibres [68], the cytoskeleton can be modified in 3D using topographic guidance, in this instance by using randomly orientated and aligned fibres [69]. Similar results were observed for other types of neural cells, such as rat dorsal root ganglia (DRGs) and mouse cerebellum C17.2 stem cells [65, 69-71]. Yang et al. also discovered that the neurites of cerebellum C17.2 stem cell cultured on aligned poly(L-lactic acid) (PLLA) scaffolds elongate in the direction of fibre alignment, following contact guidance [65]. The degree of alignment and porosity of fibrous scaffolds are interrelated; fully aligned electrospun fibres have very small interfibre spacings as a result of increased density, which has a significant influence on cellular behaviour. When the density of aligned electrospun poly(L-lactide) fibres was increased the neurite density from chick embryonic dorsal root ganglia (DRGs) was also enhanced (Figure 2.4) [64]. However, despite this there was no significant difference in neurite length following density changes [64]. We have also shown that neurites of embryonic cortical neurons cultured in vitro follow the direction of electrospun fibres when the distance between them was greater than 15 μm. Neurites were shown to travel across fibres when the interfibre distance was between 2 and 15 μm, and avoid areas with interfibre distance smaller than 1 μm [39]. Electrospun PCL scaffolds with random and partially aligned morphologies have also been implanted in the rat brain, with random fibre morphology allowing neurite infiltration after 60 days, whereas partially aligned scaffolds did not (Figure 2.5) [38].

Another parameter that may be crucial in neural tissue engineering is the fibre diameter. Electrospun fibres ranging in diameter from 1μm to 5μm may be optimal for directing neurite outgrowth on aligned electrospun scaffold, as there were minimal instances where neurites crossed individual electrospun fibres. [64]. This has also been shown for neurites extending from mouse cerebellum c17.2 stem cells where PLLA aligned nanofibres were superior at directing elongation compared to microfibres [65]. However, it is possible that the effects observed occur due to the fibre diameters influencing the density of the scaffolds

Table 2.2. Electrospun natural and synthetic polymers for neural tissue engineering

Polymer	Diameter (μm)	Cell type (* indicates in vivo application)	Ref.
Natural polymer			
Chitosan	0.7 ± 0.502 ; 0.126 ± 0.02	Murine Schwann cells into injured sciatic nerve of rats	[72, 73]
Laminin	0.1416 (5%)	Human adipose stem cells *	[74]
Silk fibroin	0.404 – 1.977	Rat bone marrow MSC, vascular endothelia cells, neurons	[75]
Synthetic polymer			
PLLA	0.15-0.5 (2%), 0.8-3 (5%); 1.325 + 0.383 , 0.759 + 0.179, 0.293 + 0.065	Mouse cerebellum stem cells c17.2; chick DRG, Schwann cells	[65, 76]
PCL; PCL/PEG	0.45 ± 0.1 (partially aligned), 0.35 ± 0.125 (random)	Implantation of MSC into rat caudate putamen *	[38, 77]
PLGA	0.76±0.30 ; 0.25± 0.11 (aligned), 0.36±0.13 (random)	Mouse cortical neurons; Rat pheochromocytoma 12 cells (PC12)	[39, 78]
Composite polymer			
PCL/ gelatin	0.113 ± 0.033 (PCL/gel. 50:50), 0.189 ± 0.056 (PCL/gel. 70:30), 0.431 ± 0.118 (PCL)	Nerve stem cells (c17.2 cells)	[79]
PCL/Collagen; PLCL /Collagen	0.541±0.164; 0.23 ± 0.031	Chick DRGs, Schwann cells; MSCs	[71, 80]
PCL/ chitosan	0.63 (PCL), 0.45 (chitosan), 0.19 (PCL/chitosan)	Rat Schwann cells (RT4-D6P2T)	[62]

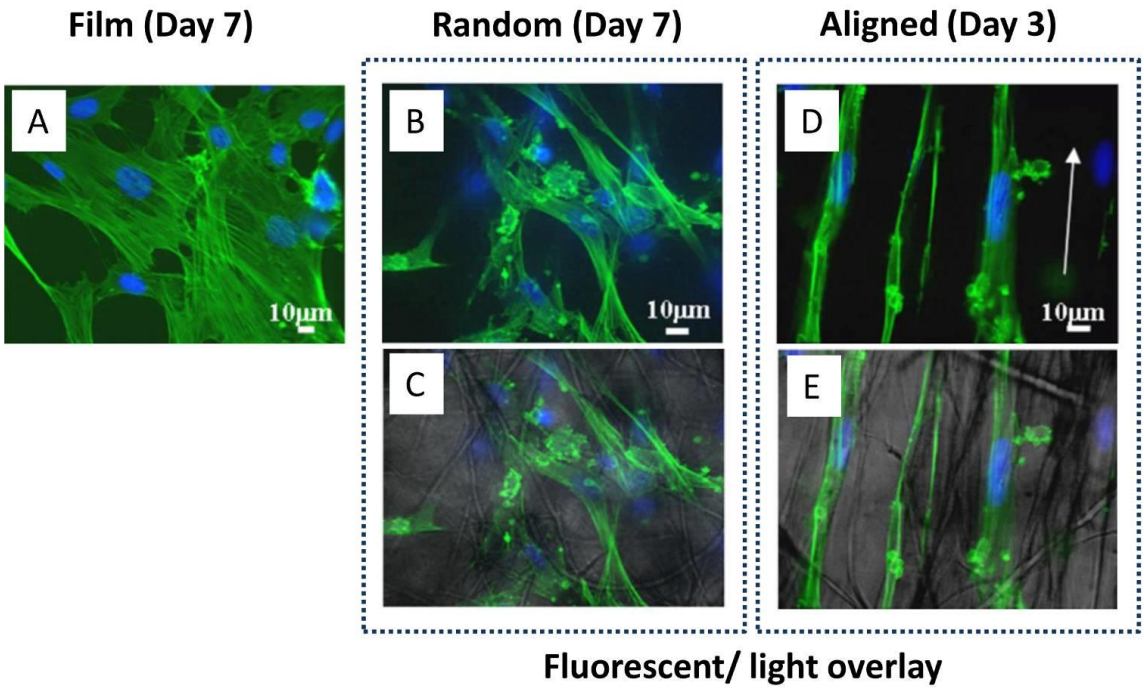

Figure 2.3 . Human Schwann cells cultured on PCL films and electrospun scaffolds with aligned and random fibre orientation. Cells were stained with actin cytoskeleton (green), highlighting the orientation of neuritic processes, and DAPI (blue), to identify cell nuclei within culture [68] (the figure has been modified).

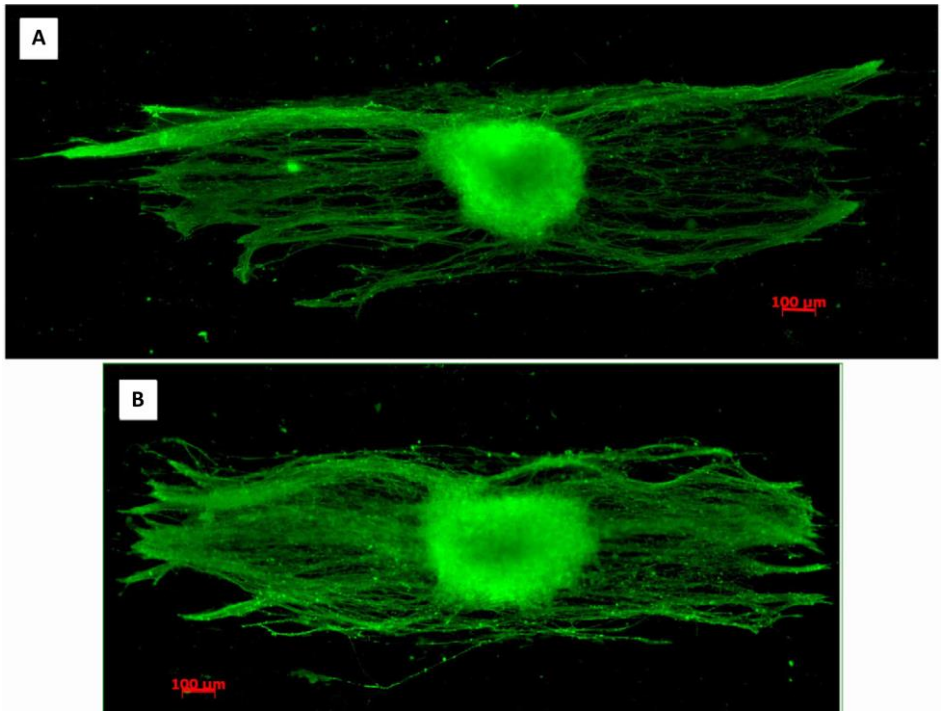

Figure 2.4 The influence of fibre density on neurite outgrowth and neurite length (neurofilament staining) after 5 days of culturing DRG cells on low density (A) and higher density (B) electrospun

PLLA fibres. An increase in electrospun nanofibre density increased the density of neurites [64] (the figure has been modified).

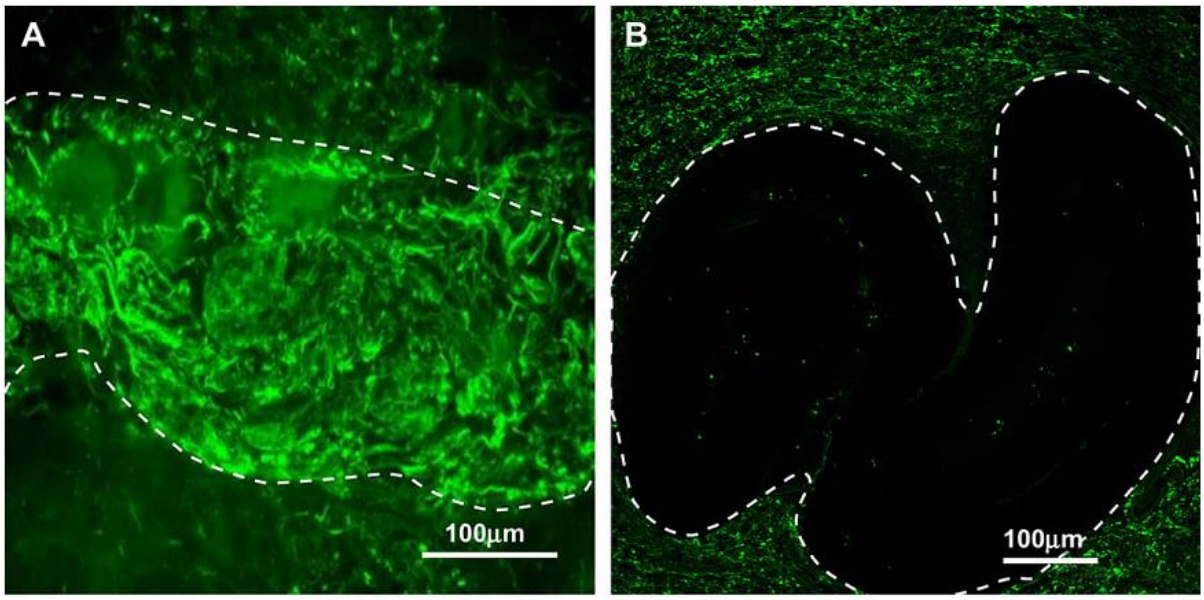

Figure 2.5 Neurofilament staining (green) was used to visualize neurite penertration into electrospun PCL scaffolds with random orientation (A) and, scaffolds with partial alignment (B). Dotted line represents the border the the scaffold. Note, neurites readily penetrated PCL scaffolds of random but not aligned fibre orientation [38].

2.3.3 Self-assembling peptide scaffolds

The self-assembling peptide scaffolds have been applied in tissue engineering including bone, nerve and cartilage regeneration and reconstruction [81, 82]. Self-assembly is driven by non-covalent bonding and spontaneous organisation of peptides into nanostructures such as nanotubes, vesicles, nanofibres, helical ribbons and β-sheets (Figure 2.6a). This organisation can be triggered by changes in temperature, pH, or ionic strength [82-84]. Self assembling peptides are often amphiphilic with hydrophobic terminals self organising to form the core of a nanofibre, and the hydrophilic terminals forming the outer layer which can interact with water molecules; therefore self assembling peptide scaffolds can contain up to 99.9% water

and form a hydrogel matrix [85]. Additionally, self-assembling peptide scaffolds can be functionalised with different biological molecules such as the laminin sequence, IKVAV, which increases cell attachment and neurite extension [83, 86, 87]. Self-assembling peptide scaffolds that have been used in neural tissue engineering are summarised in Table 2.3.

Figure 2.6 shows the uniform structure of self-assembled nanofibres composed of peptide amphiphilic molecules. The fibre diameters formed are typically 10 to 20 nm and the porosity can vary from about 5 to 200 nm [88]. Self-assembling peptide amphiphile (PA) scaffolds (based on RADA16-I peptide) with a diameter of approximatley 10 nm have previously been implanted into the injured cortex where they facilitated regeneration. This regeneration was evident by the absence of cavities 6 weeks after implantation, compared to saline injected animals (Figure 2.7) [89]. The hydrogel reduced the extent of secondary injury, possibly due to its ability to promote rapid haemostasis, angiogenesis, reduce the amount of gliosis and facilitate cells migration into the lesion. Yang et al. investigated amphiphilic diblock copolypeptide hydrogels (DCHs) composed of poly(L-leucine) (L) and poly(L-lysine) (K) with different concentrations [90]. An increase in cell migration and proliferation of oligodendrocytes, astrocytes, microglia as well as angiogenesis were evident in the hydrogel after implantation in the caudate putamen nucleus (CPN) of mice brains. However, no significant neurite outgrowth was detected in the scaffolds after 8 weeks [90].

Cellular regeneration and proliferation has also been demonstrated using rat PC12 cells cultured within self-assembling scaffolds, $(RADA)_3IKVAV(RADA)_3$ and $(RADA)_4IKVAV$ (Figure 2.8) [87]. The self assembling peptide $(RADA)_3IKVAV(RADA)_3$ significantly increased the number of rat PC12 cells after 7 days compared to $(RADA)_4IKVAV$ and $(RADA)_4$ based scaffolds (without IKVAV), demonstrating that the position of the IKVAV

epitope in the peptide is important. Additionally cell viability was maintained in the $(RADA)_3IKVAV(RADA)_3$ scaffolds for day 28. However, no neurite outgrowth was evident in this case either, yet it was evident in 2D culture conditions, presumable due to a lack of signal polarity or the small pore size of the hydrogel restricting neurite outgrowth.

Table 2.3 Self assembling peptides for neural tissue engineering

Peptides	Biological recognition molecule	Fibre diameter	In vitro/ vivo	Ref.
$C_{16}H_{31}O$-NH-AAAGGGEIKVAV-COOH (IKVAV PA)	IKVAV	7-8 nm	Rat DRG, rat DRGn	[86]
RADA16-I		10 nm	Schwann cells, NPCs	[91]
bsp-RGD(15), GRGDSP	RGD		Adult hippocampal NSCs	[92]
RAD16-I/ RAD16-II		10-20 nm	Rat PC12 cells, mouse cerebellar neurons, mouse/ rat hippocampal neurons	[93]
CCCCGGGS$^{(PO4)}$RGD	IKVAV		Mice (spinal cord injury)	[88]
RADA	IKVAV		Rat PC12 cells	[87]
RADA16-I	IKVAV	10 nm	Rats (cortex)	[89]
RADA16		10 nm	Adult rat NSCs	[94]
CCCCGGGS$^{(PO4)}$RGD	IKVAV	5-8 μm	Murine NPCs	[95]
RAD16-I		10 nm	Young/ adult hamsters (midbrain SC)	[96]

Abbreviations: dorsal root ganglions (DRG) and neurons (DRGn), Arg-Gly-Asp (RGD), Arg-Ala-Asp-Ala(RADA), neural progenitor cells (NPCs), GGGNGEPRGDTYRAY [bsp-RGD(15)], superior colliculus (SC)

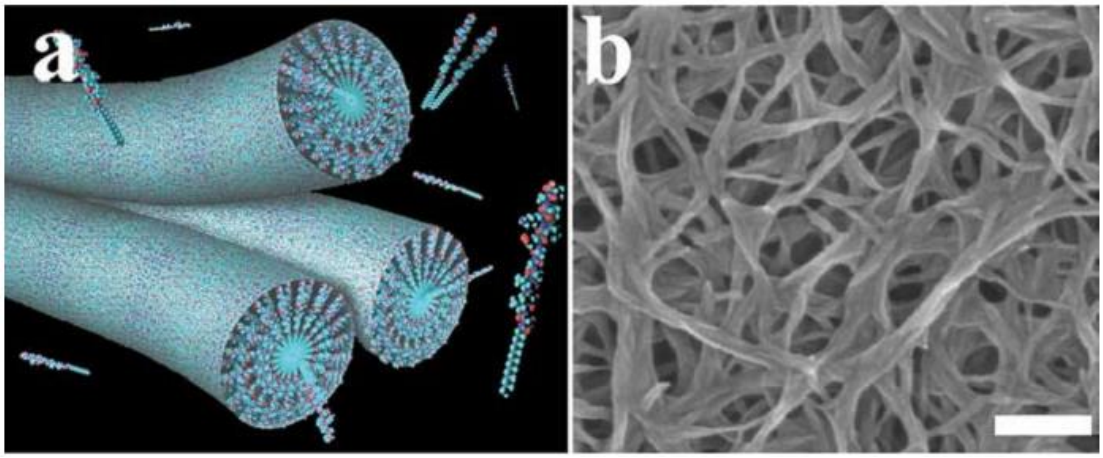

Figure 2.6 Schematic showing a cross-sectional view of self assembling peptide-amphiphile (PA) nanofibres presenting the laminin epitope IKVAV at the hydrophilic terminus. (a); and the scanning

electron micrograph of the nanofibre scaffold (b). Scale bar = 200 nm [88].

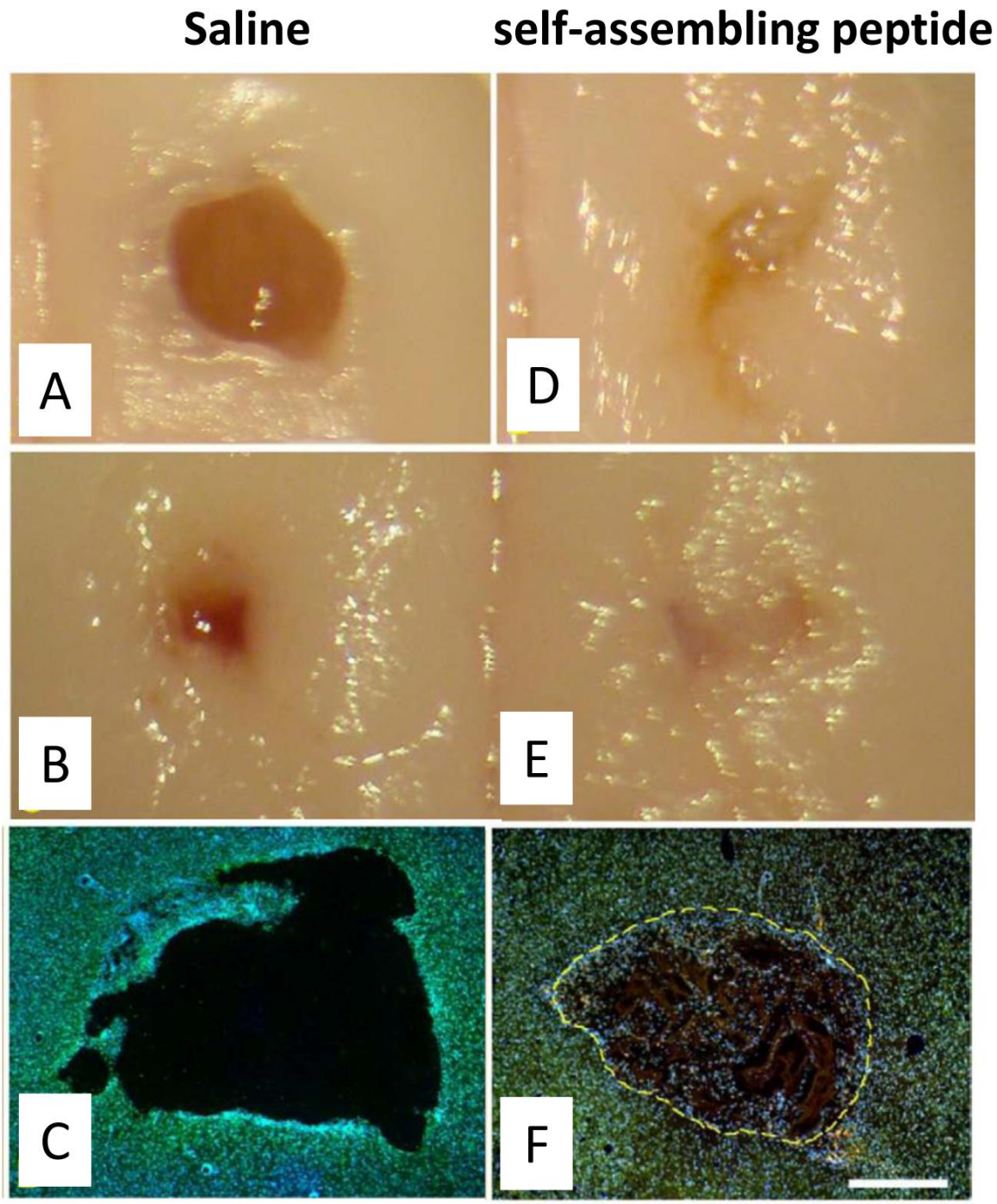

Figure 2.7 Cortical tissue regeneration and reconstruction: control group treated by injection of saline (A, B and C) and experimental group treated with self assembling scaffolds $(RADA)_{16}$ (D, E right and F). C and F show Nissl staining (cell RNA in the rough endoplasmic reticulum of nuclei) and DAPI (nuclei) double staining. Scale bar: A,B,D,E= 100 μm; C, F= 500 μm [89] (the figure has been modified).

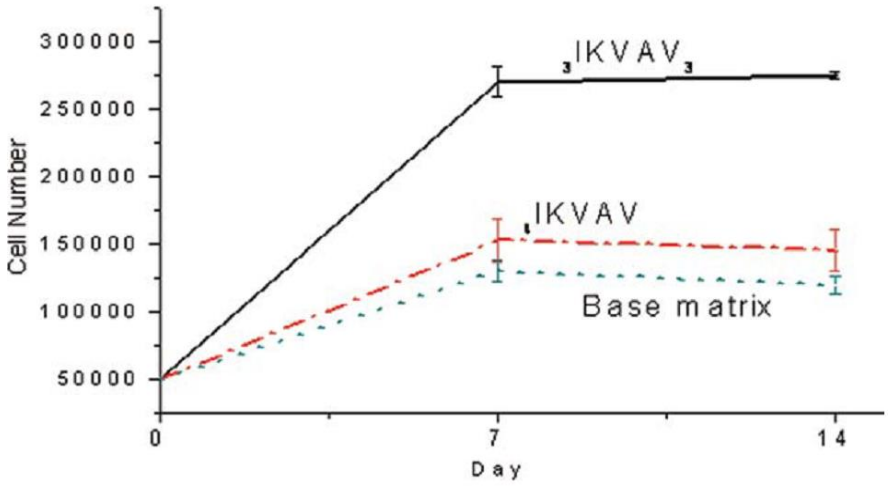

Figure 2.8 Cell proliferation and viability of PC12 cells cultured on self-assembling peptide scaffolds biofunctionalised with the laminin epitope IKVAV. $_3$IKVAV$_3$ represents (RADA)$_3$IKVAV(RADA)$_3$ and $_4$IKVAV represents (RADA)$_4$IKVAV. Increased proliferation is evident when the IKVAV is inserted between RADA sequences ($_3$IKVAV$_3$) compared to the end of the peptide chain ($_4$IKVAV). The base matrix (RADA)$_4$ lacks the IKVAV epitope [87].

2.4 BIOFUNCTIONALISATION OF SCAFFOLDS

The ultimate goal of neural tissue engineering is to promote cell survival and integration (including neurite outgrowth, guidance and connectivity) of endogenous or exogenous cells into the injured site in order to repair damaged neural tissue. While to some extent this can be achieved through optimising the morphology and the mechanical properties of the scaffold, biomolecular stimulation may also be essential. By delivering appropriate biological molecules to target tissues, we can move closer towards the fabrication of niche cellular microenvironments that are necessary to modulate neuronal behaviour. Here, we will discuss different biological stimulators that have been employed in neural tissue engineering, as well as the methods of biofunctionalisation.

2.4.1 Biological molecules for neural tissue engineering

The selection of suitable biological molecules to tether or release from scaffolds is reliant on the target tissue. The common types of molecules that have been utilised in neural tissue engineering include neurotrophins, such as brain derived neurotrophic factor (BDNF) [46] and nerve growth factor (NGF) [97], peptides sequences, such as laminin derived IKVAV [98], or ECM proteins, such as collagen I, fibronectin and laminin [99-101]. There are a variety of methods employed for the biofunctionalisation of scaffolds, such as covalent crosslinking, blending and physical adsorption. The method of biofunctionalisation depends on the property and chemistry of scaffolds and the nature of binding molecules. An appropriate presentation method should maximise the bioactivity of the scaffold [102, 103] and minimise chronic inflammatory reactions after implantation [27]. For instance, covalently immobilised growth factors may amplify their trophic effect compared to soluble analouges due to multivalency, prevention of protein internalisation, as well as the comparatively high local concentrations of the growth factor on the scaffold surface compared to delivery in solution [104]. Interestingly immobilisation of growth factors can activate different signalling pathways compared to soluble factors. For instance, sustained signalling from immobilised epidermal growth factor (EGF) to PC12 cells induced differentiation and neurite formation, whereas soluble EGF stimulated cell proliferation [105]. Whilst there are numerous molecules and proteins that can influence cell proliferation, differentiation and migration, we will focus on neurotrophins.

2.4.1.1 Neurotrophins

Neurotrophins are a family of proteins that have multiple functions in the CNS and PNS, including promoting survival, proliferation, differentiation, axonal outgrowth, synaptogenesis

and even apoptosis under certain conditions [106, 107]. Neurotrophins have similar structures, and include BDNF, NGF, neurotrophin-3 (NT-3) and neurotrophin-4/5 (NT-4/5) [108, 109]. They are synthesised in the brain in variable quantities and with regional distribution [110]. There are two types of neurotrophin receptors, tyrosine kinase (Trk) receptors and the p75 neurotrophin receptor (p75NTR). Some neurotrophin receptors, such as p75, bind to different neurotrophins, whilst others are neurotrophin specific [111]. Therefore, it is important to consider the receptors that are specific to each individual neural cell type so that an appropriate neurotrophin can be selected prior to scaffold functionalisation.

In the PNS, NGF, BDNF and NT-3 are crucial factors for controlling neuron differentiation and survival. NT-3 expression can be observed during embryogenesis, where it facilitates cell proliferation [112] and supports the differentiation of new neurons and synaptogenesis. For instance, along with BDNF, it is necessary for inner ear innervations during embryonic development [113]. During the early stage of the prenatal development, NT-3 encourages the survival and differentiation of sensory neurons which shifts to rely mainly on NGF upon maturity [114]. Additionally, BDNF acts to support dorsal root ganglion (DRG) and other sensory neurons [113]. As the postnatal PNS develops the role of neurotrophins transfers from encouraging neuronal survival to facilitating neuronal differentiation [114]. Whilst the roles of neurotrophins in development of the CNS and PNS are highlighted here, it is equally important that these proteins are present in neural repair – processes that are likely to recapitulate the events of development. Finally, several neurotrophins have also been shown to protect neurons after CNS and PNS injury [112].

Neurotrophins have been widely employed in neural tissue engineering. However, the efficiency of neural reconstruction varies with the concentration and delivery of the

neurotrophin. In addition, their combination with biomaterials used to fabricate neural tissue engineering scaffolds i.e. stable coupling and/or encapsulation, is also an important design consideration.

A number of studies have biofunctionalised scaffolds using NGF. Krewson et al. encapsulated NGF into poly(ethylene-*co*-vinyl acetate) (EVAc) hydrogels and showed that it had a positive influence on neurite outgrowth from PC12 cells cultured on the surface of the hydrogels [115]. However recently, NGF has successfully been immobilised onto the surface of scaffolds, preventing cell internalisation [1]. It was proposed that the signalling vehicles containing phosphorylated TrkA (and not the NGF) may provide signalling for axonal outgrowth and survival. The concentration of chemically immobilised NGF has a pronounced affect on the survival of cervical ganglia (SCG) neurons and gradients of immobilised NGF could provide guidance cues to axons and increase the density of axon branching without an internalisation of NGF into neurons [1]. Similarly, aligned and random electrospun scaffolds produced from poly(ethylene glycol) and poly(ε-caprolactone) (PCL–PEG) copolymers were biofunctionalised with NGF via covalent attachment. This results in enhanced neurite elongation and alignment of mesenchymal stem cells (MSCs) compared to non-biofunctionalised scaffolds [77]. Accumulative release of NGF from silk fibroin scaffolds has also been achieved and shown to be bioactive in the presence of PC12 cells [116]. Additionally, studies have examined the effects of presenting combinations of neurotrophins. In this regard NGF and NT-3 gradients, immobilised on poly(2-hydroxyethyl-methacrylate) scaffolds, promoted neurite elongation from DRG neurons, highlighting the potential for such strategies in the spinal cord and peripheral nerve injuries [97].

Furthermore, we have shown that BDNF immobilised on electrospun PCL scaffolds enhanced NSCs proliferation and was superior in supporting cortical neural stem cells and controlling their lineage specification compared with soluble protein used in culture with cells plated on the electropun scaffolds without tethered BDNF [46]. In an in vivo study for the reconstruction of the rat spinal cord, BDNF was engineered with a polypeptide, TKKTLRT, which specifically binds to collagen, allowing sustained release from aligned fibrous collagen scaffolds and overcoming the short half life (ca. 30 min) of BDNF in vivo [117]. Nerve filaments in the vicinity of the injury were greater when BDNF was released from collagen scaffolds compared to the collagen control group after 15 weeks [117]. Saltzman and coworkers fabricated poly(ethylene vinyl acetate) (EVAc) and alginate scaffolds with varying concentrations and continuous release rates of BDNF for implantation into the dorsal hippocampus of rats [118]. This study highlights the importance of dose and the duration of the delivery of trophic factors, as desensitisation and down regulation of neuron plasticity were observed after a continuous delivery of BDNF. Hence, it is critical to optimise the appropriate dose of specific neurotrophins released or presented on scaffolds for the future development of neural tissue engineering.

2.4.1.2 ECM proteins and protein derived sequences

Cellular activity is regulated by interactions with the surrounding ECM. While the ECM is unique for each tissue type, it typically consists of fibronectin (FN), laminin (LM), collagen, tenascin and thrombospondin [119]. Laminin, tenascin and thrombospondin can encourage cell proliferation [100], whilst laminin and collagens modulate the differentiation of neural precursor cells into neurons and can also influence cell adhesion and neurite growth [99, 120]. However, in the brain there are low levels of fibrous proteins, as the ECM is predominantly composed of lecticans, proteoglycans, hyaluronic acid, and tenascins [121]. These play a

crucial role during axonal elongation, neuron differentiation and migration in both the CNS and PNS, and are therefore likely to be important in neural repair. For instance, during development of the spinal cord, various ECM molecules, (including LM, S-laminincollagen and F-spondin) have a tightly regulated temporal and spatial expression pattern to control the migration of growth cones and hence axonal elongation and neuron migration [101].

Many ECM molecules have been used to biofunctionalise synthetic scaffolds to fabricate neural tissue analogues, as an attempt to replicate developmental steps and encourage regeneration in the adult brain. For instance, laminin gradients deposited on the surface of electrospun blends of PCL and PEG increased the number of attached Schwann cells, highlighting the potential to direct neurite outgrowth in PNS injuries [122]. Laminin derived peptides CYIGSR and CSIKVAV have also been attached on lysine capped PLLA [K-(CH2)n-PLLA] films for the culture of mouse cerebellum c17.2 stem cells [123]. Superior cell viability and attachment was observed on the modified film after 5 days compared to the unmodified PLLA films and the tissue culture plate control. Furthermore the morphology of neurons and extent of neurite outgrowth increased on the peptide modified PLLA films. Similarly, hydrogels composed of copolymers of 2-hydroxylethyl methacrylate and 2-aminoethyl methacrylate, poly(HEMA-*co*-AEMA), have been biofunctionalised with two laminin derived oligopeptides, CDPGYIGSR and CQAASIKVAV [124]. Biofunctionalised hydrogels increased both cell number and neurite length of primary chick DRGs compared to the unmodified scaffold [124].

Table 2.4 shows a variety of recent studies that have used different biological molecules for scaffold biofunctionalisation. Additionally, different biofunctionalisation methods, such as covalent and non-covalent crosslinking, co-electrospinning and physical adsorption, is

summarised.

Table 2.4 Biofunctionalised scaffolds for neural tissue engineering

Scaffolds & preparation	Biomolecule/ peptide/ cell addition & biofunctionalisation	In vitro/ in vivo	Results	Ref.
P(MMA-*co*-AA); electrospinning	Collagen type I; EDC/ NHS activation (amino groups)	Rat cortical NSCs	Cell attachment, cell spread, cell viability	[125]
PCL-PEG-DIAMINE; electrospinning	Ferritin-LN (EDC/ NHS activation); external magnetic field (LN attachment/ gradient)	Schwann cells	Cell attachment, cell number	[122]
PCL, PLA; electrospinning	Polypyrrole (PPy); polymerisation	Chick embryo DRGs	Neurite length: aligned Fibres (1723±339 μm)/ randomly orientated fibres (946±164μm)	[126]
PDL; PDL solution coated on coverslips	IKVAV peptide-amphiphile (self-assembly); electric crosslinking	Rat DRGs, DRGn	Cell viability, neuron adhesion, neurite outgrowth	[86]
P(HEMA-*co*-AEMA); copolymerisation	CDPGYIGSR/ CQAASIKVAV (LN-derived oligopeptides); covalent crosslinking (sulfo-SMCC)	Primary chick DRGs	Cell adhesion, neurite outgrowth	[124]
Fibrin; polymerisation	Bidomain peptide (Factor XIIIa)/ heparin/ NT-3, PDGF; covalent/ noncovalent crosslinking	RW4 mouse embryonic SCs	Cell differentiation (neural progenitors, neurons, oligodendrocytes)	[127]
Silk fibroin; air-dried (film), freeze-dried (tube)	NGF; air dried, freeze dry (-20, -196 ℃)	PC12 cells	Cell differentiation,	[116]
PDLLA; frozen (liquid nitrogen), freeze-dried	BDNF; dissolve in polymer solution	Female Fischer rats	Cell survival/ angiogenesis, no much axonal regeneration	[128]
PLGA; injection molding	FITC-D, primary SCs; dissolve in polymer solution	Female Sprague-Dawley rats	Axon regeneration	[129]
Poly(Dex-MA-*co*-AEMA); copolymerisation	CRGDS, CDPGYIGSR/ CQAASIKVAV; physical adsorption	Chick embryos DRGs	Cell adhesion, neurite outgrowth, cell penetration	[98]
PLGA/ PLLA; salt-leaching process	RA, NGF, NT-3; medium supplements	hESC	Cell number, maturity, cell differentiation (nestin, βIII-tubulin)	[107]
PLLA; electrospinning	LN; covalent crosslinking, physical adsorption, co-electrospinning	Rat PC12 cells	Cell viability, neurite outgrowth, axon extension	[130]
PLA film; hot shrinking machine	AG73-G_3- $(PPG)_5$; hydrophobic adsorption	PC12 cells	Neurite outgrowth	[131]
Lysine-capped PLLA/ PLLA; drop-cast	CYIGSR/CSIKVAV; covalent crosslinking (sulfo-SMCC)	Mouse cerebellum C17.2 SCs	Cell viability, neurite outgrowth	[123]
RADA16-I peptide nanofibres; self-assembly	Schwann cells/ NPCs	Female rats	Host cell migration, blood vessel growth, axon growth	[91]
RADA16-I peptide nanofibres;		Adult NSCs	Cell proliferation	[132]

self-assembly				
PEG–heparin hybrid gel; covalent crosslinking	RGD peptide/ FGF-2; covalent (RGD)/ noncovalent (FGF-2) crosslinking	Primary nerve cells, NSCs, Wistar rats	NSCs differentiation, propagation, axon dendrite outgrowth	[133]
PSF NGCs/ agarose hydrogels	LN-1/ NGF; covalent crosslinking (photochemical conjugation technique)	Adult male rats	Bridging peripheral nerve gaps (20mm)	[134]
Collagen type I /gelatin/ nano-silver; freeze-dried/ crosslinking (Genipin)	LN; adsorption/ freeze-dry	Male rabbits	Nerve regeneration	[135]

Abbreviations: Poly(methyl methacrylate-*co*-acrylic acid) [P(MMA-*co*-AA)], laminin (LN), N-(3-dimethylaminopropyl)-N-ethylcarbodiimide hydrochloride /N- Hydroxysuccinimide (EDC/NHS), polycaprolactone- polyethylene glycol- diamine (PCL-PEG-DIAMINE), copolymer 2-hydroxylethyl methacrylate/ 2-aminoethyl methacrylate [P(HEMA-*co*-AEMA)], sulfo-(N-maleimidomethyl) cyclohexane-1 -carboxylate (sulfo-SMCC), platelet-derived growth factor (PDGF), poly(D,L-lactic acid) (PDLLA/PLA), fluorescein isothyocyanate-dextran (FITC-D), copolymer methacrylated dextran (Dex-MA)/ aminoethyl methacrylate (AEMA) [poly(Dex-MA-*co*-AEMA)], human embryonic stem cells (hESC), retinoic acid (RA), hydroxyapatite (HAp), Cys-Tyr-Ile-Gly-Ser-Arg (CYIGSR), Cys-Ser-Ile-Lys-Val-Ala-Val (CSIKVAV), poly(ethylene glycols) (PEG), basic fibroblast growth factor (FGF-2), polysulfone (PSF), nerve guidance channels (NGCs)

2.5 SCAFFOLDS THAT PROMOTE REPAIR

In the preceding pages we have outlined a number of scaffolds, their functionalisation and the associated affect on neural stem cells and their derivatives; predominantly in an in vitro setting. This knowledge is instrumental in understanding the potential of neural tissue engineering scaffolds for neural repair in vivo. Below, we briefly outline a number of neural injuries, current therapies, limitations in current therapies and finally discuss the potential of scaffolds to improve repair.

2.5.1 Neural injuries and the common difficulty in current therapy

Within the CNS and PNS, injury can be classified as acute (e.g. stroke, traumatic brain injury (TBI), spinal cord injury (SCI) and peripheral nerve injury), or chronic injuries (for example neurodegenerative disease including Parkinson's disease (PD) and Huntington Disease). A common feature in all neural injuries is the loss of neurons either due to the primary impact or the subsequent secondary injury. Additionally the loss of supporting neural cells, such as oligodendrocytes and astrocytes, can also occur. Such damage in the CNS is permanent due to a limited ability to regenerate lost neural cells and a failure to restore normal physiological functions [136, 137]. Although there are self repair processes within the PNS, self-restoration depends on the segment of the injured peripheral nerve, intensity of injury, lesion distance and, where applicable, timing of intervention/surgery [138, 139]. Damage to the CNS (and instances of PNS injury) can result in motor, sensory, cognitive and/or autonomic dysfunction, resulting in a variety of disabilities in patients.

Evidently there are various treatments for patients suffering from neural injuries, depending on the type of injury. Unfortunately many of these are limited in their efficacy either from the outset or with time (in the context of progressive neurodegenerative disorders). For example, many neurodegenerative diseases, result in the loss of select cell populations and consequent neurotransmission [140]. In this regard, therapies often focus on restoring this neurochemical transmission through the administration of pharmacological agents that replace the neurotransmitter, hyper-stimulate receptors or slow the degradation of residual transmitter in the brain. Commonly these drugs are reliant on a residual population of neurons within the brain, cells that are progressively degenerating and therefore treatments wane in efficacy with

time. Furthermore, in some instances the side effects from these pharmacological drugs can eventually be more debilitating than the disease itself. For example, L-DOPA (the precursor in dopamine synthesis) is the most widely used drug in the treatment of PD that aims to restore dopamine transmission in the brain [141]. However the majority of patients on the drug develop unwanted excessive movements (dyskinesias) typically within 5 years of treatment [142]. Furthermore levodopa is reliant on surviving dopamine neurons in the brain to convert the precursor molecule to dopamine, a population of cells that are progressively degenerating.

Alternative pharmacotherapies aim to slow the neurodegeneration by reducing toxic molecules from the brain. For example in motor neuron disease too much of the neurotransmitter glutamate is cytotoxic to motor neurons [143]. Drugs that block glutamate release, such as amantadine, have been shown to modestly slow progression however also present negative side effects [142]. Alternative efforts to slow disease progression have investigated the possibility of infusing neurotrophins into the site of cell loss, however such approaches are commonly reliant on the use of infusion cannula and pumps that can be cumbersome and associated with additional tissue damage at the site of implantation [140].

Whilst trophic factors have been shown to slow disease progression in animal models of neural injuries, it is often difficult to administer these compounds long term and in a regulated releasing manor. Therefore there is a need for alternative approaches to protect remaining cells, restore connectivity and continuously deliver controllable amount of trophic factors for long term with minimal invasion.

Stroke presents another neural injury that could benefit from the utilisation of scaffolds. In stroke there is a ‘core’ area of severe ischemia, in which necrosis of neurons occurs, as a result of altered blood flow in the brain. Surrounding the core is the ‘ischemic penumbra’; an area also of reduced blood flow yet still viable cerebral tissue [144]. If this area is not treated within hours it results in cavity formation through loss of tissue and there is no current therapy to deal with this. Recently, plasma polymerised allylamine treated biodegradable poly(lactic-*co*-glycolic acid) polymer particles, which can completely fill the resultant cavity, were incorporated with neural stem cells and used as scaffolds for brain repair. It was demonstrated that the scaffolds integrated well within the brain and formed primitive neural tissue to fill the void [145]. Therefore, if a scaffold that mimics morphological features of the brain parenchyma and releases neurotrophins with appropriate timing were implanted within the cavity, it may be possible to promote endogenous repair through promoting angiongenesis, cell survival and synapsogenesis.

Whilst we have highlighted a couple examples of treatments for neural injuries we direct the readers to the following reviews for an overview of some of the current therapies for neurodegenerative diseases [141, 142, 146, 147]. In all, current therapies for neural injuries are limited. They fail to address the primary cell loss and have little effect on protecting remaining cells, consequently offering no long term symptomatic relief or disease modification.

In contrast to existing therapies, cell transplantation; either to deliver trophins and/or deliver replacement cells provides hope for many neural injury sufferers. To date, PD has received the most significant attention for cell replacement therapy (CRT), due to the localised nature of cell loss and the fact that it is predominantly one cell type (dopamine neurons) that are

required to restore motor function in patients [148]. However, Huntington's disease (HD), motor neuron disease (MND) and stroke are also examined for the plausibility of cell replacement therapies (CRT), both in the laboratory and clinical trials. CRT involves the transplantation of new neurons (e.g. dopamine neurons) to replace those lost as a consequence of the disease [149]. These cells are commonly isolated from fetal tissue, however there is increasing efforts to obtain transplantable cells from pluripotent stem cell sources [150]. Excitingly, proof of principle for CRT in PD has been achieved using fetal tissue enriched with dopamine neurons. These grafts were capable of partially reinnervating the brain, releasing dopamine and inducing functional recovery for up to 10 years in some patients [149]. However more detailed studies have revealed that CRT technologies require further refinement before they can be employed as mainstream therapies [151]. Some of the major caveats of CRT are limited tissue availability, reliability, poor cell survival and insufficient graft innervation in the host brain [152]. Key efforts over the past 30 years have focused on promoting the survival and appropriate integration of transplanted cells, namely for PD, but more recently for other neural injuries.

Combining cell replacement therapy with the delivery of trophins could provide a more conducive cellular microenvironment for repair. In addition to the reliance on cell therapy, this could be enhanced through the use of tissue engineering scaffolds, whereby replacement cells can be both physically supported by the scaffold as well as exposed to the appropriate biological molecules that encourage the survival, differentiation and integration.

2.6 THE POTENTIAL OF SCAFFOLDS IN NEURAL TISSUE ENGINEERING

We have illustrated a number of limitations of the current therapies for neural injuries. The future of CNS repair relies in efficiently protecting remaining neurons and glia cells, replacing lost neurons and/or regulating inflammatory responses. It is proposed that scaffolds may significantly improve neural repair in this regard, through the physical and trophic support of endogenous and/or newly transplanted cells, as well as the regulation of scar tissue.

2.6.1 Promoting the survival and connectivity of remaining cells through physical and trophic support

Polymeric scaffolds can act as a physical support to the remaining cells to promote survival, proliferation and restore the connections between cells at the injured site. For example, implantation of electrospun PCL scaffolds with random orientation in the brain of rats resulted in endogenous neurite penetration of the scaffolds after 60 days [38]. Inverted colloidal crystal (ICC) scaffolds, modified with two peptides and combined with bone marrow stromal cells (BMSCs), has also been implanted into the injured spinal cord of rats, neuron survival was promoted compared to BMSCs transplants alone [153]. Furthermore, scaffolds can provide a chemical support by acting as a delivery system for trophic factors to dominate or manipulate cell behaviour thereby promoting repair. A key advantage of using scaffolds as a ‘delivery system’ is that it can be provided in a controlled spatial and temporal manner without the need for current invasive approaches, such as implantation of infusion probes. [142]. In many instances this can also have the concomitant influence of delivering growth factors in a superior manner whilst also provided a synthetic ECM to better support

residual endogenous and/or transplanted cells [46]. The delivered trophins can be chosen to encourage cell proliferation and integration or suppress inhibitory molecules that prevent or restrict axonal outgrowth and connectivity. For example, in amyotrophic lateral sclerosis, where CNTF has been shown to reduce motor neuron death, implantation of polymer capsules that encapsulated fetal cells were found to release CNTF demonstrating the clinic relevance of tissue engineering scaffolds [154]. This encapsulated cell based therapy has been shown as a potential method to overcome many of the side effects that arise from the systemic delivery of growth factors. Hence, engineered scaffolds can encourage endogenous neural repair by providing physical support for remaining neural cells and axons, as well as trophic support to stimulate cell survival and connectivity.

Tissue engineering scaffolds could also be employed to recruit endogenous stem cells for repair following neural injury. Within the adult brain there are two well described neurogenic niches; the subventricular zone (SVZ) and the dentate gyrus (DG) of the hippocampus [155]. These areas generate a constant pool of stem cells. Moreover, following injury these niches have been shown to up-regulate stem cell proliferation and migration into injury sites, predominantly into the cortex and striatum. In particular the work of Arvidsson et al. showed in an animal model of stroke that new neurons in the SVZ were redirected into the injury site, differentiated and thereby promoted self-repair. [155].

According to more recent research, there are potentially other stem cell niches in the adult brain however their existence remain a topic of debate [156, 157]. Regardless, neural repair as a result of these residual stem cells is insufficient to negate the degenerative processes seen in many neurodegenerative diseases or acute neural injuries. Therefore ways to boost the production of stem cells within these niches, as well as the migration and differentiation of

cells exiting the niche could see improved self repair process after neural injuries. It is well established that various mitogens including leukemia inhibitory factor, EGF and fibroblast growth factor-2, promote the proliferation of stem cells. Further, morphogens, such as TGF-3β promote the migration of neuroblasts within the brain. Hence, the potential of scaffolds to physically support the niche and provide additional mitogens and morphogens could lead to enhanced stem cell turn over, migration and integration into injury sites.

2.6.2 Support the integration of newly transplanted cells

Tissue engineering scaffolds may also be employed to support transplanted cells. Similar to promoting survival and integration of residual cells at the injury site, scaffolds can provide physical and chemical support to transplanted cells. Transplanted cells require structural support to survive and form appropriate connections within neural networks. In support, Park et al. transplanted neural stem cells together with poly(glycolic acid) (PGA) scaffolds in an animal model of hypoxia-ischemia (stroke). The results showed the ability of transplanted cells to repopulation the lesion site, undergo cellular differentiation and reconstruction of tissue connections [158]. Importantly, previous CRT studies in Parkinsonian rodents have also demonstrated the benefit of residual cell for graft integration and survival [159]. Here, the residual host fibres provided scaffolding for the axons of newly grafted neurons to climb and connect with target tissues, thereby also prompting survival. In light of this knowledge, improved scaffolding, provided by tissue engineered scaffolds, should enhance survival and integration of transplanted cells. Recently, neural stem/progenitor cells (NSCPs) have been combined with chitosan guidance channels and implanted into the injured spinal cord of adult rats (a compression injury). Combining the transplantation of cells with chitosan channels enhanced the survival of the NSCPs compared to when the cells were injected into lesion cavity alone [160]. While this is a significant discovery further optimisation of the scaffold

will be required, as there was no significant difference in functional recovery between the groups. In this regard, chemical support from neural tissue engineering scaffolds will be required to enhance the maintenance of transplanted cells, whilst allowing them to integrate within the parenchyma and undertake reparative processes, synaptogensis etc.

2.6.3 Controlling inflammation, scar formation and secondary injury

Another major consideration in neural repair is the role of inflammation. Following neural injury there are two phases of glial cell proliferation; an early phase to remove dead cells, and late phase for the delivery of trophins to promote repair. Many studies have shown the detrimental influence of microglia activation on the survival of neurons [161] and even axonal sprouting in the brain parenchyma that results following injury [162, 163]. The administration of antibotics such as minocycline, which is known to inhibit microglia activation, has been reported to increase neurogenesis in vivo [161]. However, the role of microglia during adult neurogenesis has proven to be much more complex [164] with neurogenesis depending on the degree of microglia activation, as in some instances microglia have been shown to play a positive role through the secretion of neurotrophic molecules [165, 166]. Additionally, they can also support progenitor survival, proliferation, differentiation and migration [164].

Similarly, astrocytes are activated during the inflammatory cascade. While astrocytes play a cytotrophic role in the healthy brain, defending against tissue insult and clearing dead and damaged cells to return to its homeostatic state following injury, they can also become reactive [167] and are detrimental, as seen in MND [38]. Following injury astrocytes increase the production of cytoskeletal filaments, which in the later stages can result in the formation

of a scar (a dense fibrous collagenous membrane) that physically and biochemically impede axonal regeneration within the parenchyma.

In the later stages of regeneration microglia and astrocytes contribute cytotrophically providing nutrients such as glucose [38]. Therefore the activation of microglia and astrocytes during the inflammatory cascade cannot be considered pro or anitneurogenic. The role of microglia and astrocytes in inflammation must be further investigated, specifically the timing and level (mild verses chronic) of the activation, to gain an understanding of the influences that determine whether inflammation will play a defensive or trophic role towards neurogenesis and neural repair. It will be essential to harness the trophic abilities or glia cells activated during the cascade of inflammatory events to encourage the survival of neuronal progenitor cells and associated neurogenesis and recovery in the adult.

2.6.4 Secondary injury

In instances of acute neural injury, the initial tissue insult is generally followed by a cascade of impairments, referred to as secondary injury, which is the main cause of subsequent neuron death [146]. For example, in TBI, secondary injuries include cerebral oedema or brain swelling, resulting from the increased accumulation of vasogenic fluid in the brain that subsequently increases the intracerebral pressure and decreases cerebral pressure [146, 168, 169]. This leads to cerebral ischaemia and hypoxaemia. In addition, because of insufficiencies in cerebral blood flow and oxygen concentration, the destruction of healthy brain tissue within the parenchyma results in cerebral ischemia, progressive neurodegeneration and in some instances mortality [146, 168, 169].

Another example is the secondary injury in spinal cord injury. Here, the injured segment of

the spinal cord progresses to a secondary stage as a result of inflammation, disrupted vascular regulations, lipid peroxidation, excitotoxicity, disturbances of homeostatic electrolytes, necrosis and apoptosis [170]. SCI caused by mechanical impact can also destroy the surrounding microvascular environment and local vascular autoregulation inducing petechial hemorrhage, intravascular thrombosis and oedema. The development of such symptoms can also lead to hypoperfusion and ischaemia around the injuries [147]. In turn hypoperfusion leads to lipid peroxidation, another pathological imbalance, which progressively causes the disruption of mitochondrial respiration, metabolism and cell development [171]. The cascade of secondary injury also induces progressive neuronal and glial cell death including necrosis and apoptosis, which seriously contributes to the dysfunction of motor and sensory neurons [172]. Moreover the apoptotic death of oligodendrocytes and the following demyelination of white matter decrease the insulation and conduction of neurons [173-177].

Neural tissue engineering scaffolds potentially have an important role in the regulation of inflammatory responses following neural injury. First, implanted scaffolds must be biocompatible without causing further inflammation. In this regard, Nisbet et al. has shown that certain scaffolds can in fact dampen the inflammatory response, and thereby support repair. In this study they demonstrated that activated astrocytes and microglia cells remained at homeostatic level after implantation of xyloglucan hydrogel in the caudate putamen of rats [27]. Moreover, within this study neurite infiltration corresponded to astrocytes migration inside the implanted xyloglucan hydrogel (modified with PDL); with higher PDL concentration resulting in more neurite penetration [27].

Chemically, scaffolds may be engineered to deliver biological molecules to suppress inflammation, reduce secondary injuries and thereby promote repair. For example,

chondroitinases, enzymes that cleave proteoglycans within scar tissue, have been shown to promote axonal growth and neural repair in animal models of spinal cord injury [178]. Such proteins could be biofunctionalised onto scaffolds prior to implantation, thereby promoting axon growth beyond the typical glial scar. Additionally, anti-inflammatory factors could be delivered via scaffolds post injury to attempt reduce inflammation (astrocytosis) and hence encourage neural regeneration and reconstruction.

2.7 PERSPECTIVES AND FUTURE DIRECTIONS

Various biological molecules, such as neurotrophins, ECM proteins and protein derived sequences have been widely used in conjunction with neural tissue engineering scaffolds in vitro and in vivo. However, a greater understanding of the complex interactions between the target tissue and biofunctionalised scaffolds is required, as well as an understanding of integrin interactions and the associated intracellular signalling, before scaffolds can be engineered for the purpose of neural tissue repair in a clinical setting.

Within the nervous system, the cellular microenvironment varies significantly depending on location of the injury, the time after injury and signalling cascades present at any given time. However, to date most research has been limited to investigating the influence of a single signalling molecule in isolation in vitro. Therefore, to further develop the field it is essential to explore the validity of presenting multiple biological molecules with precise timing during the regeneration phases, to biochemically recapitulate some of the events that occur during neural development to encourage repair in the adult. In this regard, biofunctionalised scaffolds could, for example, promote repair of neural tissue by preventing further cytotoxic damage at the same time as protecting remaining cells and boost the endogenous repair from

stem cell niches.

The combination of cells/stem cells with biofunctionalised scaffolds offers exciting prospects for the future. It may be possible to regulate the survival and integration of host or graft derived neural cells through scaffold support. In this regard, scaffolds may provide a more chemically and physically optimised milieu to support regeneration. Furthermore, these scaffolds can be 'custom designed' to meet the needs of each neural injury. As such, some injuries will benefit from an improved physical environment in which scaffolds provide a framework to promote axonal growth whilst other injuries will benefit from the long term delivery trophic cues to promote survival and/or influence cellular differentiation. In all, the field of engineered scaffolds for neural repair in vivo remains in its infancy. The coming decades will bare witness to exciting developments in the merging of bioengineering and cell therapy for the treatment of neural injuries.

2.8 CONCLUDING REMARKS

Bioengineered scaffolds offer exciting prospects for the future of neural repair. In order to promote regeneration it will be essential to fabricate scaffolds that provide physical support, promoting cell attachment, survival and encouraging neurite/axon growth. In many instances the morphology and physical properties can also be ultilised to improve cell scaffold interactions. Furthermore, appropriate scaffolds will most likely involve the incorporation of appropriate biological cue/s to encourage cell survival, migration, proliferation differentiation and/or axonal outgrowth, of endogenous or newly implanted cells. The importance of biofunctionalisation is highlighted in neural development, where mitogens, morphogens and neurotrophins are involved and synchronised to orchestrate the maturation of the brain and its

precise connectivity. In this regard, it is important to acknowledge that the appropriate biomolecule or combinations thereof, will need to be delivered in an appropriate temporal and spatial manner. Scaffolds provide a novel approach to present such cues in a highly orchestrated manner.

In the future many questions remain to be answered in order to gain a full understanding, and ability to exploit the benefits, of bioengineered scaffolds for neual repair. For instance; what is the most suitable combination of biological cues for injured neural tissue? How should the release rate and presentation of biological cues be exploited to satisfy the needs for neural regeneration? What is the nature of the interaction between the scaffold and cells of interest? These questions, along with many other fundamental and critical biological questions must be addressed in order to develop a scaffold that could potentially be employed in a clinical setting.

2.9 ACKNOWLEDGMENTS

D. N. is grateful to the Australian Research Council (A. R. C.) for an Australian Postdoctoral Fellowship. We also acknowledge the ARC Discovery Project Grant DP0985433 for funding. We also acknowledge the Bethlehem Griffith Research Foundation grant awarded to D. N. and C. P.

2.10 REFERENCES

1. Yu LMY, Miller FD, Shoichet MS. The use of immobilized neurotrophins to support neuron survival and guide nerve fiber growth in compartmentalized chambers. Biomaterials 2010;31(27):6987-6999.

2. Willerth SM, Sakiyama-Elbert SE. Approaches to neural tissue engineering using scaffolds for drug delivery. Advanced Drug Delivery Reviews 2007;59(4-5):325-338.

3. Leipzig ND, Wylie RG, Kim H, Shoichet MS. Differentiation of neural stem cells in three-dimensional growth factor-immobilized chitosan hydrogel scaffolds. Biomaterials 2011;32(1):57-64.

4. Willerth SM, Arendas KJ, Gottlieb DI, Sakiyama-Elbert SE. Optimization of fibrin scaffolds for differentiation of murine embryonic stem cells into neural lineage cells. Biomaterials 2006;27(36):5990-6003.

5. Yao L, O'Brien N, Windebank A, Pandit A. Orienting Neurite Growth in Electrospun Fibrous Neural Conduits. J Biomed Mater Res Part B 2009 Aug;90B(2):483-491.

6. Jha BS, Colello RJ, Bowman JR, Sell SA, Lee KD, Bigbee JW, et al. Two pole air gap electrospinning: Fabrication of highly aligned, three-dimensional scaffolds for nerve reconstruction. Acta Biomaterialia 2011;7(1):203-215.

7. Stephane W, Van Diep D, Norma S, Jean de V, Araceli E-J. Prevention of gliotic scar formation by NeuroGel allows partial endogenous repair of transected cat spinal cord. Journal of Neuroscience Research 2004;75(2):262-272.

8. Piantino J, Burdick JA, Goldberg D, Langer R, Benowitz LI. An injectable, biodegradable hydrogel for trophic factor delivery enhances axonal rewiring and improves performance after spinal cord injury. Experimental Neurology 2006;201(2):359-367.

9. Li GN, Hoffman-Kim D. Tissue-Engineered Platforms of Axon Guidance. Tissue Engineering Part B: Reviews 2008;14(1):33-51.

10. Murakami K, Aoki H, Nakamura S, Nakamura S-i, Takikawa M, Hanzawa M, et al. Hydrogel blends of chitin/chitosan, fucoidan and alginate as healing-impaired wound dressings. Biomaterials 2010;31(1):83-90.

11. Wei L, Cai C, Lin J, Chen T. Dual-drug delivery system based on hydrogel/micelle composites. Biomaterials 2009;30(13):2606-2613.

12. Karoubi G, Ormiston ML, Stewart DJ, Courtman DW. Single-cell hydrogel

encapsulation for enhanced survival of human marrow stromal cells. Biomaterials 2009;30(29):5445-5455.

13. Liu K, Li Y, Xu F, Zuo Y, Zhang L, Wang H, et al. Graphite/poly (vinyl alcohol) hydrogel composite as porous ringy skirt for artificial cornea. Materials Science and Engineering: C 2009;29(1):261-266.

14. Nicodemus GD, Bryant SJ. Cell Encapsulation in Biodegradable Hydrogels for Tissue Engineering Applications. Tissue Engineering Part B: Reviews 2008;14(2):149-165.

15. Drury JL, Mooney DJ. Hydrogels for tissue engineering: scaffold design variables and applications. Biomaterials 2003;24(24):4337-4351.

16. Biancamaria B. Hydrogels for tissue engineering and delivery of tissue-inducing substances. Journal of Pharmaceutical Sciences 2007;96(9):2197-2223.

17. Xiaojun Y, Ravi VB. Dorsal root ganglia neurite extension is inhibited by mechanical and chondroitin sulfate-rich interfaces. Journal of Neuroscience Research 2001;66(2):303-310.

18. Nisbet RD, Kylie EC, Malcolm KH, David IF, John SF. Neural tissue engineering of the CNS using hydrogels. Journal of Biomedical Materials Research Part B: Applied Biomaterials 2008;87B(1):251-263.

19. Straley KS, Foo CWP, Heilshorn SC. Biomaterial Design Strategies for the Treatment of Spinal Cord Injuries. Journal of Neurotrauma 2006;27(1):1-19.

20. Tian WM, Hou SP, Ma J, Zhang CL, Xu QY, Lee IS, et al. Hyaluronic Acid-poly-D-Lysine-Based Three-Dimensional Hydrogel for Traumatic Brain Injury. Tissue Engineering 2005;11(3-4):513-525.

21. Nisbet DR, Moses D, Gengenbach TR, Forsythe JS, Finkelstein DI, Horne MK. Enhancing neurite outgrowth from primary neurones and neural stem cells using thermoresponsive hydrogel scaffolds for the repair of spinal cord injury. Journal of Biomedical Materials Research Part A 2009;89A(1):24-35.

22. Horn EM, Beaumont M, Shu XZ, Harvey A, Prestwich GD, Horn KM, et al. Influence of cross-linked hyaluronic acid hydrogels on neurite outgrowth and recovery from spinal cord injury. Journal of Neurosurgery: Spine 2007;6(2):133-140.

23. Newton D, Mahajan R, Ayres C, Bowman JR, Bowlin GL, Simpson DG. Regulation of material properties in electrospun scaffolds: Role of cross-linking and fiber tertiary structure. Acta Biomaterialia 2009;5(1):518-529.

24. Leipzig ND, Shoichet MS. The effect of substrate stiffness on adult neural stem cell behavior. Biomaterials 2009;30(36):6867-6878.

25. Dillon GP, Xiaojun Y, Sridharan A, Ranieri JP, Bellamkonda RV. The influence of physical structure and charge on neurite extension in a 3D hydrogel scaffold Journal of Biomaterials Science, Polymer Edition 1998;9:1049-1069.

26. Crompton KE, Goud JD, Bellamkonda RV, Gengenbach TR, Finkelstein DI, Horne MK, et al. Polylysine-functionalised thermoresponsive chitosan hydrogel for neural tissue engineering. Biomaterials 2007;28(3):441-449.

27. Nisbet DR, Rodda AE, Horne MK, Forsythe JS, Finkelstein DI. Implantation of Functionalized Thermally Gelling Xyloglucan Hydrogel Within the Brain: Associated Neurite Infiltration and Inflammatory Response. Tissue Engineering Part A 2010;16(9):2833-2842.

28. Duconseille E, Woerly S, Kelche C, Will B, Cassel JC. Polymeric hydrogels placed into a fimbria-fornix lesion cavity promote fiber (re)growth: a morphological study in the rat. Restor Neurol Neurosci 1998 Dec;13(3-4):193-203.

29. Hynd MR, Frampton JP, Dowell-Mesfin N, Turner JN, Shain W. Directed cell growth on protein-functionalized hydrogel surfaces. Journal of Neuroscience Methods 2007;162(1-2):255-263.

30. Thonhoff JR, Lou DI, Jordan PM, Zhao X, Wu P. Compatibility of human fetal neural stem cells with hydrogel biomaterials in vitro. Brain Research 2008;1187:42-51.

31. Xu T, Molnar P, Gregory C, Das M, Boland T, Hickman JJ. Electrophysiological characterization of embryonic hippocampal neurons cultured in a 3D collagen hydrogel. Biomaterials 2009;30(26):4377-4383.

32. Tsai EC, Dalton PD, Shoichet MS, Tator CH. Matrix inclusion within synthetic hydrogel guidance channels improves specific supraspinal and local axonal regeneration after complete spinal cord transection. Biomaterials 2006;27(3):519-533.

33. Kunze A, Bertsch A, Giugliano M, Renaud P. Microfluidic hydrogel layers with multiple gradients to stimulate and perfuse three-dimensional neuronal cell cultures. Procedia Chemistry 2009;1(1):369-372.

34. Nakaji-Hirabayashi T, Kato K, Iwata H. Hyaluronic acid hydrogel loaded with genetically-engineered brain-derived neurotrophic factor as a neural cell carrier. Biomaterials 2009;30(27):4581-4589.

35. Woerly S, Pinet E, de Robertis L, Van Diep D, Bousmina M. Spinal cord repair with PHPMA hydrogel containing RGD peptides (NeuroGel(TM)). Biomaterials 2001;22(10):1095-1111.

36. Baumann MD, Kang CE, Tator CH, Shoichet MS. Intrathecal delivery of a polymeric nanocomposite hydrogel after spinal cord injury. Biomaterials 2010;31(30):7631-7639.

37. Nisbet DR, Yu LMY, Zahir T, Forsythe JS, Shoichet MS. Characterization of neural stem cells on electrospun poly(ε-caprolactone) submicron scaffolds: evaluating their potential in neural tissue engineering. J Biomater Sci-Polym Ed 2008;19(5):623-634.

38. Nisbet DR, Rodda AE, Horne MK, Forsythe JS, Finkelstein DI. Neurite infiltration and cellular response to electrospun polycaprolactone scaffolds implanted into the brain. Biomaterials 2009;30(27):4573-4580.

39. Nisbet DR, Pattanawong S, Ritchie NE, Shen W, Finkelstein DI, Horne MK, et al. Interaction of embryonic cortical neurons on nanofibrous scaffolds for neural tissue engineering. J Neural Eng 2007;4:35-41.

40. Nisbet DR, Forsythe JS, Shen W, Finkelstein DI, Horne MK. A Review of the Cellular Response on Electrospun Nanofibers for Tissue Engineering. J Biomater Appl 2009 Jul;24(1):7-29.

41. Kyung Hwa H, Jong Lyoul P, In Hwan S, Ji Ho Y, Tae Jin K. Preparation of antimicrobial poly(vinyl alcohol) nanofibers containing silver nanoparticles. Journal of Polymer Science Part B: Polymer Physics 2006;44(17):2468-2474.

42. Hsu F-Y, Hung Y-S, Liou H-M, Shen C-H. Electrospun hyaluronate-collagen nanofibrous matrix and the effects of varying the concentration of hyaluronate on the characteristics of foreskin fibroblast cells. Acta Biomaterialia 2010;6(6):2140-2147.

43. Vargas EAT, do Vale Baracho NC, de Brito J, de Queiroz AAA. Hyperbranched polyglycerol electrospun nanofibers for wound dressing applications. Acta Biomaterialia 2010;6(3):1069-1078.

44. Yang L, Fitie Carel FC, van der Werf KO, Bennink ML, Dijkstra PJ, Feijen J. Mechanical properties of single electrospun collagen type I fibers. Biomaterials 2008;29(8):955-962.

45. Zhang X, Thomas V, Xu Y, Bellis SL, Vohra YK. An in vitro regenerated functional human endothelium on a nanofibrous electrospun scaffold. Biomaterials 2010;31(15):4376-4381.

46. Horne MK, Nisbet DR, Forsythe JS, Parish CL. Three-Dimensional Nanofibrous Scaffolds Incorporating Immobilized BDNF Promote Proliferation and Differentiation of Cortical Neural Stem Cells. Stem Cells Development 2010;19(6):843-852.

47. Vaz CM, van Tuijl S, Bouten CVC, Baaijens FPT. Design of scaffolds for blood vessel tissue engineering using a multi-layering electrospinning technique. Acta Biomaterialia 2005;1(5):575-582.

48. Huang Z-M, Zhang YZ, Kotaki M, Ramakrishna S. A review on polymer nanofibers

by electrospinning and their applications in nanocomposites. Composites Science and Technology 2003;63(15):2223-2253.

49. Pan H, Li L, Hu L, Cui X. Continuous aligned polymer fibers produced by a modified electrospinning method. Polymer 2006;47(14):4901-4904.

50. Thompson CJ, Chase GG, Yarin AL, Reneker DH. Effects of parameters on nanofiber diameter determined from electrospinning model. Polymer 2007;48(23):6913-6922.

51. Eda G, Liu J, Shivkumar S. Solvent effects on jet evolution during electrospinning of semi-dilute polystyrene solutions. European Polymer Journal 2007;43(4):1154-1167.

52. Murugan R, Ramakrishna S. Design Strategies of Tissue Engineering Scaffolds with Controlled Fiber Orientation. Tissue Engineering 2007;13(8):1845-1866.

53. Murugan R, Ramakrishna S. nano-features scaffolds for tissue engineering: a review of spinning methodologies. tissue engineering 2006;12:435-446.

54. Sell S, Barnes C, Matthew S, McClure M, Madurantakam P, Grant J, et al. Review extracellular matrix regenerated: tissue engineering via electrospun biomimetic nanofibers. polym Int 2007;56:1349-1360.

55. Theron SA, Zussman E, Yarin AL. Experimental investigation of the governing parameters in the electrospinning of polymer solutions. Polymer 2004;45(6):2017-2030.

56. Chronakis IS. Novel nanocomposites and nanoceramics based on polymer nanofibers using electrospinning process--A review. Journal of Materials Processing Technology 2005;167(2-3):283-293.

57. Sill TJ, von Recum HA. Electrospinning: Applications in drug delivery and tissue engineering. Biomaterials 2008;29(13):1989-2006.

58. Martins AR, R.L.; Neves, N.M. Electrospinning: processing technique for tissue engineering scaffolding International Materials Reviews 2008;53(5):257-274.

59. Baker BM, Handorf AM, Ionescu LC, Li WJ, Mauck RL. New directions in nanofibrous scaffolds for soft tissue engineering and regeneration. Expert Rev Med Devices 2009 Sep;6(5):515-532.

60. Wang Y, Yong T, Ramakrishna S. nanofibers and their influence on cells for tissue regeneration. Aust J Chem 2005;58:704-712.

61. Seidlits SK, Lee JY, Schmidt CE. Nanostructured scaffolds for neural applications. Nanomedicine 2008 Apr;3(2):183-199.

62. Prabhakaran MP, Venugopal JR, Chyan TT, Hai LB, Chan CK, Lim AY, et al. Electrospun Biocomposite Nanofibrous Scaffolds for Neural Tissue Engineering. Tissue Engineering Part A 2008;14(11):1787-1797.

63. Venugopal J, Prabhakaran MP, Low S, Choon AT, Zhang YZ, Deepika G, et al. Nanotechnology for nanomedicine and delivery of drugs. Curr Pharm Design 2008 Aug;14(22):2184-2200.

64. Wang HB, Mullins ME, Cregg JM, Hurtado A, Oudega M, Trombley MT, et al. Creation of highly aligned electrospun poly-L-lactic acid fibers for nerve regeneration applications. J Neural Eng 2009 Feb;6(1):15.

65. Yang F, Murugan R, Wang S, Ramakrishna S. Electrospinning of nano/micro scale poly(L-lactic acid) aligned fibers and their potential in neural tissue engineering. Biomaterials 2005;26(15):2603-2610.

66. Meng ZX, Wang YS, Ma C, Zheng W, Li L, Zheng YF. Electrospinning of PLGA/gelatin randomly-oriented and aligned nanofibers as potential scaffold in tissue engineering. Materials Science and Engineering: C 2010;30(8):1204-1210.

67. Yang F, Murugan R, Ramakrishna S, Wang X, Ma YX, Wang S. Fabrication of nano-structured porous PLLA scaffold intended for nerve tissue engineering. Biomaterials 2004;25(10):1891-1900.

68. Chew SY, Mi R, Hoke A, Leong KW. The effect of the alignment of electrospun fibrous scaffolds on Schwann cell maturation. Biomaterials 2008;29(6):653-661.

69. Gupta D, Venugopal J, Prabhakaran MP, Dev VRG, Low S, Choon AT, et al. Aligned and random nanofibrous substrate for the in vitro culture of Schwann cells for neural tissue engineering. Acta Biomaterialia 2009;5(7):2560-2569.

70. Chow WN, Simpson DG, Bigbee JW, Colello RJ. Evaluating neuronal and glial growth on electrospun polarized matrices: bridging the gap in percussive spinal cord injuries. Neuron Glia Biology 2007;3(02):119-126.

71. Schnell E, Klinkhammer K, Balzer S, Brook G, Klee D, Dalton P, et al. Guidance of glial cell migration and axonal growth on electrospun nanofibers of poly-[epsilon]-caprolactone and a collagen/poly-[epsilon]-caprolactone blend. Biomaterials 2007;28(19):3012-3025.

72. Sangsanoh P, Suwantong O, Neamnark A, Cheepsunthorn P, Pavasant P, Supaphol P. In vitro biocompatibility of electrospun and solvent-cast chitosan substrata towards Schwann, osteoblast, keratinocyte and fibroblast cells. European Polymer Journal 2010;46(3):428-440.

73. Wang W, Itoh S, Matsuda A, Aizawa T, Demura M, Ichinose S, et al. Enhanced nerve regeneration through a bilayered chitosan tube: The effect of introduction of glycine spacer into the CYIGSR sequence. Journal of Biomedical Materials Research Part A 2008;85A(4):919-928.

74. Neal R, McClugage III, S., Link, M., Sefcik, L., Ogle, R., Botchwey, E. Laminin Nanofiber Meshes That Mimic Morphological Properties and Bioactivity of Basement Membranes. Tissue Engineering Part C: Methods 2009;15(1):11-21.

75. Zhang F, Zuo BQ, Zhang HX, Bai L. Studies of electrospun regenerated SF/TSF nanofibers. Polymer 2009;50(1):279-285.

76. Wang HB, Mullins ME, Cregg JM, McCarthy CW, Gilbert RJ. Varying the diameter of aligned electrospun fibers alters neurite outgrowth and Schwann cell migration. Acta Biomaterialia 2010;6(8):2970-2978.

77. Cho YI, Choi JS, Jeong SY, Yoo HS. Nerve growth factor (NGF)-conjugated electrospun nanostructures with topographical cues for neuronal differentiation of mesenchymal stem cells. Acta Biomaterialia 2010;6(12):4725-4733.

78. Lee JY, Bashur CA, Goldstein AS, Schmidt CE. Polypyrrole-coated electrospun PLGA nanofibers for neural tissue applications. Biomaterials 2009;30(26):4325-4335.

79. Ghasemi-Mobarakeh L, Prabhakaran MP, Morshed M, Nasr-Esfahani M-H, Ramakrishna S. Electrospun poly([var epsilon]-caprolactone)/gelatin nanofibrous scaffolds for nerve tissue engineering. Biomaterials 2008;29(34):4532-4539.

80. Prabhakaran MP, Venugopal JR, Ramakrishna S. Mesenchymal stem cell differentiation to neuronal cells on electrospun nanofibrous substrates for nerve tissue engineering. Biomaterials 2009;30(28):4996-5003.

81. Zhang S, Gelain F, Zhao X. Designer self-assembling peptide nanofiber scaffolds for 3D tissue cell cultures. Seminars in Cancer Biology 2005;15(5):413-420.

82. Kyle S, Aggeli A, Ingham E, McPherson MJ. Production of self-assembling biomaterials for tissue engineering. Trends in Biotechnology 2009;27(7):423-433.

83. Holmes TC. Novel peptide-based biomaterial scaffolds for tissue engineering. Trends in Biotechnology 2002;20(1):16-21.

84. Zhang S, Altman M. Peptide self-assembly in functional polymer science and engineering. Reactive and Functional Polymers 1999;41(1-3):91-102.

85. Yanlian Y, Ulung K, Xiumei W, Horii A, Yokoi H, Shuguang Z. Designer self-assembling peptide nanomaterials. Nano Today 2009;4(2):193-210.

86. Zou Z, Zheng Q, Wu Y, Song Y, Wu B. Growth of rat dorsal root ganglion neurons on a novel self-assembling scaffold containing IKVAV sequence. Materials Science and Engineering: C 2009;29(7):2099-2103.

87. Li Q, Chau Y. Neural differentiation directed by self-assembling peptide scaffolds presenting laminin-derived epitopes. Journal of Biomedical Materials Research Part A

2010;94A(3):688-699.

88. Tysseling-Mattiace VM, Sahni V, Niece KL, Birch D, Czeisler C, Fehlings MG, et al. Self-assembling nanofibers inhibit glial scar formation and promote axon elongation after spinal cord injury. J Neurosci 2008 Apr;28(14):3814-3823.

89. Guo J, Leung KKG, Su H, Yuan Q, Wang L, Chu T-H, et al. Self-assembling peptide nanofiber scaffold promotes the reconstruction of acutely injured brain. Nanomedicine: Nanotechnology, Biology and Medicine 2009;5(3):345-351.

90. Yang C-Y, Song B, Ao Y, Nowak AP, Abelowitz RB, Korsak RA, et al. Biocompatibility of amphiphilic diblock copolypeptide hydrogels in the central nervous system. Biomaterials 2009;30(15):2881-2898.

91. Guo J, Su H, Zeng Y, Liang Y-X, Wong WM, Ellis-Behnke RG, et al. Reknitting the injured spinal cord by self-assembling peptide nanofiber scaffold. Nanomedicine: Nanotechnology, Biology and Medicine 2007;3(4):311-321.

92. Ananthanarayanan B, Little L, Schaffer DV, Healy KE, Tirrell M. Neural stem cell adhesion and proliferation on phospholipid bilayers functionalized with RGD peptides. Biomaterials 2010;31(33):8706-8715.

93. Holmes TC, de Lacalle S, Su X, Liu GS, Rich A, Zhang SG. Extensive neurite outgrowth and active synapse formation on self-assembling peptide scaffolds. Proc Natl Acad Sci U S A 2000 Jun;97(12):6728-6733.

94. Gelain F, Bottai D, Vescovi A, Zhang S. Designer Self-Assembling Peptide Nanofiber Scaffolds for Adult Mouse Neural Stem Cell 3-Dimensional Cultures. PLoS ONE 2006;1(1):e119.

95. Silva GA, Czeisler C, Niece KL, Beniash E, Harrington DA, Kessler JA, et al. Selective Differentiation of Neural Progenitor Cells by High-Epitope Density Nanofibers. Science 2004 February 27, 2004;303(5662):1352-1355.

96. Ellis-Behnke RG, Liang Y-X, You S-W, Tay DKC, Zhang S, So K-F, et al. Nano neuro knitting: Peptide nanofiber scaffold for brain repair and axon regeneration with functional return of vision. Proc Natl Acad Sci U S A 2006 March 28, 2006;103(13):5054-5059.

97. Moore K, Macsween M, Shoichet M. Immobilized Concentration Gradients of Neurotrophic Factors Guide Neurite Outgrowth of Primary Neurons in Macroporous Scaffolds. Tissue Engineering 2006;12(2):267-278.

98. Levesque SG, Shoichet MS. Synthesis of cell-adhesive dextran hydrogels and macroporous scaffolds. Biomaterials 2006;27(30):5277-5285.

99. Tresco PA, Seil FJ. Tissue engineering strategies for nervous system repair. Prog

Brain Res: Elsevier, 2000. p. 349-363.

100. Reichardt LF, Tomaselli KJ. Extracellular Matrix Molecules and their Receptors: Functions in Neural Development. Annual Review of Neuroscience 1991;14(1):531-570.

101. Letourneau PC, Condic ML, Snow DM. Interactions of developing neurons with the extracellular matrix. J Neurosci 1994 March 1, 1994;14(3):915-928.

102. Doran MR, Markway BD, Aird IA, Rowlands AS, George PA, Nielsen LK, et al. Surface-bound stem cell factor and the promotion of hematopoietic cell expansion. Biomaterials 2009;30(25):4047-4052.

103. Doran MR, Markway BD, Croll TI, Sara S, Munro TP, Cooper-White JJ. Controlled presentation of recombinant proteins via a zinc-binding peptide-linker in two and three dimensional formats. Biomaterials 2009;30(34):6614-6620.

104. Ito Y. Covalently immobilized biosignal molecule materials for tissue engineering. Soft Matter 2008;4(1):46-56.

105. Ito Y, Chen G, Imanishi Y, Morooka T, Nishida E, Okabayashi Y, et al. Differential Control of Cellular Gene Expression by Diffusible and Non-Diffusible EGF. Journal of Biochemistry 2001 May 1, 2001;129(5):733-737.

106. Lim K-C, Lim ST, Federoff HJ. Neurotrophin secretory pathways and synaptic plasticity. Neurobiology of Aging 2003;24(8):1135-1145.

107. Levenberg S, Burdick JA, Kraehenbuehl T, Langer R. Neurotrophin-Induced Differentiation of Human Embryonic Stem Cells on Three-Dimensional Polymeric Scaffolds. Tissue Engineering 2005;11(3-4):506-512.

108. McDonald JW, Stefovska VG, Liu XZ, Shin H, Liu S, Choi DW. Neurotrophin potentiation of iron-induced spinal cord injury. Neuroscience 2002;115(3):931-939.

109. Lanave C, Colangelo AM, Saccone C, Alberghina L. Molecular evolution of the neurotrophin family members and their Trk receptors. Gene 2007;394(1-2):1-12.

110. Persson H. Neurotrophin production in the brain. Seminars in Neuroscience 1993;5(4):227-237.

111. Yano H, Chao MV, Ugo Gulini MGWQ, Gabriella M. Neurotrophin receptor structure and interactions. Pharmacochem Libr: Elsevier, 2000. p. 253-260.

112. Lessmann V, Gottmann K, Malcangio M. Neurotrophin secretion: current facts and future prospects. Progress in Neurobiology 2003;69(5):341-374.

113. Fritzsch B, Silos-Santiago I, Bianchi LM, Fari 鋼 s I. The role of neurotrophic factors in regulating the development of inner ear innervation. Trends in Neurosciences

1997;20(4):159-164.

114. Davies AM, Callow JA. Chapter 5 Developmental changes in the neurotrophic factor survival requirements of peripheral nervous system neurons. Prog Brain Res: Elsevier, 1998. p. 47-56.

115. Krewson CE, Klarman ML, Saltzman WM. Distribution of nerve growth factor following direct delivery to brain interstitium. Brain Research 1995;680(1-2):196-206.

116. Uebersax L, Mattotti M, Papaloizos M, Merkle HP, Gander B, Meinel L. Silk fibroin matrices for the controlled release of nerve growth factor (NGF). Biomaterials 2007;28(30):4449-4460.

117. Han Q, Sun W, Lin H, Zhao W, Gao Y, Zhao Y, et al. Linear Ordered Collagen Scaffolds Loaded with Collagen-Binding Brain-Derived Neurotrophic Factor Improve the Recovery of Spinal Cord Injury in Rats. Tissue Engineering Part A 2009;15(10):2927-2935.

118. Sirianni RW, Olausson P, Chiu AS, Taylor JR, Saltzman WM. The behavioral and biochemical effects of BDNF containing polymers implanted in the hippocampus of rats. Brain Research 2010;1321:40-50.

119. de Curtis I. Neuronal interactions with the extracellular matrix. Current Opinion in Cell Biology 1991;3(5):824-831.

120. Yu X, Dillon GP, Bellamkonda RV. A Laminin and Nerve Growth Factor-Laden Three-Dimensional Scaffold for Enhanced Neurite Extension. Tissue Engineering 1999;5(4):291-304.

121. Ruoslahti E. Brain extracellular matrix. Glycobiology 1996 July 1, 1996;6(5):489-492.

122. Valmikinathan CM, Wang JP, Smiriglio S, Golwala NG, Yu XJ. Magnetically Induced Protein Gradients on Electrospun Nanofibers. Comb Chem High Throughput Screen 2009 Aug;12(7):656-663.

123. He L, Liao S, Quan D, Ngiam M, Chan CK, Ramakrishna S, et al. The influence of laminin-derived peptides conjugated to Lys-capped PLLA on neonatal mouse cerebellum C17.2 stem cells. Biomaterials 2009;30(8):1578-1586.

124. Yu TT, Shoichet MS. Guided cell adhesion and outgrowth in peptide-modified channels for neural tissue engineering. Biomaterials 2005;26(13):1507-1514.

125. Li WS, Guo Y, Wang H, Shi DJ, Liang CF, Ye ZP, et al. Electrospun nanofibers immobilized with collagen for neural stem cells culture. J Mater Sci-Mater Med 2008 Feb;19(2):847-854.

126. Jingwei X, Matthew RM, Stephanie MW, Xiaoran L, Daniel WM, Shelly ES-E, et al. Conductive Core-Sheath Nanofibers and Their Potential Application in Neural Tissue

Engineering. Advanced Functional Materials 2009;19(14):2312-2318.

127. Willerth SM, Rader A, Sakiyama-Elbert SE. The effect of controlled growth factor delivery on embryonic stem cell differentiation inside fibrin scaffolds. Stem Cell Research 2008;1(3):205-218.

128. Patist CM, Mulder MB, Gautier SE, Maquet V, Jerome R, Oudega M. Freeze-dried poly(,-lactic acid) macroporous guidance scaffolds impregnated with brain-derived neurotrophic factor in the transected adult rat thoracic spinal cord. Biomaterials 2004;25(9):1569-1582.

129. Moore MJ, Friedman JA, Lewellyn EB, Mantila SM, Krych AJ, Ameenuddin S, et al. Multiple-channel scaffolds to promote spinal cord axon regeneration. Biomaterials 2006;27(3):419-429.

130. Koh HS, Yong T, Chan CK, Ramakrishna S. Enhancement of neurite outgrowth using nano-structured scaffolds coupled with laminin. Biomaterials 2008;29(26):3574-3582.

131. Kakinoki S, Yamaoka T. Stable modification of poly(lactic acid) surface with neurite outgrowth-promoting peptides via hydrophobic collagen-like sequence. Acta Biomaterialia 2010;6(6):1925-1930.

132. Gelain F, Unsworth LD, Zhang S. Slow and sustained release of active cytokines from self-assembling peptide scaffolds. Journal of Controlled Release 2010;In Press, Uncorrected Proof.

133. Freudenberg U, Hermann A, Welzel PB, Stirl K, Schwarz SC, Grimmer M, et al. A star-PEG-heparin hydrogel platform to aid cell replacement therapies for neurodegenerative diseases. Biomaterials 2009;30(28):5049-5060.

134. Dodla MC, Bellamkonda RV. Differences between the effect of anisotropic and isotropic laminin and nerve growth factor presenting scaffolds on nerve regeneration across long peripheral nerve gaps. Biomaterials 2008;29(1):33-46.

135. Ding T, Luo Z-J, Zheng Y, Hu X-Y, Ye Z-X. Rapid repair and regeneration of damaged rabbit sciatic nerves by tissue-engineered scaffold made from nano-silver and collagen type I. Injury 2010;41(5):522-527.

136. Pettikiriarachchi JTS, Parish CL, Shoichet MS, Forsythe JS, Nisbet DR. Biomaterials for Brain Tissue Engineering. Australian Journal of Chemistry 2010;63(8):1143-1154.

137. Walker P, Aroom K, Jimenez F, Shah S, Harting M, Gill B, et al. Advances in Progenitor Cell Therapy Using Scaffolding Constructs for Central Nervous System Injury. Stem Cell Reviews and Reports 2009;5(3):283-300.

138. Campbell WW. Evaluation and management of peripheral nerve injury. Clinical

Neurophysiology 2008;119(9):1951-1965.

139. Navarro X, Viv M, Valero-Cabr A. Neural plasticity after peripheral nerve injury and regeneration. Progress in Neurobiology 2007;82(4):163-201.

140. Alexi T, Borlongan CV, Faull RLM, Williams CE, Clark RG, Gluckman PD, et al. Neuroprotective strategies for basal ganglia degeneration: Parkinson's and Huntington's diseases. Progress in Neurobiology 2000;60(5):409-470.

141. Goole J, Amighi K. Levodopa delivery systems for the treatment of Parkinson's disease: An overview. International Journal of Pharmaceutics 2009;380(1-2):1-15.

142. Singh N, Pillay V, Choonara YE. Advances in the treatment of Parkinson's disease. Progress in Neurobiology 2007;81(1):29-44.

143. Licker V, Koari E, Hochstrasser DF, Burkhard PR. Proteomics in human Parkinson's disease research. Journal of Proteomics 2009;73(1):10-29.

144. Thrift AG, Srikanth VK, Howard MF, Md, Kenneth R, Md Mpa Frcpc Fcahs F, et al. Stroke: Epidemiology and Pathology. Brocklehurst's Textbook of Geriatric Medicine and Gerontology (SEVENTH EDITION). Philadelphia: W.B. Saunders, 2010. p. 478-483.

145. Bible E, Chau DYS, Alexander MR, Price J, Shakesheff KM, Modo M. The support of neural stem cells transplanted into stroke-induced brain cavities by PLGA particles. Biomaterials 2009;30(16):2985-2994.

146. Ghajar J. Traumatic brain injury. The Lancet 2000;356(9233):923-929.

147. Kwon BK, Tetzlaff W, Grauer JN, Beiner J, Vaccaro AR. Pathophysiology and pharmacologic treatment of acute spinal cord injury. The Spine Journal 2004 2004/8//;4(4):451-464.

148. Androutsellis-Theotokis A, Rueger MA, McKay RDG, Jeffrey HK, Mark HT. Stem Cell Therapies for Parkinson's Disease. In: Jeffrey K, Mark T, editors. CNS Regeneration (Second Edition). San Diego: Academic Press, 2008. p. 161-180.

149. Winkler C, Kirik D, Bjorklund A. Cell transplantation in Parkinson's disease: how can we make it work? Trends in Neurosciences 2005;28(2):86-92.

150. Rosser AEab, Zietlow Rb, Dunnett SBb. Stem cell transplantation for neurodegenerative diseases. Current Opinion in Neurology 2007;20(6):688-692.

151. B. Dunnett S, E. Rosser A, Craig H, Dwaine E. Neural Transplantation in Parkinson's Disease. In: Caraig H, dwaine E, editors. Cellular Transplantation from laboratory to clinic. Burlington: Academic Press, 2007. p. 439-454.

152. Shufaro Y, Reubinoff BE. Therapeutic applications of embryonic stem cells. Best Practice & Research Clinical Obstetrics & Gynaecology 2004;18(6):909-927.

153. Yang J-T, Kuo Y-C, Chiu K-H. Peptide-modified inverted colloidal crystal scaffolds with bone marrow stromal cells in the treatment for spinal cord injury. Colloids and Surfaces B: Biointerfaces 2011;84(1):198-205.

154. Aebischer P, Schluep M, Deglon N, Joseph JM, Hirt L, Heyd B, et al. Intrathecal delivery of CNTF using encapsulated genetically modifiedxenogeneic cells in amyotrophic lateral sclerosis patients. Nature medicine 1996;2:696-699.

155. Arvidsson A, Collin T, Kirik D, Kokaia Z, Lindvall O. Neuronal replacement from endogenous precursors in the adult brain after stroke. nature medicine 2002;8:963-970.

156. Conover J, Notti R. The neural stem cell niche. Cell and Tissue Research 2008;331(1):211-224.

157. Ventura RE, Goldman JE. Dorsal Radial Glia Generate Olfactory Bulb Interneurons in the Postnatal Murine Brain. The Journal of Neuroscience 2007 April 18, 2007;27(16):4297-4302.

158. Park KI, Teng YD, Snyder EY. The injured brain interacts reciprocally with neural stem cells supported by scaffolds to reconstitute lost tissue. Nat Biotech 2002;20(11):1111-1117.

159. Thompson LH, Grealish S, Kirik D, Björklund A. Reconstruction of the nigrostriatal dopamine pathway in the adult mouse brain. European Journal of Neuroscience 2009;30(4):625-638.

160. Bozkurt GMDP, Mothe AJP, Zahir TP, Kim HB, Shoichet MSP, Tator CHMDP. Chitosan Channels Containing Spinal Cord-Derived Stem/Progenitor Cells for Repair of Subacute Spinal Cord Injury in the Rat. Neurosurgery 2010;67(6):1733-1744.

161. Ekdahl CT, Claasen J-H, Bonde S, Kokaia Z, Lindvall O. Inflammation is detrimental for neurogenesis in adult brain. Proc Natl Acad Sci U S A 2003 November 11, 2003;100(23):13632-13637.

162. Batchelor PE, Liberatore GT, Wong JY, Porritt MJ, Frerichs F, Donnan GA, et al. Activated Macrophages and Microglia Induce Dopaminergic Sprouting in the Injured Striatum and Express Brain-Derived Neurotrophic Factor and Glial Cell Line-Derived Neurotrophic Factor. J Neurosci 1999 March 1, 1999;19(5):1708-1716.

163. Berry M, Hunter AS, Duncan A, Lordan J, Kirvell S, Tsang WL, et al. Axon–glial relations during regeneration of axons in the adult rat anterior medullary velum. Journal of Neurocytology 1998;27(12):915-937.

164. Ekdahl CT, Kokaia Z, Lindvall O. Brain inflammation and adult neurogenesis: The dual role of microglia. Neuroscience 2009;158(3):1021-1029.

165. Schwartz M. Macrophages and Microglia in Central Nervous System Injury: Are They Helpful or Harmful? J Cereb Blood Flow Metab 2003;23(4):385-394.

166. Streit WJ, Walter SA, Pennell NA. Reactive microgliosis. Progress in Neurobiology 1999;57(6):563-581.

167. Asada H, Ip NY, Pan L, Razack N, Parfitt MM, Plunkett RJ. Time course of ciliary neurotrophic factor mRNA expression is coincident with the presence of protoplasmic astrocytes in traumatized rat striatum. Journal of Neuroscience Research 1995;40(1):22-30.

168. Mark WG, Brian JZ. Pathophysiology of traumatic brain injury. Mount Sinai Journal of Medicine: A Journal of Translational and Personalized Medicine 2009;76(2):97-104.

169. Maas AIR, Stocchetti N, Bullock R. Moderate and severe traumatic brain injury in adults. The Lancet Neurology 2008;7(8):728-741.

170. Fehlings MG, Baptiste DC. Current status of clinical trials for acute spinal cord injury. Injury 2005;36(2, Supplement 1):S113-S122.

171. Yezierski RP, Allan IB, Akimichi K, Gordon MS, Gerald W, Thomas DA, et al. Pain Following Spinal Cord Injury. The Senses: A Comprehensive Reference. New York: Academic Press, 2008. p. 387-400.

172. McDonald JW, Becker D, Huettner J, Robert L, John G, Brigid H, et al. Spinal Cord Injury. In: Robert L, John G, Brigid H, Douglas M, Roger P, James T, et al., editors. Handbook of Stem Cells. Burlington: Academic Press, 2004. p. 701-712.

173. Whalley K, O'Neill P, Ferretti P. Changes in response to spinal cord injury with development: Vascularization, hemorrhage and apoptosis. Neuroscience 2006;137(3):821-832.

174. Terayama R, Bando Y, Murakami K, Kato K, Kishibe M, Yoshida S. Neuropsin promotes oligodendrocyte death, demyelination and axonal degeneration after spinal cord injury. Neuroscience 2007;148(1):175-187.

175. Park E, Velumian AA, Fehlings MG. The Role of Excitotoxicity in Secondary Mechanisms of Spinal Cord Injury: A Review with an Emphasis on the Implications for White Matter Degeneration. Journal of Neurotrauma 2004;21(6):754-774.

176. Dong H, Fazzaro A, Xiang C, Korsmeyer SJ, Jacquin MF, McDonald JW. Enhanced Oligodendrocyte Survival after Spinal Cord Injury in Bax-Deficient Mice and Mice with Delayed Wallerian Degeneration. J Neurosci 2003 September 24, 2003;23(25):8682-8691.

177. Blight AR. Miracles and molecules-progress in spinal cord repair. Nat Neurosci 2002:1051-1054.

178. Yick LW, Wu W, So KF, Yip HK, Shum DKY. Chondroitinase ABC promotes axonal regeneration of Clarke's neurons after spinal cord injury. Neuroreport 2000;11(5):1063-1067.

Chapter 3

Materials and Methods

Contents

3.1 MATERIALS AND METHODS

3.1.1 PCL scaffold preparation

3.1.1.1 Electrospun PCL scaffold

A 10% (w/v) PCL solution was prepared by dissolving PCL (Sigma) in 3:1 (v/v) chloroform and methanol (Merk Pty Ltd, Australia) at room temperature. The solution was then loaded into a 10 mL glass syringe with an 18 - gauge needle for electrospinning at a potential of +20 kV and -5 kV with a 0.394 mL/h flow rate and a working distance of 10 cm. The PCL fibres were collected on aluminum foil. The collected PCL scaffolds were removed from the aluminum foil immediately after electrospinning and placed in a vacuum oven overnight at 30 ℃. Scaffolds were then immersed in 0.05 M ethylenediamine (Sigma Uldrich, USA) diluted with 2-propanol (Merck Pty, Australia) for 15 minutes at room temperature. The samples were washed in ice chilled milliQ water three times for 10 minutes and stored in a desiccator under vacuum. Circular punch biopsies (6mm in diameter) were cut from the PCL scaffolds for use in vitro (in 96-well plates) or alternatively scaffolds were cut into squares (0.5cm2) for in vivo implantation. The final samples were sterilized in 70% ethanol for 15 minutes and washed with sterilized PBS 3 times prior to *in vitro* and *in vivo* experiments.

3.1.1.2 Biofunctionalisation of PCL scaffolds with neurotrophic factors

For immobilisation of neurotrophic factors onto the PCL scaffolds, 4-(*N*-maleimidomethyl)cyclohexane-1-carboxylic acid 3-sulfo-*N*- hydroxysuccinimide ester sodium salt (sulfo-SMCC) was used as a cross-linker, as previously described by Horne [1]. In brief, a 2.5 mg/mL sulfo-SMCC solution (Sigma Aldrich, USA) was prepared in PBS with 1 hour agitation at room temperature prior to filtration (0.22 μm filter). The PCL scaffolds, treated with ED, were immersed in sulfo-SMCC for 2 hours at room temperature, prior to being transferred to a solution containing neurotrophins. The tested protein solutions were recombinant human GDNF (0.5 or 4 μg/ml, R & D Systems, USA) overnight at 4 ℃.

3.1.2 Composite scaffolds preparation

3.1.2.1 Electrospun PLLA scaffolds and short fibre fabrication

A 15.9wt% of PLLA (in chloroform (Merk Pty, Ltd, Australia) and acetone at 3:1 (v/v) ration with 1mM dodecyl trimethyl ammonium bromide (DTAB) was electrospun at a flow rate of 0.8mL/hr, a 20kV voltage, a working distance of 5cm from a mandrel (5cm diameter) rotating at a speed of 300 RPM for 40min. The PLLA electrospun scaffolds were then immersed in 5% ethylenediamine (ED) (Sigma Alrich Pty Ltd) in 2-isopropanol (IPA) for 10 minutes and washed three times with milliQ water. The hydrolysed PLLA scaffolds were either sonicated

(4:6 second on:off pulse sonication) in water for approximately 10 minutes to fabricate short fibres which were collected after centrifuged or alternatively cut into short fibers (20um in length) on a freezing microtome. The collected short fibres was sterilised in 80% ethanol for 10 min and washed twice in PBS, with the short fibers pelleted between each wash.

To attach GDNF onto short fibres, a 5 mM sulfo-succinimidyl 1-(N-maleimidomethyl)-cyclohexane-1-carboxylate (sulfo-SMCC) solution in PBS was prepared 1 hr prior and filtered with 0.2 μm membrane. The sterile short fibres were placed in sulfo-SMCC for two hours and transferred in 0.5ug/mL GDNF over night at 4℃. The functionalised short fibres were washed twice with PBS and stored, ready for in vitro or in vivo application.

3.1.2.2 PDL functionalised xyloglucan

PDL functionalised xyloglucan was produced according to previously described protocol [2, 3]. After UV sterilisation xyloglucan was mixed at a concentration of 3.75(wt/v)% in HBSS media for in vitro studies, and 1.67(wt/v)% in HBSS and cell suspension for *in vivo* studies.

3.1.3 Materials characterisation

3.1.3.1 Scanning electron microscopy (SEM)

The scaffolds (PCL, xyloglucan and xyloglucan mixed with short fibres) were coated with 2 nm of platinum using a Cressington sputter coater. PCL samples were tilted at 45 degrees and splutter coated at approximately 50-100 turns/per minute for 30 seconds. A scanning electron microscope was then used for examination of the scaffold architecture (JEOL JSM-840A SEM W filament). The SEM variables were set as: 20.0 kV (accelerating voltage), 8 mm (working distance), 3000X (magnification) and 1×10^{-9} A (probe current). Fibre diameter and interfiber distance were measured using Image J software.

3.1.3.2 Enzyme-linked immunosorbent assay

An enzyme-linked immunosorbent assay (ELISA) was used to verify the attachment of neurotrophic factors onto the scaffolds in samples prepared in parallel to those scaffolds used *in vitro* and *in vivo*. Scaffolds (PCL, PCL with soluble proteins or PCL+immobilised proteins) were washed 3 times in PBST (PBS containing 0.05% Tween-20) prior to blocking in 5% normal goat or donkey serum. The scaffolds were then immersed in primary antibodies (goat anti-GDNF antibody: 1 μg/mL; rat anti-NGF: 2 ng/ml; rabbit anti-laminin: 1:100; rabbit anti-BDNF: 1:750 (R & D Systems, USA)) prepared in PBST for 2 hours at 37 ℃. The

scaffolds were then washed three times in PBST before being incubated in anti-goat/ anti-rat/ anti-rabbit horseradish peroxidase (HRP, 1:2000 in PBST solution containing 2% donkey serum). Scaffolds were again washed (3x10 minutes in PBST) and placed in a 96-well plate where the bound HRP activity was assayed by color development using TMB microwell peroxidase system (R & D Systems, USA). The reaction was stopped by addition of 1M HCl, and finally the absorbance (450 nm) was measured with a microtitre plate reader (SpectraMax). ELISA was performed on triplicate scaffolds for each treatment group and repeated for each independent *in vitro* experiment (>3) as well as prior to *in vivo* implantation of scaffolds. For the study protein (GDNF) stability (chapter 5), the scaffold samples and supernatants were collected at time points (0,1,3 and 7days) after protein attachment and kept in -80 ℃ before testing.

A GDNF standard curve was generated to determine the amount of GDNF tethered onto the scaffolds by ELISA. A 96-well plate was coated with 100 µL/ per well of GDNF capture antibody (4µg/mL, R&D Systems) overnight at room temperature. After three washes with PBST, the plate was dried and blocked by adding 300 µL of PBS containing 2.5% gelatin and 0.05% Tween20 (the solution was heated to dissolve gelatin and allowed to cool) for an hour at 37°C in an incubator. After washes, 100 µL of GDNF solution at different concentrations was added and incubated for two hours at room temperature. Standard curve GDNF concentrationsincluded 0, 50, 100, 200, 500, 1000, 2000 and 10,000 pg/ml. After three

washes, the ELISA procedure was performed as described above in parallel with the GDNF-tethered scaffolds of interest.

3.1.3.3 X-ray photoelectron spectroscopy analysis

XPS with an AXIS-HSi spectrometer (Kratos Analytical) and a monochromated Al K source at a power of 144 W (12 kV × 12 mA), and 1 × 0.5 mm aperture was applied for sample characterisation [2]. Samples including xyloglucan and PDL grafted xyloglucan were firstly dissolved in milliQ water and placed on silicon wafers before air dried. The samples were ready to measure at an emission angle of 0°. A survey spectrum was then performed to determine the amount of PDL present in grafted xyloglucan. N/C ration for PDL was expected to be around 0.33 ($C_6H_{14}N_2O_2$), the N/C ration in PDL grafted xyloglucan were measured to calculate the ration of PDL verse xyloglucan using a linear model (molecular weights were used to transplant the data into per xyloglucan repeat unit).

3.1.3.4 Isothermal rheology

A Rheometric Scientific^{TM} rheometer was conducted to investigate the thermal gelation time of xyloglucan and xyloglucan grafted with PDL [2]. 2.5 (wt/v)% of the hydrogel was prepared in HBSS media. Isothermal rheology was performed to measure the elastic (G') and shear

(G”) moduli using parallel plate configuration at a frequency of 0.1 Hz and a strain rate of 1.25%.

3.1.4 Animals for *in vitro* and *in vivo* studies

All procedures were conducted in accordance with the Australian National Health and Medical Research Council’s published Code of Practice for the Use of Animals in Research, and experiments were approved by the Florey Neuroscience Institute animal ethics committee. Mice and rats were housed on a 12 h light/dark cycle with ad libitum access to food and water. Cells used for *in vitro* culturing and transplantation were obtained from mice that were time mated overnight, with visualisation of a vaginal plug on the following morning taken as embryonic day (E) 0.5. Tissue was isolated at mouse embryonic day 14.5 (E14.5) for cortical cultures and E12.5 for ventral midbrain cells. *In vitro* culturing of primary cortical or ventral midbrain cells was performed using tissue obtained C57BL/6 time mated mice while donor tissue for transplantation was obtained from C57BL/6 time-mated mice expressing green fluorescent protein (GFP) under the β-actin promoter. The ubiquitous expression of GFP within the donor tissue enabled distinction of the grafted cells within the host brain.

3.1.4.1 Isolation of primary cortical and ventral midbrain cells

Tissue was isolated from embryos at times corresponding to the peak in neurogenesis for that given tissue region (E12.5- ventral midbrain cells and E14.5 for cortical cells). Consequently

isolated cell preparations, for in vitro and in vivo application, included a heterogenous population of cells including neural stem cells, neural progenitors and immature neuronsPregnant mice were anesthetised with isoflurane prior to cervical dislocation. The collected embryos were immersed in chilled L15 medium (Invitrogen), the brains removed and cortices or ventral midbrain microdissected. Subsequently the tissue fragments were incubated in 0.1%DNase and 0.05% trypsin (in magnesium and calcium free Hank's buffered saline solution, HBSS) for 15 minutes followed by 3 gentle washes in HBSS. Finally, the tissue fragments were dissociated in N2 media consisting of a 1:1 mixture of F12 and MEM supplemented with 15 mM HEPES buffer, 1 mM glutamine, 6 mg/ml glucose (Sigma-Aldrich), 1.5 mg/ml bovine serum albumin and 1% N2 supplement (all purchased from Invitrogen).

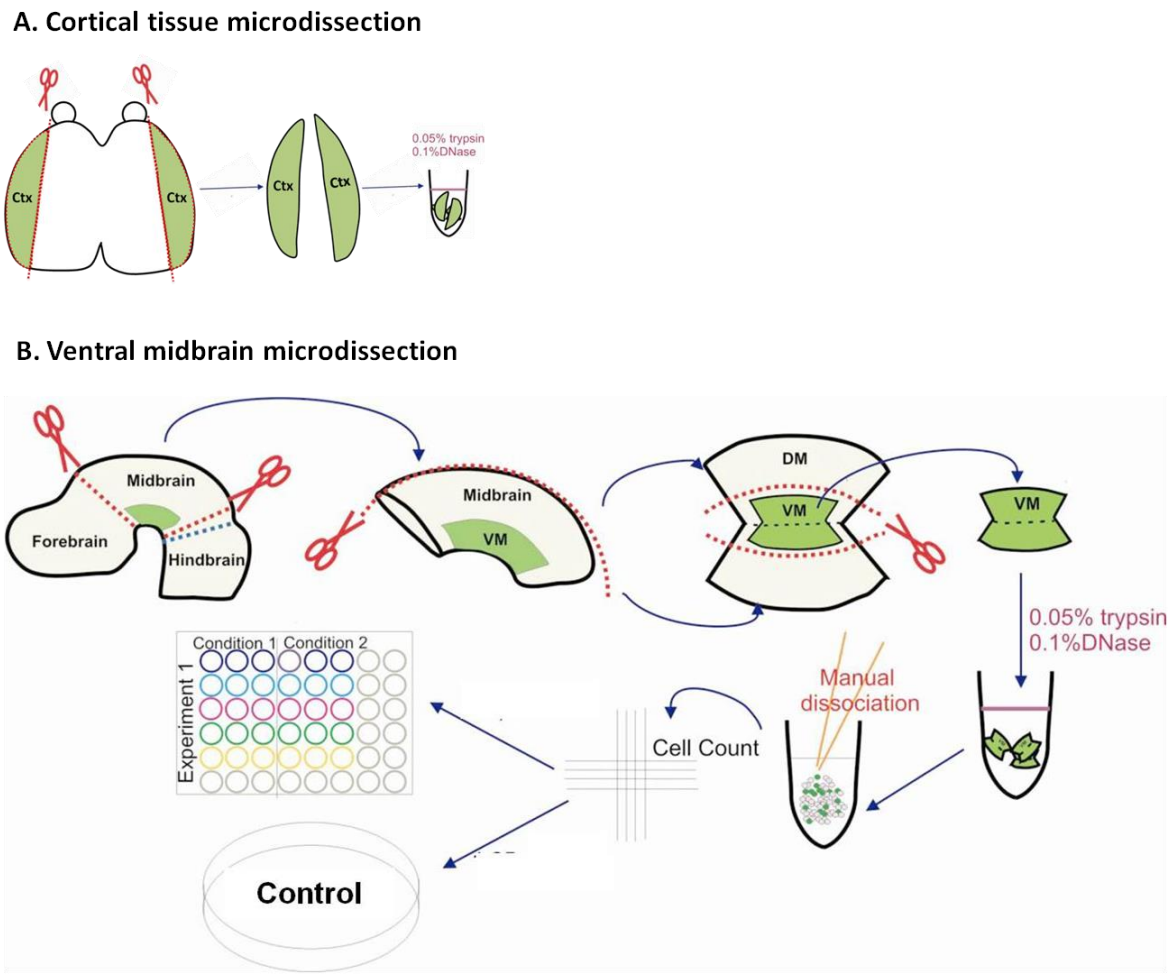

Figure 3.1 The schematic illustration of cortical tissue and ventral midbrain micro-dissection

For *in vitro* culturing, cells were seeded at a density of 175,000 cells /cm^2 onto either poly-D-lysine-coated coverslips or prepared scaffolds and incubated at 37 ^{o}C in 5% CO_2 for 72 hours. After 3 days, the cells were fixed with 4% paraformaldehyde for 20 minutes, washed and stored in PBS containing 0.025% sodium azide until the time of immunocytochemistry. For *in vivo* transplantation, the cells were suspended at a density of 100,000 cells/μL in HBSS containing 0.1% DNase and stored on ice until the time of implantation. Each embryo provides enough primary neural cells to each experimental animal (recipient).

3.1.5 *In vitro* studies

To assess biocompatibility of scaffolds, cells were suspended at a density of 5.4 x 10^5 cells/mL. 100 μL added on scaffolds in each well (5.4 x 10^4 cells/well, 96 wells, 0.3 cm^2/ well) and incubated for days in N2 media consisting of a 1:1 mixture of F12 and MEM supplemented with 15 mM HEPES buffer, 1 mM glutamine, 6 mg/ml glucose (Sigma-Aldrich), 1.5 mg/ml bovine serum albumin and 1% N2 supplement (all purchased from Invitrogen). After days of culturing, cells were fixed with 4% paraformaldehyde (PFA) for 20 minutes and washed 3 times for 5 minutes with PBS. Experimental groups in each chapter are listed as below:

Chapter 4: control (glass coated with PDL), PCL scaffolds and PCL scaffolds tethered with GDNF with/ without vortex.

Chapter 5: control (glass coated with PDL), and PCL scaffolds with/ without ED treatment

Chapter 6: control (glass coated with PDL), PCL scaffolds, PCL scaffolds with soluble GDNF and PCL scaffolds tethered with GDNF

Chapter 7: control (glass coated with PDL), xyloglucan, xyloglucan with short fibres, and xyloglucan with short fibres mobilized with GDNF

3.1.5.1 Immunohistochemistry

Cultures were subsequently incubated in a primary antibody solution (containing 0.3% TritonX and 5% of goat/ donkey serum) at 4 ℃ overnight. Primary antibodies and dilution factors were as follows: chicken anti-GFP (1:1000, abcam), mouse anti-β tubulin (TUJ, 1:1500, Promega, USA, neuronal marker), rabbit anti-glial fibrillary acidic protein (GFAP, 1:800, Dako Cytomation, Denmark, astrocyte marker), rabbit anti-NG2 (NG2, 1:500 Millipore, oligodendrocyte marker), mouse anti-nestin (Nestin, 1:200, Millipore, neural stem cell marker) and rabbit anti-tyrosine hydroxylase (TH, 1:400 Pelfreeze, dopaminergic neuron marker) [1, 4] (see table 3.1 for the antibody details). The cell cultures were then washed for 10 minutes in PBS (three times) before the secondary antibodies were subsequently added and incubated for one hour at room temperature. Secondary antibodies (1:300 in PBS containing 0.3% TritonX and 2% of goat/ donkey serum) were as follows: DyLight 594 goat anti-mouse (Alexa), DyLight 633 goat anti-rabbit (Alexa), DyLight 488/ 549 conjugated donkey anti-mouse (Jackson ImmunoResearch), DyLight 549/ 649 conjugated donkey anti-rabbit (Jackson immunoResearch), DyLight 488/ 549/ 649 conjugated donkey anti-chicken (Jackson ImmunoResearch). After another 10 minutes wash in PBS, Hoechst (1:1000 in PBS, nuclei marker) was applied for 5 minutes, followed by two washes (10 minutes) in PBS. The samples were slide mounted (Dako, USA) and imaged using a fluorescence microscope. The samples were stored at 4 ℃ in the dark prior to imaging.

Table 3.1 the list of antibodies used in the thesis

Cell markers/ Antibodies	Cell types/ Neurotrophins/ Receptors	Concentrations/ Companies
Hoechst	Nuclei	1:1000 Sigma
Nestin	Neural stem cell	1:200 Millpore
GFAP	Astrocyte	1:800 Dako
NG2	Oligodendrocyte	1:500 Millpore
TUJ	Immature neurons	1:1500 Promega
NeuN	Neuron	1:200 Millpore
TH	Dopaminergic cell	1:400 Pelfreeze
GFP	Green florescent protein cell	1:1000 ABCAM
BDNF	Brain-derived neurotrophic factor	1:750 R&D
GDNF	Glial-cell derived neurotrophic factor	1 µg/ml R&D
CD11b	Microglia/ macrophages	1:20 Chemicon
Erk1/2	Erk1/ 2	1:1000 Cell signalling
Phospho-Erk1/2	Phosphorylation Erk1/ 2	1:2000 Cell signalling

3.1.6 *In vivo* studies

3.1.6.1 An animal model of Parkinson's disease (chapter 7)

Female Swiss mice were anesthetized in 5% isoflurane gas until no reflex was observed at which point the level of anaesthetic was reduced to 2%. An incision (2-2.5 cm) was cut on the scalp to reveal the skull, lateral craniotomies were drilled at + 1.0 mm AP (anterior- posterior), - 2.0 mm ML (median- lateral) from bregma. To create Parkinson's disease mouse model (chapter 7), 6-hydroxydopamine (6-OHDA, sigma) was prepared at a concentration of 2 µg/µl in 0.2mg/ml ascorbic acid solution. The glass capillary was filled with 1.5µl of the

6-OHDA solution (3µg) and injected at -3.2 mm AP, 1.4 mm ML and -4.5 mm DV (6-OHDA was kept in a dark and chilled environment during surgery). The wound was then sutured, iodine was applied to the wound. Three weeks after the animals were ready for scaffold implantation with cell transplantation.

3.1.6.2 Implantation of primary cortical cells into the intact brain of rats (chapter 5 and 6)

Male Wistar rats were anesthetized in 5% isoflurane gas until no reflex was observed at which point the level of anesthetic was reduced to 2%.An incision (2-2.5 cm) was cut on the scalp to reveal the skull. Bi-lateral craniotomies were drilled at + 1.0 mm AP (anterior-posterior), ± 2.5 mm ML (median- lateral) from bregma; the sterile scaffolds were rolled to facilitate insertion into a 21 G needle. The needle was then injected at - 7.0 mm DV (dorsal-ventral) to create the cavity, being retracted to - 5.0 mm for scaffold insertion. A plunger was subsequently inserted into the needle to push the scaffold through the needle as it was slowly withdrawn from the brain. The top of the scaffold was left exposed above the surface of the brain to enable subsequent cell injection adjacent or into the core of the scaffolds. A 50 µm glass capillary was connected to the 5 µL Hamilton syringe as the injecting device and a 150,000 cells (1.5 µL) injected. The cell suspension (GFP+ cortical cells) was slowly injected at 3 depths (0.5ul/site): - 5.0 mm, -4.5 mm and -4.0 mm DV (dorsal- ventral). When injecting at each site, the glass capillary was left in situ for 2 minutes to allow the tissue and cells to

settle. Upon completion of the cell implantation the protruding scaffold was gentle pushed below the surface of the brain. After implantation, the wound was sutured, iodine was applied to the wound. Upon completion of surgery animals received an intramuscular injection of analgesic (Meloxicam, 3mg/kg). Rats were immunosuppressed by way of daily cyclosporine injection (CyclosporineA, 10mg/kg/day). Each experimental group had 6 animals and the groups were listed as below:

Chapter 5: cells alone and PCL scaffolds

Chapter 6: cells alone, PCL scaffolds and PCL scaffolds treated with GNDF

In the consideration of the size of implanted scaffolds and brain, rats were selected for the *in vivo* studies in chapter 5 and 6. Mouse donor tissue was used due to the availability of GFP mice, but not rats. GFP-labeled mouse cells enabled the ability to distinguish the transplanted cells (GFP+) from the host cells (GFP-). As a consequence of xenografting (i.e. grafting of cells across different species) daily cyclosporine injection was required to suppress the immune system.

3.1.6.3 Implantation of primary ventral midbrain cells into mouse brain of Parkinson's disease (chapter 7)

The surgery procedure was according to previously described section 3.1.6.2 except preparation of the composite scaffolds and implantation coordinates. 2μL of composite scaffolds were mixed with 1μL of cell suspension (GFP+ cortical cells, 150,000 cells/ μL) before implantation, and ended with a cell density of 50,000/ μL in the composite scaffolds. Lateral craniotomies were drilled at + 1.0 mm AP (anterior- posterior), - 2.0 mm ML (median- lateral) from bregma. 2μL of the scaffolds pre-mixed with cells solution was then injected into the brains of Parkinsonian mice at – 3.2 mm DV from bregma. When injecting at each site, the glass capillary was left in situ for 2 minutes to allow the tissue and cells to settle. After implantation, the wound was sutured, iodine was applied to the wound. Upon completion of surgery animals received an intramuscular injection of analgesic (Meloxicam, 3mg/kg). In chapter 7 the experimental groups included cells alone, cells in xyloglucan, cells in xyloglucan with short fibres, and cells in xyloglucan with short fibres mobilised with GDNF (n = 6). Mice were selected due to the finical consideration. And the donor and recipient species were the same, so no daily cyclosporine injection was required to suppress the immune system.

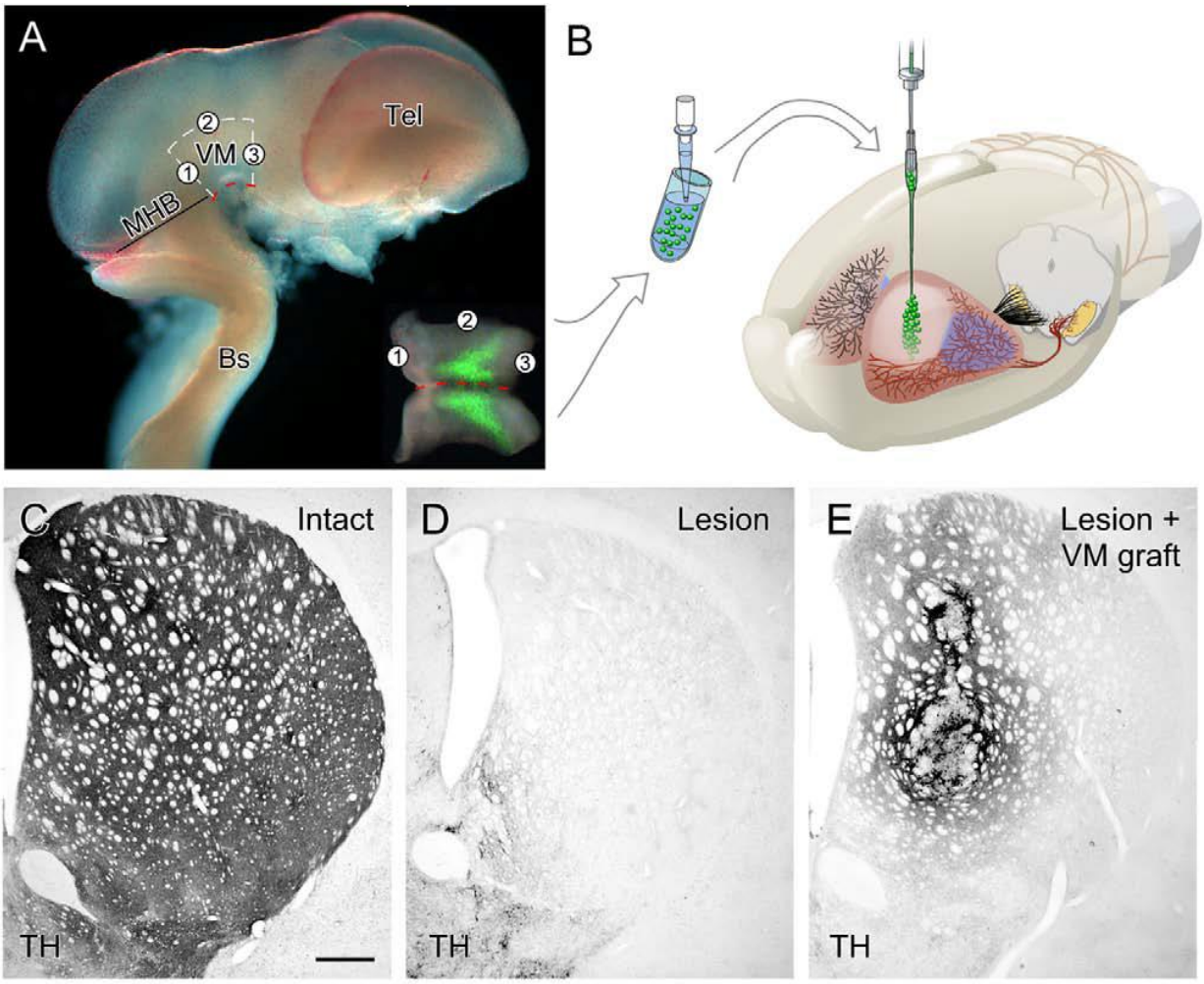

Figure 3.2 Cell transplantation into mouse brain of PD (A) The dashed lines area shows the dissected VM region for cell grafting, (B) shows the VM cell transplantation into the brain of PD after tissue preparation, (C) darkly stained area shows the healthy network of TH-positive fibers from mDA neurons, (D) after injection of 6-OHDA to create the animal model of PD, no TH-positive fibers from mDA neuron can be observed, and (E) illustrates the TH-positive fibers from grafted VM cells after cell transplantation for 6 weeks. [5]

3.1.6.4 Animal perfusion and tissue sectioning

Rats/ mice received a lethal dose of sodium pentobarbitone (Lethabarb, 100mg/kg) prior to intracardial perfusion with 400 mL (rats)/ 50 mL (mice) of warmed PBS followed by 400 mL

(rats)/ 50 mL (mice) of 4% PFA. The brain was then removed and post-fixed in 4% PFA for two hours followed by cryopreservation in 30% sucrose. The brains were frozen using dry ice and stored in a - 80 ℃ freezer prior to sectioning. The brain tissue was either sectioned on a cryotstat and mounted on slides (Chapter 5 and 6) or sectioned by 40 μm in a free floating method (Chapter 7).

3.1.6.5 Tissue chromogenic staining and immunohistochemistry

The tissue slides were washed 3 times for 10 minutes in PBS and quenched in endogenous peroxidase (10%, methano ,10%, hydrogen peroxide and 80% PBS) for 20 minutes before washing. Primary antibody was applied overnight at room temperature prior to washing. Primary antibodies and dilution factors were as follows: chicken anti-GFP (1:1000, abcam), rabbit anti-GFP (1:20000, abcam), rabbit GFAP (1:800) and mouse OX-42 (1:500) (see table 3.1 for the antibody details). Blocking solution (10% NGS serum in PBTA) was then applied for 30 minutes. Secondary antibody (Biotinylated anti-rabbit (DAKO), 1:500 in PBTA) was then added on the slides for 1.5 to 2 hours at room temperature. Vectastain® ABC system kit (20μL A, 20μL B and 5mL PBS) was prepared 30 minutes beforehand. The slides were in the washing procedure before incubating in ABC for 1 hour at room temperature. The slides were again washed before DAB (DAB 100mL: 1 Aliquot (1mL at 50 mg/mL), 2.5 mL of 1% Cobalt Chloride, 2 mL of 1% Ammonium Nickel Sulphate and 94.5 mL PB (0.1 M)) was

applied for 10 minutes. Peroxide H_2O_2 (1%) was applied on the slides for 5 minutes (for free floating the tissue was ready to mount on gelatine slides, dehydrate and mount with DPX medium). The slides were washed in PBS before immersing in H_2O (2 times), 50% ethanol, 70% ethanol, 90% ethanol, 100% ethanol, 100% ethanol and X3B (2 times) for 1 min for each step. Afterward the tissue slides were mounted with DPX medium. Immunohistochemistry procedures were performed as previously described in section 3.1.5.1 after quenching and washing steps.

3.1.6.6 Statistical analysis

Each culture condition was run in triplicate (three scaffolds) on at least 3 independent experiments. All cultures were examined using an inverted fluorescent microscope (Zeiss Axiovert 200) and imaged at 20x magnification (Cell D software, Olympus). Cell counts were made from 10 fields of view per scaffold. Cell counts included: total viable cell (Hoechst+ non-pyknotic nuclei), dead cells (Hoechst+ condensed pyknotic nuclei), total neural stem cells (Nestin+ cells), total neurons (TUJ+ cells), total astrocytes (GFAP+ cells), total oligodendrocytes (NG2+ cells), total dopaminergic neurons (tyrosine hydroxylase, TH+). *In vivo* cell counts included: GFP+ graft derived cells, nestin+, GFAP+, TUJ+ and NG2+ cells. Area of GFP+ staining, TUJ+, GFAP+ and NG2+ were calculated using ImageJ. The observer was blinded to the experimental conditions and each brain was graded for its level

(density) of innervation surrounding the graft and throughout the stratal tissue. The grading was as follows: 0 = no evident innervation surrounding the graft, 1 = low level of innervation, 2 = moderate density, 3 = high density. All data are expressed as mean + SD/ mean + SEM. Student t-tests or one way ANOVAs with Tukey post-hoc tests were used to show significant differences between groups with the level of significance set at 0.05. *, $P \leq 0.05$; ** $p \leq 0.01$; ***, $p \leq 0.001$.

3.1.6.7 Measurement of cell viability *in vitro* and *in vivo*

Hoechst is a common dye often used to specifically stain the nuclei of living or fixed cells in culture and tissues [4]. Hoechst nucleic acid stain is a conventional cell-permeant nuclear dye that expresses blue fluorescence when bound to double-stranded DNA (dsDNA); the blue fluorescence can then be observed by a fluorescence microscope [6]. This dye is commonly used to distinguish dead cells (cells displaying a condensed pyknotic nuclei reflective to apoptotic cell death, figure 3.3) from living cells (that displays large, and non-pyknotic nuclei, figure 3.3). Pyknotic verses non-pyknotic cells on glass or on/in scaffolds could be clearly distinguished. By counting pyknotic and non-pyknotic nuclei, the cell viability *in vitro* can be quantified. Within this thesis cell viability reflects the viable (non-pyknotic) cells as a percentage of total cells (viable and pyknotic).

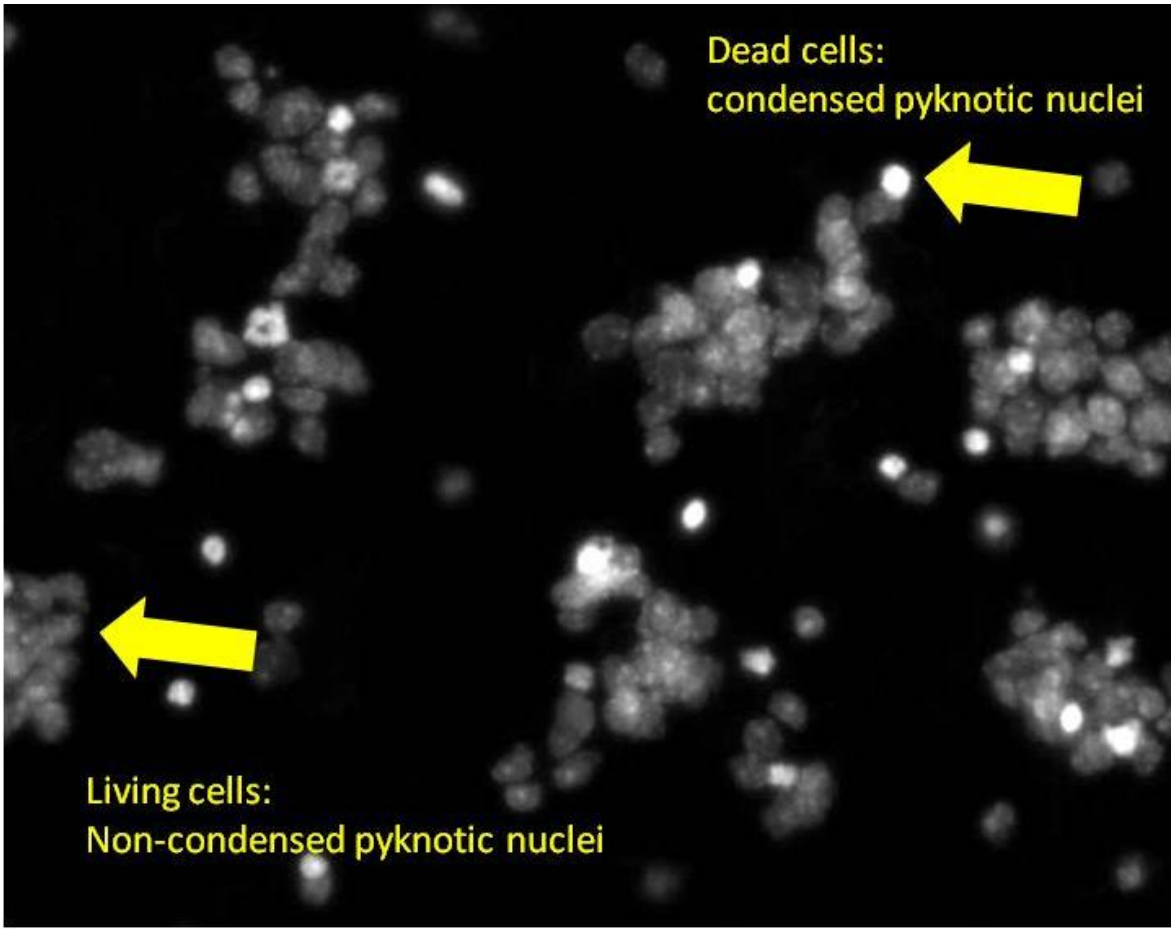

Figure 3.3 Cells stained by Hoechst. Dead cells display a condensed pyknotic nuclei reflective to apoptotic cell death from living cell display large, and non-pyknotic nuclei.

3.2 REFERENCES

[1] Horne MK, Nisbet DR, Forsythe JS, Parish CL. Three-Dimensional Nanofibrous Scaffolds Incorporating Immobilized BDNF Promote Proliferation and Differentiation of Cortical Neural Stem Cells. Stem Cells Development. 2010;19:843-52.

[2] Nisbet DR, Moses D, Gengenbach TR, Forsythe JS, Finkelstein DI, Horne MK. Enhancing neurite outgrowth from primary neurones and neural stem cells using thermoresponsive hydrogel scaffolds for the repair of spinal cord injury. Journal of Biomedical Materials Research Part A. 2009;89A:24-35.

[3] Nisbet DR, Rodda AE, Horne MK, Forsythe JS, Finkelstein DI. Implantation of Functionalized Thermally Gelling Xyloglucan Hydrogel Within the Brain: Associated Neurite Infiltration and Inflammatory Response. Tissue Engineering Part A. 2010;16:2833-42.

[4] Tønnesen J, Parish CL, Sørensen AT, Andersson A, Lundberg C, Deisseroth K, et al. Functional Integration of Grafted Neural Stem Cell-Derived Dopaminergic Neurons Monitored by Optogenetics in an <italic>In Vitro</italic> Parkinson Model. PLoS ONE. 2011;6:e17560.

[5] H. Thompson L, Björklund A. Transgenic reporter mice as tools for studies of transplantability and connectivity of dopamine neuron precursors in fetal tissue grafts. In: Joost Verhaagen EMHIHJWABBGJB, Dick FS, editors. Prog Brain Res: Elsevier; 2009. p. 53-79.

[6] Riddle A, Ling Luo N, Manese M, Beardsley DJ, Green L, Rorvik DA, et al. Spatial Heterogeneity in Oligodendrocyte Lineage Maturation and Not Cerebral Blood Flow Predicts Fetal Ovine Periventricular White Matter Injury. The Journal of Neuroscience. 2006;26:3045-55.

Chapter 4

Characterisation of the stability and bio-functionality of tethered proteins on bioengineered scaffolds

Contents

Monash University

Declaration for Thesis Chapter 4

Declaration by candidate

In the case of Chapter 4, the nature and extent of my contribution to the work was the following:

Nature of contribution	Extent of contribution (%)
Planning, research and article writing	90%

The following co-authors contributed to the work. Co-authors who are students at Monash University must also indicate the extent of their contribution in percentage terms:

Name	Nature of contribution	Extent of contribution (%) for student co-authors only
Bradley J. Turner	Assisted in research	
Clare L. Parish	Assisted in planning & corrected manuscript	
David R. Nisbet	Assisted in planning & corrected manuscript	

Candidate's Signature	[redacted]	**Date** 16.5.2013

Declaration by co-authors

The undersigned hereby certify that:

(1) the above declaration correctly reflects the nature and extent of the candidate's contribution to this work, and the nature of the contribution of each of the co-authors.
(2) they meet the criteria for authorship in that they have participated in the conception, execution, or interpretation, of at least that part of the publication in their field of expertise;
(3) they take public responsibility for their part of the publication, except for the responsible author who accepts overall responsibility for the publication;
(4) there are no other authors of the publication according to these criteria;
(5) potential conflicts of interest have been disclosed to (a) granting bodies, (b) the editor or publisher of journals or other publications, and (c) the head of the responsible academic unit; and
(6) the original data are stored at the following location(s) and will be held for at least five years from the date indicated below:

Location(s)	**Department of Materials Engineering, Monash University**

[Please note that the location(s) must be institutional in nature, and should be indicated here as a department, centre or institute, with specific campus identification where relevant.]

Signature 1	Bradley J. Turner [redacted]	**Date** 16.5.2013
Signature 2	Clare Parish [redacted]	16.5.2013
Signature 3	David Nisbet [redacted]	16.5.2013

Characterisation of the stability and bio-functionality of tethered proteins on bioengineered scaffolds

Ting-Yi Wang [1,2], Bradley J. Turner [1], David R. Nisbet [3*], Clare L. Parish [2*]

[1] Florey Institute of Neuroscience & Mental Health, The University of Melbourne, Parkville, Australia, 3010. [2] Department of Materials Engineering, Monash University, Clayton, Australia, 3800. [3] Research School of Engineering, The Australian National University, Canberra, Australia, 0200.

Corresponding Authors: C.L. Parish [redacted] or D.R. Nisbet [redacted]

Key words: protein tethering, Polycaprolactone, scaffolds, protein stability, GDNF, neurons.

Running title: Stability and functionality of immobilised protein

Abbreviations: E, embryonic day; ED, ethylene diamine; ELISA, enzyme-linked immunosorbent assay; GDNF, glial derived neurotrophic factor; iGDNF, immobilised glial derived neurotrophic factor; iGDNF(v), immobilised glial derived neurotrophic factor scaffolds that have been exposed to vortexing; NSC, neural stem cell; PCL, poly ε-caprolactone.

Acknowledgements: This research was supported by funding from the Australian Research council (DP DP130103131) and Bethlehem Griffith Research Foundation. The authors would like to acknowledge: Ms Francesca Maclean for electrospinning, Dr Francesca Ercole for assistance with the determination of attached amines, Ms Alexandra Rodriguez for SEM imaging and Ms Kiara for critical reading of the manuscript. D.R.N was supported by an Australian Research Council Australian Postdoctoral Fellowship and subsequently an NHMRC Career Development Fellowship (APP1050684). C.L.P was supported by Senior Medical Research Fellowship provided by the Viertel charitable Foundation, Australia. Access to the facilities of the Centre for Advanced Microscopy (CAM) with funding through the Australian Microscopy and Microanalysis Research Facility (AMMRF) is gratefully acknowledged.

4.1 ABSTRACT

Various engineering applications have been utilised to deliver molecules and compounds in both innate and biological settings. In the context of biological applications, the timely delivery of molecules can be critical for cellular and organ function. As such, previous studies have demonstrated the superior benefit of long-term protein delivery, by way of protein-tethering onto bioengineered scaffolds, compared to conventional delivery of soluble protein in vitro and in vivo. Despite such benefits little knowledge exists regarding the stability, release kinetics and functionality of these proteins over time. As way of example, here we examined the stability, degradation and function of a protein, glial derived neurotrophic factor (GDNF), which is known to influence neuronal survival, differentiation and neurite morphogenesis. Enzyme-linked immunosorbent assays revealed that GDNF, covalently tethered onto polycaprolactone (PCL) electrospun nanofibrous scaffolds, remained present on the scaffold surface for 14 days, with no evidence of protein leaching or degradation. The tethered GDNF protein remained functional and capable of activating downstream signalling cascades, as revealed by its capacity to phosphorylate intracellular ERK in a neural cell line. Furthermore, immobilisation of GDNF protein promoted cell survival and differentiation in culture at both 3 and 7 days, further validating prolonged functionality of the protein, well beyond the minutes to hours timeframe observed for soluble proteins under the same culture conditions. This study provides important evidence of the stability and functionality kinetics of tethered molecules.

4.2 INTRODUCTION

Soluble proteins in their natural physiological environment execute their function and are then degraded by enzymes, oxidation, hydrolysis and other reactions over relatively short periods of time; thereby losing their original bio-functionality. As such, repeated synthesis and delivery from the local environment is required for ongoing activity [1]. When soluble proteins are extrinsically introduced in vivo to influence cellular responses (e.g. to promote tissue repair or influence disease progression) they are also only present for short periods of time (typically minutes to hours), due to diffusion into the local physiological environment and degradation. Hence methods of ongoing delivery must be employed which typically rely on the use of cumbersome catheters and infusion pumps. Consequently there is increasing interest to develop improved methodologies to enable the stable delivery of molecules and proteins, and to ensure these factors can be administered in temporally and spatially appropriate manners.

Work by us and others has already demonstrated that protein immobilisation onto bioengineered scaffolds can provide means to control the localisation of biological molecules, create longer lasting stimuli and can be controlled by way of substrata (scaffold) degradation. We demonstrated that both brain derived neurotrophic factor (BDNF) and glial-cell derived neurotrophic factor (GDNF) tethered onto electrospun nanofibrous scaffolds, were capable of promoting primary neural cell proliferation and influencing differentiation in vitro, to a greater extent than culturing cells in the presence of soluble protein [2, 3] (chapter 6). Furthermore, we showed that tethered GDNF maintained long-term biofunctionality in vivo; supporting the survival, differentiation and integration of transplanted primary neural cells for

up to 28 days [3]. Work by others has similarly demonstrated the benefit of tethered proteins. As way of example, photochemically bound nerve growth factor on microporous poly(2-hydroxyethylmethacrylate) was shown to encourage neurite outgrowth of PC12 cells [4]; methacrylamide chitosan immobilised with rat interferon-γ promoted neural differentiation of adult neural stem/progenitor cells [5, 6]; and tethered epidermal growth factor (EGF) on poly(methyl methacrylate)-*graft*-poly(ethylene oxide) significantly enhanced mesenchymal stem cell (MSC) spreading and survival compared to saturating concentrations of soluble EGF [7].

Despite evidence for the benefit of immobilised proteins, little attention has been paid to the amount of protein tethered to biomaterial surfaces, stability of tethered proteins, protein degradation rate, the release kinetics of tethered molecules or the duration of functionality of the protein. Here we investigated the stability of a tethered protein, GDNF, and its functionality using primary cultures isolated from the developing ventral midbrain, enriched with dopaminergic neurons. GDNF has been shown to promote the survival, differentiation and neurite growth, most notably of dopaminergic neurons in vitro and in vivo [8, 9]. GDNF has additionally been shown to delay degeneration of dopaminergic neurons in Parkinsonian animals as well as promote the survival and integration dopamine neurons following transplantation into animal models of the disease [10-13]. GDNF thereby represents an example whereby prolonged protein delivery could have a significant impact on disease progression and treatment. Our findings demonstrated that GDNF remained present and functional on the scaffold surface long term, with no evidence of degradation or leaching, thereby demonstrating stability and functionality of tethered molecules.

4.3 MATERIALS AND METHODS

4.3.1 Synthesis of electrospun scaffolds

Electrospun fibres were produced from polycaprolactone (PCL, Mn 70-90k, Sigma Aldrich, USA), dissolved in a 3:1 (v/v) solution of chloroform (Chem-Supply, USA) and methanol (Chem-Supply, USA). A home built electospinner consisting of a syringe pump (KD-100, KD Scientific, Holliston, USA) and an adjustable DC voltage power supply (Model RR 50-1.25R/230/DDPM, Gamma High Voltage Research, Ormond Beach, FL, USA) was employed using a voltage of 20 kV and a 21G needle. A flow rate of 2 mL/hr and a working distance of 13cm were used and electrospinning took place a room temperature. After collection, the scaffolds were dried in a vacuum oven overnight and stored in a desiccator prior to use. The scaffolds were then aminolysed by immersion in 0.05 M ethylene diamine (ED, Sigma Aldrich, USA), diluted in 2-propanol (Merck Pty, Australia) for 15 min at room temperature. The samples were subsequently washed three times, and sterilised in 70% ethanol for 15 minutes.

4.3.1.1 Confirmation of aminolysation

Scaffolds treated with ethylenediamine (ED, Sigma Alrich Pty Ltd) were dissolved in 100 µL of tetrahydrofuran and 100 µL of PBS, and reacted with 100 µL of fluorescamine (Molecular Probes, 10mg/mL in acetone). The solutions were detected by a plate reader with ex/em = 390/475-490 nm. For the standard curve amine concentrations included 1.49×10^{-6}, 1.12×10^{-6}, 7.45×10^{-7}, 1.49×10^{-7}, 7.45×10^{-8}, 1.49×10^{-8}, 7.45×10^{-9} and 0 mol/g of ED in PBS.

4.3.2 Protein tethering on PCL scaffolds

For immobilisation of GDNF onto PCL scaffolds, 4-(N-maleimidomethyl) cyclohexane-1-carboxylic acid 3-sulfo-N- hydroxysuccinimide ester sodium salt (sulfo-SMCC, Sigma Aldrich, USA) was used as a cross-linker. A 2.5 mg/mL sulfo-SMCC solution was prepared in PBS for an hour at room temperature prior to filtration (0.22 mm filter). The PCL scaffolds, treated with ED, were immersed in sulfo-SMCC for 2 hours at room temperature, prior to being transferred to a recombinant human GDNF solution (4 mg/ml; R & D Systems, USA) overnight at 4 ℃. To ensure that GDNF protein was attached and not adsorbed onto the scaffolds, some scaffolds were vortexed in PBS following protein immobilisation. Amounts of tethered protein, stability and functionality were compared between: PCL scaffolds (PCL), PCL scaffolds tethered with GDNF (PCL_iGDNF) and PCL scaffolds tethered with GDNF and vortexed (PCL_iGDNF(v)).

4.3.2.1 Enzyme-linked immunoabsorbent assay

Enzyme-linked immunoabsorbent assays (ELISA) were performed as described previously [3]. In brief, PCL scaffolds, ± GDNF attachment, were incubated in 1 mg/mL of goat anti-GDNF antibody (R & D Systems, USA) containing 5% donkey serum in PBST (PBS containing 0.05% Tween-20) for 2 hours at room temperature. The scaffolds were washed three times in PBST before being immersed in anti-goat horseradish peroxidase (HRP, 1:2000 in PBST solution containing 2% donkey serum) for 1 hour. After 3 washes in PBST, scaffolds were placed in a 96-well plate where the bound HRP activity was assessed by color development using TMB microwell peroxidase system (R & D Systems, USA). 30 µl of 1M HCl was added to each well to stop the reaction, and the absorbance (450 nm) was measured with a microtitre plate reader (SpectraMax). A standard curve for GDNF was performed (0 -

10,000pg/ml, Figure.4.1) from which the amount of tethered GDNF protein per scaffold could be determined and compared across treatments. To determine the stability of tethered GDNF over time, scaffold samples were collected immediately after protein attachment (day 0) and at day 3, 7 and 14 days after attachment and storage in PBS. Collected scaffolds and supernatant were stored at -80 °C until determination of protein levels by sandwich ELISA.

4.3.3 Immunoblotting

The dopaminergic neural stem cell line, SN4741, was cultured in DMEM, 10% FBS, L-glutamine (2 mM), penicillin/streptomycin (50 U/ml) and glucose (0.6%) in an incubator at 37 °C. For analysis of intracellular GDNF signalling, 100,000 cells were seeded onto PCL scaffolds with or without tethered GDNF for 1 day. Cells were lysed in ice-cold buffer containing 20 mM Tris-Cl, pH 7.5, 150 mM NaCl, 1% Triton X-100, 1% protease inhibitor cocktail (Sigma), 50 mM NaF and 0.2 mM Na3VO4 for 20 min on ice. Lysates were centrifuged at 14,000 rpm for 20 minute at 4 °C to collect supernatants. Protein was quantified using the bicinchoninic acid assay kit (Pierce) using bovine serum albumin standards.

Protein (50 µg) were electrophoresed through 12.5% SDS polyacrylamide gels and transferred to Immobilon PVDF-FL membrane (Millipore). Membranes were blocked with 5% skim milk in Tris-buffered saline with Tween-20 (TBST), pH 8.0, for 30 minutes and incubated with mouse pERK1,2 (1:2,000, #9106, Cell Signalling Technology) and rabbit total ERK1,2 (1:1,000, #9102, Cell Signalling Technology) antibodies in 3% BSA in TBST overnight at 4 °C . Blots were washed 3 x in TBST for 10 minutes and incubated with IRDYe 680 and 800CW conjugated secondary antibodies (1:10,000) followed by 3 x washes in TBST for 10 minutes and detected using the Odyssey Classic infrared imaging system.

Blots were quantified by taking the ratio of pERK/ERK bands and subtracting background intensity.

4.3.4 Microdissection and culturing of cortical neural stem cells/progenitors

All procedures were conducted in accordance with the Australian National Health and Medical Research Council's published Code of Practice for the Use of Animals in Research, and experiments were approved by the Florey Neuroscience Institute animal ethics committee. C57BL/6 mice were housed on a 12 hour light/dark cycle with ad libitum access to food and water. Cells used for *in vitro* culturing were obtained from mice that were time mated overnight, with visualisation of a vaginal plug on the following morning taken as embryonic day (E) 0.5. Ventral midbrain tissue was isolated at mouse embryonic day 11.5 (E11.5).

Pregnant mice (E11.5) were anesthetised with isoflurane prior to cervical dislocation. The collected embryos were immersed in chilled L15 medium (invitrogen), the brains removed and ventral midbrain microdissected. Subsequently the tissue fragments were incubated in 0.1%DNase and 0.05% trypsin (in magnesium and calcium free Hank's buffered saline solution, HBSS) for 15 minutes followed by 3 gentle washes in HBSS. Finally, the tissue fragments were dissociated in N2 media consisting of a 1:1 mixture of F12 and MEM supplemented with 15 mM HEPES buffer, 1 mM glutamine, 6 mg/ml glucose (Sigma-Aldrich), 1.5 mg/ml bovine serum albumin and 1% N2 supplement (all purchased from Invitrogen). Cells were seeded at a density of 175,000 cells /cm^2 onto either poly-D-lysine-coated coverslips or PCL scaffolds and incubated at 37 ^oC in 5% CO_2 for 3 and 7 days. After

3 days and 7 days, the cells were fixed with 4% paraformaldehyde for 20 minutes, washed and stored in PBS containing 0.025% sodium azide until the time of immunocytochemistry.

4.3.4.1 Immunocytochemistry

Fixed cultures were incubated overnight in the following primary antibodies (diluted in 0.3% Triton-X and 5% donkey serum): mouse anti-β tubulin (TUJ, 1:1500, Promega, USA, neuronal marker) and rabbit anti-tyrosine hydroxylase (TH, 1:400 Pelfreeze, rate limiting enzyme in dopamine synthesis and marker of dopaminergic neurons). Cultures were then washed for 10 minutes in PBS before the secondary antibodies were subsequently added and incubated for an hour at room temperature. Secondary antibodies (1:300 in PBS containing 0.3% Triton X and 2% of goat/ donkey serum) were as follows: DyLight 488 donkey anti-rabbit (Jackson immunoResearch), DyLight 549 donkey anti-mouse (Jackson immunoResearch). After washing in PBS, Hoechst (1:1000 in PBS, nuclei marker) was applied for 5 minutes, followed by two washes. The samples were then slide mounted (Dako, USA) and imaged using a fluorescence microscope.

4.3.5 Statistical analysis

All ELISAs, western blots and cell cultures were performed on $\geq$ 3 independent experiments with 3 coverslips or scaffolds included for each condition in each experiment. For assessments of cell viability and differentiation, 10 fields of view per coverslip or scaffold were imaged using a Zeiss200 inverted microscope (images captured at 20x magnification). All data are expressed as mean $\pm$ SD. Student t-tests or one way ANOVAs with tukey post-hoc tests were used to show significant differences between groups with the level of significance set at 0.05.

4.4 RESULTS AND DISCUSSION

Due to the high surface area to volume ratio, tuneable surface chemistry and biomimetic environment, electrospun scaffolds have been applied as a delivery system of biological molecules to influence cell behaviour in vitro and in vivo [14, 15]. As proof of principle, we previously demonstrated that the three-dimensional structure of electrospun PCL scaffolds could be exploited to deliver neurotrophins BDNF and GDNF in vitro to influence cell survival, proliferation and differentiation [2, 3] (chapter 6). Furthermore, implantation of GDNF functionalised scaffolds promoted the engraftment of neural transplants for up to 28 days [3]. However in these former studies, and others like it exploring the benefits of tethered proteins, there remains insufficient knowledge pertaining to the amount of immobilised protein on the scaffold surface, the stability of the tethered protein or the bio-functionality of the molecules over time. In the present study we examined the stability of immobilised GDNF on electrospun PCL scaffolds over 14 days and the biological effects on primary neurons in cultures. Specifically, we examined the ability of tethered GDNF protein to activate intracellular signalling pathways and to promote survival and dopaminergic differentiation of ventral midbrain cells for up to 7 days in culture.

4.4.1 Confirmation of protein immobilisation and maintained presentation without degradation

The electrospun PCL scaffolds were treated with ethylenediamine (ED) to produce amine groups on the fibre surface for protein (GDNF) attachment via a crosslinker, succinimidyl 4-(*N*maleimidomethyl)-cyclohexane-1-carboxylate (SMCC) [2]. The amount of fluorescamine on the scaffolds after aminolysation was measured to be 1.2×10^{-11} mol/ g. Subsequent GDNF attachment onto the scaffolds, via SMCC crosslinking, was confirmed by ELISA.

Figure 4.1A showed significant levels of GDNF on the scaffold (PCL_iGDNF; 975 ± 115 pmol/ml), compared to PCL scaffolds alone (75 + 45; reflective of background readings) or in the absence of the SMCC crosslinker (PCL_sGDNF, 180 + 30 pmol/ml; reflective of physically adsorbed GDNF into the scaffold), suggesting GDFN was chemically attached to scaffolds via the crosslinker SMCC. To confirm that the majority of the protein was tether, and not adsorbed onto the scaffolds, we vortexed the scaffolds for had been immobilised with GDNF to 'shake-off' any protein embedded but not tethered to the PCL fibers. Under these conditions, no significant difference was seen in GDNF levels on PCL_iGDNF and PCL_iGDNF with vortexing (PCL_iGDNF: 975 ± 115, and PCL_iGDNF(v): 650 ± 60, respectively, Figure 4.1A), suggesting that the majority of the protein was chemically attached via SMCC.

To examine the stability of tethered GDNF on scaffolds, the immobilised scaffolds were placed in a 96-well plate, immersed in PBS and stored stationarily in an incubator at 37℃ for up to 14 days, with PCL scaffold samples collected at day 0 (i.e. upon completion of protein immobilisation), day 3, 7 and 14 and supernatant collected at days 1, 3, 7 and 14. All samples were stored at -80 ℃ prior to performing ELISAs. Importantly, we confirmed that freezing of scaffolds had no effect on the stability of the protein, with no significant difference observed in the amount tethered protein at day 0 from fresh verses frozen PCL_iGDNF samples (975 ± 115 and 810 ± 100, respectively, Figure 4.1A-B).

Examination of PCL_iGDNF scaffolds, with or without vortexing, showed no significant difference in GDNF concentration over time (day 0, 3, 7 or 14), demonstrating that the protein remained tethered on the scaffold without degradation for at least 14 days (Figure 4.1B). Results from the supernatant revealed that any adsorbed protein leached from the

scaffold within 24 hours (245 + 75 pmol/ml, Figure 4.1C), and was comparable to the difference observed between iGDNF (PCL_iGDNF: 819 + 100 pmol/ml, Figure 4.2B) and vortexed iGDNF (PCL_iGDNF(v): 515 + 50 pmol/ml, Figure 4.1B). Interestingly, GDNF was only marginally detectable in the supernatant at 3, 7 and 14 days, indicating that the protein measured in the supernatant after 24hrs had subsequently degraded, and thereby further highlighting the benefit of protein tethering for biological applications. Additional longer-term studies are required to assess the rate of degradation of tethered protein on electrospun scaffold surfaces. Degradation of chemically attached proteins is likely to occur through surface erosion of the electrospun scaffolds, hence proteins are likely to remain present in culture for several months.

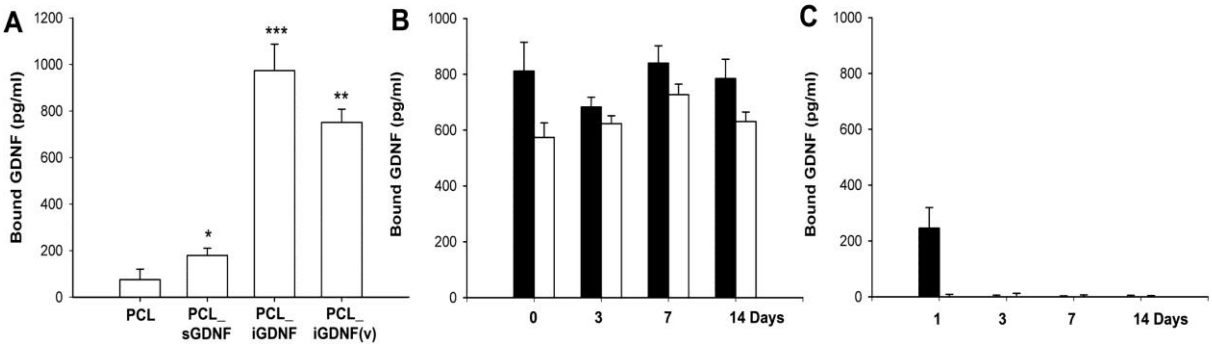

Figure 4.1: Confirmation of protein tethering and stability on electrospun nanofibers.

(A) Immobilisation of GDNF on PCL scaffolds (iGDNF) significantly increases the presentation of protein in culture in the comparison with PCL scaffolds. The majority of protein was firmly attached as reflected by vortexing to remove excess adsorbed protein (iGDNF(v)). (B) Amount of GDNF present on scaffolds at 0, 3, 7 and 14 days after attachment without vortexing (black bars) and with (white bars). No significant decrease was observed in the amount of GDNF on the scaffolds over time, indicative of protein stability. (C) A small amount of GDNF was adsorbed onto the scaffolds at the time of tethering, which leached from the biomaterial within the first day, and subsequently degraded. Data represents Mean $\pm$ SEM. *P < 0.05, **P < 0.01, ***P < 0.001, One-way ANOVA with Tukey post-hoc test.

Here we demonstrate the ability to covalently tether GDNF onto the surface of electrospun PCL scaffolds using the sulfo-SMCC protein crosslinking reaction. This conjunction is dependent on the protein of interest possessing sulfhydryls (thiols, -SH), which readily react with the maleimide group within the sulfo-SMCC at pH 6.5-7.5. However, it is still possible for maleimides to react with amines, such as those found on the N-terminus of a protein or peptide [16]. At pH > 7.5 the reactivity of maleimides to aimines begins to increase and as our reactions were conducted in PBS (pH 7.4) the same chemistry can be used to tether a protein that do not possess a free sulfhydryl group, although the reactivity will be slower. However, It should be noted that hydrolysis of the maleimide group is a possibility during such a conjugation. In this regard, the ability to tether a particular protein may therefore be dependent on the structure of the protein to be tether (i.e. the binding affinity of the maleimide). Furthermore, whilst it may be possible to attach a number of different proteins using this approach it will also be important to ensure that such crosslinking does not interfere with the cellular accessibility of the surface protein.

4.4.2 The biofunctionality of tethered GDNF on cultured neurons

Next we investigated the bio-functionality of tethered GDNF on neural cells in culture, the SN4741 cell line was originally derived by Son et al (1999). In brief, a clonal SN DA neuronal progenitor cell line, arrested at an early DA developmental stage (E14), was established from mice [16]. The phenotypic and morphological differentiation of these cells could be manipulated by environmental cues in vitro and were therefore optimal for studying intracellular signaling of dopaminergic neurons in response to soluble and tethered GDNF. Note, the heterogeneity of ventral midbrain primary cultures (containing only 10% DA neurons) rendered them unsuitable for such cell signaling studies. Using a dopaminergic neural cell line (SN4741), known to express the GDNF receptors c-ret and GFRa1, we

examined the ability of tethered GDNF to induce intracellular phosphorylation of ERK1 and ERK2, key components of the GDNF- ERK signalling pathway. Comparable levels of total ERK1 and 2 could be detected in cells cultured on both PCL or PCL_iGDNF. However, the presence of GDNF significantly increase the phosphorylation of ERK2 (Figure 4.2A), indicating that tethered GDNF was capable of mediating intracellular GDNF signalling. Quantification of band density revealed a significant (4.4-fold) increase in the ratio of phospho-ERK to total ERK following culturing on tethered GDNF (Figure4. 2). Figure 4.2C illustrating the ability of GDNF to to phosphorylate intracellular Erk1/2 of SN4741 cells *in vitro* treated with soluble GDNF (30ng/ml). The results show notable amount of GDNF (57.2 ± 18.5 ng/mL, standard curve not shown) present and activation of p-ERK when tethered to the scaffold similar to soluble GDNF (Figure 4.3). Further to the inclusion of this control data, additional western blots have confirmed the longevity of presentation of functional GDNF following immobilized on PCL. New data illustrates that increased p-Erk at 1hr after soluble GDNF but not after 3days. By comparison, immobilization of GDNF on PCL maintains the ability to activate intracellular GDNF signaling, as reflected by maintained p-ERK activation.

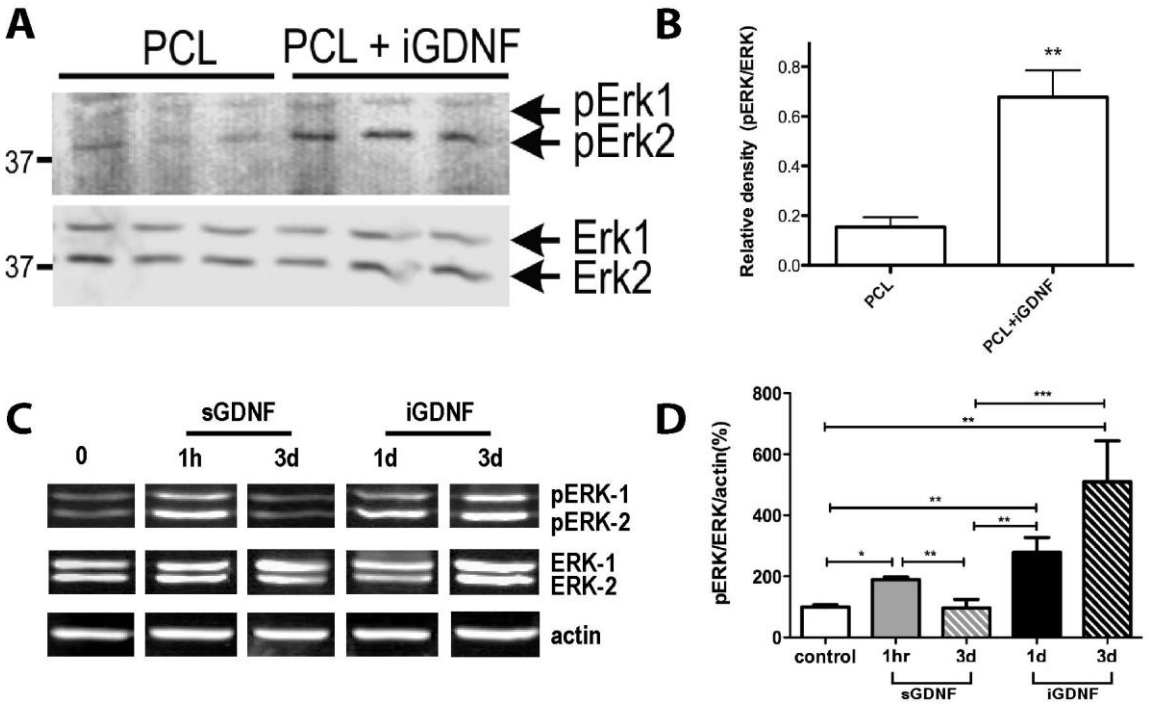

Figure 4.2: Phosphorylation of intracellular ERK confirms functionality of tethered GDNF.

(A) Culturing of SN4741 neural cells on PCL+iGDNF, but not PCL alone, resulted in phosphorylation of intracellular Erk determined by immunoblot analysis, indicitive of intracellular signalling in response to GDNF presentation. (B) Ratio of phospho-ERK/total ERK level. Tethered GDNF results in a 4.4-fold increase in pERK/ERK level compared to culturing on PCL. (C-D) Phospho-ERK levels were significantly elevated after 1 hr stimulation of SN4741 cells with soluble GDNF, but returned to basal levels within 3days. By contrast culturing cells on iGDNF resulted in maintained elevated pERK levels (at 1d and 3d in culture). Data represents Mean $\pm$ SEM. *P < 0.05, **P < 0.01, ***P < 0.001, Students t-test and One-way ANOVA.

Finally we examined the ability of tethered GDNF to not only induce a intracellular response, but also provide a prolonged effect on neural progenitors in culture. In vitro and in vivo GDNF has been shown to promote the survival of various neural populations [17-19], including ventral midbrain dopaminergic progenitors [20-24]. After 3 days in culture, we demonstrated that tethered GDNF significantly improved the viability of VM cells (Hoechst labelled non-pyknotic nuclei) in culture compared to cells cultured on PDL coated glass (56.37% $\pm$ 0.96 and 44.04% $\pm$ 1.78, respectively), or PCL scaffolds alone (46.74% $\pm$ 2.86), Figure 4.3A,C-F. Similarly immobilised GDNF enhanced the number of tyrosine

Hydroxylase immunoreactive (TH+) dopaminergic cells in culture, Figure 4.4 B,K-N. After 7 days, cells cultured in the presence of immobilised GDNF showed no decrease in cell viability or the proportion of dopaminergic neurons compared to 3 days in culture, demonstrating maintained activity of GDNF, whilst cells cultured on PCL alone showed significantly reduced viability over time (Figure 4.4). These findings demonstrate the benefits of maintained presentation and functionality of tethered protein.

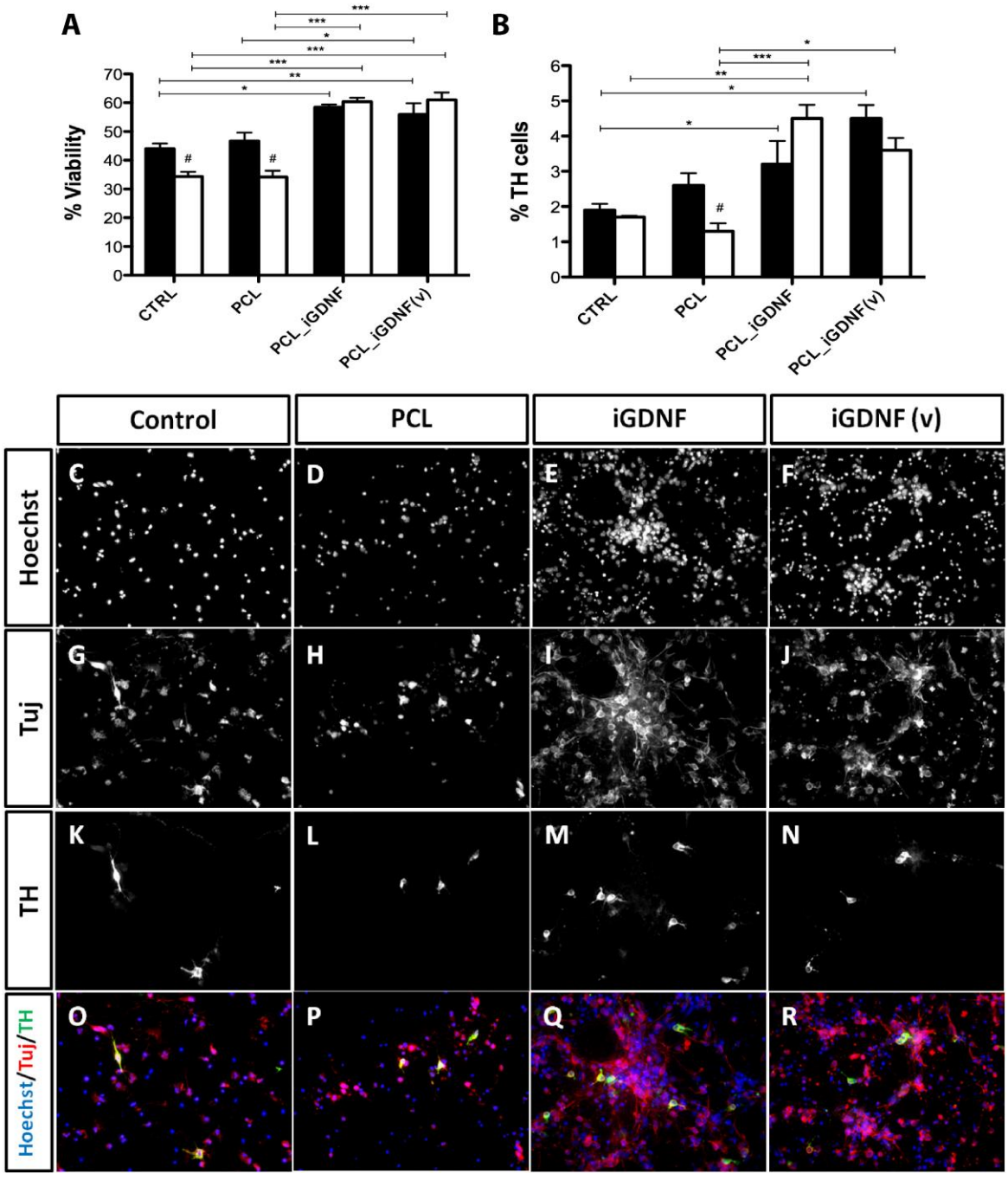

Figure 4.4: GDNF immobilization enhances cell viability and differentiation. (A) Protein tethering, with or without vortexting, significantly increased the viability and (B) proportion of tyrosine Hydroxylase-immunoreactive (TH+) cells in ventral midbrain cultures, compared to culturing on PDL-coated glass (control) or PCL. Black bars: 3 DIV, White bars: 7 DIV. Prolonged culturing (7DIV) resulted in a significant decrease in cell viability and TH cells, effects that could be prevented by maintained presentation of GDNF in culture. (C-F) Representative photomicrographs of Hoechst labelled nuclei, (G-J) TUJ+ neurons, (K-N) TH+ dopaminergic neurons, and (O-R) merged images of VM cells cultured on PDL-coated glass (control), PCL, PCL with immobilized GDNF (PCL_iGDNF), and PCL with immobilized GDNF and vortexed (PCL_iGDNF(v)). Data represents Mean + SEM. *P < 0.05, $^{\#}$P < 0.05, **P < 0.01, ***P < 0.001, One-way ANOVA with Tukey post-hoc test.

The development of assays to provide long-term presentation of molecules is important for increasing our understanding of physiological processes. Most in vitro studies focused on understanding the role of a given molecule in development, adult homeostasis or disease rely on application of soluble proteins in culture; effects that are rapid and transient and often do not reflect the ongoing presentation of a protein that typically occurs in nature. In addition to providing a more relevant assay to understand these basal and pathophysiological functions, the use of tethered proteins can also aid in the development of new treatments. For example, long term delivery of GDNF in vivo, by way of protein tethering onto bioengineered scaffolds, such as microspheres, could be exploited to stall disease progression in PD, or promote the survival and integration of newly transplanted dopaminergic neurons for patients. The development of such protein/molecule tethering technologies will be dependent on ongoing validation of protein/molecule stability and function, using methodologies such as those described here.

4.5 CONCLUSION

Bio-engineering scaffolds, surface immobilised with proteins, have been investigated for their potential to influence cellular responses in vitro and in vivo. While the benefits of tethered proteins have been recognised for some years now, there has been a notable lack of research concentrating on their stability and bio-functionality kinetics. Here we demonstrate, by way of GDNF example, that tethered protein on electrospun scaffolds are stable for 14 days (with no evidence of degradation), capable of activating intracellular signalling cascades, and maintaining cellular effects (GDNF influencing cell viability and differentiation). These findings hold significant potential for the use of biomaterials in presenting and maintaining the activity of proteins in vitro and in vivo, and may impact on the ability to enhance tissue repair.

4.6 REFERENCES

[1] Tessmar JK, Gopferich AM. Matrices and scaffolds for protein delivery in tissue engineering. Advanced Drug Delivery Reviews. 2007;59:274-91.
[2] Horne MK, Nisbet DR, Forsythe JS, Parish CL. Three-Dimensional Nanofibrous Scaffolds Incorporating Immobilized BDNF Promote Proliferation and Differentiation of Cortical Neural Stem Cells. Stem Cells Development. 2010;19:843-52.
[3] Horie N, Maag A-L, Hamilton SA, Shichinohe H, Bliss TM, Steinberg GK. Mouse model of focal cerebral ischemia using endothelin-1. Journal of Neuroscience Methods. 2008;173:286-90.
[4] Frisén J, Johansson CB, Lothian C, Lendahl U. Central nervous system stem cells in the embryo and adult. CMLS, Cell Mol Life Sci. 1998;54:935-45.
[5] Elkabetz Y, Studer L. Human ESC-derived Neural Rosettes and Neural Stem Cell Progression. Cold Spring Harbor Symp Quant Biol. 2008;73:377-87.
[6] Muotri AR, Gage FH. Generation of neuronal variability and complexity. Nature. 2006;441:1087-93.
[7] Pickens CL, Airavaara M, Theberge F, Fanous S, Hope BT, Shaham Y. Neurobiology of the incubation of drug craving. Trends in Neurosciences. 2011;34:411-20.
[8] Haniu M, Hui J, Young Y, Le J, Katta V, Lee R, et al. Glial Cell Line-Derived Neurotrophic Factor: Selective Reduction of the Intermolecular Disulfide Linkage and Characterization of Its Disulfide Structure. Biochemistry. 1996;35:16799-805.
[9] Consales C, Volpicelli F, Greco D, Leone L, Colucci-D'Amato L, Perrone-Capano C, et al. GDNF signaling in embryonic midbrain neurons in vitro. Brain Research. 2007;1159:28-39.
[10] Nakajima K, Hida H, Shimano Y, Fujimoto I, Hashitani T, Kumazaki M, et al. GDNF is a major component of trophic activity in DA-depleted striatum for survival and neurite extension of DAergic neurons. Brain Research. 2001;916:76-84.
[11] Ortiz-Ortiz MA, Moran JM, Ruiz-Mesa LM, Bonmatty RG, Fuentes JM. Protective effect of the glial cell line-derived neurotrophic factor (GDNF) on human mesencephalic neuron-derived cells against neurotoxicity induced by paraquat. Environmental Toxicology and Pharmacology. 2011;31:129-36.
[12] Sandhu JK, Gardaneh M, Iwasiow R, Lanthier P, Gangaraju S, Ribecco-Lutkiewicz M, et al. Astrocyte-secreted GDNF and glutathione antioxidant system protect neurons against 6OHDA cytotoxicity. Neurobiology of Disease. 2009;33:405-14.
[13] Alexi T, Borlongan CV, Faull RLM, Williams CE, Clark RG, Gluckman PD, et al. Neuroprotective strategies for basal ganglia degeneration: Parkinson's and Huntington's diseases. Progress in Neurobiology. 2000;60:409-70.
[14] Nisbet DR, Rodda AE, Horne MK, Forsythe JS, Finkelstein DI. Neurite infiltration and cellular response to electrospun polycaprolactone scaffolds implanted into the brain. Biomaterials. 2009;30:4573-80.
[15] Nisbet DR, Forsythe JS, Shen W, Finkelstein DI, Horne MK. A Review of the Cellular Response on Electrospun Nanofibers for Tissue Engineering. J Biomater Appl. 2009;24:7-29.
[16] Son JH, Chun HS, Joh TH, Cho S, Conti B, Lee JW. Neuroprotection and Neuronal Differentiation Studies Using Substantia Nigra Dopaminergic Cells Derived from Transgenic Mouse Embryos. The Journal of Neuroscience. 1999;19:10-20.
[17] Chen Y, Ai Y, Slevin JR, Maley BE, Gash DM. Progenitor proliferation in the adult hippocampus and substantia nigra induced by glial cell line-derived neurotrophic factor. Experimental Neurology. 2005;196:87-95.
[18] Enomoto H. Regulation of neural development by glial cell line-derived neurotrophic factor family ligands. Anat Sci Int. 2005;80:42-52.

[19] Lee C-S, Tee LY, Dusenbery S, Takata T, Golden JP, Pierchala BA, et al. Neurotrophin and GDNF family ligands promote survival and alter excitotoxic vulnerability of neurons derived from murine embryonic stem cells. Experimental Neurology. 2005;191:65-76.
[20] Kauhausen J, Thompson LH, Parish CL. Cell intrinsic and extrinsic factors contribute to enhance neural circuit reconstruction following transplantation in Parkinsonian mice. The Journal of Physiology. 2013;591:77-91.
[21] Rosenblad C, Martinex-Serrano A, Bjorklund A. glial cell line-derived neurotrophic factor increases survival, growth and function of intrastriatal fetal nigral dopaminergic grafts. Neuroscience. 1996;75:979-85.
[22] Björklund A, Rosenblad C, Winkler C, Kirik D. Studies on Neuroprotective and Regenerative Effects of GDNF in a Partial Lesion Model of Parkinson's Disease. Neurobiology of Disease. 1997;4:186-200.
[23] Redmond DE, Elsworth JD, Roth RH, Leranth C, Collier TJ, Blanchard B, et al. Embryonic substantia nigra grafts in the mesencephalon send neurites to the host striatum in non-human primate after overexpression of GDNF. The Journal of Comparative Neurology. 2009;515:31-40.
[24] Rangasamy SB, Soderstrom K, Bakay RAE, Kordower JH. Chapter 13 - Neurotrophic factor therapy for Parkinson’s disease. In: Anders B, Cenci MA, editors. Prog Brain Res: Elsevier; 2010. p. 237-64.

Chapter 5

Optimizing implantation of electrospun PCL scaffolds with primary neural cell transplantation in vivo

Contents

5.1 INTRODUCTION

5.1.1 Combination of electrospun scaffolds and stem cells for neural tissue engineering

Cell transplantation has been widely studied for brain injury with small lesions or neurodegenerative disease [1-4]. In terms of an extensive and severe lesion in the injured brain, a physical support is likely to be necessary and/or beneficial to replace lost tissue, restore architecture and support regenerating and/or new cells [5-7]. Recently, investigation into the viability of transplanting neural cells that have been pre-seeded onto tissue engineering scaffolds has been explored. Modified poly (D,L-lactic-co-glycolic) acid (PLGA) particle scaffolds with a diameter of 50-100 μm were cultured with neural stem cells (MHP36) for implantation [8]. The neural stem cells were cultured on the particles for a few days and transplanted into the injured cavity, whereby they interacted with the endogenous cells [8]. In another study, amnion-derived multipotent progenitor (AMP) cells were combined with collagen scaffolds for transplantation in animals with penetrating ballistic-like brain injury (PBBI); and the migration and viability of the cells were observed [9]. Compared to the transplanted cells or implants alone, the combined AMP/ collagen implant was found to reduce the axonal degeneration induced previously before implantation, facilitate cell penetration including astrocytes and neural progenitors, and AMP cell migration [9]. Human

marrow stromal cells (hMSCs) were delivered via collagen scaffolds into rats with cortical impact as TBI models [5]. Result shows rats treated with collagen scaffolds seeded with hMSCs had significant improvement in both sensor and motor function compared to the hMSCs transplantation alone [5]. Additionally a combination of collagen scaffolds and hMSCs showed a decrease in the injured volume in the cortex and enhanced protection for neurons in the specific hippocampal area after traumatic brain injury (TBI) [5]. Another study also demonstrated that a combination of hMSCs and collagen scaffolds in TBI models provided extensive vascular formation in the dentate gyrus, hippocampus (CA1 and CA3) and cortex [10].

In summary, studies have shown the advantages of applying scaffolds as a cell carrier for implantation in animals with severe damage to brain tissue. In terms of different combinations of scaffolds and cells, further research is required. Therefore, in this chapter an implantation method together with cell transplantation in the intact brain was optimized to estimate the potential of bioengineered scaffolds for repair in brain injuries/ neurodegenerative diseases, which may involve large lesions, cystic cavities and lost neural pathways. I investigated two different methods to combine scaffolds and cells for implantation purpose, and adopted one for the following research. The optimized implantation method can well control the location and quantity of cell grafts, which is crucial

to maximize the efficiency of cell transplantation to the desired sites in the brain. Additionally the method allows grafted cells being contact with implanted scaffolds, which promote fibre penetration, grafts survival and did not induce inflammatory response after 28 days implantation.

5.2 METHODS

The preparation of electrospun PCL scaffold and ED treatment were prepared according to section 3.1.1.1 (chapter 3). The structure of scaffolds was examined by SEM as previously described in section 3.1.3.1. Sections 3.1.4.1 and 3.1.5 provides details for *In vitro* studies. The cell culture results were stained and analyzed as described in section 3.1.5.1. The experimental groups *in vitro* included: control (glass coated with PDL), and PCL scaffolds with/ without ED treatment. The in vivo study included two groups, cells alone and PCL scaffolds. Each embryo provides enough primary neural cells for cell transplantation to each experimental animal (recipient), and each group contained 5 animals.

5.3 RESULTS AND DISSCUSSION

5.3.1 Electrospun PCL scaffolds support survival and differentiation of GFP+ primary neural cells *in vitro*

Scaffolds for implantation should be nontoxic to cells and not cause a chronic inflammatory response in the physiological environment. Therefore PCL scaffolds were cultured with dissociated primary cortical cells to observe the toxicity prior to *in vivo* experimentation. Numerous viable primary cortical cells were observed under control and PCL culture conditions (distinguished by GFP+ staining and plump, non-pyknotic Hoechst labeled nuclei). After 24hrs, cell viability was approximately 80% under all three culture conditions (PDL-coated glass, PCL and PCL-ED) (figure5.1).

The results demonstrate that GFP primary cortical cells were able to adhere, proliferate and differentiate into all 3 neural phenotypes on PCL scaffolds (Figure 5.2-5.3); additionally neurons possessed visible neurites (axons and dendrites). Overall the *in vitro* study shows that the electrospun PCL scaffolds were biocompatible and capable of supporting primary cortical cells to survive and differentiate after culturing for 24 hours.

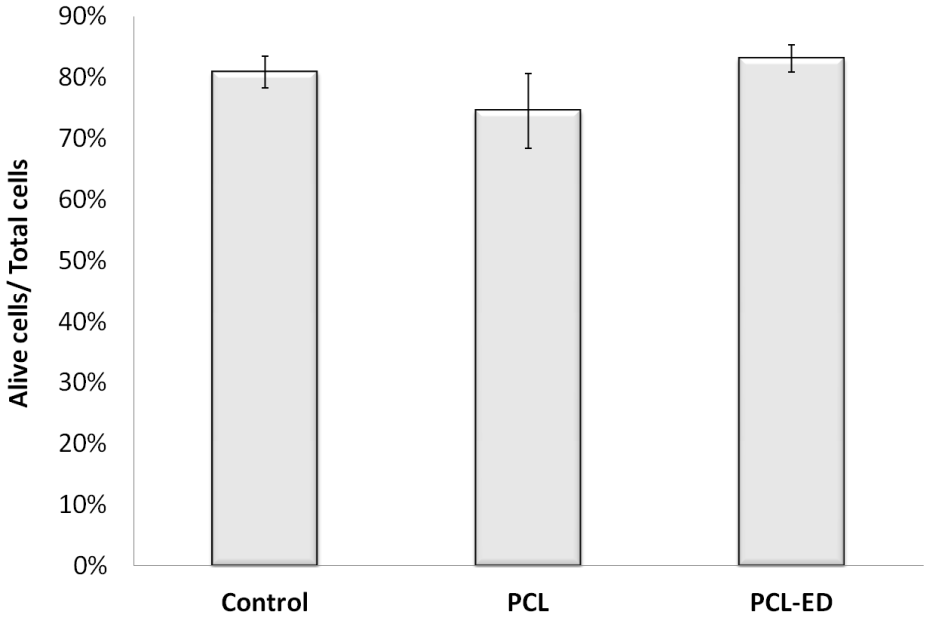

Figure 5.1 GFP cell viability of control, PCL, PCL-ED groups for 1 day cell culture. Mean ± SD (n=3)

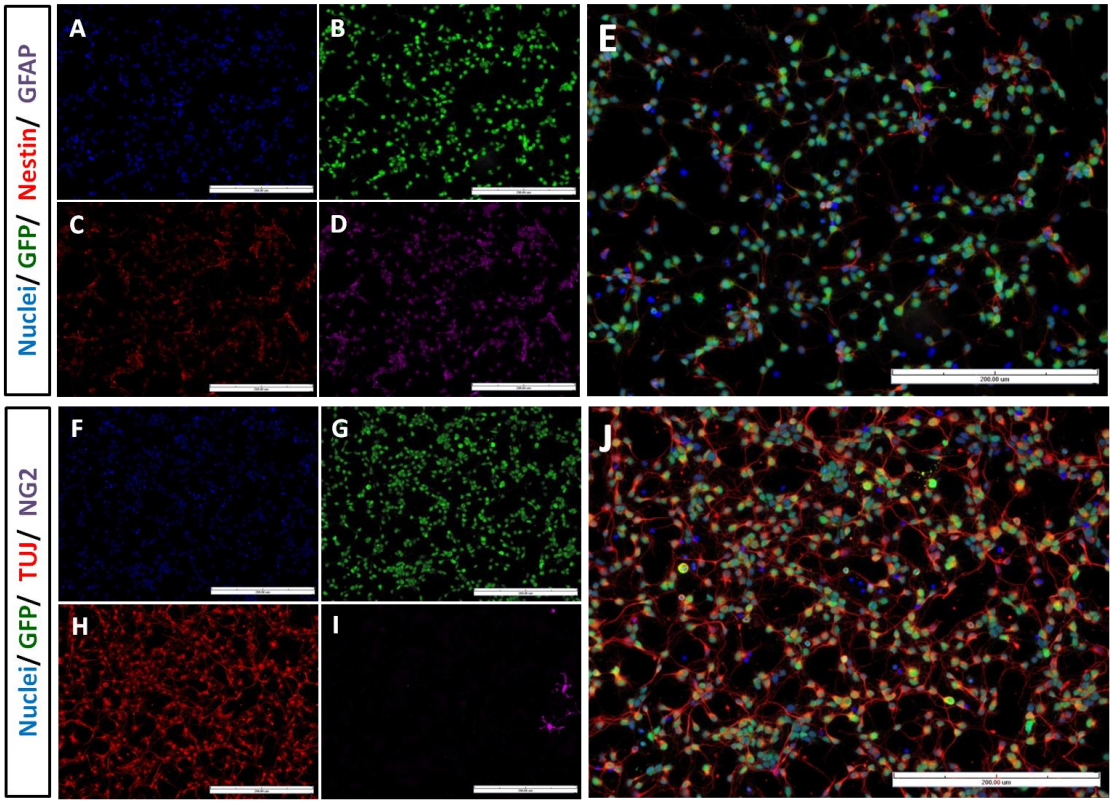

Figure 5.2 (A-J) Fluorescent staining images of GFP primary cortical cells cultured on PDL coated glass (Control). Image (A, F) Hoechst labeled nuclei, (B, G) GFP cortical cells, (C) Nestin+ NSCs, (D)

GFAP+ astrocytes, (E) merge of images of A-D; (H) TUJ+ neurons, (I) NG2+ oligodendrocytes and (J) merge of images of F-I. (scale bar = 200 μm).

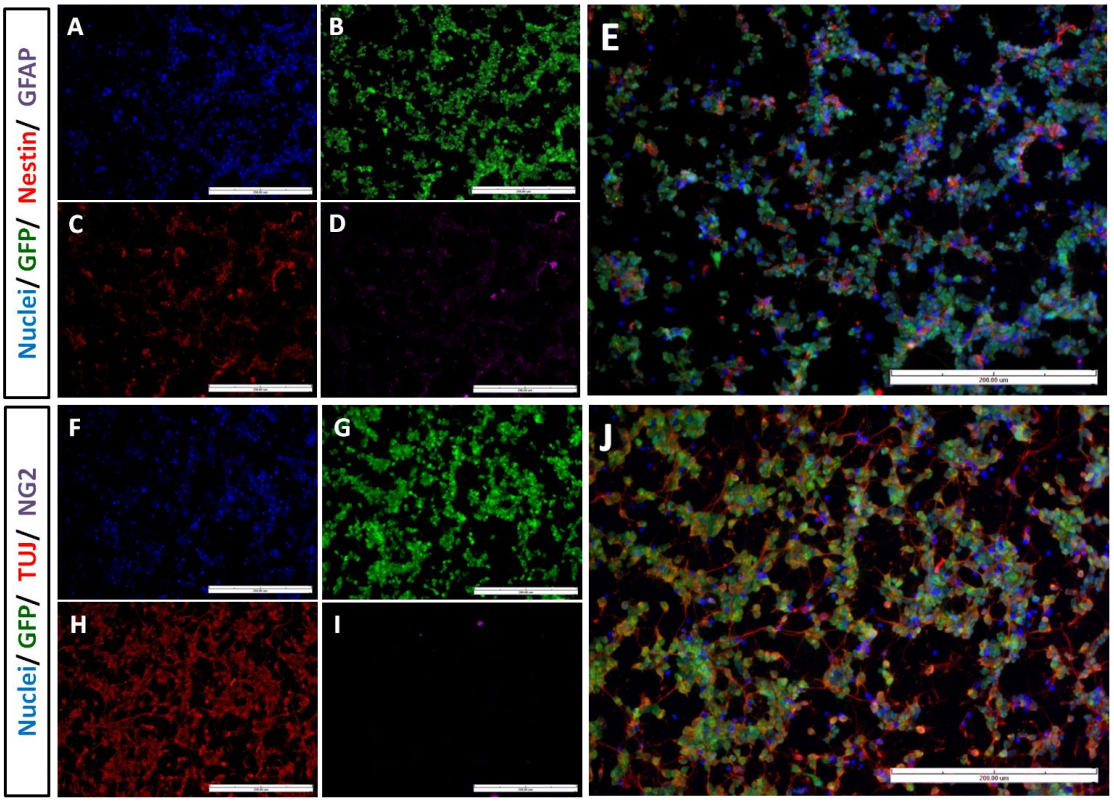

Figure 5.3 (A-J) Fluorescent staining images of GFP primary cortical cells cultured on electrospun PCL scaffold treated with ED as a control group. Image (A, F) Hoechst labeled nuclei, (B, G) GFP cortical cells, (C) Nestin+ NSCs, (D) GFAP+ astrocytes, (E) merge of images of A-D; (H) TUJ+ neurons, (I) NG2+ oligodendrocytes and (J) merge of images of F-I. (scale bar = 200 μm).

In order to optimize the method of combining electrospun scaffold implantation and cell transplantation *in vivo*, the electrospun PCL scaffolds were pre-seeded with cells and rolled by applying a force in one direction from side to side before implantation. Before conducting implantation of the pre-seeded scaffolds, the influence of rolling scaffolds for the implantation with cultured green fluorescent protein (GFP) primary cortical cells pre-seeded

was studied. Figure 5.4 shows that the morphology of GFP primary cortical cells was dramatically changed, and all the cells cultured on the scaffolds had been compressed and detached following rolling. This result led to a need to change the way that cells and scaffolds were introduced into the brain without affecting the viability and differentiation capability. I therefore examined the possibility of dual implantations. The PCL scaffolds were rolled and implanted into the brain and subsequently a cell suspension transplanted either into the cavity of the coiled PCL or adjacent to the rolled scaffolds which had been implanted prior.

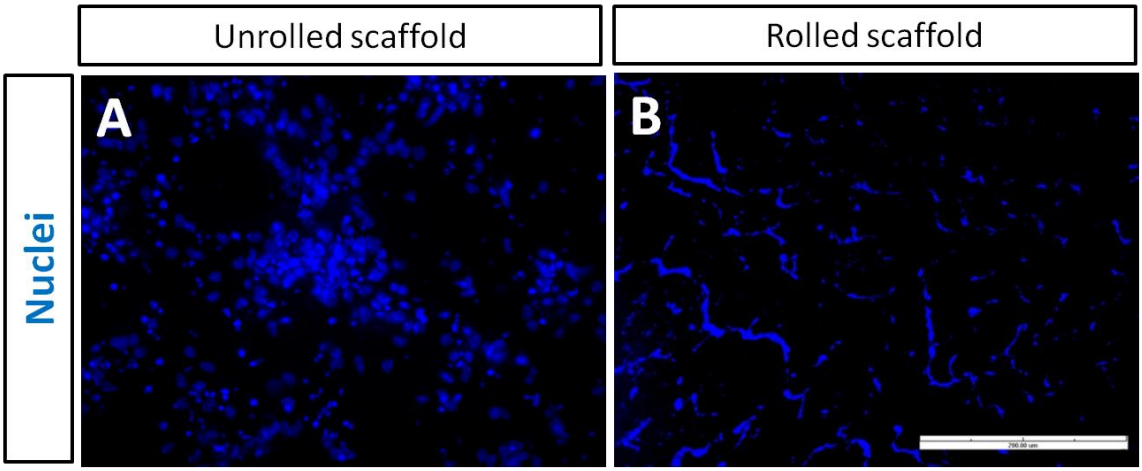

Figure 5.4 The influence of rolling scaffolds cultured with GFP cells on cell morphology and viability. blue: Hoechst labeled nuclei (scale bar = 200 μm).

5.3.2 *In vivo* experiments

5.3.2.1 Histological results

The transplanted GFP primary cortical cells were shown to survive after injecting either into the PCL scaffolds cavity or adjacent to the rolled electrospun PCL scaffolds *in vivo* for 28 days. Figure 5.5 highlights the interaction between transplanted GFP cells and the implanted PCL scaffolds. Additionally, penetration of GFP cells into PCL scaffolds was observed. The transplanted cells seemed to be attracted to the implanted PCL scaffolds, as the result of migration from the injection sites to the scaffold surface (Figure 5.5 (C)). This result indicated that the methodology of sequential implantation (PCL scaffolds followed by cell grafting) was successful. The result shows more cell infiltration and migration when they were injected adjacent to the rolled PCL scaffolds (Figure 5.5 (A, C)), and clear evidence of fiber infiltration was observed with higher magnification in figure 5.5 (B) and (D).

Further immunohistochemistry analysis was required to determine the cellular behaviour of the implanted GFP+ cells; including assessment of differentiation, migration and neurite penetration. Grafted cells were able to differentiate into neurons and astrocytes as shown in figure 5.6 (A) and (E). Additionally clear cellular process infiltration from grafted cells (GFP+), presumably neurites, was observed. These fibres penetrated through the thickness of

implanted scaffolds (Figure 5.7). The method of implanting the cells adjacent to implanted scaffolds showed greater beneficial and convincing results than cells implanted into the cavity. Grafted cells migrated toward and surround scaffolds when they were deposited adjacent to scaffolds, which create more contacting area between grafted cells and scaffolds eventually. In contrast, when cells were deposited in the cavity of implanted scaffolds pockets of air remained trapped in the scaffold cavity, having a negative impact on cell survival, migration and differentiation (Figure 5.8). Additionally cells deposited in the cavity might have less propensity to differentiate into neurons or astrocytes compared to cells adjacent to scaffolds that show greater GFP+ and GFAP+ overlap and GFP+TUJ+ overlap (Figure 5.6). The possible reasons might be the insufficient space for cell development and isolation from nutrients provide by the host tissue when cells were trapped in the cavity of scaffolds. Moreover when cells transplanted adjacent to implanted scaffolds, it shows an increase in extend processes (TUJ+ neurites) into the scaffolds (Figure 5.6, 5.8).

Assessment of grafted cell differentiation revealed that a notable about of the GFP staining area overlayed with TUJ staining, indicating that grafted cells were able to differentiate into neurons and develop neurite that infiltrated into implanted scaffolds *in vivo* (Figure 5.8). Both figure 5.5 and 5.6 showed more mature neurons stained by NeuN and less mature neurons marked by TUJ in figure 5.8. Different degrees of maturity of neurons were stained by

different markers to show the distribution and grafted cell differentiation.

As shown in figure 5.6 and 5.7 tremendous host derived astrocytes penetrated into the scaffolds. It is crucial to determine whether astrocyte penetration had a positive or negative consequence on the grafted cells, and was it a source of neurotrophic factors capable of attracting grafted NSCs into the scaffolds. Immunohistochemistry revealed that BDNF, but not GDNF, was deposited through the implanted scaffolds (Figure 5.9) and overlayed with astrocyte penetration through scaffolds (Figure 5.10). BDNF expression appeared in close association with astrocytes and may support survival and integration of grafted cells [11].

It is notoriously difficult to isolate the graft without also isolating significant amounts of surrounding host tissue. Consequently the signal (amount of BDNF presented through secretion to the scaffold) can be significantly diluted and provide an inaccurate assessment of levels. The choice for immunohistochemistry was therefore selected, whereby the cell graft and implanted scaffold can be examined in vivo. Additionally negative control staining was performed (absence of the primary antibody) to confirm that the labeling observed in figure 5.9 and 5.10 was due to the presentation of BDNF secretion and not non-specific labeling.

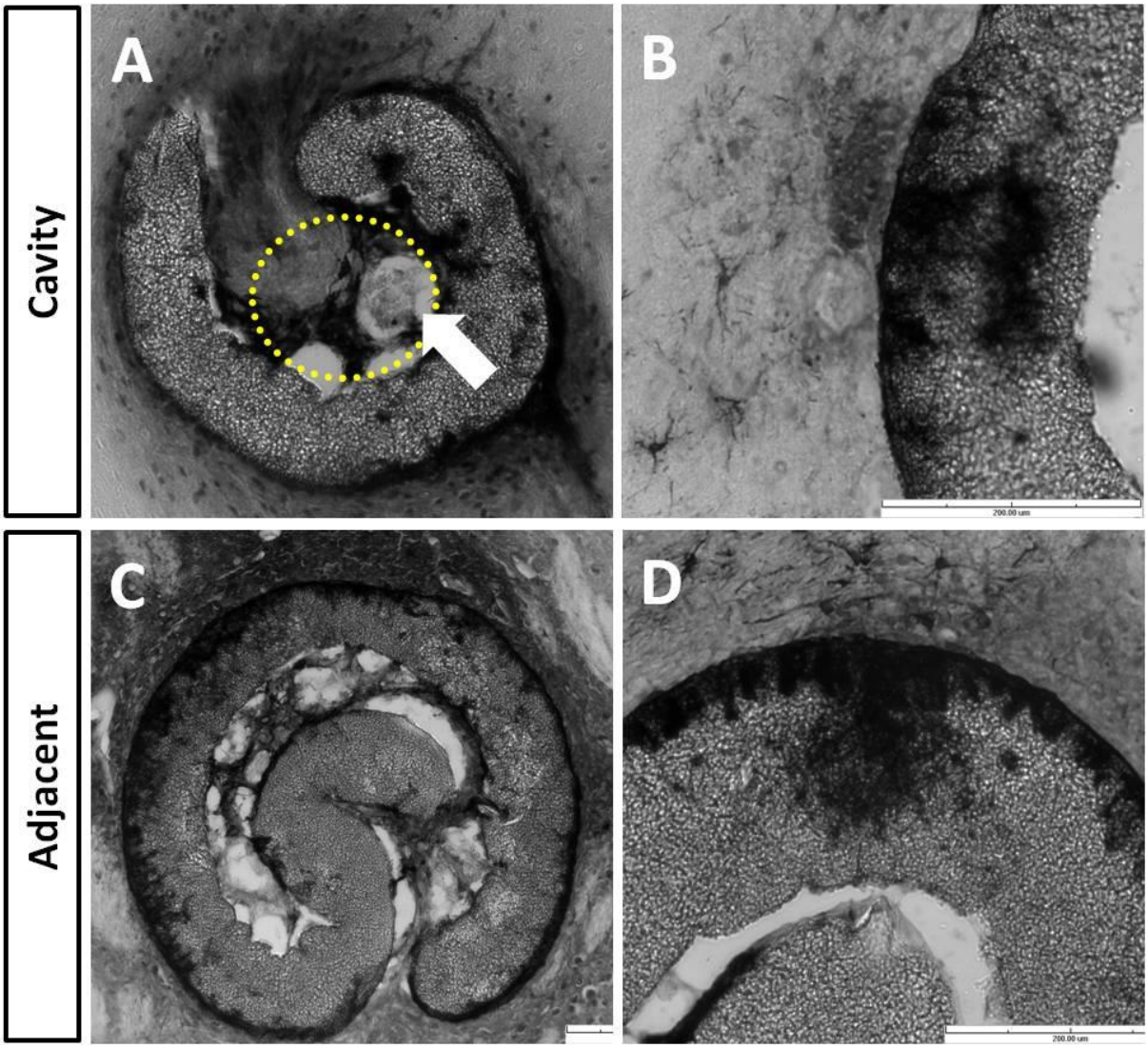

Figure 5.5 The interaction between transplanted GFP primary cortical cells and implanted electrospun PCL scaffolds after implantation in male rats for 28 days. Cells injected in the cavity of rolled scaffolds (the yellow circle shows the injecting site) with different magnifications (A, B), and adjacent to the rolled scaffolds (the injecting site was located on the top left of the image) with different magnifications (C, D). The dark area shows GFP cells. (scale bar = 200 μm)

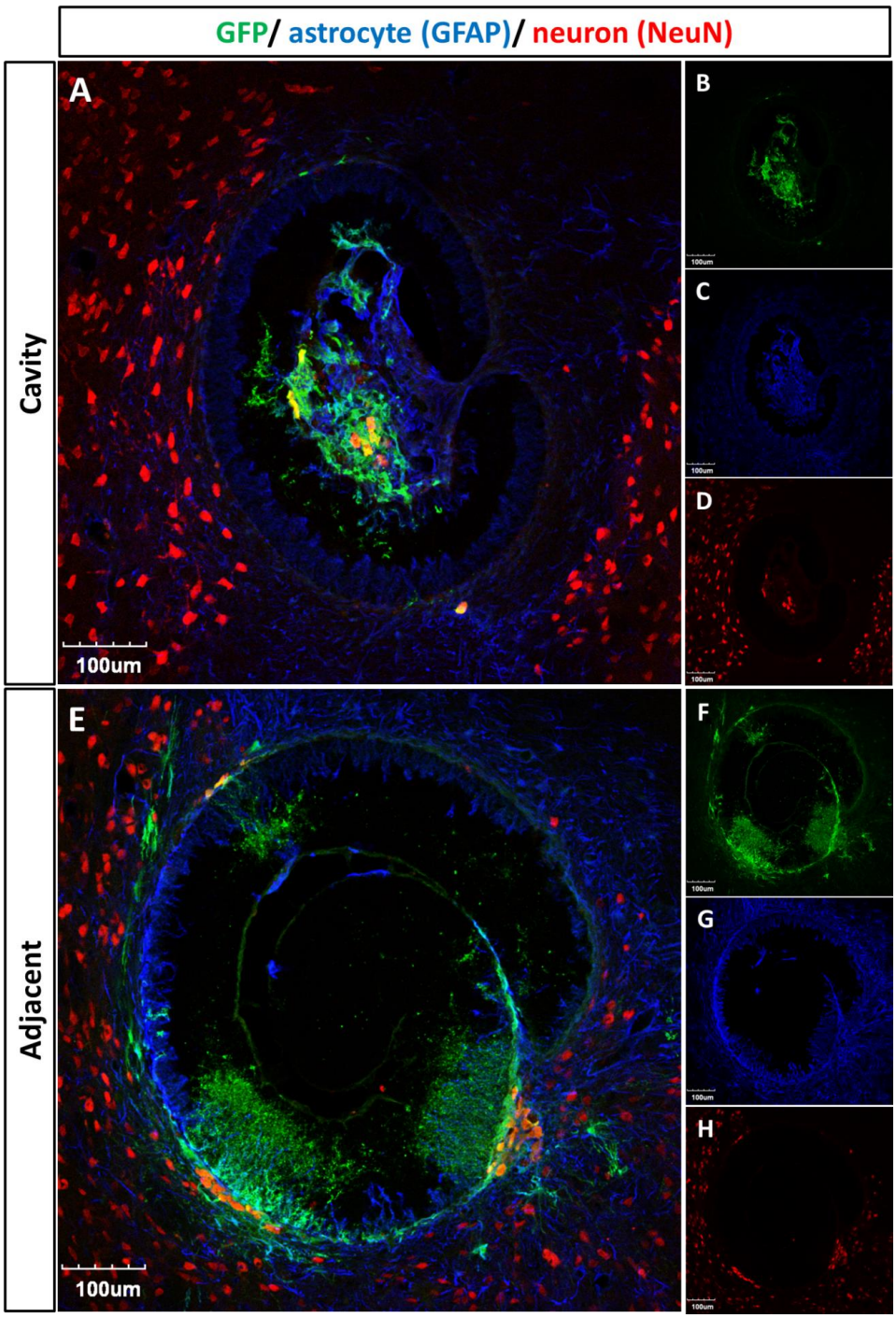

Figure 5.6 Fluorescent staining images of GFP primary cortical cells transplanted with PCL scaffolds *in vivo* for 28 days. (A-D) the cell injected in the cavity of implanted scaffolds and (E-H) adjacent to scaffolds. (A) correspond to (B-D) and (E) correspond to (F-H); (B, F) GFP positive cells (GFP^+), (C, G) astrocyte process ($GFAP^+$) and (D, H) mature neurons ($NeuN^+$).

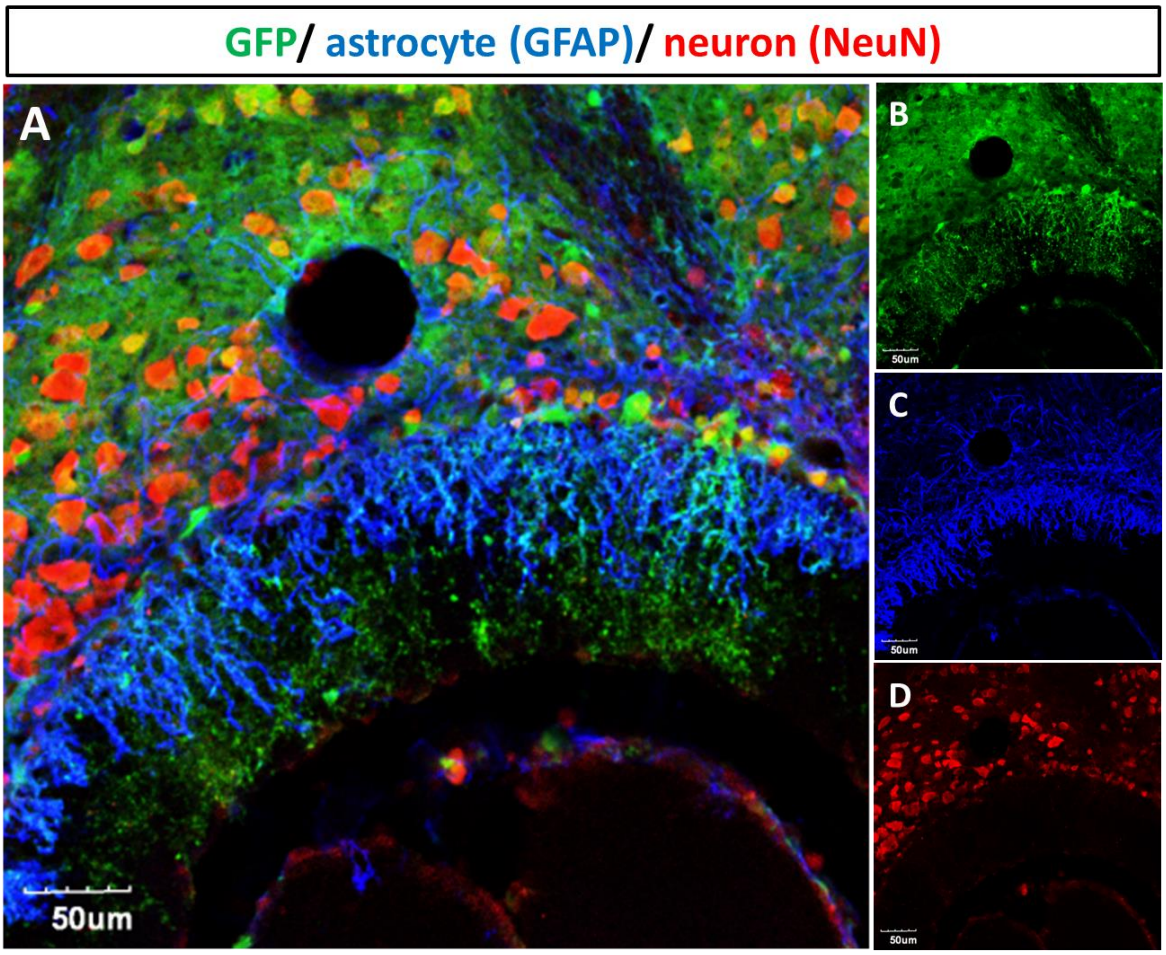

Figure 5.7 Fluorescent staining images of GFP primary cortical cells transplanted with PCL scaffolds *in vivo* for 28 days with high magnification. (A) correspond to (B-D); (B) GFP positive cells (GFP^+), (C) astrocyte process ($GFAP^+$) and (D) mature neurons ($NeuN^+$).

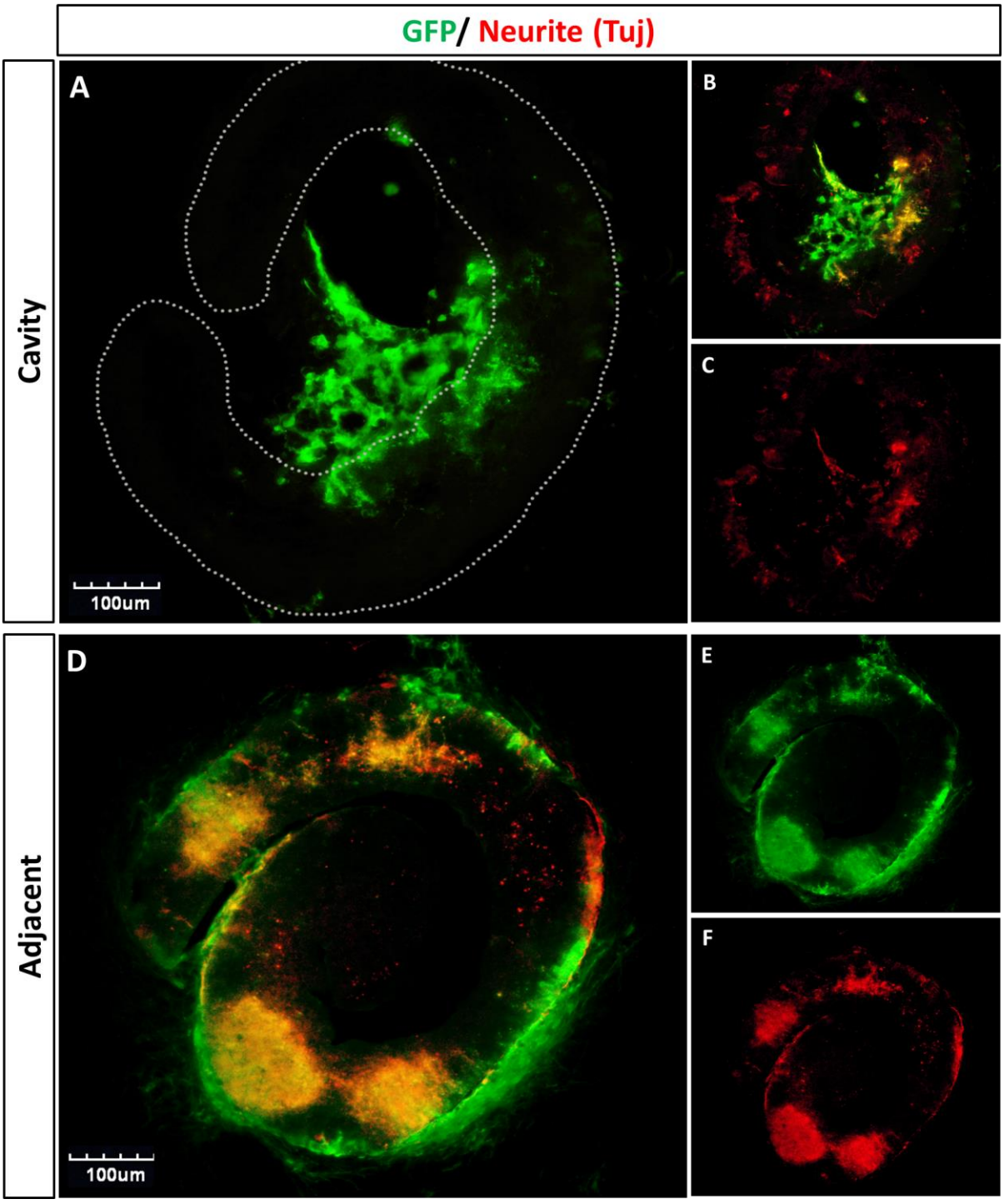

Figure 5.8 Fluorescent staining images of GFP primary cortical cells transplanted with PCL scaffolds *in vivo* for 28 days. (A-C) the cell injected in the cavity of implanted scaffolds and (D-F) adjacent to scaffolds. (A) corresponds to (B-C) and (D) corresponds to (E-F); (B, E) GFP positive cells (GFP^+) and (C, F) mature neurons ($NeuN^+$).

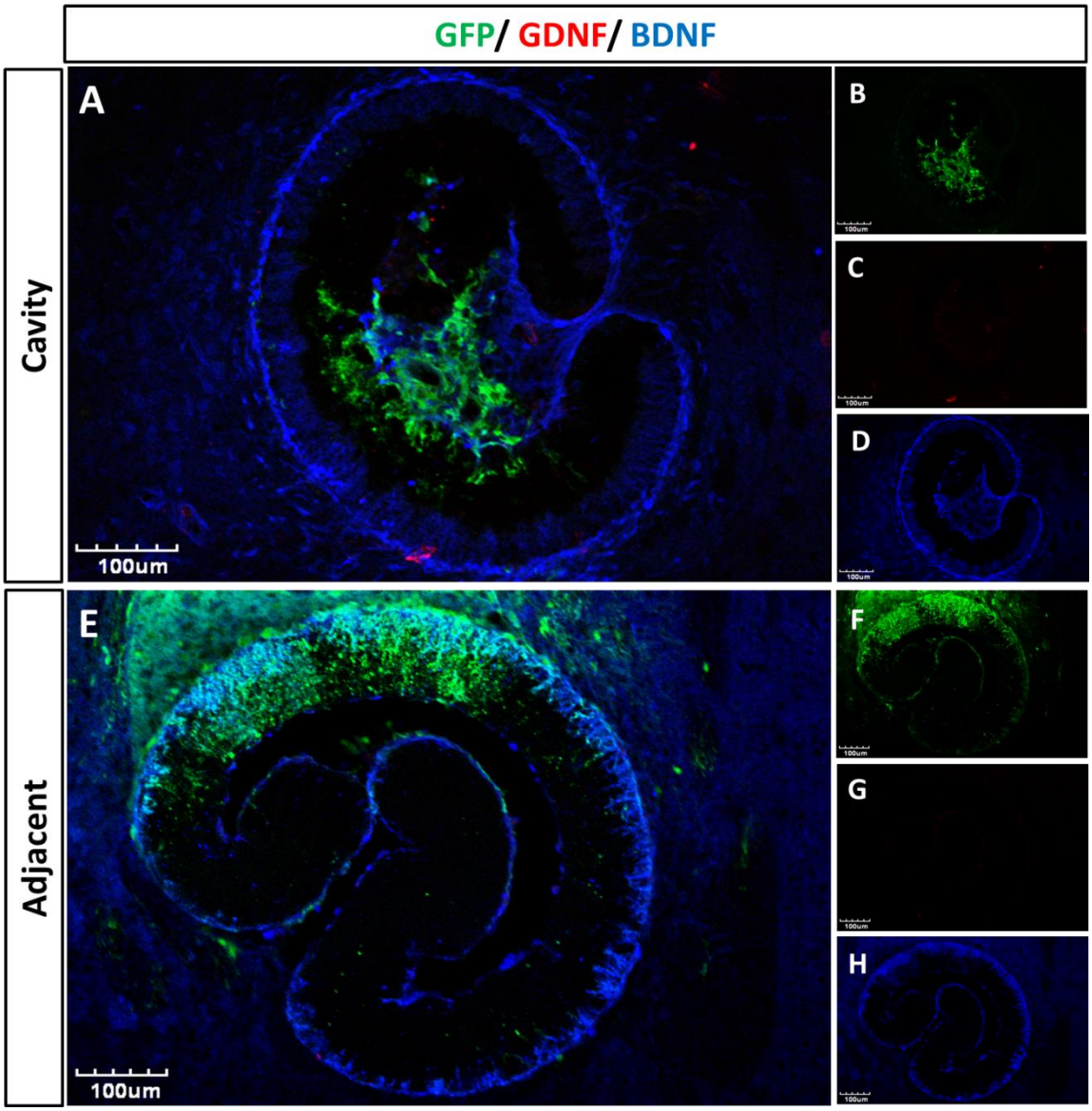

Figure 5.9 Fluorescent staining images of GFP primary cortical cells transplanted with PCL scaffolds *in vivo* for 28 days. (A-D) the cell injected in the cavity of implanted scaffolds and (E-H) adjacent to scaffolds. (A) corresponds to (B-D) and (E) corresponds to (F-H); (B, F) GFP positive cells (GFP^+), (C, G) GDNF deposition ($GDNF^+$) and (D, H) BDNF deposition ($BDNF^+$).

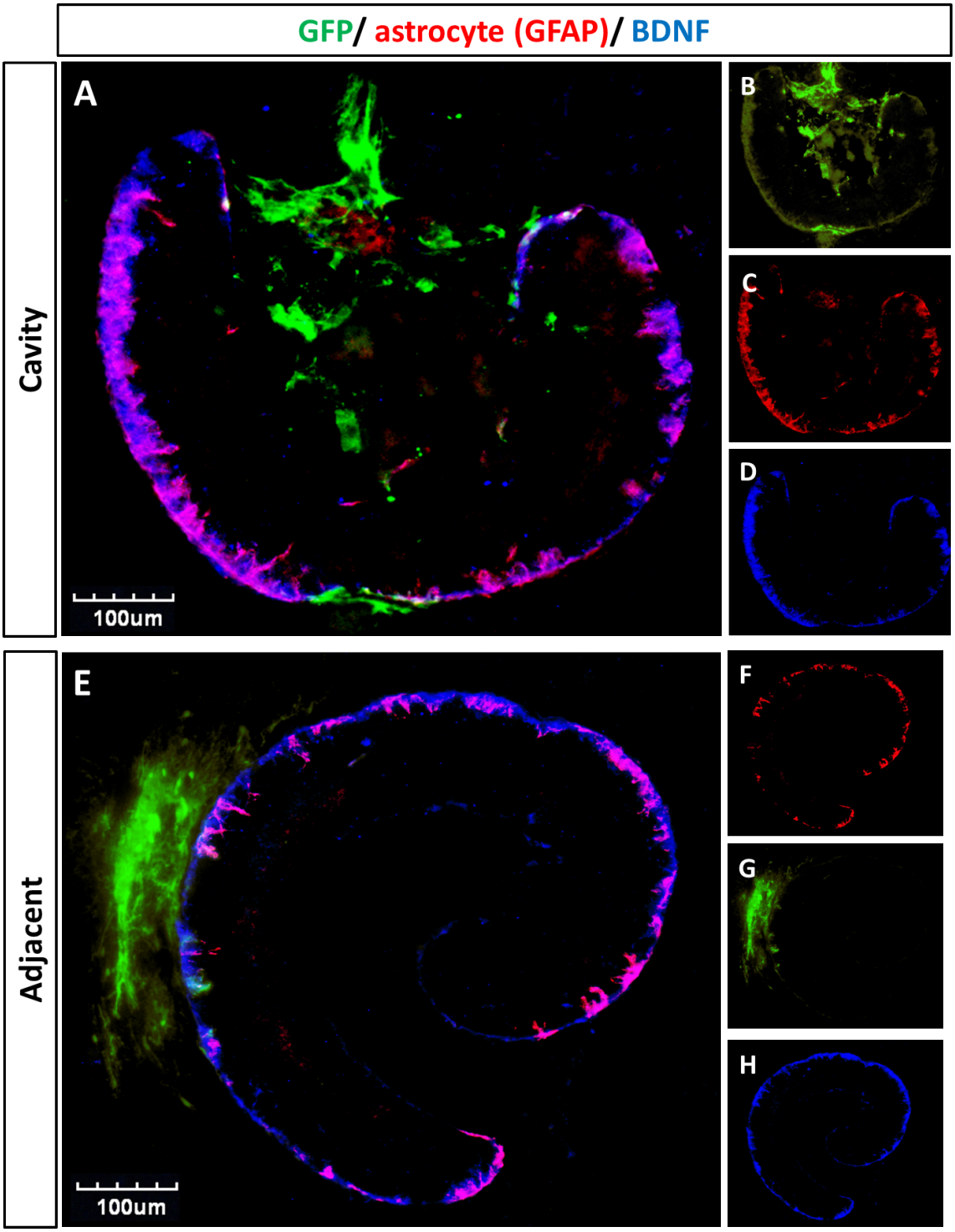

Figure 5.10 Fluorescent staining images of GFP primary cortical cells transplanted with PCL scaffolds *in vivo* for 28 days. (A-D) the cells injected in the cavity of implanted scaffolds and (E-H) adjacent to scaffolds. (A) corresponds to (B-D) and (E) corresponds to (F-H).

Overall the scaffolds were biocompatible and can sustain primary cortical cells in culture. However rolling the scaffolds pre-cultured with primary cortical cells was not a feasible and sterile option to combine scaffolds and grafted cells for implantation purpose, which causes cells shearing off and death. Therefore, an implantation method introducing scaffolds and grafted cells was optimized; the suspension of GFP primary cortical cells was injected in the core, and adjacent to the previously implanted PCL scaffolds. According to the preliminary data this method facilitated cell delivery *in vivo*, with the cells not only surviving but also migrating to and penetrating inside the scaffolds. The results show that cells transplanted adjacent to scaffolds was more promising compared to cells deposited in the cavity of rolled scaffolds due to the negative influence from empty space created inside scaffolds during implantation (note the acellular regions inside the cavity of the rolled scaffold, arrowhead figure 5.5). Added to this, the placement of cells inside the center of the scaffold reduced the graft host interface, including both physical and trophic support. Additionally abundant host-derived astrocytes penetrated into scaffolds, in addition to BDNF deposition after 28 days implantation. The penetration of astrocytes seemed to have a positive impact on the grafts by promoting BDNF secretion; further research is required to investigate the effects of BDNF secretion on NSC development in this context

5.4 CONCLUSION

It is important to fabricate scaffolds that promote cell attachment and penetration for application in brain injury, and this will most likely involve the incorporation of primary cortical cells to encourage cell differentiation and proliferation. The preliminary work here indicates that electrospun scaffolds have the potential to provide a physical support for neural cells adhesion, and maintain cell proliferation and differentiation. Therefore the implantation of PCL scaffolds, in combination with primary cortical cells, may have the potential to encourage regeneration within the injured brain.

Electrospun PCL scaffolds were capable to provide GFP primary cortical cells to adhere, proliferate and differentiate. However GFP primary cortical cells were not able to survive the physical force applied to rolled PCL scaffolds prior to implantation. A new method of combining GFP primary cortical cells with PCL scaffolds was optimised and achieved *in vivo* as a pilot study, with survival, migration and penetration (into the scaffolds) of the transplanted cells being observed. Therefore the implantation method was adopted going forward for this PhD research.

5.5 REFERENCES

[1] Lindvall O, Odin P. Clinical application of cell transplantation and neurotrophic factors in CNS disorders. Curr Opin Neurobiol 1994 Oct;4(5):752-7. 1994.
[2] Longhi L, Zanier ER, Royo N, Stocchetti N, McIntosh TK. Stem cell transplantation as a therapeutic strategy for traumatic brain injury. Transplant Immunology. 2005;15:143-8.
[3] Parish CL, Arenas E. Stem-cell-based strategies for the treatment of Parkinson's disease. Neurodegener Dis 2007;4(4):339-47. 2007.
[4] Rosser AEab, Zietlow Rb, Dunnett SBb. Stem cell transplantation for neurodegenerative diseases. Current Opinion in Neurology. 2007;20:688-92.
[5] Lu D, Mahmood A, Mauney JR, Qu C, Hong X, Kaplan D, et al. Collagen Scaffolds Populated With Human Marrow Stromal Cells Reduce Lesion Volume and Improve Functional Outcome After Traumatic Brain Injury. Neurosurgery. 2007;61:596-603 10.1227/01.NEU.0000290908.38438.B2.
[6] Madigan NN, McMahon S, O'Brien T, Yaszemski MJ, Windebank AJ. Current tissue engineering and novel therapeutic approaches to axonal regeneration following spinal cord injury using polymer scaffolds. Respiratory Physiology & Neurobiology. 2009;169:183-99.
[7] Park KI, Teng YD, Snyder EY. The injured brain interacts reciprocally with neural stem cells supported by scaffolds to reconstitute lost tissue. Nat Biotech. 2002;20:1111-7.
[8] Bible E, Chau DYS, Alexander MR, Price J, Shakesheff KM, Modo M. Attachment of stem cells to scaffold particles for intra-cerebral transplantation. Nat Protocols. 2009;4:1440-53.
[9] Chen Z, Lu XCM, Shear DA, Dave JR, Davis AR, Evangelista CA, et al. Synergism of human amnion-derived multipotent progenitor (AMP) cells and a collagen scaffold in promoting brain wound recovery: Pre-clinical studies in an experimental model of penetrating ballistic-like brain injury. Brain Research. 2010;In Press, Corrected Proof.
[10] Xiong Y, Qu C, Mahmood A, Liu Z, Ning R, Li Y, et al. Delayed transplantation of human marrow stromal cell-seeded scaffolds increases transcallosal neural fiber length, angiogenesis, and hippocampal neuronal survival and improves functional outcome after traumatic brain injury in rats. Brain Research. 2009;1263:183-91.
[11] Nisbet DR, Rodda AE, Horne MK, Forsythe JS, Finkelstein DI. Neurite infiltration and cellular response to electrospun polycaprolactone scaffolds implanted into the brain. Biomaterials. 2009;30:4573-80.

Chapter 6

Promoting engraftment of transplanted neural stem cells/progenitors using biofunctionalised electrospun scaffolds

Contents

Monash University

Declaration for Thesis Chapter 6

Declaration by candidate

In the case of Chapter 6, the nature and extent of my contribution to the work was the following:

Nature of contribution	Extent of contribution (%)
Planning, research and article writing	

The following co-authors contributed to the work. Co-authors who are students at Monash University must also indicate the extent of their contribution in percentage terms:

Name	Nature of contribution	Extent of contribution (%) for student co-authors only
John S. Forsythe	Assisted in planning & corrected manuscript	
Clare L. Parish	Assisted in planning, research & corrected manuscript	
David R. Nisbet	Assisted in planning, research & corrected manuscript	

Candidate's Signature	[redacted]	**Date** 16.5.2013

Declaration by co-authors

The undersigned hereby certify that:

(1) the above declaration correctly reflects the nature and extent of the candidate's contribution to this work, and the nature of the contribution of each of the co-authors.
(2) they meet the criteria for authorship in that they have participated in the conception, execution, or interpretation, of at least that part of the publication in their field of expertise;
(3) they take public responsibility for their part of the publication, except for the responsible author who accepts overall responsibility for the publication;
(4) there are no other authors of the publication according to these criteria;

(5) potential conflicts of interest have been disclosed to (a) granting bodies, (b) the editor or publisher of journals or other publications, and (c) the head of the responsible academic unit; and
(6) the original data are stored at the following location(s) and will be held for at least five years from the date indicated below:

Location(s)	**Department of Materials Engineering, Monash University**

[Please note that the location(s) must be institutional in nature, and should be indicated here as a department, centre or institute, with specific campus identification where relevant.]

Signature 1	John Forsythe	**Date**
Signature 2	Clare Parish [redacted]	16.5.2013
Signature 3	David Nisbet [redacted]	16.5.2013

Promoting engraftment of transplanted neural stem cells/progenitors using biofunctionalised electrospun scaffolds

Ting-Yi Wang,[1,2], John S. Forsythe,[1], David R. Nisbet,[3*], Clare L. Parish,[2,4*]

[1,] Department of Materials Engineering, Monash University, Clayton, Australia, 3800. [2] Florey Neuroscience Institute, The University of Melbourne, Parkville, Australia, 3010.[3] Research School of Engineering, The Australian National University, Canberra, Australia, 0200, [4] Department of Anatomy & Neuroscience, The University of Melbourne, Parkville, Australia, 3010.

* Equal contribution

Corresponding Authors: C.L. Parish [redacted] Florey Neuroscience Institute, The University of Melbourne, Parkville, Victoria, Australia 3010. [redacted]; or D.N. Nisbet [redacted] Research School of Engineering, The Australian National University, Canberra ACT, Australia 0200. P[redacted]

Abbreviations: CNS, central nervous system; CRT, cell replacement therapy; E, embryonic day; ED, ethylene diamine; ELISA, enzyme-linked immunosorbent assay; GDNF, glial derived neurotrophic factor; GFP, green fluorescent protein; iGDNF, immobilised glial derived neurotrophic factor; NSC, neural stem cell; PCL, poly ε-caprolactone; sGDNF, soluble glial derived neurotrophic factor.

6.1 ABSTRACT

With the brain's limited capacity for repair, new and innovative approaches are required to promote regeneration. While neural transplantation for a number of neural disease/injuries have been demonstrated, major limitations in the field include poor cell survival and integration. This, in part, is due to the non-conducive environment of the adult brain, failing to provide adequate chemical and physical support for new neurons. Here we examine the capacity of fibrous poly ε-caprolactone (PCL) scaffolds, biofunctionalised with immobilised glial cell-derived neurotrophic factor (GDNF), to influence primary cortical neural stem cells/progenitors *in vitro* and enhance integration of these cells following transplantation into the brain parenchyma. Immobilisation of GDNF was confirmed prior to *in vitro* culturing and at 28 days after implantation into the brain, demonstrating long-term delivery of the protein. *In vitro*, we demonstrate that PCL with immobilised GDNF (iGDNF) significantly enhances cell viability and neural stem cell/progenitor proliferation compared to conventional 2-dimensional cultureware. Upon implantation, PCL scaffolds including iGDNF enhanced the survival, proliferation, migration, and neurite growth of transplanted cortical cells, whilst suppressing inflammatory reactive astroglia.

Keywords: Polycaprolactone, scaffold, neural stem cell, brain, nerve tissue engineering, transplantation, growth factors, GDNF, plasticity.

6.2 INTRODUCTION

Development of the central nervous system (CNS) is dependent on a tightly orchestrated sequence of events involving the appropriate temporal and spatial presentation of chemical cues and physical support. These same sequences of events are required to repair the injured CNS, however they are either inhibited or significantly attenuated to an extent that repair is extremely limited. Furthermore, current therapies for the treatment of CNS disease or trauma are non-existent, minimally effective and/or associated with unwanted side effects, thereby highlighting the need for new innovative therapies. In this regard, stem cells, due to their self-renewing and differentiation capacity, have received significant attention for their potential in cell-based therapies. While cell transplantation using stem cells/progenitors has shown promise for a number of neurological conditions, and in some clinical trials (see reviews [1-3]), extensive variability, poor cell survival and insufficient integration/reinnervation remain common limitations impeding their further development. Combined, this highlights the need for the development of technologies to improve the microenvironment for transplanted stem cells and residual endogenous cells in an effort to promote neural repair. In this regard the engineering and functionalisation of biomaterials are of increasing interest.

While numerous biomaterials are available, electrospinning of polymers has drawn attention for neural repair due to the ability to recapitulate the local tissue environment through the manipulation of fiber alignment, diameter and inter-fibre distance. These scaffolds provide physical support for new and residual cells, while also maintaining the architecture at the injury site [4-6]. In particular, a number of studies to date have demonstrated the ability of poly (ε-caprolactone) (PCL) to support neural cells *in vitro* and *in vivo* (see reviews [7-9]). Previously we showed the ability of PCL to support neural stem cells (NSC) *in vitro*, resulting in altered proliferation, differentiation and enhanced neurite growth [10-12]. Additionally we have demonstrated that, following implantation into the brain, host derived neurites surrounding the injury site were capable of penetrating the PCL scaffolds, thereby demonstrating biocompatibility and integration [13]. It now remains to be determined to what extent these scaffolds are able to support transplanted NSC/progenitors *in vivo.*

In addition to providing physical support, scaffolds can also be utilised to present chemical cues. A number of studies to date have demonstrated the benefits of administering proteins to influence cell transplantation. Proteins have been administered intra-cerebrally to promote cell survival or suppress cell death cascades, enhance differentiation of transplanted cell and encourage axonal growth and connectivity on implanted cells [14-17]. However, delivery of these proteins is commonly dependent on the co-transplantation of overexpressing cells,

implantation of cannulas and infusion pumps or viral infection of host tissue. Each of these approaches are hindered by problems, including inability to accurately control the site of protein expression, mis-expression in neighbouring nuclei resulting in inappropriate targeting of axons, compromised translation of genes to proteins in cases of severe trauma as well as the inability to down regulate proteins after new cells have appropriately integrated. This highlights the need for improved methods of *in vivo* protein delivery. Several studies now have demonstrated the ability to tether proteins onto scaffolds. In many instances the presentation of immobilised proteins has been shown to be superior to soluble proteins, as endocytosis is prevented, thereby prolonging the period of cellular stimulation [18-20]. We recently immobilised brain derived neurotrophic factor onto PCL scaffolds where it was shown to influence cellular proliferation as well as promote the differentiation of neurons and oligodendrocytes from cortical neural stem cells in culture [12]. Whilst immobilised proteins have been examined *in vitro*, their ability to induce long-term functional outcomes *in vivo*, particularly in the context of supporting neural transplants, requires further investigation.

As two of the major stumbling blocks for the integration of neural transplants into the injured brain are poor cell survival and inadequate reinnervation of the host tissue, in the present study we chose to examine the effects of tethered glial derived neurotrophic factor (GDNF) on cortical neural stem/progenitor cells *in vitro* and *in vivo*. GDNF has been shown to

regulate neural cell behaviour including survival, proliferation, differentiation, and neurite outgrowth *in vitro* [21-24]. Additionally, *in vivo* delivery of GDNF using conventional methods has improved the survival rate and/or neurite growth of both endogenous and transplanted neurons in a number of models of neural injuries [25-30].

The aim of this study was to investigate the potential for electrospun PCL fibrous scaffolds to present tethered GDNF to support cortical neural stem/progenitor cell *in vitro* and upon transplantation. We investigated their ability to support cell survival, proliferation, differentiation and enhance neurite growth, thereby enhancing graft integration.

6.3 MATERIALS & METHODS

6.3.1 Preparation of poly (ε-caprolactone) scaffolds and aminolysation

Poly(ε-caprolactone) (PCL) was obtained from Sigma Aldrich (St Louis, MO, USA, molecular weight = 70000 – 90000). Polymer solutions of 10% (w/v) were prepared for electrospinning by dissolving the PCL in 5 ml of chloroform and methanol (Merck Pty Ltd, Australia) at a ratio of 3:1 (v/v). The solution was placed in a glass syringe with a 18 - gauge needle for electrospinning at +20 kV to -5 kV with a 0.394 mL/h flow rate and a working distance of 10 cm from the plate. The collected PCL scaffolds were dried in a vacuum oven overnight at 30 ℃. Scaffolds were then cut into squares (0.5 cm^2) and aminolysed by immersion in 0.05 M ethylenediamine (ED, Sigma Aldrich, USA) diluted with 2-propanol (Merck Pty, Australia) for 15 minutes at room temperature. The samples were subsequently washed in milliQ water three times for 10 minutes and stored in a desiccator under vacuum. The samples were sterilised in 70% ethanol for 15 minutes and washed with sterilised PBS prior to *in vitro* and *in vivo* testing.

6.3.2 Scanning electron microscopy (SEM)

The scaffolds were coated with 2 nm of platinum using a Cressington sputter coater. PCL

samples were tilted at 45 degrees and splutter coated at approximately 50-100 turns/per minute for 30 seconds. A scanning electron microscope was then used for examination of the scaffold architecture (JEOL JSM-840A SEM W filament). The SEM variables were set as: 20.0 kV (accelerating voltage), 8 mm (working distance), 3000X (magnification) and 1×10^{-9} A (probe current). Fibre diameters were measured using Image J software.

6.3.3 Biofunctionalisation of PCL scaffolds with glial-cell line derived neurotrophic factor

For immobilisation of GDNF onto the PCL scaffolds, 4-(*N*-maleimidomethyl)cyclohexane-1-carboxylic acid 3-sulfo-*N*- hydroxysuccinimide ester sodium salt (sulfo-SMCC) was used as a cross-linker, as previously described by Horne et al., 2010. In brief, a 2.5 mg/mL sulfo-SMCC solution (Sigma Aldrich, USA) was prepared in PBS with 1 hour agitation at room temperature prior to filtration (0.22 μm filter). The PCL scaffolds, treated with ED, were immersed in sulfo-SMCC for 2 hours at room temperature, prior to being transferred to a solution containing recombinant human GDNF (0.5 or 4 μg/ml; R & D Systems, USA) overnight at 4 ℃.

6.3.4 Confirmation of GDNF attachment by enzyme-linked immunosorbent assay and immunhistochemistry

An enzyme-linked immunosorbent assay (ELISA) was used to verify the attachment of

GDNF onto the scaffolds in samples prepared in parallel to those scaffolds used *in vitro* and *in vivo*. Scaffolds (PCL, PCL with soluble GDNF or PCL+immobilised GDNF) were washed 3 times in PBST (PBS containing 0.05% Tween-20) prior to blocking in 5% normal donkey serum. The scaffolds were then immersed in 1 μg/mL of goat anti-GDNF antibody (R & D Systems, USA) prepared in PBST for 2 hours at 37 ℃. The scaffolds were then washed three times in PBST before being incubated in anti-goat horseradish peroxidase (HRP, 1:2000 in PBST solution containing 2% donkey serum). Scaffolds were again washed (3x10 minutes in PBST) and placed in a 96-well plate where the bound HRP activity was assayed by color development using TMB microwell peroxidase system (R & D Systems, USA). The reaction was stopped by addition of 1M HCl, and finally the absorbance (450 nm) was measured with a microtitre plate reader (SpectraMax). ELISA was performed on triplicate scaffolds for each treatment group and repeated for the 3 independent *in vitro* cultures as well as the *in vivo* implantation of scaffolds.

The attachment of GDNF onto the PCL-ED scaffolds was additionally confirmed by immunohistochemistry at 28-days after implantation. Brain sections containing the scaffolds were mounted onto slides for immunostaining against GDNF. All slides were washed (3 x 10 minutes in PBS) and quenched in endogenous peroxidase (10%, methanol, 10%, hydrogen peroxide and 80% PBS) for 20 minutes before additional washes. Subsequently the primary

antibody, goat anti-GDNF (2 μg/mL) prepared in PBS containing 0.3% triton-X, was applied overnight at room temperature. The next day the slides were washed prior to blocking in 10% donkey serum in PBS for 30 minutes. The secondary antibody, biotinylated anti-goat (1:500, DAKO), was added for 1.5 hours at room temperature. The sections were then incubated in avidin peroxidase (Vectastain® ABC system kit) and then reacted with diaminobenzidine (DAB, Sigma). The slides were washed in PBS before dehydrating in ethanol, delipiding in X3B and coverslipping with DPX mounting medium.

6.3.5 Animals

All procedures were conducted in accordance with the Australian National Health and Medical Research Council's published Code of Practice for the Use of Animals in Research, and experiments were approved by the Florey Neuroscience Institute animal ethics committee. Mice and rats were housed on a 12 h light/dark cycle with ad libitum access to food and water. Cells used for *in vitro* culturing and transplantation were obtained from mice that were time mated overnight, with visualisation of a vaginal plug on the following morning taken as embryonic day (E) 0.5. All tissue was isolated at mouse embryonic day 14.5 (E14.5). *In vitro* culturing of primary cortical cells was performed using tissue obtained C57BL/6 time mated mice while donor tissue for transplantation was obtained from C57BL/6 time-mated mice expressing green fluorescent protein (GFP) under the β-actin promoter. The ubiquitous

expression of GFP within the donor tissue enabled distinction of the grafted cells within the host brain.

6.3.5.1 Preparation of primary cortical cell suspensions for *in vitro* and *in vivo* application

Pregnant mice (E14.5) were anesthetised with isoflurane prior to cervical dislocation. The collected embryos were immersed in chilled L15 medium (invitrogen), the brains removed and cortices microdissected. Subsequently the tissue fragments were incubated in 0.1%DNase and 0.05% trypsin (in magnesium and calcium free Hank's buffered saline solution, HBSS) for 15 minutes followed by 3 gentle washes in HBSS. Finally, the tissue fragments were dissociated in N2 media consisting of a 1:1 mixture of F12 and MEM supplemented with 15 mM HEPES buffer, 1 mM glutamine, 6 mg/ml glucose (Sigma-Aldrich), 1.5 mg/ml bovine serum albumin and 1% N2 supplement (all purchased from Invitrogen).

For *in vitro* culturing, cells were seeded at a density of 175,000 cells /cm^2 onto either poly-D-lysine-coated coverslips or prepared PCL scaffolds and incubated at 37 ^oC in 5% CO_2 for 3 days. After 3 days, the cells were fixed with 4% paraformaldehyde for 20 minutes, washed and stored in PBS containing 0.025% sodium azide until the time of immunocytochemistry. For *in vivo* transplantation, **t**he cells were suspended at a density of 100,000 cells/μL in HBSS containing 0.1% DNase and stored on ice until the time of

implantation.

6.3.5.2 Cell transplantation and PCL implantation

Twenty-four male Wistar rats received implants of either: PCL scaffolds, GFP cells, GFP cells + PCL scaffold or GFP cells + PCL_iGDNF scaffold. In all animals, immune suppression (Cyclosporine A, 15 mg/kg, subcutaneous) was commenced 24 hours prior to transplantation, and 10 mg/kg given daily thereafter for 28 days.

Rats were anesthetised using 5% isoflurane (Baxter; Deerfield, IL, USA), and the level of anaesthesia subsequently maintained at 2% for the duration of the surgery. The rats were placed into a stereotaxic frame (Kopf) and an incision made in the scalp to reveal the skull. Bi-lateral craniotomies were drilled overlying the striatum at 1.0 mm anterior and 2.5 mm lateral to bregma. The sterile scaffolds were rolled and inserted into a 21 G needle. The needle was then stereotaxically implanted into the striatum at 1.0 mm anterior and 2.5 mm lateral relative to bregma, and to a depth of 5.0 mm below the dural surface. A plunger was subsequently inserted into the needle making contact with the top of the previously loaded scaffold. This remained static as the needle was removed leaving the scaffold in the desired location.

Micro-transplantation, using a fine glass capillary (50 µm internal diameter) attached to a 5 µl Hamilton syringe, was used to deliver a total of 1 µl of the cortical GFP neural stem/progenitor cell suspension (100,000 cells) into the striatum (1.0 mm anterior and 2.5 mm lateral to bregma, 3.5 mm below the dural surface), directly adjacent to the scaffold.

Four weeks after transplantation, animals received a terminal dose (100 mg/kg, i.p.) of sodium pentobarbitone (Virbac; Peakhurst, Australia) and were transcardially perfused with warmed saline (0.9% w/v), followed by ice-cold paraformaldehyde (4% w/v in 0.1M phosphate buffer). The brains were post-fixed for 2 hours in 4% paraformaldehyde and cryo-protected overnight in sucrose (30% w/v in 0.1M phosphate buffered saline) before being coronally sectioned on a cryostat (10 series collected at a section thickness of 20 µm).

6.3.6 Immunohistochemistry

Immunohistochemical procedures on primary cortical cultures or brain sections mounted on slides were performed as previously described [31]. Primary antibodies and dilution factors were as follows: chicken anti-GFP (1:1000, abcam), rabbit anti-GFP (1:20000, abcam), mouse anti-β tubulin (TUJ1, 1:1500, Promega, USA; neuronal marker,) and rabbit anti-glial fibrillary acidic protein (GFAP, 1:800, Dako Cytomation, Denmark; astrocyte marker), rabbit anti-NG2 (NG2, 1:500 Millipore; oligodendrocyte marker) and mouse anti-nestin (Nestin,

1:200, Millipore, neural stem cell marker). Secondary antibodies for (i) direct detection were used at a dilution of 1:200 DyLight 488, 549 or 649 conjugated donkey anti-mouse, anti-chicken or anti-rabbit (Jackson ImmunoResearch); and (ii) indirect with streptavidin-biotin amplification—biotin conjugated anti-rabbit (1:500; Jackson ImmunoResearch) as described above. All i*n vitro* cultures were counter-stained with the nuclear marker Hoechst (1:1000, Invitrogen) for 5 minutes.

From *in vitro* cultures, all PCL scaffolds and coverslips were slide mounted and, along with immunostained brain sections, coverslipped using DAKO mounting media. Brightfield and fluorescent images were captured using either a Zeiss epifluorescent or Olympus confocal microscope.

6.4 RESULTS & DISCUSSION

The future of cell based therapies for the treatment of neural injuries, resulting from trauma or neurodegenerative disease will be dependent on improved methodologies to promote the survival and integration of new cells into the host tissue. In the present study, we examined the ability of electrospun PCL scaffolds functionalised with immobilised GDNF to provide structural and chemical support for cortical neural stem cells/progenitors in vitro and following cell transplantation. Specifically, we examined cell survival, proliferation, and differentiation in vitro and in vivo, as well as graft integration (fiber growth) upon transplantation.

6.4.1 Characterisation of PCL and GDNF immobilisation

Electrospun scaffolds have been extensively studied due to their bio-mimetic properties to the extracellular matrix in the physiological environment [32, 33]. Previously we demonstrated that random alignment of PCL fibres, together with greater interfibre distances, were superior at supporting neurons and neurite growth *in vitro* and *in vivo*, in comparison to aligned fibres having smaller interfibre distances [11-13]. Therefore, in the present investigation electrospun PCL scaffolds were specifically fabricated with random fibre alignment, a micron fiber diameter and micron inter-fiber distances, in order to encourage cell infiltration and the

ingrowth of cellular processes (i.e. neurites). Using SEM, we confirmed that the resultant electrospun fibers had a mean fiber diameter of 2.3 $\pm$ 0.6 μm (figure 6.1 A).

The PCL scaffolds were chemically functionalised with the neurotrophin, GDNF, in an effort to influence cell survival, differentiation and to promote neurite growth. The tethering of GDNF onto PCL scaffolds was confirmed with ELISA prior to *in vitro* culturing and *in vivo* implantation into the host brain, as well as by immunohistochemistry at 28 days after implantation (Figure 6.1). Initially the electrospun PCL scaffolds were aminolysed via treatment with ethylene diamine (ED). The resultant presentation of amine moieties on the surface of the scaffolds was important for attachment of the cross-linker sulfo-SMCC and subsequent GDNF tethering. ELISA results demonstrated that a significantly greater amount of GDNF was attached on PCL scaffolds in the presence of the sulfo-SMCC cross-linker (PCL_iGDNF) compared to its soluble counterpart (PCL_sGDNF), Fig. 6.1 B. This was true whether low (0.5 μg/ml) or higher (4 μg/ml) concentrations of GDNF were used for conjugation. As higher concentrations of GDNF resulted in more GDNF attachment compared to low (1.4 + 0.1 and 0.9 $\pm$ 0.2, respectively), this dose was used for protein tethering in all subsequent *in vitro* and *in vivo* studies. Interestingly, the addition of GDNF in the absence of sulfo-SMCC cross-linker (PCL_sGDNF) resulted in detectable levels of the protein by ELISA, significantly higher than the control (PCL), even in instances were wash

times were extended, Fig.1B. This indicated that a proportion of GDNF was physically adsorbed onto the surface of the PCL fibers.

GDNF attachment was additionally confirmed by immunohistochemistry at 28 days after implantation into the brain of rats. A cross section through the PCL scaffold embedded within the brain, depicted in Figure 6.1 C and D, illustrates that GDNF attachment was not only on the surface of the scaffold but throughout its entire thickness. These findings demonstrate that GDNF protein can be tethered onto electrospun PCL scaffolds via sulfo-SMCC crosslinking with concentration dependency, and maintained for at least 28 days *in vivo*, thereby establishing a long-term delivery system for proteins.

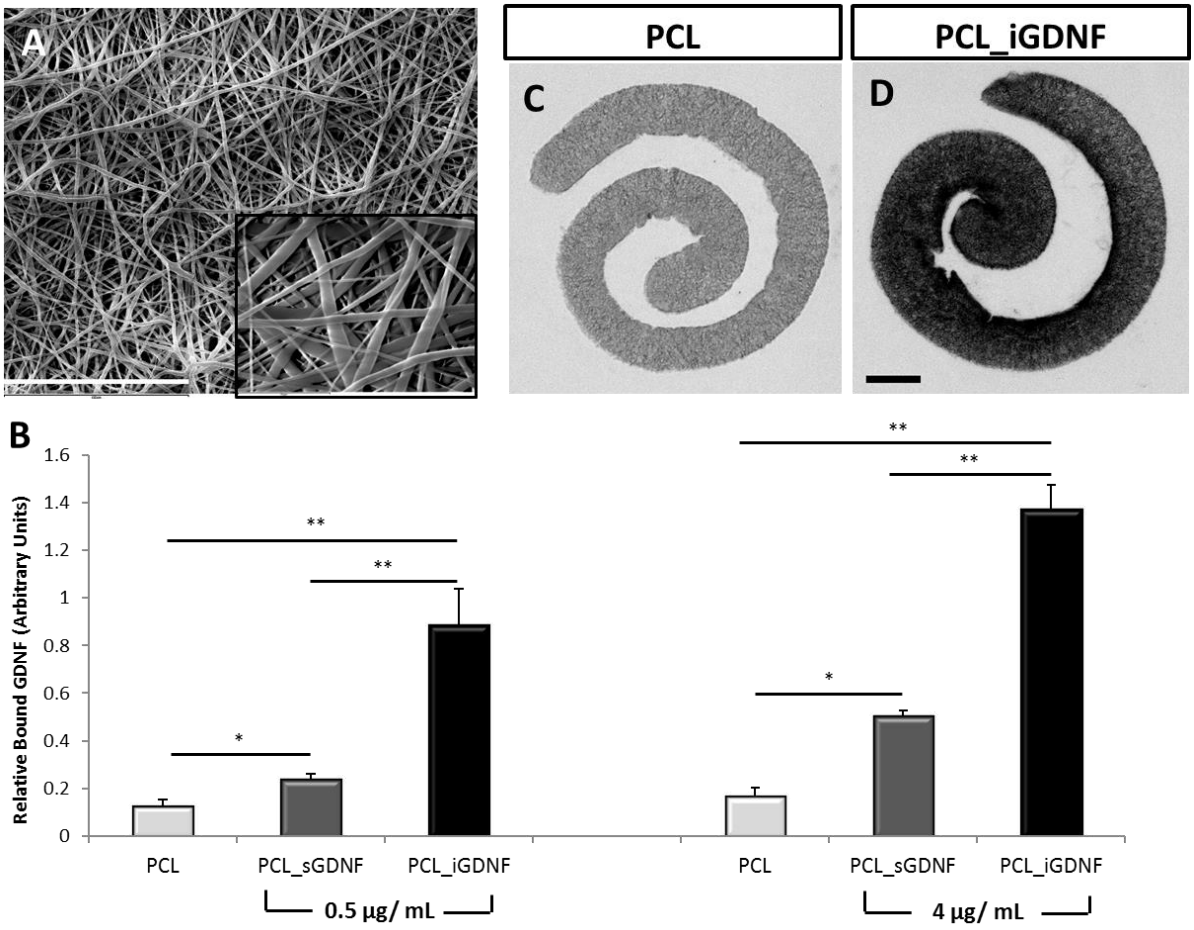

Figure 6.1 Microstructure of electrospun poly ε-caprolactone scaffold and confirmation of GDNF immobilisation. (A) SEM image shows the fibrous structure of electrospun PCL scaffolds. (B) GDNF ELISA confirms the attachment of GDNF onto PCL-ED scaffolds via sulfo-SMCC crosslinker. (C) Cross section of PCL scaffolds and (D) PCL scaffold + immobilised GDNF after implantation into the rat brain for 28 days. Immunohistochemistry against GDNF confirms the presence of immobilised GDNF after 28days in vivo. Data represents Mean + SEM. *P<0.05, **P<0.01, One way ANOVA with Tukey post-hoc test. Scale bars = 100 um.

6.4.2 Effect of modified PCL scaffolds on cell survival, proliferation and neural differentiation in vitro

In a number of neural injuries, including stroke and traumatic brain injury, cortical neurons are lost, resulting in a wide range of sensory, cognitive and motor deficits. In this regard, primary cortical cultures provide a relevant cell population in which to study the benefits of electrospun scaffolds, including physical and chemical modifications, in the support of neural transplants.

The three dimensional, as well as macroporous structure of electrospun scaffolds provides an enhanced surface area-to-volume ratio with high porosity that has been shown to influence cell survival, proliferation, differentiation and neurite growth, see review [9]. In support, we recently demonstrated the ability of PCL scaffolds to support neurospheres and their differentiation *in vitro*, in a manner superior to conventional two dimensional cultureware [12]. Here we confirmed the biocompatibility of cortical neural stem cell/progenitors on PCL as well as their responsiveness to iGDNF *in vitro*, prior to *in vivo* implantation. Cells were cultured on either PDL-coated glass coverslips (Control), PCL-ED scaffolds (PCL), PCL-ED scaffolds with soluble GDNF (PCL_sGDNF) or PCL-ED scaffolds with iGDNF (PCL_iGDNF). Primary cortical cells cultured on PDL-coated coverslips showed a viability rate of 48% $\pm$ 2% (figure 6.2 A), with a significant (37%) increase in cells when grown on

PCL (65% ± 3%). Presentation of GDNF, a neurotrophin known to promote the survival of neural cells [34], either soluble (i.e. absorbed into the scaffold, PCL_sGDNF) or tethered onto the PCL fibers (PCL_iGDNF), resulted in a significant increase in cell viability (77% ± 2% and 93% ± 6%, respectively) in the comparison with the control (glass coated with PDL) and unmodified PCL scaffolds.

We wished to ascertain whether the increased proportion of viable cells observed on modified PCL scaffolds was the consequence of survival or additional proliferation. Previous work has demonstrated that nanofibre, as well as the aminolysation of scaffolds can enhance neural stem cell proliferation [12, 35] and self-renewal of embryonic stem cells, via activation of the small GTPase Rac and phosphoinositide 3-kinase [36]. Here we demonstrate that culturing on randomly aligned PCL scaffolds of microfiber, rather than nanofibre, diameter also promoted proliferation, with a significant increase in the proportion of Nestin+ NSCs cultured on PCL compared to controls (28.3% ± 5.3% and 3.9% ± 0.7%, respectively), Figure 6.2 B,D,E,F. Electrospun scaffolds can also enhance cell adhesion *in vitro* and i*n vivo* through their high porosity and surface area to volume ratio, and by mimicking aspects of the extracellular matrix. While the increase in cell viability on PCL versus control is comparable to the increase in Nestin+ cells, we cannot disregard the possibility that PCL may also be acting to promote cell adhesion.

In addition to the physical attributes of fibrous scaffolds to enhance Nestin+ populations, GDNF has also been shown to act as a mitogen, affecting the proliferation of neural stem cells within the hippocampus and enteric nervous system [37-39]. We therefore examined the effects of tethering GDNF onto PCL scaffolds on the proportion of Nestin+ cells within primary cortical cultures. While we observed a significant increase from the controls (control: 4% $\pm$ 1%, PCL_iGDNF: 42% $\pm$ 4%), the percentage of Nestin+ were similar between PCL and PCL_iGDNF, suggesting that the physical properties of the PCL, (and not the presence of GDNF) affected Nestin+ populations (Fig 6.2 B).

Next, we demonstrated the ability of cultured cortical NSC/progenitors to differentiate into the three neural lineages; neurons, astrocytes and oligodendrocytes. The differentiation ratios were similar for cells cultured under all conditions, with TUJ+ neurons dominating the cultures (Fig 6.2 C, G-I), whilst GFAP+ astrocytes and NG2+ oligodendrocytes were notably sparse (Fig. 6.2 G and 6.2 D', respectively). The propensity for neuronal differentiation was not surprising given that the donor age of the cultures (E14.5) corresponded to a period of peak cortical neurogenesis, an event preceding gliogenesis. A comparison of the cultures revealed a significant decrease in TUJ+ cells on PCL compared to controls (Fig 6.2 C), possibly due to the enhanced proliferation observed within these cultures (Fig 6.2 B). Taken together, these findings demonstrate that electrospun PCL scaffolds were non-toxic to

primary cortical cells, capable of promoting cell viability and elicited effects on the proliferation of Nestin+ NSC and TUJ+ neuronal differentiation.

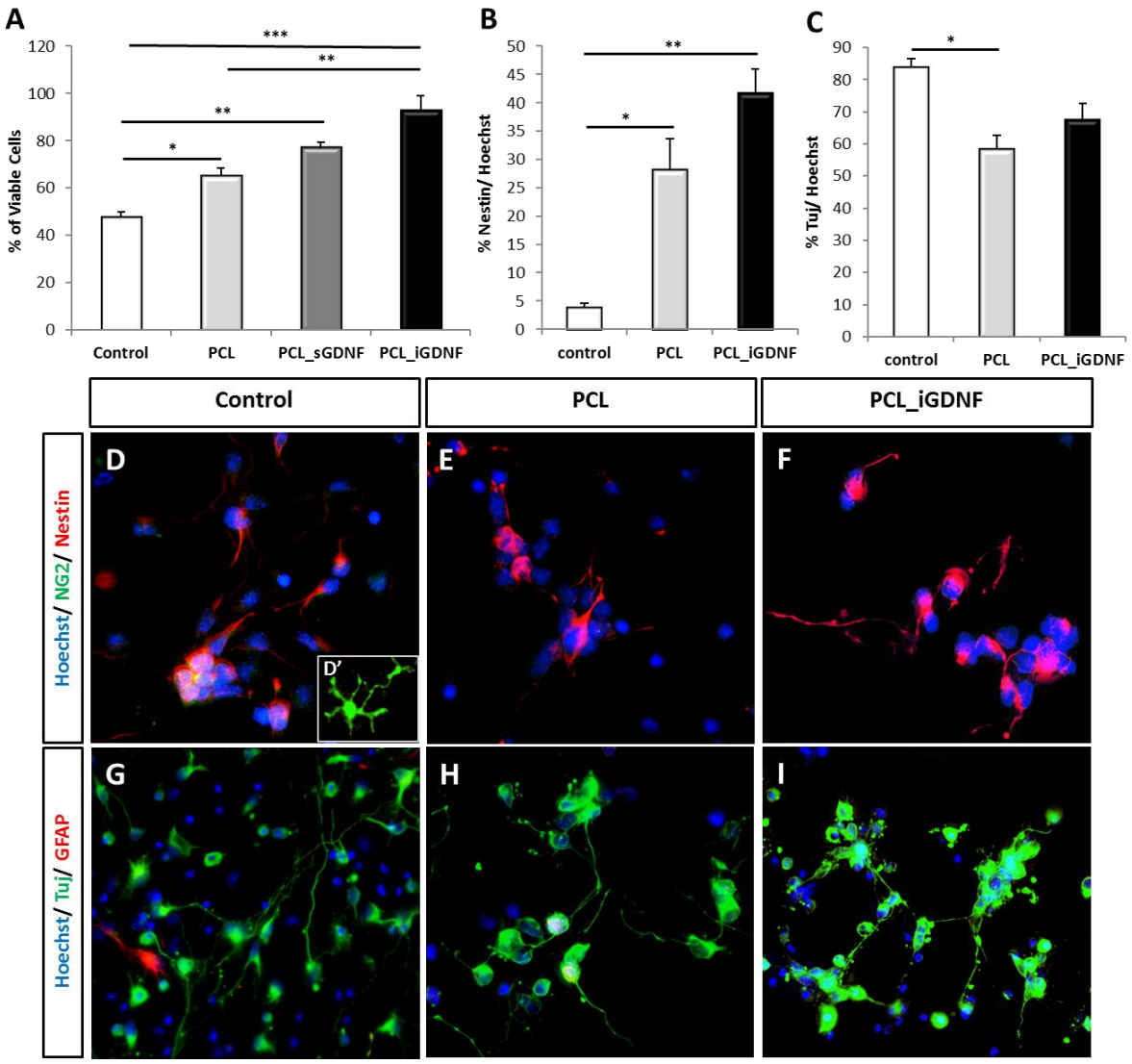

Figure 6.2 Modified PCL scaffolds, including tethered GDNF, enhances cell viability and proliferation, but has no effect on neural differentiation in vitro. (A) PCL scaffolds, and GDNF, enhance cortical cell viability and (B) proliferation of nestin+ neural stem cells/progenitors compared to culturing on PDL-coated glass coverslips (control). (C) PCL and GDNF have little effect on the differentiation of neurons, as well as astrocytes and oligodendrocytes (data not shown). (D-F, D')

Representative photomicrographs of NG2+ oligodendrocytes, nestin+ neural stem cells, (G-I) TUJ+ neurons and GFAP+ astrocytes cultured on glass, PCL and PCL_iGDNF. Cultures were co-stained with Hoechst to identify viable cells (nuclei) in culture. Data represents Mean + SEM. *P<0.05, **P<0.01, ***P<0.001, One-way ANOVA with Tukey post-hoc test. Groups: Control, PDL coated glass coverslip; PCL, PCL treated with ethylene diamine; PCL_sGDNF, PCL-ED with soluble GDNF; PCL_iGDNF, PCL-ED with Sulfo-SMCC crosslinker and immobilised GDNF.

6.4.3 Effect of modified PCL scaffolding, and GDNF, on graft survival and cell migration

Given the ability of PCL scaffolds, including tethered GDNF, to support NSCs and their derivatives *in vitro*, we next wished to examine the potential the scaffolds to support and promote the integration of neural stem/progenitor cell grafts. Our previous work examined the inflammatory response following implantation of PCL scaffolds (in the absence of a cell graft), concluding that PCL does not elicit a prolonged foreign body reaction and is capable of interfacing with the host tissue [13]. In the present study animals received implants of either: (i) PCL scaffold, (ii) GFP+ cells, (iii) GFP+ cells adjacent to a PCL scaffolds or (iv) GFP+ cells adjacent to a PCL scaffolds with iGDNF. Donor tissue (E14.5 cortex) was isolated from GFP mice to enable visualisation of grafted cells and their fiber innervation (GFP+) within the host tissue (GFP-). All animals receiving cell transplants displayed viable grafts at 28 days, as indicated by the presence of GFP+ staining. All cell grafts were localised within the striatal target of the host brain and showed no signs of neural overgrowth.

Quantification of GFP+ cells demonstrated that PCL had no deleterious effect on the survival of transplanted cells, showing trends towards increased cell survival (> 2-fold increase in the number of grafted GFP+ cells in the presence verses the absence of PCL, Fig. 6.3 A). iGDNF resulted in a significant (317%) increase in GFP+ cells compared to implants of cells alone (3070 $\pm$ 480 and 970 $\pm$ 270, respectively, Fig. 6.3 A-D), demonstrating that GDNF was capable of maintaining its trophic effects following tethering and implantation.

Next we examined the effects of PCL on cell migration. In the absence of a cell graft, Hoechst+ nuclei were observed within the implanted scaffold, indicating that large interfibre distance was sufficient to allow cell penetration, that host-derived cells were capable of undergoing migration and, demonstrating the biocompatibility of PCL *in vivo*. In the presence of a GFP+ graft, notably more (> 3-fold) cells were observed within the scaffold, presumably due to the high number of migrating neuroblasts present within the embryonic donor tissue. Previous studies have shown that GDNF is responsible for the tangential migration of cortical GABA neurons within the ventral telencephalon during development [40]. Here we show that tethered GDNF similarly evokes an effect on the migration of transplanted cortical cells, resulting in a significant increase in the number of Hoechst+ nuclei within the scaffolds (Fig. 6.3 E-H). Whilst GDNF was tethered onto the surface, figure 6.1 B illustrates that approximately a third of the protein was absorbed and therefore likely to gradually diffuse

from the scaffold, forming a gradient capable of attracting neuroblasts. The propensity for more cells to remain within the scaffold at 28 days is likely due to the presence of the tethered protein.

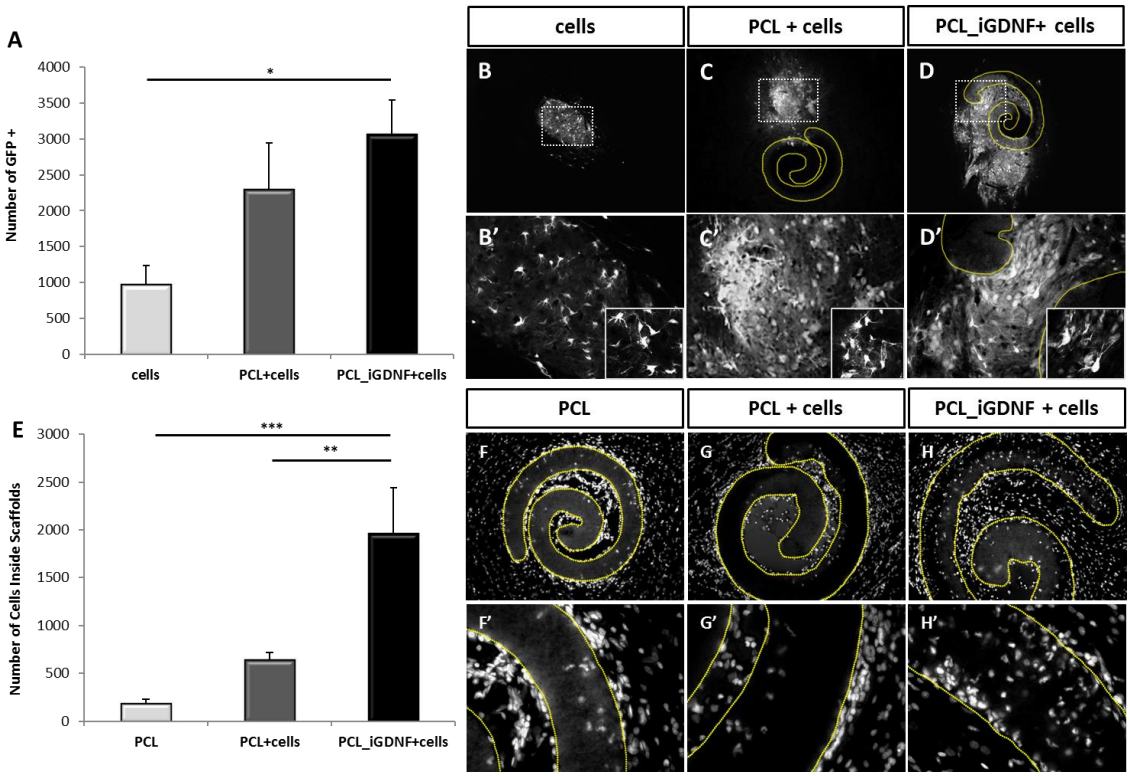

Figure 6.3 PCL scaffolds, and immobilised GDNF, support GFP+ grafted cells and cell migration. (A) Tethered GDNF significantly increases the number of GFP+ in vivo following implantation. (B) Micrographs of GFP+ grafted cells within the rat striatum and (C) adjacent to a PCL scaffold and (D) PCL scaffold with tethered GDNF. (B'-D') Higher magnification of images B-D. (E) GDNF promotes the migration of cells onto the implanted scaffold. (F) Images showing hoechst labeled cells that have migrated onto the PCL scaffold in the absence of a GFP+ graft (i.e. host derived cells), (G) in the presence of a GFP+ cell graft and (H) the effect of GDNF on the migration of these cells. Yellow dotted lines show the outline of implanted scaffolds. Data represents Mean + SEM. *P<0.05, **P<0.01, One-way ANOVA with Tukey post-hoc test. Groups: Cells = GFP+ graft in

the absence of PCL; PCL = PCL scaffold in the absence of GFP+ graft; PCL+ cells = GFP+ cortical cell graft adjacent to PCL-ED implant; PCL_iGDNF = GFP+ cortical cell graft adjacent to PCL-ED implant with immobilised GDNF.

6.4.4 Effects of PCL scaffolding on the proliferation and differentiation of transplanted NSCs/progenitors

In support of our past and present *in vitro* findings (Fig. 6.2 B and [12]), there was a notable increase in Nestin+ NSCs within the graft when additionally exposed to iGDNF via PCL scaffolds (Fig. 6.4 A,E,F,G) in the comparison with cell transplantation alone. Nestin is an intermediate filament protein expressed in dividing cells during development of the nervous system (CNS) and becomes downregulated upon differentiation when it is then replaced by tissue-specific intermediate filament proteins. The increase in the percentage of Nestin+/ GFP+ cells here (Fig. 6.4 A) demonstrates the ongoing support of immature neurons within the graft and accounts for the increase in total GFP+ cells as show in figure 6.3 A. Further studies, involving longer graft survival periods, are required to observe the maturation/identity of these graft-derived NSC/progenitors, however based upon the following differentiation findings, we speculate that the majority of these cells will adopt a neuronal fate.

Next, we examined the effect of PCL±iGDNF on those graft-derived GFP+ cells that had undergone differentiation *in vivo*. Similar to *in vitro* culturing, TUJ+ neurons remained the predominant cell type within all grafts. Exposure of the transplanted cells to PCL (±GDNF) had little effect on the differentiation ratio of TUJ+ neurons or NG2+ oligodendrocytes, with similar proportions observed in all treatments (Fig. 6.4 B,C). Importantly however, as PCL and PCL+iGDNF resulted in notable and significant increases in total GFP cells the overall yield of neurons and oligodendrocytes within these grafts were enhanced. Finally we observed that the presentation of GDNF to the graft resulted in a significant decrease in GFAP+ reactive astrocytes (Fig. 6.4 D, H-,J). This is important, as the introduction of grafts within the brain results in iatrogenic injury, which is followed by an inflammatory response that includes astrocytes proliferating locally and becoming reactive. It is the persistence of these activated astrocytes that results in glial scarring and prevents neurons and axons from entering the injury site and promoting reinnervation. Interestingly, the use of biomaterials in a cell transplantation have previously been shown to reduce astrogliosis [41] and furthermore, a recent study has attributed the benefits of GDNF in spinal cord axonal regeneration to the ability of this protein to inhibit reactive astrocytes [42]. We therefore believe that the ability to limit the associated astrocytosis contributed to the superior graft survival observed, and may also be important in controlling glial scarring.

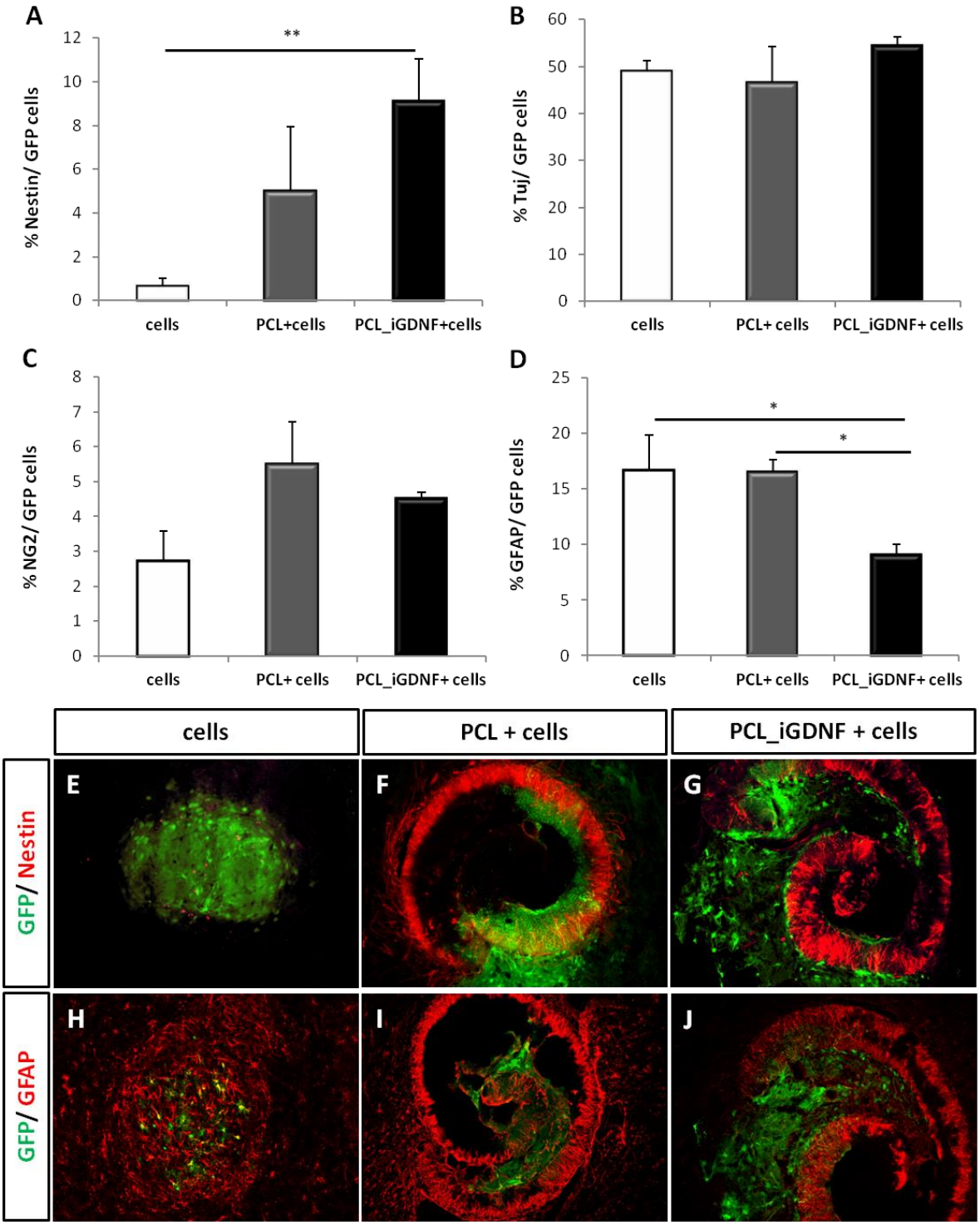

Figure 6.4 Effect of PCL and GDNF immobilisation on the differentiation and proliferation of GFP+ transplanted cortical cells. (A) Quantification of the proportion of neural stem cells (Nestin+GFP+), (B) neurons (TUJ+GFP+), (C) oligodendrocytes (NG2+GFP+) and (D) astrocytes (GFAP+GFP+) within rat striatal grafts. PCL and GDNF have no effect on the differentiation of

grafted cortical cells, but significantly enhance the proportion of graft-derived neural stem cells. (E-G) Representative photomicrographs of nestin+GFP+ neural stem cells and, (H-J) GFAP+GFP+ astroglia within the graft and. Data represents Mean + SEM, **P<0.01, One-way ANOVA with Tukey post-hoc test.

6.4.5 Influence of PCL scaffolding and tethered GDNF on graft integration

The use of GFP donor tissue not only allowed for visualisation and quantification of grafted cells, but also the extensive network of processes emanating from these cells. This enabled assessment and comparisons of the total area innervated by the grafts within the striatum, as well as penetrating the scaffolds. Figure 6.5 A-C shows GFP immunolabeling of grafted cells and their fiber network from representative animals receiving (A) cells (B) cells + PCL or (C) cells + PCL_iGDNF. Grafting adjacent to PCL_iGDNF scaffolds resulted in increased numbers of GFP+ cells relatively to cell transplantation alone but not unmodified PCL scaffolds (Fig. 6.3 A), presumably due to improved support for grafted cells and proliferation of graft derived Nestin+ cells. Not surprisingly, the increase in cell number resulted in similar trends of enhanced graft size (i.e area covered by GFP+ staining, Fig. 6.5 A-D). Further examination of the ability of grafted cells to respond to tethered GDNF was demonstrated by an increase in the area of the scaffold covered by GFP+ staining compared to grafting alongside PCL alone (26% ± 6% and 8% ± 2%, respectively, Fig. 6.5 E-G), suggesting that the trophin was capable of eliciting effects not only on cell number and proportion, but

additionally on GFP+ fibers. Finally, we examined the identity of GFP+ fiber growth penetrating the scaffolds to ascertain whether iGDNF promoted the infiltration of neurites (neuronally derived axons and dendrites), astroglia fibers or oligodendrocyte processes. The presence of tethered GDNF (PCL_iGDNF) resulted in a significant (> 2-fold) increase in the penetration of TUJ+ neurites (PCL+cells: 15% ± 2%, PCL_iGDNF+cells: 42% ± 10%, Fig. 6.6). Interestingly, neuronal differentiation was not altered across the grafted groups (figure 6.4 B), indicating that the increased neurite penetration observed in the presence of iGDNF was due to neurite extension, a previously ascribed role for GDNF in development [43] and following cell transplantation [44].

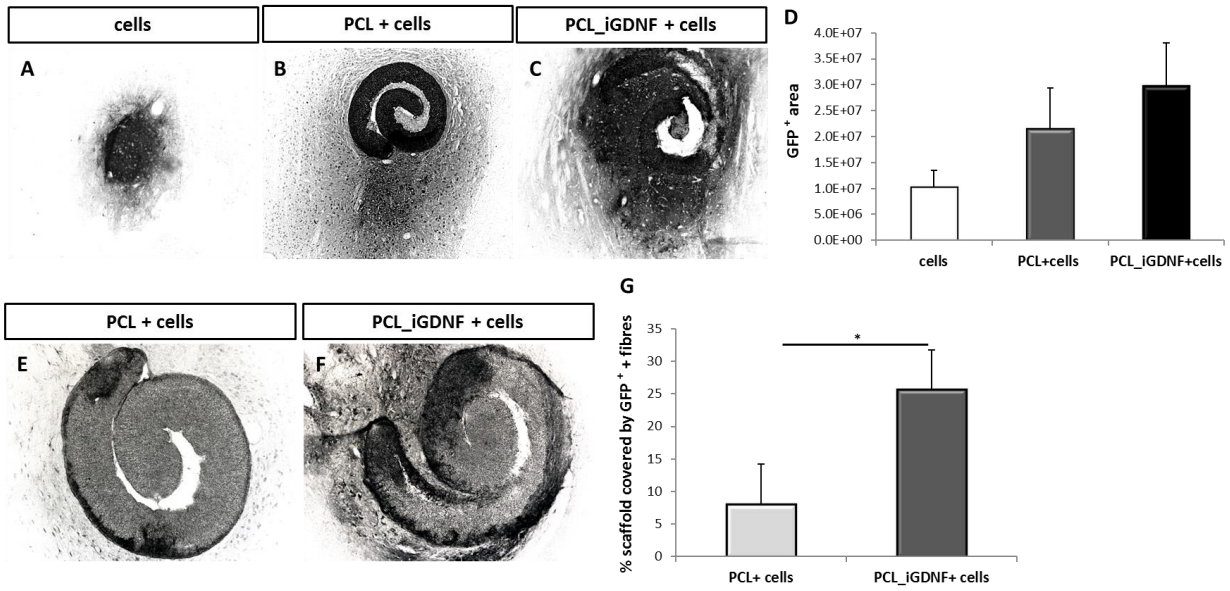

Figure 6.5 Effect of PCL and GDNF on graft area and fiber penetration of the scaffold. (A) Images showing the size of a GFP+ graft within the striatum, (B) adjacent to a PCL scaffold and (C) a PCL scaffold with immobilised GDNF. (D) Quantification of the area of the grafts transplanted adjacent to PCL scaffolds and PCL tethered with GDNF, as determined by the area of GFP+ staining. (E-F) Representative images showing the influence of GDNF on the penetration of GFP+ fibers into the scaffold. (G) Quantification of the proportion of the scaffold covered by GFP+ labeling. GDNF results in a significant increase in GFP+ fiber infiltration. Data represents Mean + SEM, *P<0.05, One-way ANOVA with Tukey post-hoc test and students t-test.

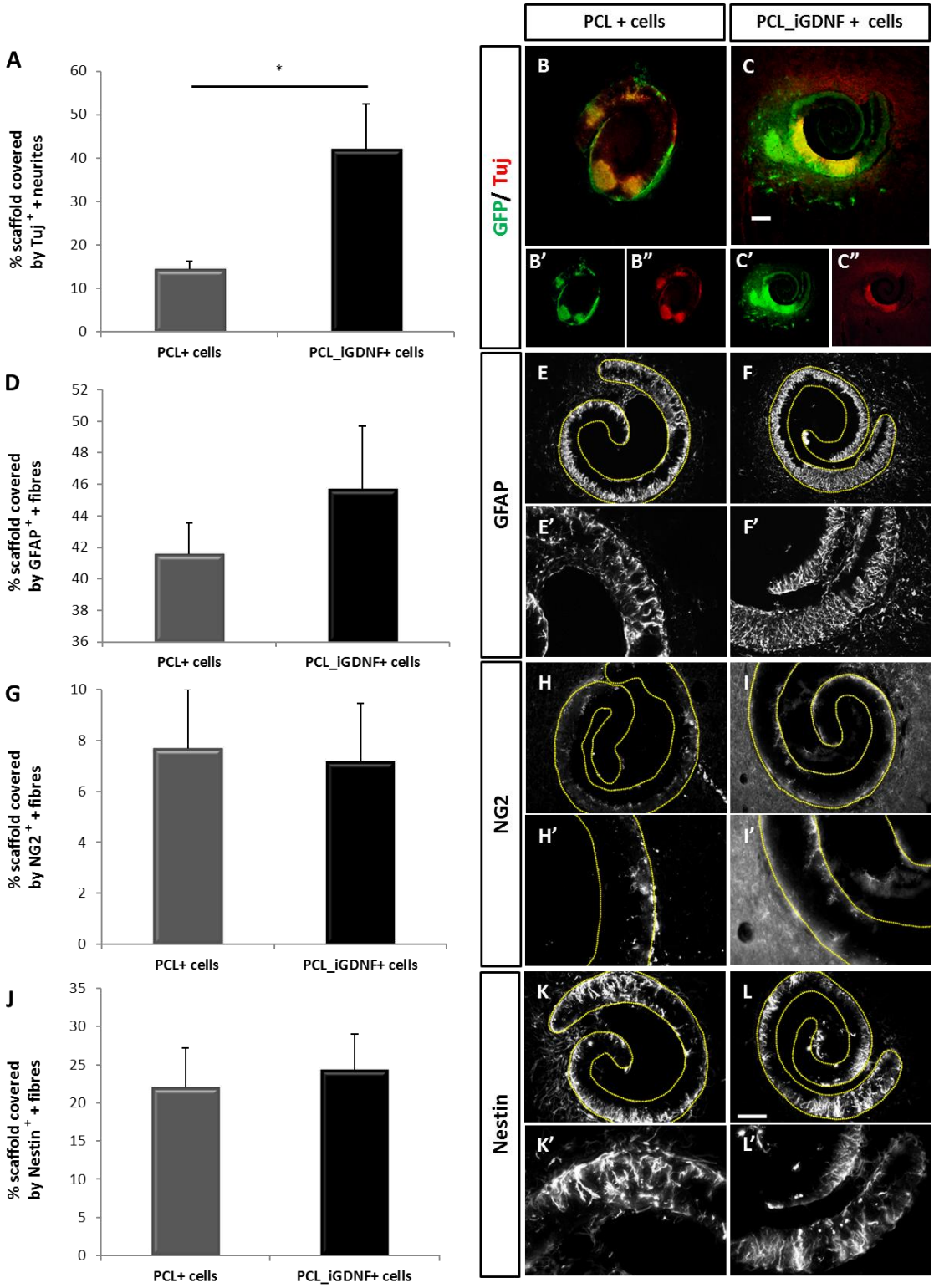

Figure 6.6 Immobilised GDNF promotes neurite growth into the scaffolds, but has no effect on astrocytic, oligodendrocytic or nestin+ processes. (A) Quantification of proportion of scaffold covered by neurites (TUJ+), (D) astrocyte processes (GFAP+), (G) oligodendrocyte processes (NG2+)

and, (J) neural stem cell processes (Nestin+) in the presence or absence of immobilised GDNF. (B-C) Representative images of TUJ+, (E-F) GFAP+, (H-I) NG2+ and (K-L) Nestin+ fibers penetrating the scaffold from grafted cortical neural cells. Data represents Mean + SEM, *P<0.05, One-way ANOVA with Tukey post-hoc test.

6.5 CONCLUSION

Brain tissue engineering aims to develop biologically functional scaffolds to repair, replace and/or regenerate damaged neural tissue. Although a number of scaffolds have been utilized, electrospun fibres remain attractive due to their high surface area to volume ratio, porosity and fibrous three dimensional structure. While there is an abundance of literature detailing various methods to optimise the morphology of these fibers and their use *in vitro*, there is seemingly a lack of research focused on their chemical modification and *in vivo* application. Here we demonstrate that the physical attributes of electrospun PCL can support NSC/progenitors *in vitro* as well as following transplantation. Furthermore, the tethering of proteins onto the scaffolds enables prolonged exposure to functional trophic cues capable of positively impacting cellular proliferation, differentiation and neuritic growth in the comparison with the cell transplantation alone *in vivo*, thereby improving the integration of transplanted cells.

6.6 ACKNOWLEDGEMENTS

We wish to thank Alexandra Rodriguez for critical reading of the manuscript. This research was supported by funding from the Bethlehem Griffith Research Foundation. D.R.N was supported by an Australian Research Council Australian Postdoctoral Fellowship. C.L.P was supported by an NHMRC Career Development Award, and subsequently Senior Medical Research Fellowship provided by the Viertel charitable Foundation, Australia.

6.7 REFERENCES

1. Parish CL, Arenas E. Stem-cell-based strategies for the treatment of Parkinson's disease. Neurodegener Dis 2007;4(4):339-47 2007.
2. Winkler C, Kirik D, Bjorklund A. Cell transplantation in Parkinson's disease: how can we make it work? Trends in Neurosciences 2005;28(2):86-92.
3. Lindvall O, Kokaia Z, Martinez-Serrano A. Stem cell therapy for human neurodegenerative disorders–how to make it work. Nature Medicine 2004;10:S42-S50.
4. Lee JY, Bashur CA, Goldstein AS, Schmidt CE. Polypyrrole-coated electrospun PLGA nanofibers for neural tissue applications. Biomaterials 2009;30(26):4325-4335.
5. Prabhakaran MP, Venugopal JR, Ramakrishna S. Mesenchymal stem cell differentiation to neuronal cells on electrospun nanofibrous substrates for nerve tissue engineering. Biomaterials 2009;30(28):4996-5003.
6. Schnell E, Klinkhammer K, Balzer S, Brook G, Klee D, Dalton P, et al. Guidance of glial cell migration and axonal growth on electrospun nanofibers of poly-ε-caprolactone and a collagen/poly-ε-caprolactone blend. Biomaterials 2007;28(19):3012-3025.
7. Pettikiriarachchi JTS, Parish CL, Shoichet MS, Forsythe JS, Nisbet DR. Biomaterials for Brain Tissue Engineering. Australian Journal of Chemistry 2010;63(8):1143-1154.
8. Wang TY, Forsythe JS, Parish CL, Nisbet DR. Biofunctionalisation of polymeric scaffolds for neural tissue engineering. J Biomater Appl April 5, 2012.
9. Nisbet DR, Forsythe JS, Shen W, Finkelstein DI, Horne MK. A Review of the Cellular Response on Electrospun Nanofibers for Tissue Engineering. J Biomater Appl 2009 Jul;24(1):7-29.
10. Nisbet DR, Pattanawong S, Ritchie NE, Shen W, Finkelstein DI, Horne MK, et al. Interaction of embryonic cortical neurons on nanofibrous scaffolds for neural tissue engineering. J Neural Eng 2007 Jun;4(2):35-41.
11. Nisbet DR, Yu LM, Zahir T, Forsythe JS, Shoichet MS. Characterization of neural stem cells on electrospun poly(epsilon-caprolactone) submicron scaffolds: evaluating their potential in neural tissue engineering. J Biomater Sci Polym Ed 2008;19(5):623-634.
12. Horne MK, Nisbet DR, Forsythe JS, Parish CL. Three-Dimensional Nanofibrous Scaffolds Incorporating Immobilized BDNF Promote Proliferation and Differentiation of Cortical Neural Stem Cells. Stem Cells Development 2010;19(6):843-852.
13. Nisbet DR, Rodda AE, Horne MK, Forsythe JS, Finkelstein DI. Neurite infiltration and cellular response to electrospun polycaprolactone scaffolds implanted into the brain. Biomaterials 2009;30(27):4573-4580.
14. Suzuki M, Svendsen CN. Combining growth factor and stem cell therapy for

amyotrophic lateral sclerosis. Trends in Neurosciences 2008;31(4):192-198.
15. Lindvall O, Odin P. Clinical application of cell transplantation and neurotrophic factors in CNS disorders. Curr Opin Neurobiol 1994 Oct;4(5):752-7 1994.
16. Rawal N, Parish C, Castelo-Branco G, Arenas E. Inhibition of JNK increases survival of transplanted dopamine neurons in Parkinsonian rats. Cell Death Differ 2006;14(2):381-383.
17. Bregman BS, Coumans JV, Dai HN, Kuhn PL, Lynskey J, McAtee M, et al. Transplants and neurotrophic factors increase regeneration and recovery of function after spinal cord injury. Prog Brain Res 2002;137:257-273.
18. Kuhl PR, Griffith-Cima LG. Tethered epidermal growth factor as a paradigm for growth factor-induced stimulation from the solid phase. Nat Med 1996;2(9):1022-1027.
19. Ito Y, Zheng J, Imanishi Y, Yonezawa K, Kasuga M. Protein-free cell culture on an artificial substrate with covalently immobilized insulin. Proceedings of the National Academy of Sciences 1996 April 16, 1996;93(8):3598-3601.
20. Ito Y, Chen G, Imanishi Y, Morooka T, Nishida E, Okabayashi Y, et al. Differential Control of Cellular Gene Expression by Diffusible and Non-Diffusible EGF. J Biochem (Tokyo) 2001 May 1, 2001;129(5):733-737.
21. Consales C, Volpicelli F, Greco D, Leone L, Colucci-D'Amato L, Perrone-Capano C, et al. GDNF signaling in embryonic midbrain neurons in vitro. Brain Research 2007;1159:28-39.
22. Haniu M, Hui J, Young Y, Le J, Katta V, Lee R, et al. Glial Cell Line-Derived Neurotrophic Factor: Selective Reduction of the Intermolecular Disulfide Linkage and Characterization of Its Disulfide Structure. Biochemistry 1996;35(51):16799-16805.
23. Enomoto H. Regulation of neural development by glial cell line-derived neurotrophic factor family ligands. Anat Sci Int 2005;80(1):42-52.
24. Harvey BK, Hoffer BJ, Wang Y. Stroke and TGF-beta proteins: glial cell line-derived neurotrophic factor and bone morphogenetic protein. Pharmacol Ther 2005;105(2):113-125.
25. Nakajima K, Hida H, Shimano Y, Fujimoto I, Hashitani T, Kumazaki M, et al. GDNF is a major component of trophic activity in DA-depleted striatum for survival and neurite extension of DAergic neurons. Brain Research 2001;916(1-2):76-84.
26. Ortiz-Ortiz MA, Moran JM, Ruiz-Mesa LM, Bonmatty RG, Fuentes JM. Protective effect of the glial cell line-derived neurotrophic factor (GDNF) on human mesencephalic neuron-derived cells against neurotoxicity induced by paraquat. Environmental Toxicology and Pharmacology 2011;31(1):129-136.
27. Sandhu JK, Gardaneh M, Iwasiow R, Lanthier P, Gangaraju S, Ribecco-Lutkiewicz M, et al. Astrocyte-secreted GDNF and glutathione antioxidant system protect neurons against 6OHDA cytotoxicity. Neurobiology of Disease 2009;33(3):405-414.
28. Wang F, Kameda M, Yasuhara T, Tajiri N, Kikuchi Y, Liang HB, et al. GDNF-pretreatment enhances the survival of neural stem cells following transplantation in a

rat model of Parkinson's disease. Neuroscience Research 2011;71(1):92-98.
29. Alexi T, Borlongan CV, Faull RLM, Williams CE, Clark RG, Gluckman PD, et al. Neuroprotective strategies for basal ganglia degeneration: Parkinson's and Huntington's diseases. Progress in Neurobiology 2000;60(5):409-470.
30. Georgievska B, Carlsson T, Lacar B, Winkler C, Kirik D. Dissociation between short-term increased graft survival and long-term functional improvements in Parkinsonian rats overexpressing glial cell line-derived neurotrophic factor. Eur J Neurosci 2004;20(11):3121-3130.
31. Bye CR, Thompson LH, Parish CL. Birth dating of midbrain dopamine neurons identifies A9 enriched tissue for transplantation into Parkinsonian mice. Experimental Neurology 2012;236(1):58-68.
32. Meng ZX, Wang YS, Ma C, Zheng W, Li L, Zheng YF. Electrospinning of PLGA/gelatin randomly-oriented and aligned nanofibers as potential scaffold in tissue engineering. Materials Science and Engineering: C 2010;30(8):1204-1210.
33. Ashammakhi N, Wimpenny I, Nikkola L, Yang Y. Electrospinning: Methods and Development of Biodegradable Nanofibres for Drug Release. J Biomed Nanotechnol 2009 Feb;5(1):1-19.
34. Takahashi M. The GDNF/RET signaling pathway and human diseases. Cytokine & Growth Factor Reviews 2001;12(4):361-373.
35. Anuradha S, Uma Maheswari K, Swaminathan S. Fabrication of uniaxially aligned 3D electrospun scaffolds for neural regeneration. Biomed Mater 2011;6(2):025004.
36. Nur EKA, Ahmed I, Kamal J, Schindler M, Meiners S. Three-dimensional nanofibrillar surfaces promote self-renewal in mouse embryonic stem cells. Stem Cells 2006 Feb;24(2):426-433.
37. Chen Y, Ai Y, Slevin JR, Maley BE, Gash DM. Progenitor proliferation in the adult hippocampus and substantia nigra induced by glial cell line-derived neurotrophic factor. Experimental Neurology 2005;196(1):87-95.
38. Ngan ESW, Shum CKY, Poon H-C, Sham M-H, Garcia-Barcelo M-M, Lui VCH, et al. Prokineticin-1 (Prok-1) works coordinately with glial cell line-derived neurotrophic factor (GDNF) to mediate proliferation and differentiation of enteric neural crest cells. Biochimica et Biophysica Acta (BBA) - Molecular Cell Research 2008;1783(3):467-478.
39. Mwizerwa O, Das P, Nagy N, Akbareian SE, Mably JD, Goldstein AM. Gdnf is mitogenic, neurotrophic, and chemoattractive to enteric neural crest cells in the embryonic colon. Dev Dyn 2011;240(6):1402-1411.
40. Pozas E, Ibanez CF. GDNF and GFRα1 Promote Differentiation and Tangential Migration of Cortical GABAergic Neurons. Neuron 2005;45(5):701-713.
41. Park KI, Teng YD, Snyder EY. The injured brain interacts reciprocally with neural stem cells supported by scaffolds to reconstitute lost tissue. Nat Biotech 2002;20(11):1111-1117.

42. Deng L-X, Hu J, Liu N, Wang X, Smith GM, Wen X, et al. GDNF modifies reactive astrogliosis allowing robust axonal regeneration through Schwann cell-seeded guidance channels after spinal cord injury. Experimental Neurology 2011;229(2):238-250.
43. Uchida M, Enomoto A, Fukuda T, Kurokawa K, Maeda K, Kodama Y, et al. Dok-4 regulates GDNF-dependent neurite outgrowth through downstream activation of Rap1 and mitogen-activated protein kinase. J Cell Sci 2006;119:3067-3077.
44. Thompson LH, Grealish S, Kirik D, Björklund A. Reconstruction of the nigrostriatal dopamine pathway in the adult mouse brain. European Journal of Neuroscience 2009;30(4):625-638.

Chapter 7

Composite scaffolds, functionalised with glial derived neurotrophic factor, support dopaminergic neurons in vitro and promote graft integration in an animal model of Parkinson's disease

Contents

Monash University

Declaration for Thesis Chapter 7

Declaration by candidate

In the case of Chapter 7, the nature and extent of my contribution to the work was the following:

Nature of contribution	Extent of contribution (%)
Planning, research and article writing	50%

The following co-authors contributed to the work. Co-authors who are students at Monash University must also indicate the extent of their contribution in percentage terms:

Name	Nature of contribution	Extent of contribution (%) for student co-authors only
Jerani Pettikiriarachchi	Planning, research and material preparation	50%

Candidate's Signature	[redacted]	Date 16.5.2013

Declaration by co-authors

The undersigned hereby certify that:

(1) the above declaration correctly reflects the nature and extent of the candidate's contribution to this work, and the nature of the contribution of each of the co-authors.
(2) they meet the criteria for authorship in that they have participated in the conception, execution, or interpretation, of at least that part of the publication in their field of expertise;
(3) they take public responsibility for their part of the publication, except for the responsible author who accepts overall responsibility for the publication;
(4) there are no other authors of the publication according to these criteria;
(5) potential conflicts of interest have been disclosed to (a) granting bodies, (b) the editor or publisher of journals or other publications, and (c) the head of the responsible academic unit; and
(6) the original data are stored at the following location(s) and will be held for at least five years from the date indicated below:

Location(s)	**Department of Materials Engineering, Monash University**

[Please note that the location(s) must be institutional in nature, and should be indicated here as a department, centre or institute, with specific campus identification where relevant.]

Signature 1	Jerani Pettikiriarachchi	**Date**

7.1 INTRODUCTION

Although disease modifying therapies may be developed, reconstruction of the damaged brain will still be required. Cell replacement therapy (CRT) offers a long term strategy to repair this damage [1, 2]. Previous studies demonstrate that in principle CRT has convincing clinical benefits but outcomes are highly variable and there are several underlying problems that must be addressed before further clinical progress can be made [3]. Two major obstacles still exist, which are the survival of grafted cells and their integration into the host circuitry to promote functional outcomes. In this thesis engineering and nanotechnology principles were employed to produce scaffolds that can be incorporated into stem cell biology and cell replacement therapy strategies. These scaffolds offer an approach to improve survival of grafted cells and their integration into the host central nervous system (CNS) by providing physical and biochemical support [4-6].

Scaffolds to support neural circuits

Implantation of scaffolds into injury sites offers an attractive strategy to optimize neural regeneration [7]. These scaffolds can be: a) fabricated to provide a 3-dimensional (3D) support network for new cells and axons and to improve contact guidance and differentiation of primary neural cells, b) functionalized to contain surface bound trophic molecules relevant for survival, differentiation and axon guidance and c) fabricated to have controlled degradation times under physiological conditions. In this regard, scaffolds have received considerable attention for implantation to repair tissue damage, which proof of principle of these being shown in the previous chapter [8].

There are numerous different scaffolds that have been employed for brain regeneration, including hydrogels and electrospun nanofibres, to find an optimal model of the native 3D *in vivo* environment [6, 9]. It has been shown that neurones cultured on 3D electrospun nanofibres are more likely to adopt *in vivo* like morphologies, differentiate and survive longer than those cultured on 2D substrates of the same materials or conventional tissue culture-ware [4, 5]. Electrospun nanofibres provide the best simulation of the 3D *in vivo* environment of neural tissue because fibre alignment, diameter and inter-fibre distance can be characterized and regulated to generate a surface more permissive for primary neural cells cell adhesion and axon support [10-12]. Furthermore, functionalization with surface bound amines on electrospun polymer nanofibres and alterations in hydrophobicity can alter cellular responses. The mechanism for these superior characteristics is unclear, but enrichment with supportive proteins, binding, and activation of negatively charged proteins has been proposed. Whilst these advantages of nanofibres can be deployed to improve tissue culture [10, 13], their application *in vivo* is more problematic. *In vivo* nanofibrous materials are best applied to repairing peripheral nerves or spinal cord transections [14-16], where scaffolds can be 'wrapped' around the ends of transected fiber bundles to promote cell infiltration and axonal growth. In the brain paranchyma, we have implanted these scaffolds and demonstrated their ability to support endogenous cells and neurite growth [6], similarly we have shown in chapter 6 their ability to support transplanted neurons [8]. However the bulkiness of these scaffolds and their tendency to induce inflammation (at the implant-host interface) and tissue damage renders them less attractive [6]. In order to overcome this, we have begun working with temperature sensitive 'smart' xyloglucan (polysaccharide) hydrogels, which is a liquid at 4 ^{o}C but at biological temeratures will assemble into macroporous scaffolds [17]. This is also appealing for CRT because cells can be mixed into the liquid prior to implanation. On injection the fluid flows to fill extracellular voids in the CNS but promptly assembles into a

3D scaffold on which the cells can interact. Hydrogels also have the advantage of being highly permeable (for oxygen and nutrients) as well as possesses low interfacial tensions (important for cell viability and migration). Like nanofibers, hydrodels can be modified to effect cellular responses such as: promote cell migration or neurite growth (by altering gel pore size), promote neurite elongations (by alterations in charge magnitude and affect neuronal differentiation (by altering substrate elasticity) [18-22]. Consequently, a composite of nanofibers and hydrogels may present a more ideal scaffold for promoting neural tissue repair – capable of physically supporting cells and axons, being easily implantable and capable of maximal nutrient exchange.

Additional to the physical support, scaffolds are also capable of delivering molecules to promote proliferation, differentiation, survival and axonal growth *in vitro* and *in vivo* (shown in chapters 5 and 6). It is widely accepted that many ligands act at the surface rather than in a soluble form, however until recently their actions in this context could not be studied. Examination of immobilized proteins was previously hindered by difficulties in stably attaching ligands to a surface while maintaining cellular accessibility. Ligand immobilization onto a surface prevents endocytosis of the molecule, thereby prolonging the period of stimulation. Recently its has been illustrated that immobilization of brain derived neurotrophic factor (BDNF) onto nanofibrous scaffolds was superior to soluble BDNF in supporting the proliferation and differentiation of primary cortical cells *in vitro* [4]. We have also shown in the previous chapter the capacity of biofunctionalised scaffolds with immobilised GDNF to positively influence primary NSCs *in vitro* compared to control by increasing about 40% of cell survival (Figure 6.2), and enhance integration of these cells following transplantation into the brain parenchyma compare to unmodified scaffolds (as

reflected by figure 6.3 E). This provides the necessary validation of the ability of these materials to support cell transplantation.

However, in order to interface with the brain parenchyma, nanofibres and hydrogels will be used to construct 3-dimensional composite scaffolds to provide an environment more conducive to tissue re-organization. In this chapter we will employ a novel approach to form a multicomponent scaffold by imbedding short electrospun nanofibres in a hydrogel matrix. Short electrospun nanofibres will be produced using ultrasonication technology, which facilitates the bulk scission of electrospun nanofibrous membranes to produce short, discrete injectable nanofibres. The advantages of such a scaffold is that they will have the advantages of both electrospun nanofibrous and hydrogel scaffolds to a) provide a better milieu for nutrient exchange; b) provide features similar to the ECM; and c) an environment where grafted cells interact with neighbouring host tissue. Our hypothesis was that this would promote superior cell or axon adhesion, neurite elongation and alters the differentiation of transplanted cells. In this chapter we will also immobilized growth factors (GDNF) onto the scaffolds to deliver trophic factors.

This chapter will thereby assess the ability of nanofibrous/hydrogel composite scaffolds to support primary neural cells, their derivatives and neurite processes in culture as well as their ability to promote the survival and integration of neural transplants in an animal model of Parkinson's disease (PD). PD was selected due to the most progress in regards to cell replacement therapy; it therefore seems the most obvious place to start when trying to improve neural cell therapy approaches. This scaffold will encompass the benefits of both nanofibres and hydrogels to give a superior material for primary neural cells, differentiated neural cells and axons, *in vitro* and in vivo. This composite scaffold will have the unique

structural benefit of nanofibres, but the superior properties of a hydrogel for the purpose of implantation.

7.2 METHODS

Composite scaffolds, combing xyloglucan and short fibres of electrospun scaffolds, were prepared and characterised according to sections 3.1.2 and 3.1.3 (chapter 3). The scaffolds were modified and tethered with GDNF as described in section 3.1.3. Primary neurons, isolated from the developing ventral midbrain (VM) were seeded in culture as described in sections 3.1.4 and 3.1.5. The in vitro experimental groups included: control (glass coated with PDL), xyloglucan, xyloglucan with short fibres, xyloglucan with short fibres mobilized with GDNF. After confirming the biocompatibility of composite scaffolds, the scaffolds were implanted together with VM cells in the mouse brain of PD. Section 3.1.6.1 provides a detailed account of the materials and method employed to create the PD model in mice, and section 3.1.6.3 outlines the implantation cells together with composite scaffolds. Ten Weeks after implantation, animals were intracardially perfused with paraformaldehyde and their brains processed for histological examination (see sections 3.1.6.4 and 3.1.6.5).

7.3 RESULTS AND DISCUSSION

Parkinson's disease is a neurodegenerative disease characterised by the progressive degeneration of ventral midbrain dopamine neurons. Studies have demonstrated that fetal derived tissue, enriched with dopamine neurons, and transplanted into the brains of Parkinson's disease patients survived, integrated within the host circuitry and provided symptomatic relief. However extensive variability was observed between patients illustrating that there is much improvement required before such transplantations can be routinely employed in the clinic. Key areas of concern have been the survival of the transplanted neurons and their ability to adequately re-innervate the host tissue. In the present study, we examined the ability of a poly-lysine functionalised xyloglucan hydrogel scaffold incorporating short electrospun PLLA nanofibres to support the neural transplants in PD mouse models. The electrospun PLLA nanofibres were selected due to the brittle properties for sonication [23]. The short nanofibres were functionalised with immobilised GDNF so that the composite scaffold was able to provide structural and chemical support for ventral midbrain neural stem cells/ progenitors *in vitro* and following cell transplantation. Specifically, we examined viability, differentiation and neurite morphology of the cells *in vitro* as well as the survival of transplanted cells and graft integration (fiber growth) upon transplantation into an animal model of PD.

7.3.1 Characterisation of engineered scaffolds

7.3.1.1 Characterisation of the xyloglucan hydrogel

XPS was used to determine the extent of PDL grafting to the xyloglucan. Figure 7.1 shows a survey spectrum of PDL and the unmodified and modified xyloglucan, where the appearance of the nitrogen peak on the modified material is highlighted. The extent of PDL grafting was determined using and XPS to investigate the nitrogen to carbon ratio. We discovered that the N/C ratio was 0.056 ± 0.003, indicating that there was 1.30 PDL molecules immobilised to each xyloglucan repeat unit. Isothermal rheological experiments were conducted to determine the composition at which the elastic modulus of the xyloglucan hydrogels matched the modulus of neural tissue in the spinal cord (3kPa to 300kPa) (Figure 7.2) [24]. Additionally, both elastic and loss moduli have been shown to affect cell responses, and figure 7.2 shows that δ is similar before and after the PDL attachment [25, 26]. An SEM image of the xyloglucan hydrogel post PDL functionalisation (Figure 7.3) confirmed the macroporous structure that has been reported previously in the literature and its suitability for cell culture and transplantation [9]. The structure consisted of large laths, which was insensitive to the inclusion of PDL in the xyloglucan structure.

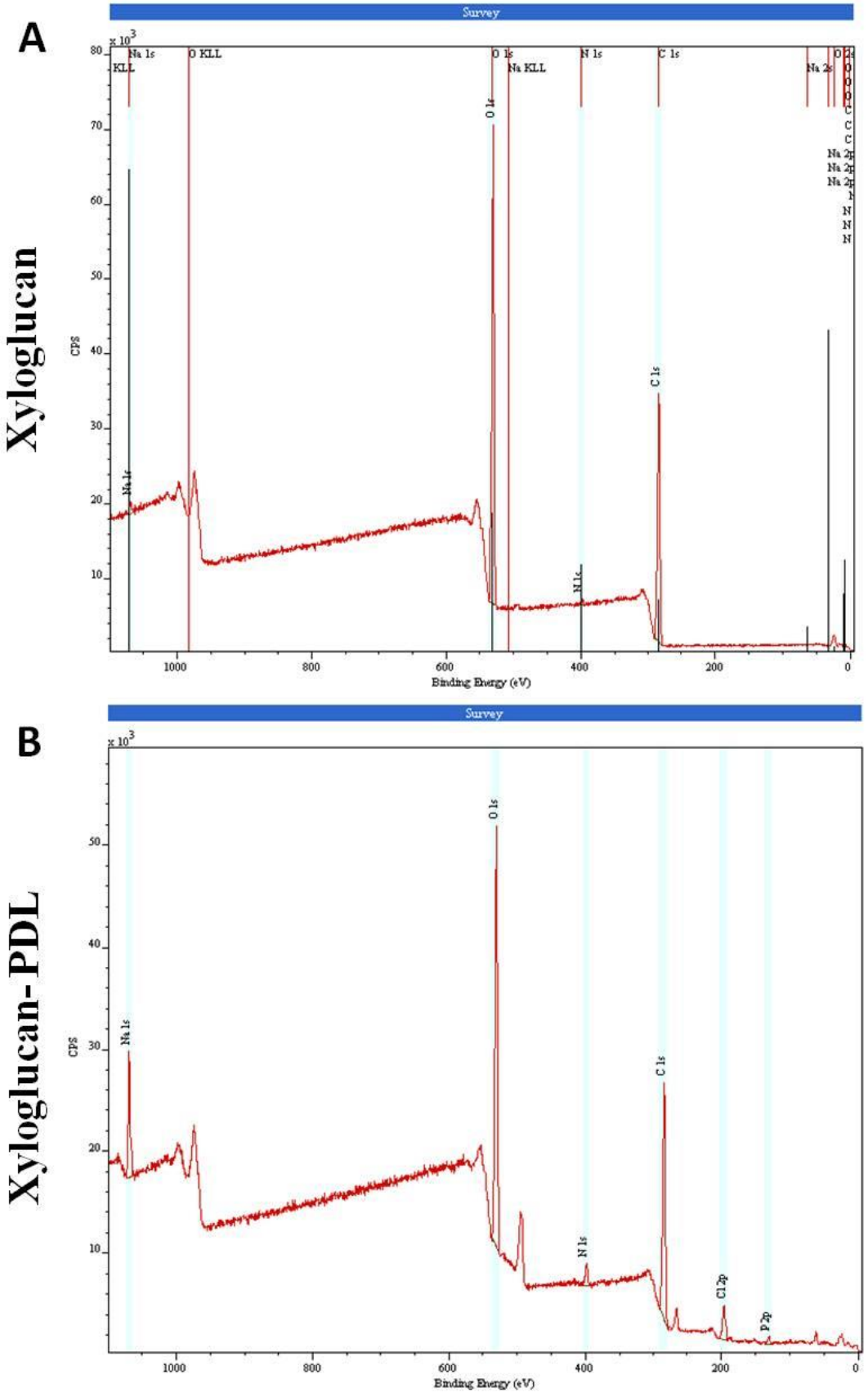

Figure 7.1 XPS of xyloglucan (A) and xyloglucan functionalised with PDL (B)

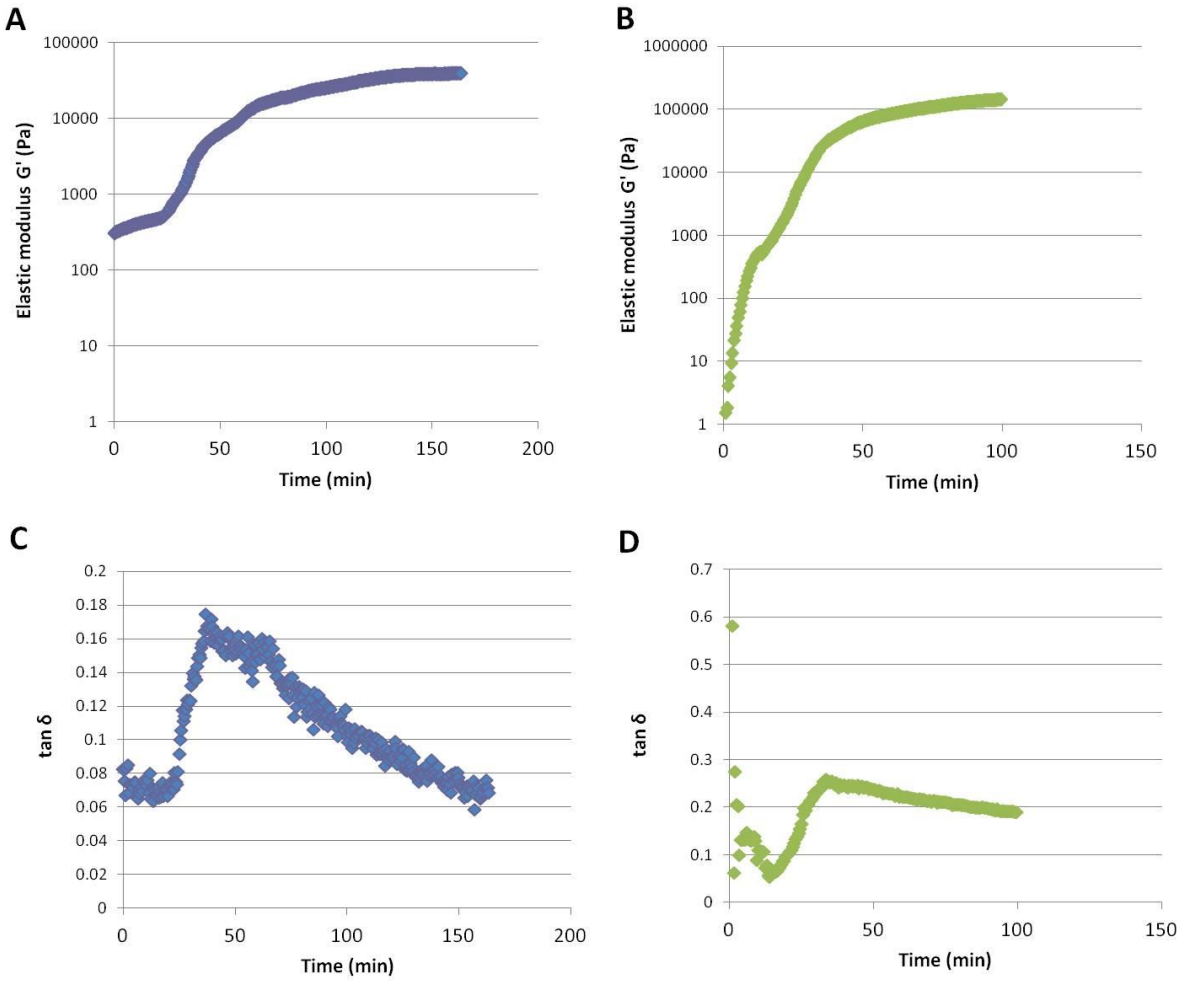

Figure 7.2 Isothermal rheological (37℃) of xyloglucan and xyloglucan functionalised with PDL. A) isothermal gelation of xyloglucan, B) isothermal gelation of xyloglucan modified with PDL, C) isothermal tan δ curve for xyloglucan, and D) isothermal tan δ curve for PDL grafted xyloglucan.

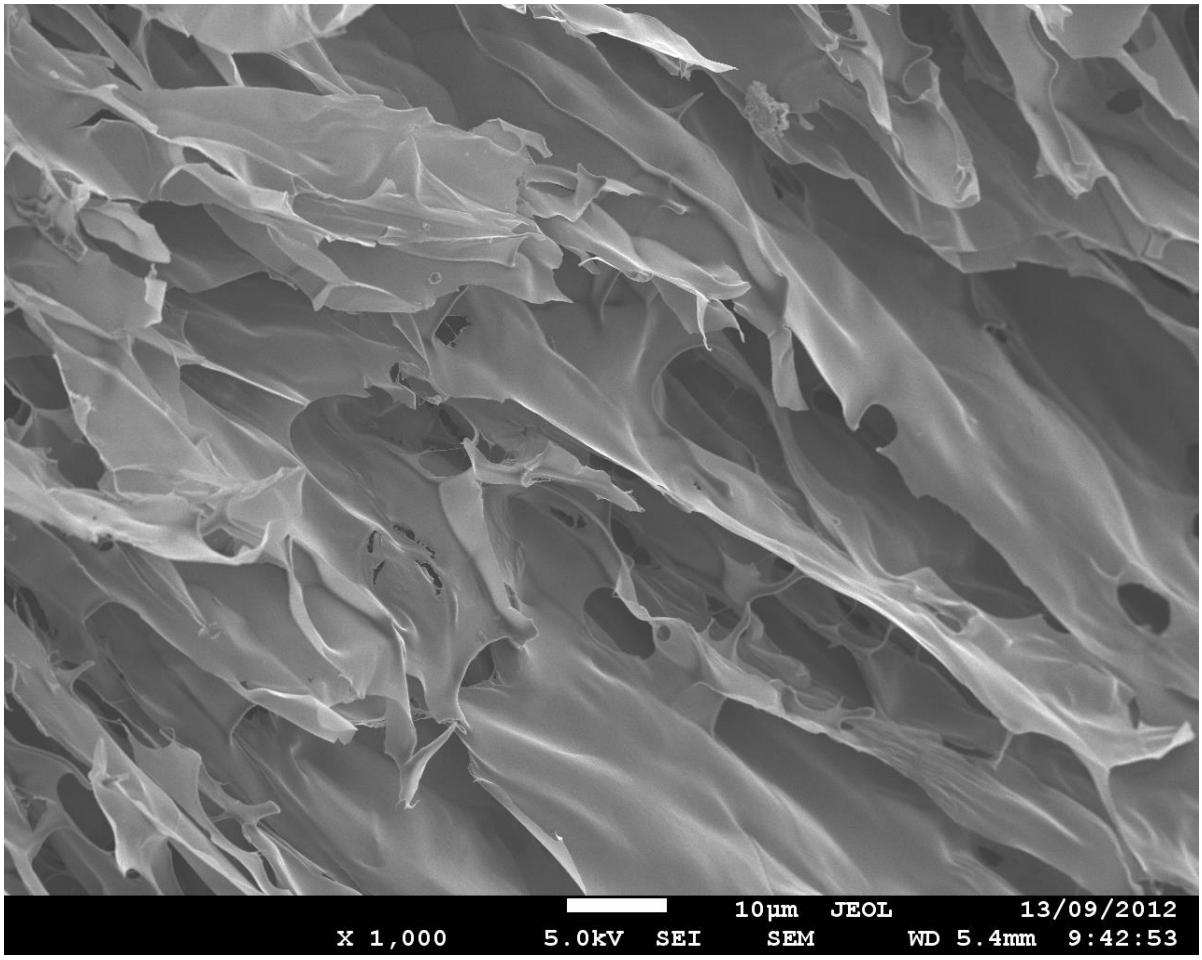

Figure 7.3 SEM picture of the morphology of 3wt% PDL functionalised xyloglucan.

7.3.1.2 Characterisation of short electrospun fibres

Poly-L-lactic acid (PLLA) nanofibres were produced via electrospinning and collected on a rotating mandrel using protocols established within our laboratories. Briefly, we utilised random PCL nanofibrous scaffolds to generate electrospun fibres that are uniform in diameter and varied from 100-900nm (Figure 7.4). We have developed methods for producing short fibres in bulk from electrospun membranes using ultrasonication. We have discovered that polymer ductility has the biggest influence over the ability to generate short fibres and their final morphology. We can break PLLA into short fibres of approximately 10 µm in length using an 80% sonication amplitude with a 4-6sec On-Off cycle for 10 min. However, due to

PLLA having a ductility that is slightly too high. The fibres need to be more brittle prior to sonication, with the degree of embitterment influencing the final length. This was achieved using ethylenediamine treatment. The architectures of the electrospun nanofibres and their ability to remain as individual, discrete short fibres upon injection was determined using confocal microscopy to image fluorescently labelled short fibres (Figure 7.5). The short fibres were injected into an agar gel of the similar elastic modulus as the brain (0.5-1 kPa) [27].

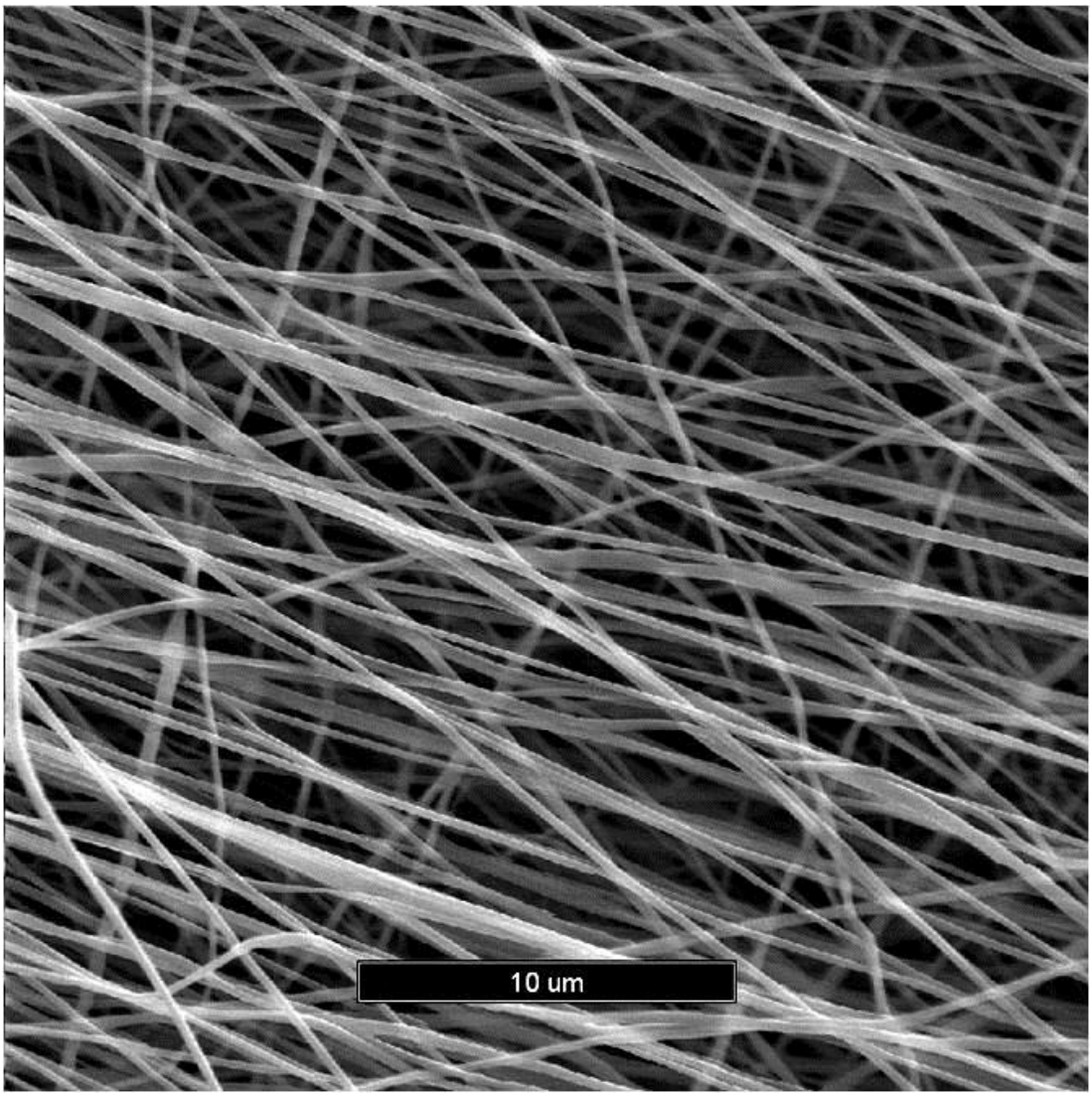

Figure 7.4 SEM image of the morphology of electrospun scaffolds

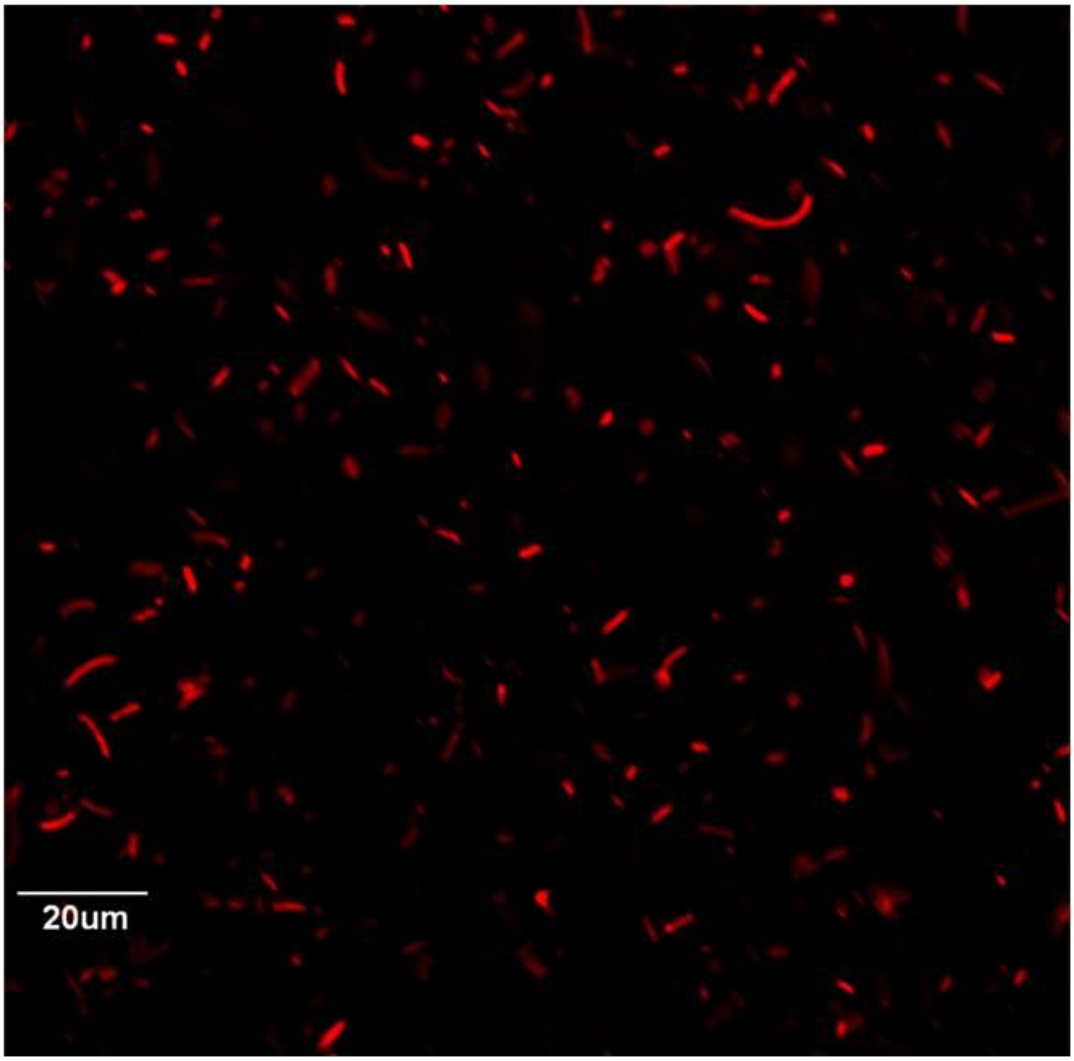

Figure 7.5 Fluorescent image of the morphology of short fibres of electrospun PLLA imbedded in agar gel

7.3.1.3 Biofunctionalisation of short electrospun fibres

The short nanofibres were biofunctionalised by directly immobilizing trophic factors to their surface. PLLA nanofibres lack the appropriate chemistry for standard coupling strategies and will therefore be treated with either ED to introduce amine moieties. Bioconjugation was then facilitated through incubation in succinimidyl-4-(N-maleimidomethyl) cyclohexane-1-carboxylate (SMCC) crosslinker. Here, as proof-of-principle, glial derived neurotrophic factor (GDNF), a neurotrophin known to promote dopamine (DA) neuron survival and axonal

growth, was immobilised onto the short fibres. Coupling efficiency was determined Enzyme-linked immunosorbent assay (ELISA) using antibodies raised against the recombinant proteins of interest (GDNF) (Figure 7.6). We have previously used these methods to validate surface chemistry and the immobilization of protein respectively (Chapter 4 and 6) [8].

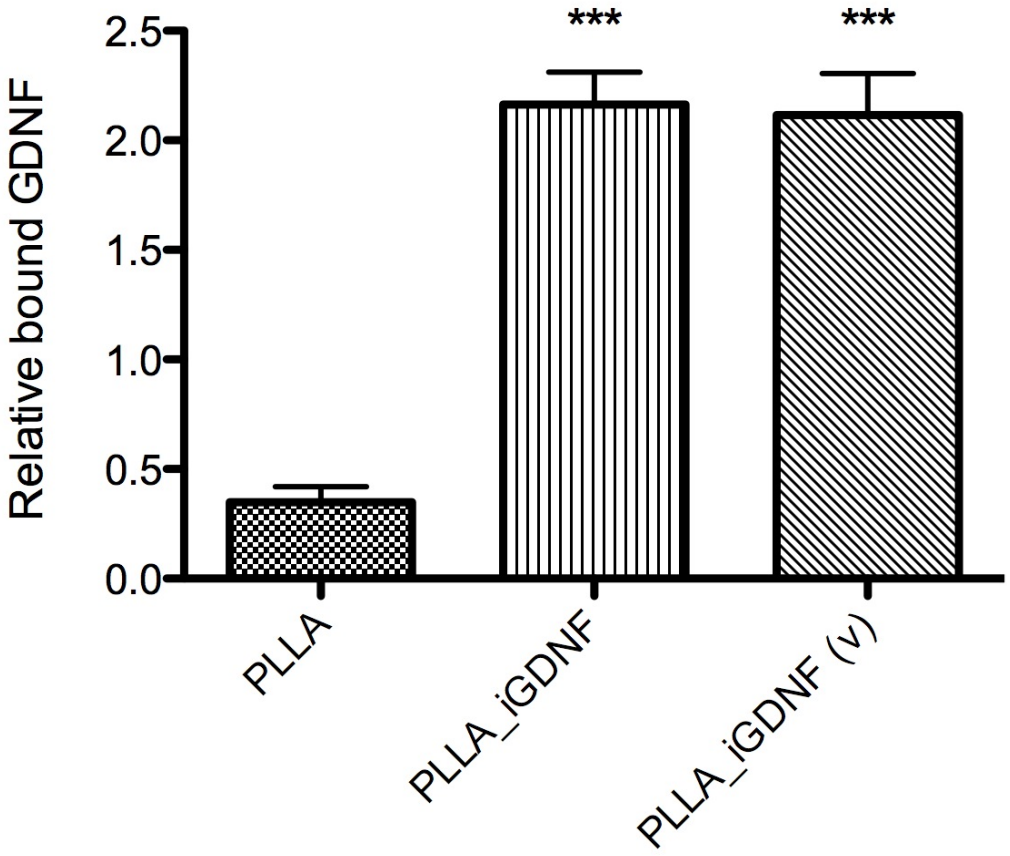

Figure 7.6 GDNF ELISA confirms the attachment of GDNF onto PCL-ED scaffolds via sulfo-SMCC crosslinker. The groups from left are (A) control PLLA; (B) an ELISA on a scaffold incubated in soluble GDNF; (C) an ELISA on a scaffold incubated in soluble GDNF with vortexing applied during the washing steps; (D) an ELISA of a scaffold with GDNF firmly attached to the surface of the fibres using SMCC; (E) an ELISA of a scaffold with GDNF firmly attached to the surface of the fibres using SMCC with vortexing applied during the washing steps. Data represents mean + SEM. *P < 0.05, **P < 0.01, One way ANOVA with Tukey post-hoc test.

Figure 7.6 shows vortexing has no influence on the amount of GDNF immobilised on the scaffolds because GDNF is covalently attached via the corsslinker SMCC to the surface and that there is minimal physical adsorption. These short, functionalised electrospun fibres were then mixed in with the PDL functionalised xyloglucan hydrogel to present GDNF within the 3D hydrogel structure. Figure 7.7 is an SEM picture of the composite scaffold where the presence of the short fibres within the xyloglucan hydrogel post gelation is clearly evident.

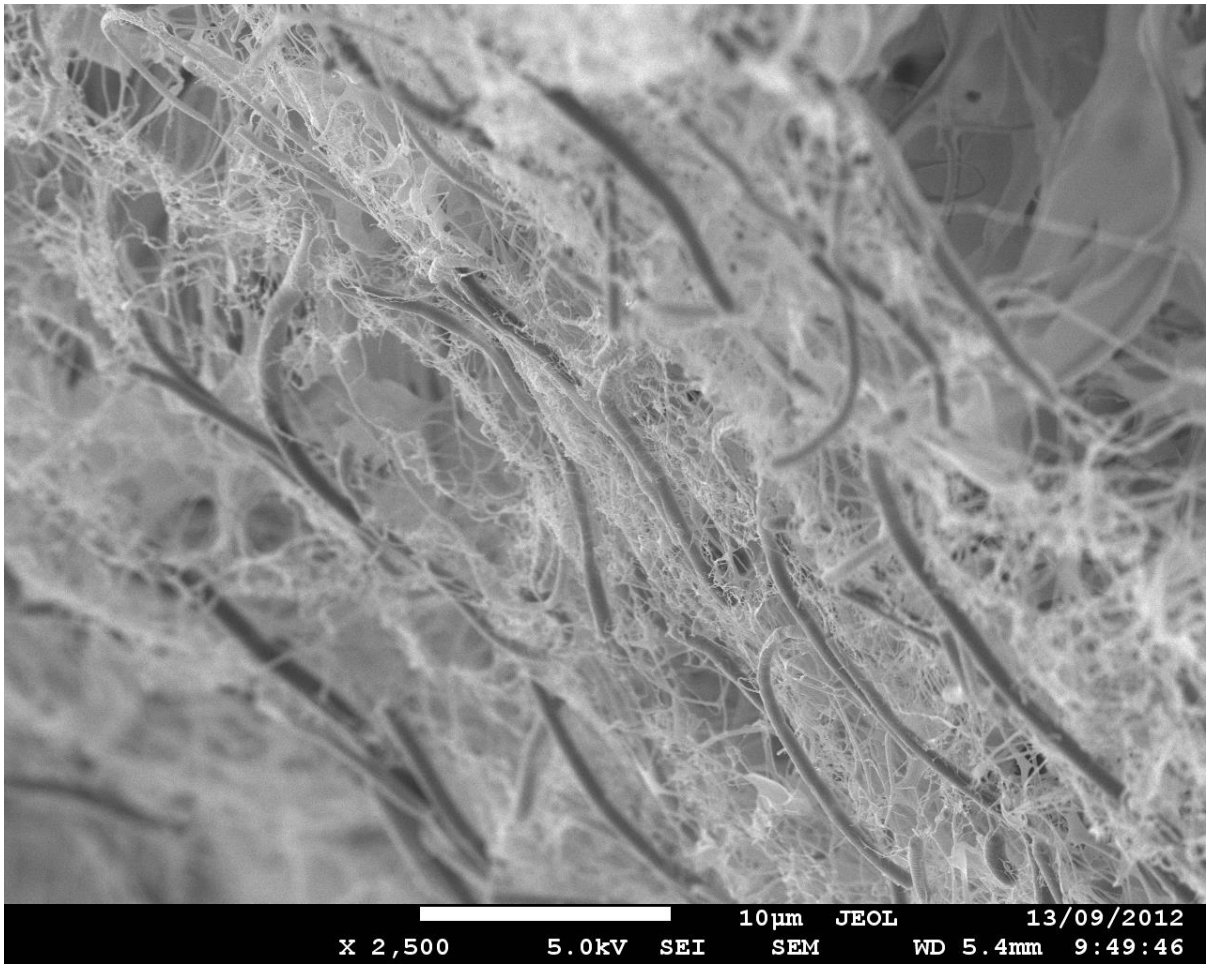

Figure 7.7 SEM picture of PLLA short fibres that have been mixed within the PDL functionalised xyloglucan hydrogel prior to gelation.

7.3.2 *In vitro* results

The experimental groups were control (glass coated with PDL), xyloglucan, xyloglucan with short fibres, and xyloglucan with short fibres immobilized with GDNF. In the previous chapter we have shown that primary cortical NSCs adopt *in vivo* like morphologies, undertake differentiation and survival longer on electrospun scaffolds compared to traditional 2D cultures. We have implanted the modified materials with the brains of adult rats demonstrating limited inflammation as well as an ability to encourage endogenous neurites to infiltrate the scaffolds. Moreover, these materials have been further optimised *in vitro* through the immobilisation of GDNF to positively influence NSC fate specification, proliferation, survival and axonal outgrowth in the comparison with control. Ligand immobilisation onto the surface of the electrospun scaffolds prevented endocytosis thereby prolonging the period of stimulation compared to soluble factors. Therefore we have demonstrated that these fibrous networks, through subsequent biochemical and physiochemical modification, are able to effectively present appropriate stimuli for *in vivo* repair. However, we recognise that the deployment of such scaffolds will be disease/injury specific, as while the fibrous morphology can encourage cell migration, differentiation and elongation their potential to encourage regeneration within lesions is debatable, as they cannot readily interface with the surrounding parenchyma. As seen in the previous chapter, the scaffolds must also be "rolled" and implanted within the host as they cannot be delivered in a minimally invasive manner through injection with a micro capillary resulting in increased tissue damage.

Therefore, in this chapter we have developed a method to circumvent these pitfalls while maintaining the benefit of growth factor presentation to providing an environment that is

more conducive to tissue re-organisation, as seen in Figure 7.7 above. We wanted to confirm the biocompatibility of the new composite scaffold through assessing the viability of primary ventral midbrain neural cells on the composite scaffolds *in vitro* for 3 days, prior to the commencement of *in vivo* studies. Figure 7.8 shows the viability of the cells indicating that there was statistically superior cell viability for the PDL xyloglucan scaffold, and the xyloglucan with the inclusion of both unfunctionalised and functionalised short fibres compared to the 2D PDL control (approximately a 2-fold increase in viability). This demonstrates the ability of all the materials to support NSCs, as well as the biocompatibility of the materials. Interestingly, there was a significant increase in cell viability for the composite scaffold with iGDNF functionalised short fibres (49.7 + 1.4%) compared to the xyloglucan material (40.3 + 1.9%) indicate the responsiveness of the cells to the immobilised growth factor. This confirmed that the presentation of GDNF, known to promote the survival of neural cells, resulted in a significant increase in cell viability when presented in the composition scaffolds, support our previous data (chapter 6).

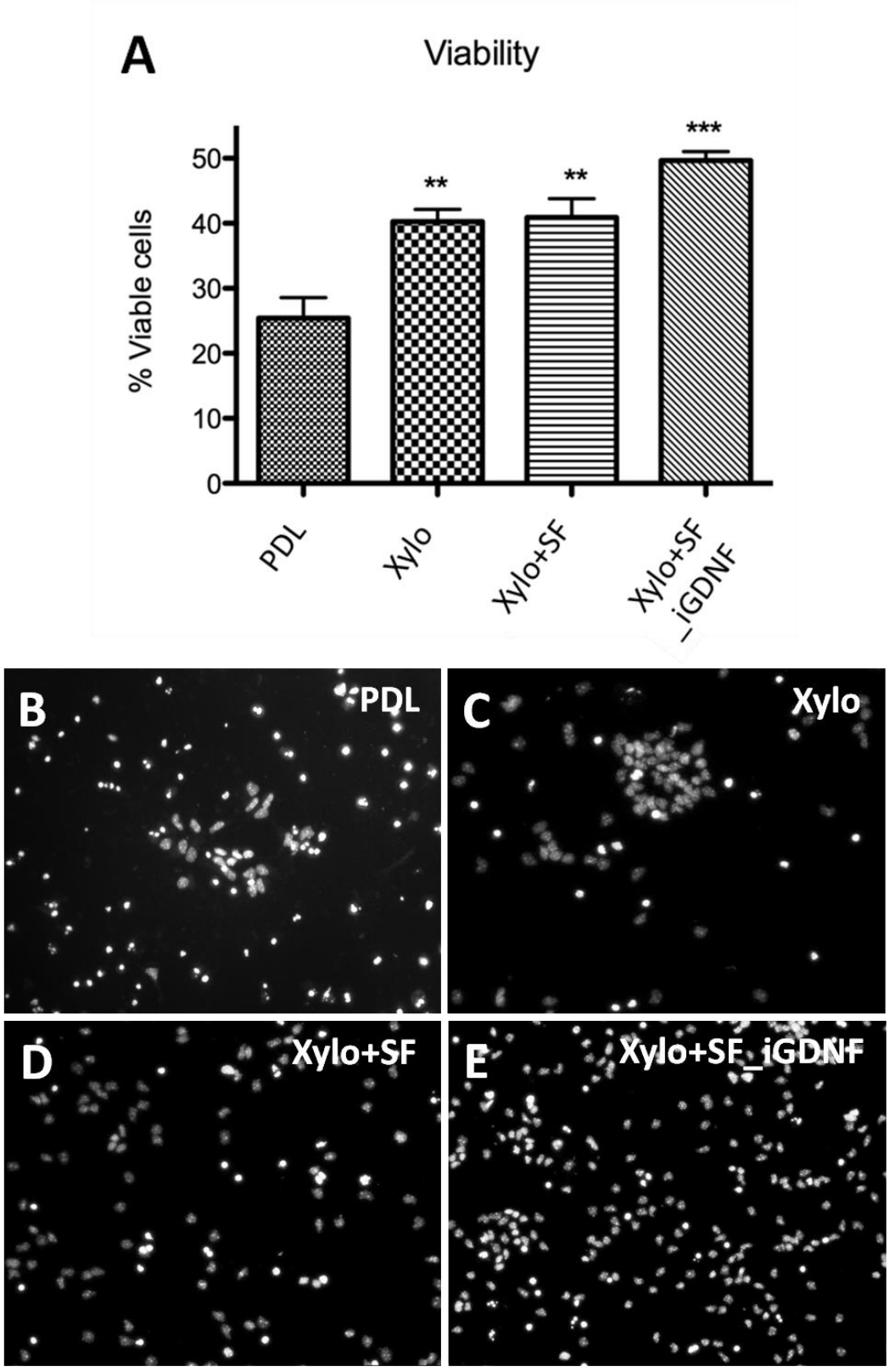

Figure 7.8 Xyloglucan hydrogel scaffolds, including short fibres and short fibres that were tethered GDNF, enhanced the cell viability compared to standard PDL controls after 3 days *in vitro*. (A) cell viability of VM cells in (B) PDL, (C) xyloglucan-PDL, (D) xyloglucan-PDL with short fibres, and (E)

xyloglucan-PDL with short fibres tethered with GDNF. Data represents mean + SEM. *P < 0.05, **P < 0.01, ***P < 0.001 One way ANOVA with Tukey post-hoc test.

Next, we demonstrated the ability of cultured ventral midbrain NSC/progenitors to differentiate into neurons (TUJ+) and more appropriately for the treatment of Parkinson's disease, dopaminergic neurones (+TH). The differentiation ratios for neurones were similar for cells cultured under all conditions, with TUJ+ neurons dominating the cultures (approximately 80% of all cells, Figure 7.9). This was not surprising, as the donor age of the cultures was 12.5 days, which was selected as it corresponded to a period of peak dopamine neurogenesis. A comparison of the cultures demonstrated a significant decrease in TH+ cells on the PDL functionalised xyloglucan scaffold with the inclusion of unfunctionalised short fibres compared to the PDL functionalised xyloglucan scaffold (0.5% + 0.09 and 1.12% + 0.33, respectively). The reason for this is likely due to slight changes in the morphology and potentially the modulus of the composite scaffold as a result of the short fibre addition. However, there is approximately a 3 fold increase in the number of TH+ cells present on the composite scaffold when GDNF was presented on the fibres (Figure 7.9 C, H-I). This is not surprising as GDNF is a neurotrophic known to promote the survival of midbrain DA neurones. Overall the result shows that the composite scaffolds maintained neuron population around 80% and increased DA neurons when GDNF was presented to the cells in culture. It indicates that the composite scaffolds sufficiently exposed tethered GDNF through short fibres to NSCs in vivo, which still retains the bio-functionality and cause biological effects after chemical conjugation.

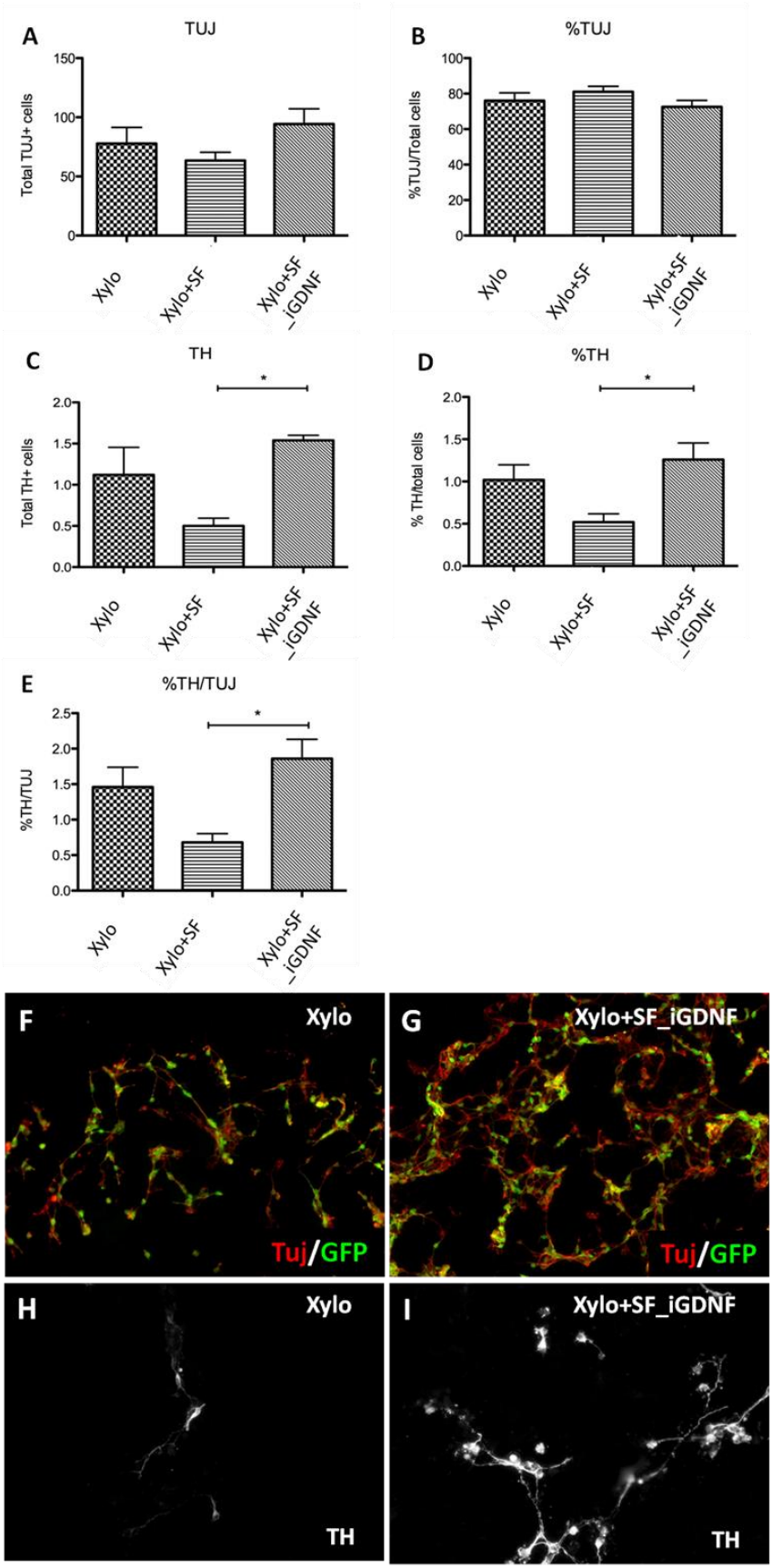

Figure 7.9 Differentiation of NSCs towards the neuronal (TUJ+) and dopaminergic (TH+) phenotype. (A) shows the total number of THU+ cells, (B) shows the percentage of TIJ+ cells, (C) shows the

total number of TH+ cells, (D) shows the percentage of TH+ cells, (E) shows the percentage of TH+/ THU+ cells in each groups. (F) represents TUJ+/ GFP cells in Xylo, and (G) xyloglucan-PDL with short fibres tethered with GDNF. (H) represents TH+ cells in Xylo, and (I) xyloglucan-PDL with short fibres tethered with GDNF. Data represents mean + SEM. *P < 0.05, **P < 0.01, One way ANOVA with Tukey post-hoc test.

In addition to promoting survival of dopaminergic neurons, GDNF is also known to promote the growth and guidance of DA axons [28]. We therefore looked at the effect of tethered GDNF (on short fibres within a hydrogel) on the morphology of DA neurites in culture (Figure 7.10). The presence of short fibres within the composite scaffold, or presentation of GDNF, had no effect on neurite number or branching of DA neurons (Figure 7.10 A, B). Examination of neurite length illustrated that the presence of SF within the xyloglucan scaffold had no effect on either total neurite length (including axon and all dendrite lengths collectively, Figure 7.10 C, F-F') or axon length (dominant neurite extending from TH+ soma, Figure 7.10 D, F-F'). Not surprisingly, the presentation of GDNF significantly increased total neurite length (Figure 7.10 C, G-G'), an effect that was specific to the DA axon (Figure 7.10 D, G-G'). This result is well documented in the literature and demonstrates our ability to form a composite nanofibrous/ hydrogel scaffolds to support primary VM cells, their derivatives and neurite processes.

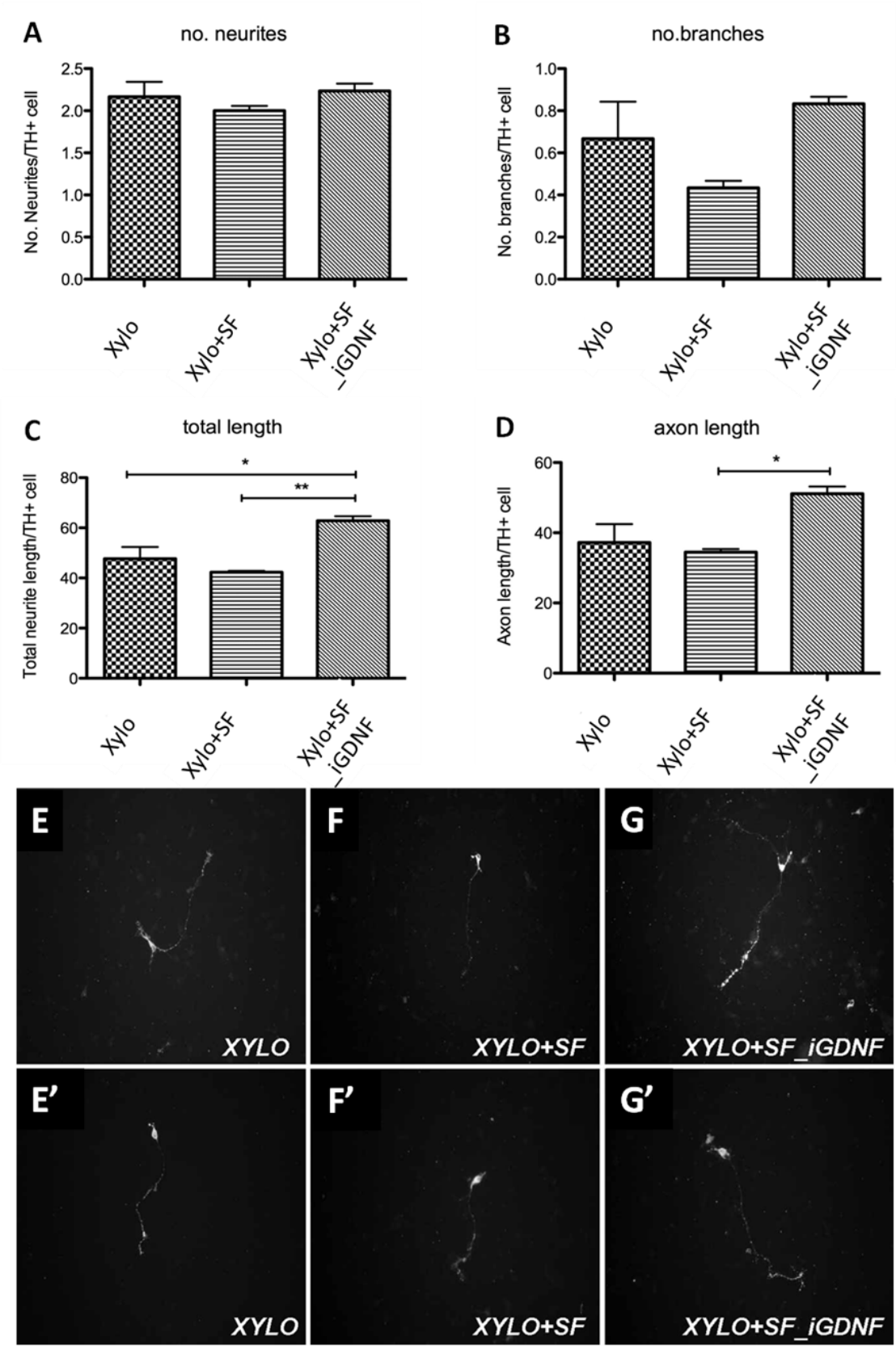

Figure 7.10 Influence of tethered GDNF on NSC process development. (A) shows the number of neurite, (B) branch, (C) total length of neurite, and (D) total length of axon of NSCs within (E-E') xyloglucan-PDL, (F-F') xyloglucan-PDL with short fibres, and (G-G') xyloglucan-PDL with short

fibres tethered with GDNF. Data represents mean + SEM. *P < 0.05, **P < 0.01, One way ANOVA with Tukey post-hoc test.

Through our *in vitro* results we believe that our composite scaffold delivers the structural benefit of nanofibres concomitantly with the superior properties of a hydrogel for the purpose of implantation. This demonstrates the potential of these scaffolds to offer improve survival of grafted cells and their integration into the host by providing physical and biochemical support.

7.3.3 *In vivo* results

Experimental conditions for the *in vivo* studies included cells alone, cells in xyloglucan, cells in xyloglucan with short fibres and cells in xyloglucan with short fibres mobilised with GDNF. The composite scaffolds tested above were implantated into the brains of PD mice together with NSCs. Tyrosine hydroxylase staining for dopamine neurons in the ventral midbrain and dopamine fibers in the striatum confirmed successful 6OHDA lesioning (Figure 7.11).

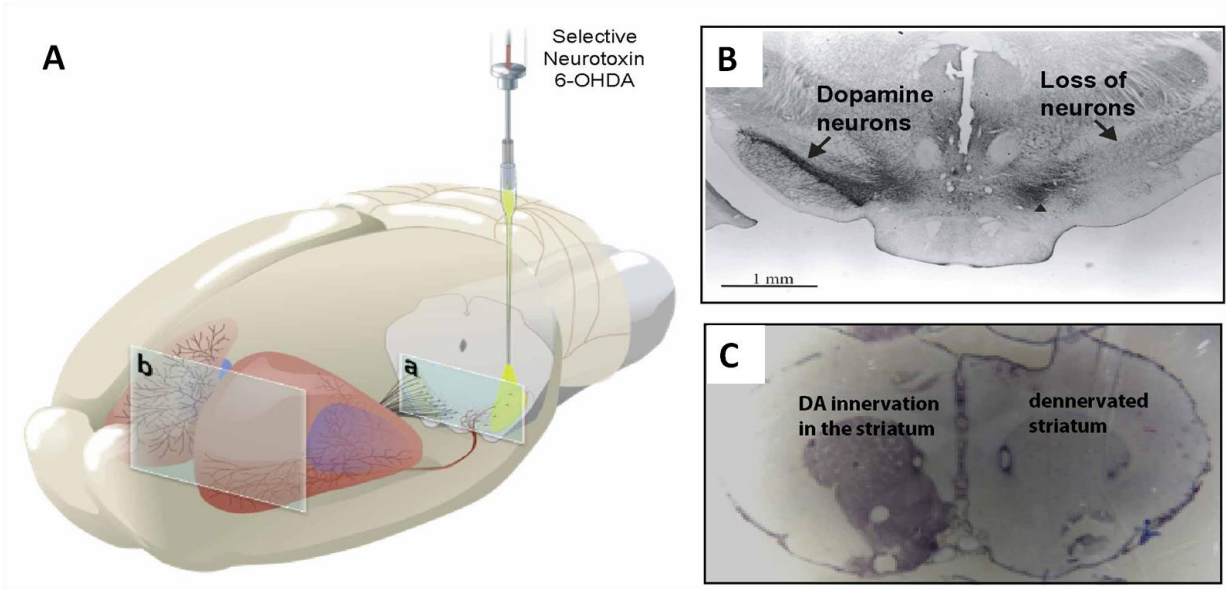

Figure 7.11 (A) Schematic illustrating unilateral injection of the dopamine selective neurotoxin, 6-hydroxydopamine (6OHDA), into the ventral midbrain. Schematic courtesy of Bengt Mattsson (Lund

University, Sweden). (B) Photomicrograph of the ventral midbrain illustrating DA neurons in the intact hemisphere (shown by tyrosine hydroxylase staining, black) and ablation of the DA neurons in the opposite hemisphere of the brain. (C) Ablation of midbrain DA neurons results in dennervation of the dopamine fibers within the target tissue (the striatum). Note the TH+ fibers in the intact striatum and absence of fibers in the lesioned hemisphere.

Whilst cell loss occurs within the VM in Parkinson's disease, cell transplants are placed ectopicallly into the target striaum, so as to restore dopamine transmission. In the present study, we utilized the TH-GFP for donor tissue so that grafted dopamine cells and fibres (GFP+) could be destinguished from host dopamine neurons and innervation (GFP-). We confirmed viable grafts (Figure 7.12 A, the presence of GFP+ dopamine neurons) in the striatum of all grafted animals after 10 weeks. Transplantation of cells together with functionalized composite scaffolds (cells + xylo + SF_iGDNF) resulted in supporting GFP+ cells (502.9 + 124.1), similar to cells + composite scaffold without GDNF (cells + xylo + SF; 275.3 + 66.9), (Figure 7.12 A). This finding, whilst not statistically significant, suggests that the GDNF bound to the short fibres may increase the survival of transplanted cells, supporting our *in vitro* observation (as shown in figure 7.12 A). Further studies, including larger groups of animals are required to fully elucidate these effects.

Next we investigated the ability of composite scaffolds (± iGDNF) to promote the integration of transplanted dopamine neurons (i.e. reinnervation) within the striatum (Figure 7.12 (B, C-E)). The use of the GFP reporter cells as donor material again allow us to not only quantify graft derived dopamine neurons, but additionally visualise and quantify the extensive network of processing that form from these cells. This allows us to compare each of the scaffolds to see if there is any advantage to presenting iGDNF on short fibres. Figure 7.12 (B) shows the density of GFP+ innervation on xyloglucan-PDL, xyloglucan-PDL with

unfuctionalised short fibres and xyloglucan-PDL-short fibres-iGDNF. While no significant difference was obsered, the transplantation of functionalized composite scaffolds (cells + xylo + SF_iGDNF) resulted in an almost 2-fold increase in GFP+ cells compared to cells + composite scaffold without GDNF (502.9 + 124.1 and 275.3 + 66.9; Figure 7.12 A). Further studies, involving larger group sizes are required to validate these trends. This is a on-going focus within the research team.

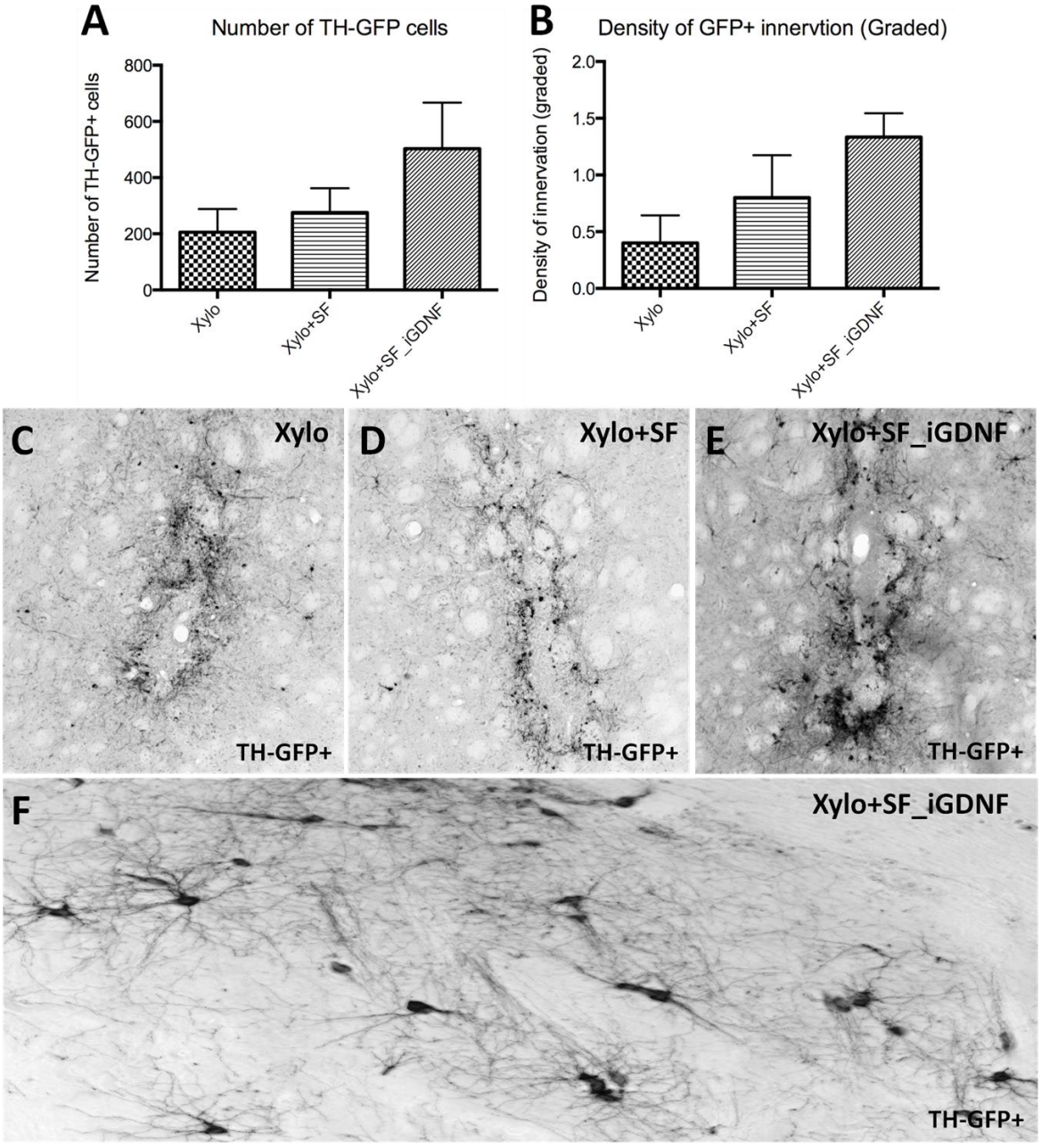

Figure 7.12 Tethered GDNF promoted the survival and innervations of grafted TH-GFP+ cells in trends; (A) shows the survival of grafted cells in each groups; (B) shows the density of innervation resulting from grafts within (C) xyloglucan-PDL, (D) xyloglucan-PDL with short fibres, and (E-F) xyloglucan-PDL with short fibres tethered with GDNF.

We also examined the inflammation caused during cell transplantation with these materials (Figure 7.13). There was no statistical difference observed in the activation of reactive astrocytes (area of GFAP+ staining) for any of the materials groups (Figure 7.13 A). While introducing substances into the brain, a subsequent inflammatory response is also induced, which can result in glial scarring and consequently inhibit the regeneration and infiltration of neurons and axons to the injured sites. As shown in the previous chapter the introduction of biomaterials modified with trophic factor in cell transplantation suppressed astrocyte differentiation *in vivo*; moreover a recent study has demonstrated the influence of GDNF in spinal cord axonal regeneration to the inhibition of reactive astrocytes [29]. Therefore we believe that the ability to limit the associated astrocytosis contributed to the superior graft survival observed, and may be crucial in reducing scar formation.

Finally we investigated the microglia activation, as it has been shown previously that xyloglucan can reduce microglia activation compared to needle sham control [9]. This was also true in this study but there was a significant increase in the number of activated microglia when unfunctionalised short fibres were included within the xyloglucan hydrogel (Figure 7.13 B, C-E). This indicated that the xyloglucan with unfunctionalised short fibres are not as biocompatible xyloglucan alone. Interestingly, when tethered GDNF was presented on the surface of the fibres the number or activated microglia subsided back down to the same level as for the xyloglucan alone material (Figure 7.13 (B)). This demonstrates our ability to incorporate biochemical and physical support into a composite scaffold to improve current cell transplantation technologies.

The composite scaffold formed within this study encompassed the benefits of nanofibers, hydrogels and growth factor presentation to give the potential to be an advanced material for stem cells survival, neurite length and axon development *in vitro*. These advanced materials resulted in significantly increased cell viability, dopaminergic differentiation and dopaminergic axonal growth (compared to cells cultured on PDL-coated glass, or unmodified xyloglucan). *In vivo* results showed trends of modified scaffolds (incorporating GDNF) to support cell transplants (improving number of grafted cells and innervation), but no statistical significance between different materials were observed after 10 weeks. Whilst this may reflect small group sizes and the necessity to repeat these studies on larger cohorts of animals (and is a likely explanation as revealed by the large error bars observed in figure 7.12), it may also reflect an inferior biocompatibility of xyloglucan. This composite scaffold incorporates the unique structural benefit of nanofibres, but also the less invasive properties of a hydrogel for the purpose of cell transplantation in the comparison with electrospun scaffolds.

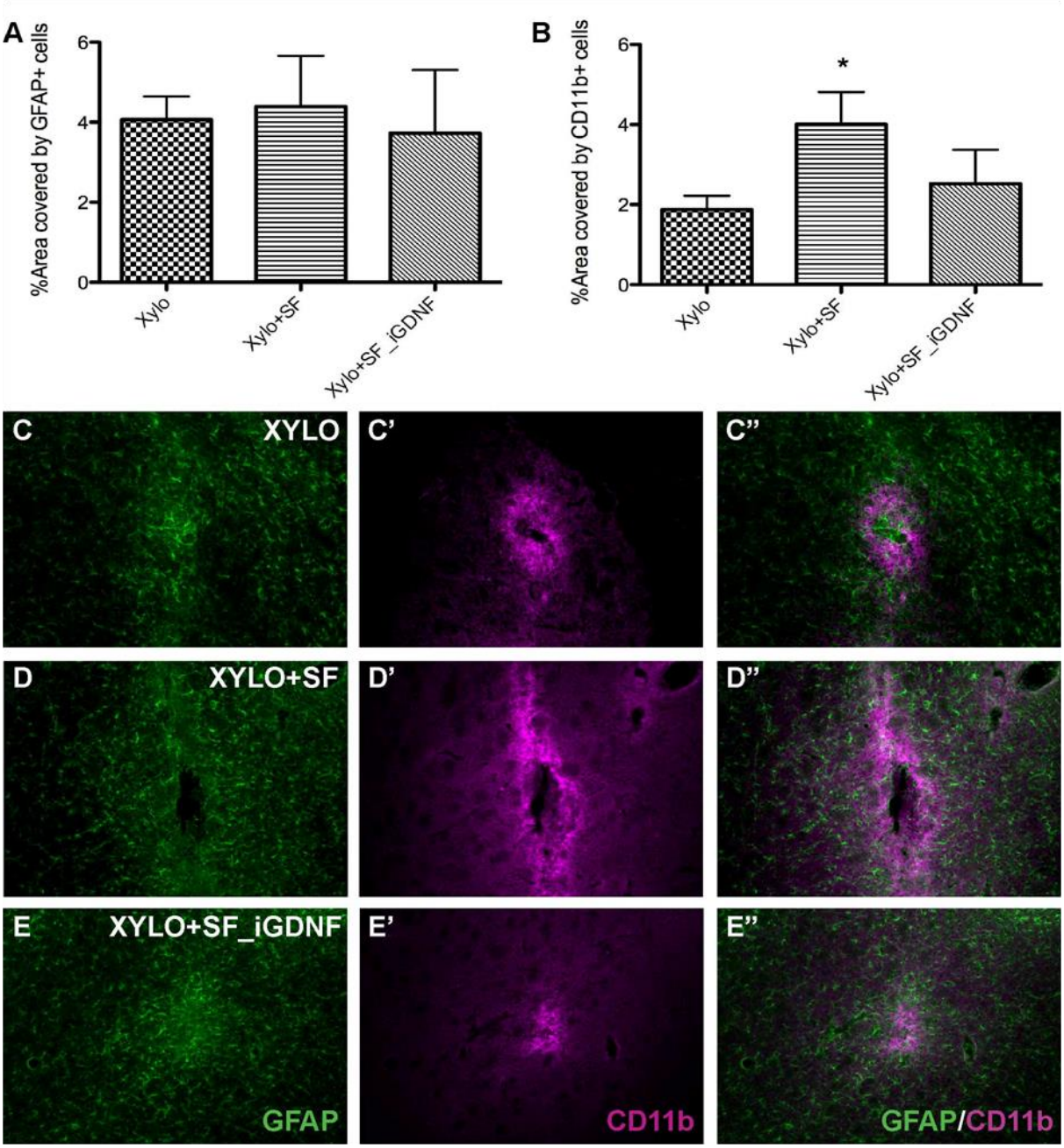

Figure 7.13 The inflammatory response caused by implanted scaffolds with grafted cells; (A) shows the percentage area covered by GFAP+ cells for each of the materials, (B) shows the percentage area covered by CD11b+ cells in (C) xyloglucan-PDL, (D) xyloglucan-PDL with short fibres, and (E) xyloglucan-PDL with short fibres tethered with GDNF. (C-E) shows GFAP+ cells, (C'-E') shows CD11b+ cells, and (C''-E'') are merged images.

7.4 CONCLUSION

The study examined the ability of composite scaffolds (including the benefits of nanofibers and a hydrogel) to support dopaminergic neurons *in vitro* and following implantation into the brain of Parkinsonian mice. Here we demonstrated that these scaffolds were biocompatible and capable of supporting ventral midbrain NSCs/ progenitors and mature neurons *in vitro* and *in vivo*. Additionally these scaffolds were utilized to present GDNF, thereby positively impacting on the survival of cells as well and their plasticity in the comparison with the absence of GDNF. Composite scaffolds including tethered GDNF show the increasing tendency in graft size (more TH-GFP cells) and striatal reinnervation (area of striatum covered by GFP+ staining). Consequently, these scaffolds could have positive impacts on 2 of the greatest stumbling blocks for cell transplantation – that is, promoting cell survival and, promoting the integration of the transplanted cells into the host brain. These scaffolds had no effect on the number of reactive astrocytes and moreover the presence of GDNF in the composite scaffolds inhibited microglia compared to the absence of GDNF, i.e. the overall the bio-functionality of the composite scaffolds was promoted by GDNF immobilisation on short fibres and the physical properties united the benefits from bother xyloglucan hydrogel and nanofibres. Collectively, these findings demonstrate that the use of composite scaffolds, such as the one employed in the present study, could have a positive impact on the integration of neural transplants for the treatment of Parkinson's disease in the future. The results also indicate some further studies are required to fully elucidate the benefits (and disadvantages) of these biofunctionalized scaffolds in vitro and in vivo. Such studies may shed more light on the biocompatibility of xyloglucan, quantity of tethered GDNF, incorporation of cells into scaffolds prior implantation. Furthermore, whilst demonstrating proof-or-principle in an animal model of PD in the present study, the knowledge gained here could additionally be

exploited to promote the survival and integration of cell transplants in a number of other neural injuries.

7.5 REFERENCES

[1] Androutsellis-Theotokis A, Rueger MA, McKay RDG, Jeffrey HK, Mark HT. Stem Cell Therapies for Parkinson's Disease. In: Jeffrey K, Mark T, editors. CNS Regeneration (Second Edition). San Diego: Academic Press; 2008. p. 161-80.
[2] Winkler C, Kirik D, Bjorklund A. Cell transplantation in Parkinson's disease: how can we make it work? Trends in Neurosciences. 2005;28:86-92.
[3] Parish CL, Arenas E. Stem-cell-based strategies for the treatment of Parkinson's disease. Neurodegener Dis 2007;4(4):339-47. 2007.
[4] Horne MK, Nisbet DR, Forsythe JS, Parish CL. Three-Dimensional Nanofibrous Scaffolds Incorporating Immobilized BDNF Promote Proliferation and Differentiation of Cortical Neural Stem Cells. Stem Cells Development. 2010;19:843-52.
[5] Nisbet DR, Pattanawong S, Ritchie NE, Shen W, Finkelstein DI, Horne MK, et al. Interaction of embryonic cortical neurons on nanofibrous scaffolds for neural tissue engineering. J Neural Eng. 2007;4:35-41.
[6] Nisbet DR, Rodda AE, Horne MK, Forsythe JS, Finkelstein DI. Neurite infiltration and cellular response to electrospun polycaprolactone scaffolds implanted into the brain. Biomaterials. 2009;30:4573-80.
[7] Wang TY, Forsythe JS, Parish CL, Nisbet DR. Biofunctionalisation of polymeric scaffolds for neural tissue engineering. J Biomater Appl.
[8] Horie N, Maag A-L, Hamilton SA, Shichinohe H, Bliss TM, Steinberg GK. Mouse model of focal cerebral ischemia using endothelin-1. Journal of Neuroscience Methods. 2008;173:286-90.
[9] Nisbet DR, Rodda AE, Horne MK, Forsythe JS, Finkelstein DI. Implantation of Functionalized Thermally Gelling Xyloglucan Hydrogel Within the Brain: Associated Neurite Infiltration and Inflammatory Response. Tissue Engineering Part A. 2010;16:2833-42.
[10] Anuradha S, Uma Maheswari K, Swaminathan S. Fabrication of uniaxially aligned 3D electrospun scaffolds for neural regeneration. Biomed Mater. 2011;6:025004.
[11] Carlberg B, Axell MZ, Nannmark U, Liu J, Kuhn HG. Electrospun polyurethane scaffolds for proliferation and neuronal differentiation of human embryonic stem cells. Biomed Mater. 2009;4:7.
[12] Chew SY, Mi R, Hoke A, Leong KW. The effect of the alignment of electrospun fibrous scaffolds on Schwann cell maturation. Biomaterials. 2008;29:653-61.
[13] Cao H, Liu T, Chew SY. The application of nanofibrous scaffolds in neural tissue engineering. Advanced Drug Delivery Reviews. 2009;61:1055-64.
[14] Tysseling-Mattiace VM, Sahni V, Niece KL, Birch D, Czeisler C, Fehlings MG, et al. Self-assembling nanofibers inhibit glial scar formation and promote axon elongation after spinal cord injury. J Neurosci. 2008;28:3814-23.
[15] Wang M, Zhai P, Chen X, Schreyer DJ, Sun X, Cui F. Bioengineered Scaffolds for Spinal Cord Repair. Tissue Engineering Part B: Reviews. 2011;17:177-94.
[16] Woerly S, Pinet E, de Robertis L, Van Diep D, Bousmina M. Spinal cord repair with PHPMA hydrogel containing RGD peptides (NeuroGel(TM)). Biomaterials. 2001;22:1095-111.
[17] Nisbet DR, Crompton KE, Hamilton SD, Shirakawa S, Prankerd RJ, Finkelstein DI, et al. Morphology and gelation of thermosensitive xyloglucan hydrogels. Biophysical Chemistry. 2006;121:14-20.

[18] Crompton KE, Goud JD, Bellamkonda RV, Gengenbach TR, Finkelstein DI, Horne MK, et al. Polylysine-functionalised thermoresponsive chitosan hydrogel for neural tissue engineering. Biomaterials. 2007;28:441-9.
[19] Horn EM, Beaumont M, Shu XZ, Harvey A, Prestwich GD, Horn KM, et al. Influence of cross-linked hyaluronic acid hydrogels on neurite outgrowth and recovery from spinal cord injury. Journal of Neurosurgery: Spine. 2007;6:133-40.
[20] Hynd MR, Frampton JP, Dowell-Mesfin N, Turner JN, Shain W. Directed cell growth on protein-functionalized hydrogel surfaces. Journal of Neuroscience Methods. 2007;162:255-63.
[21] Elkabetz Y, Studer L. Human ESC-derived Neural Rosettes and Neural Stem Cell Progression. Cold Spring Harbor Symp Quant Biol. 2008;73:377-87.
[22] Nisbet DR, Moses D, Gengenbach TR, Forsythe JS, Finkelstein DI, Horne MK. Enhancing neurite outgrowth from primary neurones and neural stem cells using thermoresponsive hydrogel scaffolds for the repair of spinal cord injury. Journal of Biomedical Materials Research Part A. 2009;89A:24-35.
[23] Inai R, Kotaki M, Ramakrishna S. structure and properties of electrospun PLLA single nanofibres. Nanotechnology. 2005;16:208-13.
[24] Straley KS, Foo CWP, Heilshorn SC. Biomaterial Design Strategies for the Treatment of Spinal Cord Injuries. Journal of Neurotrauma. 2006;27:1-19.
[25] Cameron AR, Frith JE, Cooper-White JJ. The influence of substrate creep on mesenchymal stem cell behaviour and phenotype. Biomaterials. 2011;32:5979-93.
[26] Discher DE, Janmey P, Wang Y-l. Tissue Cells Feel and Respond to the Stiffness of Their Substrate. Science. 2005;310:1139-43.
[27] Pettikiriarachchi JTS, Parish CL, Shoichet MS, Forsythe JS, Nisbet DR. Biomaterials for Brain Tissue Engineering. Australian Journal of Chemistry. 2010;63:1143-54.
[28] Nakajima K, Hida H, Shimano Y, Fujimoto I, Hashitani T, Kumazaki M, et al. GDNF is a major component of trophic activity in DA-depleted striatum for survival and neurite extension of DAergic neurons. Brain Research. 2001;916:76-84.
[29] Deng L-X, Hu J, Liu N, Wang X, Smith GM, Wen X, et al. GDNF modifies reactive astrogliosis allowing robust axonal regeneration through Schwann cell-seeded guidance channels after spinal cord injury. Experimental Neurology. 2011;229:238-50.

Chapter 8

General discussion

Contents

8.1 GENERAL CONCLUSION

The main goal of this thesis was to establish the methodology of combining implantation of bio-engineered scaffolds and transplantation of primary neural cells to promote repair of injured CNS. Additionally the modification of scaffolds with neurotrophic factors was aimed to improve the survival and integration of grafted primary neural cells *in vivo* to overcome some of the current limitations hindering cell replacement therapies and their advancement to the clinic. To maximise the capability of the bioengineered scaffolds to support cells, different types of scaffolds were combined for implantation purpose *in vivo*. Overall, the PhD thesis demonstrated a stable GDNF delivery system via electrospun scaffolds with profound effects on the survival and integration of grafted cells *in vitro* and *in vivo*. The delivery system was continuously modified to minimise the invasiveness of implantation methods by combing a hydrogel and short electrospun scaffolds nanofibres, which was proved to support grafted ventral midbrain cells in animals of PD, enhancing survival and integration.

8.1.1 Characterisation of the stability and biofunctionality of tethered GDNF on electrospun scaffolds

In chapter 4, electrospun PCL scaffolds were successfully immobilise with GDNF via a covalent conjugation (figure4.1; page116). The presentation of the protein on the scaffold was confirmed at different time points after attachment (1, 3, 7 and 14 days), and tethered GDNF on scaffolds was demonstrated to be stable without releasing and/or degrading over time (figure4.1; page116). Tethered GDNF on scaffolds were shown to be biologically active, by its ability to activate intracellular signalling (phosphorylate Erk) (figure4.2; page118) as well as support the survival and differentiation of ventral midbrain cells for up to 7 days in

culture (figure4.4;page120). Moreover the modified scaffolds directed cell differentiation into dopamine cells and enhanced the population when compared to control (glass coated with PDL) after 3 and 7 days *in vitro* (figure4.4; page120). In all, this chapter demonstrated the ability to present stable and functional proteins (GDNF as way of example) long term in a biological setting.

8.1.2 Electrospun scaffolds support primary cortical cell transplants in the intact rat brain

In chapter 5, electrospun PCL scaffolds were firstly examined for their biocompatibility and capability of supporting primary cortical cells *in vitro* (figure5.1, 5.2, 5.3; page132-133). The results show the scaffolds supported cell survival and differentiation in culture (figure5.1, 5.2, 5.3; page132-133). Once this was confirmed, we next set out to develop an implantation method combining both primary neural cells and the scaffolds. Pre-seeding cells onto the scaffold was initially trialled; however cells remained poorly attached upon rolling of the material for implantation (figure5.4; page134). Consequently, PCL scaffolds were rolled and inserted into the brain and cells subsequently implantation either into the scaffold cavity or adjacent to the scaffold. Cells expressing GFP were utilised to aid in the visualisation of graft survival and integration. According to the histological examination, the scaffolds were able to support graft survival and differentiation (figure 5.6, 5.7, 5.8, 5.9, 5.10; page 139-143). Moreover the scaffolds were demonstrated to allow neurite infiltration from both graft and host-derived cells (figure 5.5; page 138). Overall, assessment of the implantation methods and graft morphology showed that cells grafted adjacent to the scaffold demonstrate superior results and were therefore employed in subsequent studies.

Chapter 6 built on the findings of the previous chapter, to now examine and compare the improvement of graft survival and integration in the presence or absence of biofunctionalised scaffolds. First, functionalised scaffolds were demonstrated to increase cell survival and proliferation *in vitro* in the comparison with control (glass coated with PDL) and PCL scaffolds (figure 6.2; page 173). Looking at the bio-functionality of modified scaffolds *in vivo*, tethered GDNF promoted survival of grafted primary neural cells into the host tissue after 28 days in the brain of rats when compared to cell transplantation alone (figure6.3 A; page176). Additionally the electrospun scaffolds were fabricated with micron size which increases the porosity and allows cell infiltrating inside the implanted scaffolds *in vivo* (figure6.3 E; page176). As a result, both graft- and host-derived cells significantly infiltrated inside the modified scaffolds compared to unmodified materials *in vivo* (figure6.3 E; page176), suggesting the morphology and the bio-functionality of the modified scaffolds increase the likelihood of cell repopulating and replacing the scaffolds over a period of time after implantation. Similar to *in vitro* findings, tethered GDNF also encourage proliferation of grafted primary cortical cells relatively to cell transplantation alone (figure6.4 A; page179), suggesting improved repair. Furthermore the presence of modified scaffolds suppressed the number of reactive astrocyte around the graft site compared to grafts of cells alone (figure6.4 D; page179); suggesting reduced inflammation. Collectively these results demonstrate a number of benefits of bioengineered scaffolds for supporting the integration of primary neural cell-based grafts into the intact brain (figure6.3 E; page176), (figure6.5 E; page182); findings that could having important implications for enhancing neural repair in the comparison with cell transplantation alone.

8.1.3 Composite scaffolds, incorporating hydrogel and functionalised short fibres, promote the integration of neural transplant in parkinsonian mice

A conceivable scaffold for promoting neural repair in the brain needs to not only support the graft (as demonstrated in chapters 5 and 6) but be easily implantable, so as to minimise damage to the host tissue. Composite scaffolds were therefore developed that could be injected (by way of hydrogel) but still provide the 3 dimensional structural benefits of electrospun scaffolds (by embedding electrospun short fibres within the hydrogel). These composite scaffolds enhanced the survival of VM cells and increased proportion of dopamine cells *in vitro* relatively to control and xyloglucan with/ without short fibres (figure7.8 A; page212). Moreover the composite scaffolds significantly increased the total neurite length when compared to xyloglucan with/ without short fibres (figure7.10 C; page216). Upon injection into the brains of Parkinsonian mice, these composite scaffolds were capable of supporting cell survival (figure7.8 A; page212), and suppressed immunological responses (figure7.13 B; page222). According to the insignificant differences between different scaffolds in the animal study, there are improvements could be considered in the future; including a replacement to other hydrogels, an increase in quantity of tethered GDNF, an incorporation of cells into hydrogel prior implantation and an increase in animal group size.

8.2 FUTURE WORK

This thesis answers a number of questions regarding the potential of biofunctionalised scaffolds to support primary neural cells and promote their integration into the injured brain. It does however also open up a number of new questions that remain to be address, that will ensure continual advancement of the field and the likelihood of biofunctionalised scaffolds being implemented in the future for the treatment of neural injuries. The following section highlights some of the outstanding concerns.

8.2.1 Application and modification of scaffolds

8.2.1.1 Alternative scaffold materials

This thesis focuses on the potential of electrospun PCL and PLLA nanofibrous scaffolds and short fibres as well as xyloglucan hydrogels to support cells *in vitro* and *in vivo*. The field of tissue engineering however is rapidly developing and continues to identify new and improved materials from which to synthesise scaffolds. As such, self-assembling peptide scaffolds (SAPS) are one of the latest developments in bio-engineered scaffolds for tissue engineering. These scaffolds are attractive as they are based on the self assembling of a natural biological building block (amino acids) making them biocompatible and they offer the greatest functionality and cell signalling capacity, with rapid and easy synthesis into more complex structures. Peptide-based scaffolds form hydrogels by various weak non-covalent interactions in water. These interactions lead to the formation of organised supramolecular assemblies that can give rise to structures such as nanofibres and nanotubes. The nanoscale fibrillar structure and subsequent hydrogels produced by the controlled self-assembly of peptides are

therefore excellent candidates to provide some aspects of the *in vivo* cellular microenvironment necessary to support cells, and restore tissue. SAP scaffolds can also be designed to present specific protein epitopes that provide more effective graft support than presentation of the protein itself. SAPS can be designed to present epitopes for key proteins that control cell adhesion within the extracellular matrix, including fibronectin, laminin, collagen and chrondrotin sulphate. Thus, scaffolds that are capable of presenting cell-binding epitopes of proteins, including RGD, IKVAV and YIGSR, are of interest. It has been demonstrated that the laminin-derived IKVAV epitope promotes neuronal differentiation of neural progenitor cells more efficiently than laminin itself. This effect was presumed to be due to the high density of signals presented on the fibre surface (1000-fold greater than the ordered array of native laminin), as well as superior signal dynamics and spatial orientation. The ability of these SAPS, as well as other newly developed scaffolds, to support neural cells in vitro remain to be determined, as well as their capacity to support cell transplants following neural injury.

8.2.1.2 Scaffolds morphology

Scaffolds with a sphere structure in nano-size can be applied to encapsulate cells for targeting areas *in vivo* and fill the lost neural tissue/ neural pathway, and it can specifically control the number of cells carried by each sphere scaffold *in vivo*. Moreover the round shaped scaffolds can be easily implanted by injection reducing the disruption to the host tissue. Polymer solution pre-mixed with cell suspension can be electrospun to produce scaffolds encapsulating cells in round shapes. Additionally once cells are encapsulated inside scaffolds, it is isolated from the outside environment and protected by the scaffolds. The scaffolds can then be coated with different layers by immersing in solutions to enhance the bio-

functionality or modify the mechanical properties for specific applications without decreasing cell viability.

8.2.1.3 Additional protein tethering to deliver multiple factors

As proof of principle this thesis focuses on the tethering of one protein, GDNF, onto electrospun fibres. Whilst our laboratory has also previously demonstrated the ability to tether BDNF, and shown its functional benefit, further studies are required to determine whether other proteins can be similarly tethered onto nanofibres using this covalent attachment approach. It is probable and likely that attachment of some proteins will interfere with the active site of the protein and prevent cellular interaction. As such, studies similar to those performed in chapter 4 will be required for each protein of interest to ascertain its stability and functionality.

To restore the injured CNS involves complicated biological stimulations from different proteins, therefore a bio-engineered scaffold that can deliver multiple proteins either with gradual release or long lasting effects may accelerate neural repair. A combination of different proteins that promote survival (e.g. neurotrophins GDNF, BDNF, NGF) proliferation (e.g. mitogens including EGF and FGF2), differentiation and axonal growth (e.g. morphogens including Shh and Wnts) that can be tethered to scaffolds via physical adsorptions or chemical conjugations could satisfy different needs for specific applications in neural tissue engineering. As such a composite scaffold could provide multiple cues to enhance repair.

8.2.2 Cell transplantation from a different perspective for Parkinson's disease

In the context of PD, cell transplants are typically performed ectopically into the target tissue (the striatum) as a way to restore dopamine transmission, however these grafts fail to restore normal neural circuitry. Grafts into the site of cell loss (homotypic grafts) are rarely performed as the grafts survive poorly and show limited restoration of the pathway. It is believed that is largely due to the non-conducive host environment – providing inadequate chemical and physical support. It therefore remains to be determined whether bioengineered scaffolds may improve these grafts and restoration of neural circuits. Could cells be implanted into the site of cell loss (the ventral midbrain) together with a scaffold that promote survival? And added to this, could a scaffold be delivered along the pathway to promote axonal growth and guidance to the striatal target? It may be necessary to incorporate a gradient of growth factors to promote this desired trajectory. Figure 8.1 shows a possible application of scaffolds that may work towards supporting homotopic grafts and restoring neural circuitry.

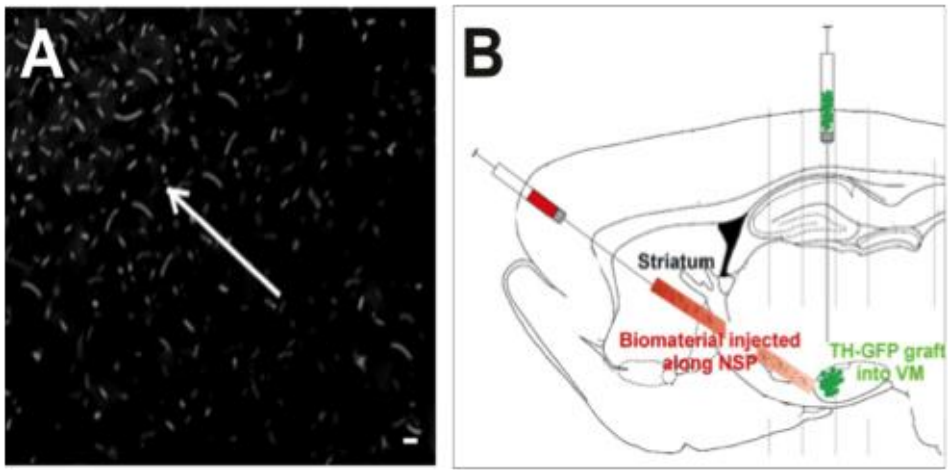

Figure 8.1 (A) Example of electrospun short fibres within a hydrogel. We are able to generate gradients of short fibres that will enable the generation of protein gradients through covalent tethering

onto these fibres. (B) Delivery of the gradient composite scaffold along the denervated pathway in a Parkinson's disease.

8.2.3 Application of bio-engineered scaffolds in other neural injuries

This thesis (chapter 7) focused on the ability of bioengineered scaffolds to support neural transplants in an animal model of Parkinson's disease. To date, PD represents the neural injury that has made the most progress in regards to cell replacement therapy. As such, clinical trials have demonstrated the ability of newly transplanted fetally derived dopamine neurons to structurally and functionally integrate into the patient brain, alleviating symptoms for up to 15 years. Variability across patients has highlighted the need for further work in the field. No other neural injury to date has shown this much progress and it therefore seems the most obvious place to start when trying to improve neural cell therapy approaches.

However it should not be disregarded that other neural injuries should also be examined in parallel. With other injuries come additional challenges that need to be addresses. Unlike PD, some neural injuries, such as traumatic brain injury (TBI) and stroke, result in tissue necrosis and the loss of tissue mass. Neural injuries with tissue loss require the development of scaffolds to restore tissue architecture, as well as provide a stimulating environment for the integration of the grafted cells. It is probable and likely that this will involve the use of composite scaffolds such as described in chapter 7. Future work is required to see the implementation of such materials in various other neural injuries.

Appendix

Supplementary information for chapter 7

Scission of electrospun polymer fibres by ultrasonication

Marini Sawawi[a,b] ,Ting Yi Wang[a], David R Nisbet[a, c],George P. Simon[a*]

[a]Department of Materials Engineering, Monash University, Clayton 3800 Victoria, Australia
[b]Faculty of Engineering, Universiti Malaysia Sarawak, Kota Samarahan 94300, Malaysia
[c]College of Engineering and Computer Science, The Australian National University, Canberra

Abstract. In this work we show that sonication alone can be used to scission bulk electrospun membranes into short fibres. The mechanism of such scission events is bubble cavitation stimulated by the ultrasonic probe, followed by bubble implosion. The tendency of polymer nanofibres to undergo failure by a scission process appears to depend primarily on the ductility of the polymer, with brittle, electrospun polymer membranes such as poly(styrene) and poly(methyl methacrylate) readily producing short fibres of approximately 10 μm. More ductile polymers such as poly (L-lactide) or poly (acrylonitrile) require additional processing after electrospinning and before sonication, to make them conducive to such sonication-based scission. Both the initial diameter of the fibres and the degree of nanofibre alignment of the electrospun membrane influence the final length of the resultant short fibres. It was found that the chemical and physical properties of the short nanofibres unaltered by the sonication process. We thus are able to demonstrate that sonication is a promising method to produce significant quantities of short, fibres of nanometre diameter and microns in length.

1 Introduction

Electrospinning has become a oft-reported technique for the fabrication of polymeric fibrous membranes that have been used for a variety of applications including membrane technologies, sensors and in particular for tissue engineering as scaffolds that mimic features of the extracellular matrix [1-6]. Electrospinning generally results in the production of a continuous fibre that deposit onto a collector as a nonwoven membrane. It is inherently difficult to spin and retrieve individual electrospun fibres in large quantities that can be readily handled. Parallel, knife-edge electrodes is a possible methods that have been used to obtain individually-aligned fibres for the purpose of single fibre testing, however very limited amounts of fibre can be produced [7, 8].

To date, there has been little work reported on producing individual, short nanometre-length fibres directly from conventionally electrospun membranes. The ability to convert an electrospun membrane into discrete, short nanofibres would be advantageous, as it would lead to a methodology to produce significant quantities of such short fibres. Such short fibres may be desirable for a number of applications, such as additives for incorporation into polymers and films to increase properties such as modulus and toughness, whilst maintaining the transparency of the nanocomposite due to the similarity of the refractive index of the nanofibres and the matrix. Short fibres would also be very useful for biomedical applications, as vessels for the containment of drugs or in tissue engineering as injectable fibrous scaffolds. In this work, we report the use of ultrasonication as a method to produce short fibres from a nonwoven, electrospun membrane, whilst also investigating the effects of materials properties and processing parameters on the process and its outcome.

* Corresponding author. [redacted]

There have been a few reports of non-ultrasonic methods to breakdown the non-woven electrospun membrane for composite reinforcement that have shown varying degrees of success. A simple method which is difficult to control is mortar grinding [9, 10] which was found most effective for brittle electrospun membranes, such as carbonised polyacrylonitrile [9]. Rubber milling [11] and cryogenic milling [12] have been shown to be better options for the scission of electrospun membranes, where the cycle and rate of the impactor can be accurately controlled. However, it is difficult to make comparisons between each of the techniques, as the characteristics of the resultant short fibres were not always well reported. Other mechanical methods such as razor blade cutting under nitrogen [13] have been used to produce short magnetic composite fibres from a mixture of a methyl methacrylate-vinyl acetate copolymer combined with superparamagnetic cobalt nanoparticles, yielding fibres of approximately 50 to 100 µm length. Another method to produce discrete fibres from the electrospun membrane has involved 1 µm step-sliced cryomicrotoming to produce short nylon electrospun fibres, however this involved tedious, repeated steps [14]. Polymer degradation using UV light was used to produce reduced poly(butadiene) electrospun fibre mats where the UV light was shined through masks with well defined slit sizes and inter-slit distances, laid on top of the mesh [15], but although this cut the fibres, the aim was to produce smaller, controlled fibre bundles, as opposed to the individual fibres we seek here.

In this work we demonstrate that we can use ultrasonication directly, under appropriate conditions, to produce short nanofibres from electrospun membranes. For this we use an ultrasonic probe, an apparatus that is already widely used in most laboratories for applications such as cleaning and mixing, and has a working frequency of 20 kHz, [16]. During sonication, bubbles in the fluid medium grow and collapse, and in so doing, release energy. These bubbles start with a diameter of some 1 µm and grow to ca. 50 µm under negative pressure [17]. Under such sonication conditions, the bubble grows in some 20 microseconds, and can collapse over a time of the order of nanoseconds [18]. This method has previously been utilised to facilitate the dispersion of carbon nanotubes in a solvent or mixture [19] and has also been shown that it can lead to carbon nanotube scission [20].

Most researchers currently use sonication for the mixing of CNTs in solution, and size reduction is often of secondary interest. The basic mechanism for the scission of carbon nanotubes has not been fully elucidated, although a number of papers have made a series of instructive observations. Recently Hennrich et al. [19] investigated the decrease in length of CNTs and the underlying mechanism during ultrasonic processing, making clear that the break-up was due to an associated cavitation phenomenon (bubble growth and collapse) within the solvent, which leads to local regions of high strain and shear stress. These include the separation, thinning and shortening of the CNTs due to the mechanical effect of sonication which occurs upon bubble implosion, yielding a maximum tensional force at the nanotube center which is similar to the observation of single molecule polymer degradation due to scission [19, 21, 22]. The mechanism of scission largely depends on the position of the nanotubes relative to the bubble during bubble implosion and how it approaches (or is drawn towards) the imploding bubble. If the long axis of the nanotube aligns normal to the bubble surface, this would lead to a high frictional force between the fibre and solvent, which causes a high tensile force at the nanotube center [19, 22]. However, nanotubes that become aligned tangential to the bubble surface would result in axial compression that results in buckling and fracture of the nanotube due to atom ejection [23, 24].

Recent modelling work by Pagani et al [24] suggests that the mode which dominates (tangential or radial) depends on the size of the nanotube. Whilst the growth of the bubble causes tangential alignment of the nanotubes, shorter nanotubes rotate radially and are drawn towards the nanotube, with subsequent tensile stretching and failure, whilst longer nanotubes do not rotate in such a fashion, but rather the opposing torques at either end cause bending

and buckling (which may also lead to failure and/or scissioning). The mode of deformation notwithstanding, the ultimate molecular failure mechanisms invoked were also often related to the precise chemical structure of the materials, such as defects in carbon nanotubes or the carbon-framework (in the case of carbon nanotubes), and may not be as relevant for polymer nanofibre scissioning. Other researchers propose alternate mechanisms to explain nanotube scission, such as bubble implosion leading to high temperatures that can cause failure on the nanotube surface [25], although others refute such claims and state that such extreme thermal events are unlikely to occur [21, 23]. It has also be proposed that bubble collapse would lead to microjets that impinge on the surface leading to their ultimate failure [26-28], and indeed, this is the mechanism by which ultrasonics is used to clean surfaces contaminated by organics, such as soiled silicon wafers. It is likely, therefore, that any scissioning of polymer nanofibres that occurs is some combination of factors may be at play, depending on material and the processing conditions. The possible mechanisms for failure in these systems will be discussed below, based on the observations made and results obtained.

To date, there has been little study on the use of sonication as a method to produce small fibres from electrospun membrane. Transverse fragmentation of fibres by first chemically-modifying poly(lactide) nanofibres by aminolysis [29, 30], in combination with some sonication has been reported, however in this case, the cutting of fibres was largely due to the chemical treatment, and the sonication was used more to disperse the resultant, chemically-cut fibres, rather than being the primary mechanism for fibre scission. One recent study has reported in passing, the direct use of ultrasonication as a means of producing short fibres from electrospun membranes. The short fibres produced were subsequently incorporated into a hydrogel for a tissue engineering applications [31] to improve interactions between the hydrogel and the cells. However, in this work sonication was used as a means to an end to produce short nanofibres, with investigation of the control of scission events and a mechanistic understanding being outside the scope of that research.

In this work we have investigated the effect of the application of ultrasonication on electrospun membranes, varying material properties and processing variables, in order to gain a more detailed understanding of how to optimise the resultant short nanofibres and obtain a mechanistic understanding of the process itself. As a point of comparison with previous methods of producing short nanofibres from electrospun membranes, we have also conducted cryogenic milling of electrospun membranes.

2 Experimental method

2.1 Materials.

Poly(L-lactide) Acid (PLLA, Inherent viscosity = 0.9-1.2 dL/g) was purchased from Lactel, USA. Polyacrylonitrile(PAN, M_w= 120,000), poly(methyl methacrylates) (PMMA, M_w= 486,000) and poly(styrene) (PS, M_w=230 000), dodecyl trimethyl ammonium bromide (DTAB), potassium bromide (KBr) and Rhodamine B were purchased from Sigma Aldrich, Australia. Chloroform, dimethylformamide (DMF) and acetone from Merck Pty Ltd, Australia. Deionised water was obtained from Direct-Q3 water purification system, Millipore.

2.2 Electrospinning.

The polymer-solvent mixture was dissolve using magnetic stirrer at room temperature overnight (except for PLLA where it was heated at 70 ^{o}C for two hours) prior use. Then, the

polymer solution was placed in a 10 mL syringe prior to electrospinning using the parameters listed in table 1 for each material. These parameters were determined through several optimisation steps to produce fibres that had diameters within the submicron range.

Table 1 Summary of final electrospinning conditions for various polymers.

Material	Solvent	Concentration (%)(w/v)	Feed rate (ml/hr)	Voltage (+ kV)	Needle size (G)	Working Distance (cm)	Surface Velocity (m/s)
PLLA	Chloroform + acetone (3:1) (with 1 mM DTAB)	13.7	1.6	20	18	16	N/A
PMMA	DMF (1 mM DTAB)	6.5	1.6	20	18	16	N/A
PAN	DMF	10	1.6	20	18	8	N/A
PS	Chloroform + DMF (1mM DTAB)	12	1.6	20	18	8	N/A
PS	Chloroform + DMF (1 mM DTAB)	8	1.6	15	18	6	6.3
PS	Chloroform + DMF (1 mM DTAB)	12	1.6	20	18	6	6.3
PS	Chloroform + DMF (1 mM DTAB)	16	1.6	20	18	6	6.3
PS (fluorescence)	1 mM Rhodamine B in Chloroform + DMF(1 mM DTAB)	12	1.6	20	18	6	6.3

To allow comparison between PLLA, PAN, PS and PMMA, all polymers were spun onto a flat collector (aluminium foil), and were stored in a desiccator under vacuum prior to use.

To explore the scission events in more detail, we primarily focused the latter work reported here on electrospun PS, which was also spun onto a rapidly rotating drum, with the surface velocity of 6.3 m/s to produce aligned electrospun membranes. For confocal microscopy fluorescently-labelled PS was prepared by mixing Rhodamine B with the Chloroform:DMF solvent (table1) to a 1 mM concentration. The fluorescent nanofibres were injected into an agar gel so that they could be imaged as discrete, dispersed fibres.

2.3 Ultrasonication.

The electrospun membranes were peeled off the collection plate, and a 1 cm^2 area with the thickness of ca 100-200 µm taken from the center of the collector was cut with a sharp knife, before being placing in a glass vial (25 mm in diameter) containing 15 ml of MiliQ water. Sonication was carried out using a Vibracell 750W (Sonics & Materials, Inc, USA) sonicator probe with a probe diameter of 13 mm, working at 20 kHz. An amplitude of 80% with a 2 s ON and 2 s OFF (2/2) lapsed time was used, with the total run time (ON time) being varied from 1 to 8 mins. The water used for this study was at ambient condition, except for the study on nucleation effect where MiliQ water was degassed in the vacuum oven for 12 hrs prior use. In general, ultrasonication was conducted in a beaker cooled by a water-ice slurry to maintain the processing temperatures below 30 ^oC, since ongoing sonication raises the solution temperature. Other less extreme methods of cooling (such as packing the sonication vessel in ice) were also undertaken in one section of the work, to allow higher temperatures of the sonication medium to be obtained and thus allow temperature to be used as a variable (temperatures up to 90^oC could be reached by this method).

After sonication was completed, a drop of the short fibres in suspension was placed on a scanning electron microscope (SEM) stub, which was covered with double-sided carbon tape to encourage adhesion to the stub. The sample was then dried overnight in the fumehood, prior to imaging using SEM.

2.4 UV irradiation of scaffolds.

In part of the work, and in particular for the PLLA scaffolds which were hard to scission directly by sonication, we also investigated the effect of surface modification of the PLLA samples by first exposing them to a combination ultraviolet-ozone environment. The PLLA membrane was irradiated by UV Ozone Procleaner^{TM} UV PC 220 (Bioforce, USA) for 12 mins with the intensity of 14.75 mW/cm^2 at a distance of approximately 1 cm, and was then sonicated.

2.5 Cryogenic milling.

Electrospun membranes with a mass of 1 g were placed into a polycarbonate vial and inserted in a Spex Freezer Mill 6870, which operates at cryogenic temperatures within a liquid nitrogen bath. The cryogenic mill, which pulverises the samples with a stainless steel magnetised impacting bullet, was set at a pre-cool time of 3 min prior to grinding of 10 minutes (5 cycles with 2 minutes run time and 2 minutes recooling), with the magnetic field oscillation rate being 5 cycles per seconds (cps).

2.6 Characterisation.

The morphology of the as-spun fibres and short fibres were characterised using either a Scanning Electron Microscope, (JEOL840A SEM) or Field Emission SEM, (JEOL 7001FEG SEM,). Prior to imaging, the sample was dried overnight in the fumehood and platinum coated at 1nm thickness with a sputter coater (Cressington 208HR, UK). The sonicated short

fibres were also characterised using the Transmission Electron Microscopy (Philips CM20TEM) where samples were placed on the copper hexagonal grid for viewing. Optical microscopy imaging of the individual short fibres injected and dispersed in a gel was carried out using confocal imaging by Olympus FV1000 (Olympus, Tokyo Japan), with 575 nm emission wavelength and objective lenses of 20x and 40x. The confocal sample was prepared by mixing agar powder with MiliQ water at 3 wt% prior to heating at 80^{o}C. The gel was then placed on to the glass slide prior to being injected with a suspension of fluorescently-labelled with Rhodamine B, Sigma Aldrich short fibres. The images were analysed by Image J software (National Institute of Health, USA) to estimate the diameter and length of the short fibres (n = 50).

A comparison between the concentration of short fibres for different types of polymers was estimated using a turbidity meter (Cyberscan TB1000, Eutech Ins, Singapore), where the various sonicated samples were placed, to determine the minimum time required for successful sonication. Any larger clusters of electrospun membrane that remained after sonication were removed using tweezers prior to the turbidity measurement, so that the turbidity results largely reflected the concentration of the short fibres produced in suspension for a given scissioning event.

In order to better understand the surface and physical properties of the nanofibres, the samples were also characterised in transmission mode by Fourier Transform Infrared spectroscopy (FTIR) using a Thermo Scientific Nicolet 6700 with scanning range of 4500 to 400 cm^{-1} and 4 cm^{-1} resolution. The samples were pre-mixed with potassium bromide (KBr) powder at 3 wt% and compressed into a disc.

Mechanical testing was conducted using an Instron 5848 microtester (USA) with 10 N load and displacement rate of 5 mm/min. The electrospun membrane with the thickness of approximately 0.3 mm was cut using dogbone shape cutter with the gauge length of 20 mm. The ultimate tensile strength (σ_{UTS}), Young's Modulus (E) and % strain to failure (ductility) were determined from five independent samples for each type of polymer.

The glass transition temperature (T_g) was estimated from endothermic curve obtained from Differential Scanning Calorimetry (Pyris DSC, Perkin-Elmer), using temperature scanning from 30^{o}C to 300^{o}C at the rate of 10^{o}C/min modes under N_2. Approximately 5mg of sample was sealed in aluminium pans for these measurements.

2.7 Statistics

PS short fibre length comparison between aligned and random fibres was made using the independent t-test, whilst the difference between short fibre length with time were analysed using one way repeated measures, analysis of variance (ANOVA). Statistical analysis for comparison between sonication of PS membranes with differing mean fibre diameters and the effect of bubble nucleation were carried out by one way between groups ANOVA with Tukey post test. All statistical analyses were performed using SPSS 19 for Windows (SPSS, Chicago, IL); *p*-values of less than 0.05 were considered to be significantly different.

3 Result and discussion

3.1 Ultrasonication of different types of electrospun polymers

Four different types of polymers were electrospun; poly (styrene) (PS), poly (methyl methacrylates) (PMMA), poly (L-lactide) (PLLA) and poly (acrylonitrile) (PAN) using the conditions shown in the first four rows of table 1. These conditions were determined by changing processing parameters until good quality fibres could be produced (that is, fibres without artefacts such as beading, for example) and their diameters ranged between 550 to 775nm. The 1 cm^2 areas cut from the membranes were then sonicated in MilliQ water. Figure

1 shows the electrospun fibres before and after sonication for what we define in this work as the “minimum sonication time” (last row of table 2) except for PAN and PLLA, where the fibre membrane remained unbroken. We define this minimum sonication time as the first time that the membrane was visually observed to fragment completely. This was ca. 40s for PMMA and 60 s for PS, whilst no such minimum sonication time observed for PAN and PLLA - even after 35 mins of sonication.

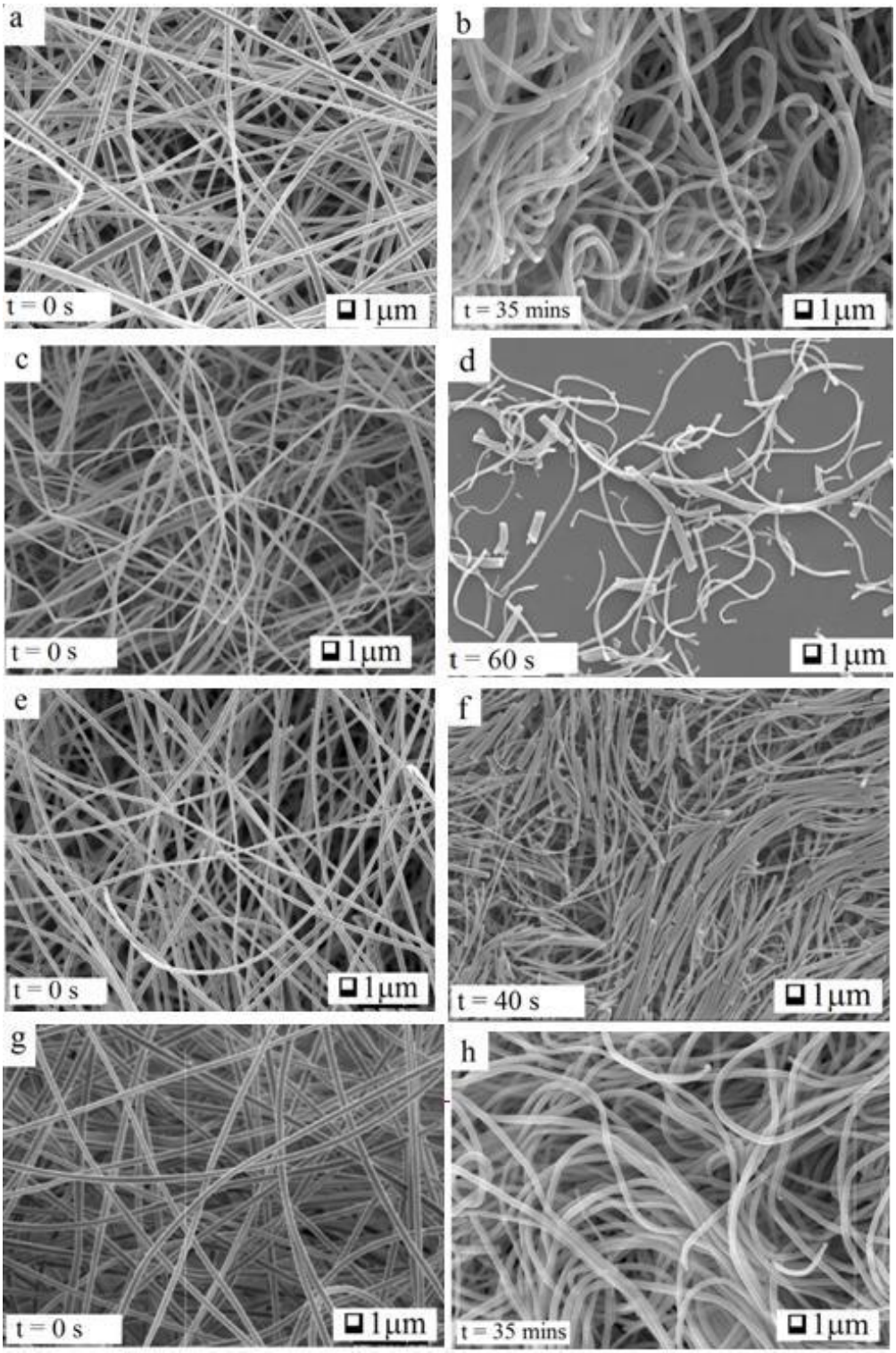

Figure 1 SEM images of the fibres before sonication (left) and after minimum sonication run time (right) at the point at which fibre membranes were visually observed to have completely fragmented (for PS and PMMA, at 60 s and 40 s, respectively), whilst for PAN and PLLA the SEM images were taken of the fibre after sonication run time of 35 mins, by which time they had still not fragmented. a,b) PLLA at 13.7 wt% with the average diameter of 770 ± 240 nm, c,d) PS at 12 wt%, average diameter = 775 ± 160nm, e,f) PMMA at 6.5 wt% , average diameter =550 ± 160 nm and g,h) PAN at 10 wt% , average diameter =640 ± 165 nm.

Figure 1 shows that within 40 s for PMMA and 60 s for PS they have been successfully scissioned into smaller lengths of 10.3 ± 5.6 µm and 10.5 ± 6.2 µm, respectively, whilst for PAN and PLLA the electrospun membrane remain intact for the entire process (i.e. 35 min, after which sonication was ceased). In the case of PS and PMMA samples, the supernatant turned whitish in colour after the minimum sonication time, highlighting the fact that short fibres were homogenously distributed in the supernatant. However, for PAN and PLLA, the membrane appeared to have been elongated due to the sonication, with a loosening of the dense, as-spun fibre mesh. It is clear that different sonication times are required for the scission of electrospun scaffolds of different materials, and in two cases even prolonged inputs of energy were not able to cause scission. It can also be seen that the sonication process does lead to some slight change in the fibre morphology where the fibres become curled. It appears that although the ultrasonication forces have not been sufficient to cause significant scission, they have caused bending and buckling of the fibres due to a range of stresses on the fibres surface [32].

For all samples, an attempt was made to quantify the degree of electrospun fibre scission using a turbidity measurement, where the results reflect the concentration of particles (in our case, short fibres) in the solution (figure 2). For this experiment, membranes of the same dimensions and thickness were used to ensure that there was approximately the same concentration of short fibres in the supernatant if all the fibres had been completely scissioned. Large, unbroken portions of the electrospun membrane were removed using tweezers prior to measurement and thus the turbidity measurement is an indication of the concentration of the short fibres that have been produced at that point in time. The measurement was performed for sonication times ranging from 10 s to 90 s for all types of fibres, although this was extended to 35 mins for the PAN and PLLA samples due to reduced visual success in scissioning.

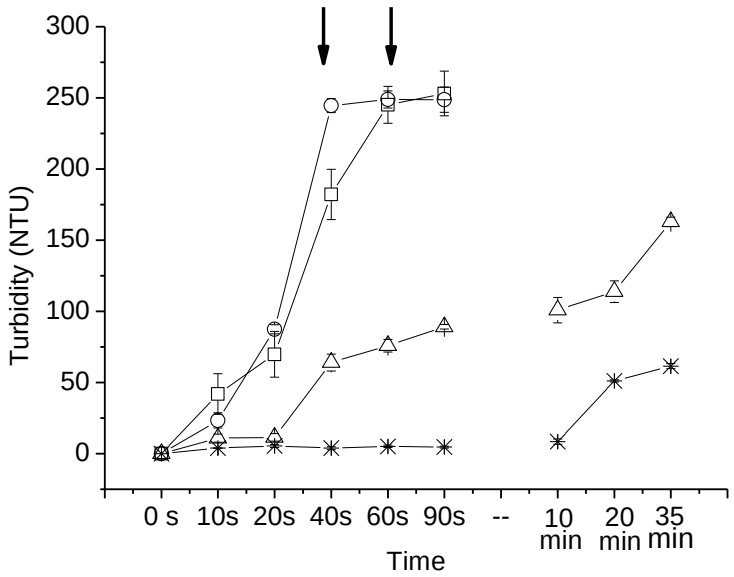

Figure 2 Turbidity measurement for PS (□), PMMA (○), PAN (Δ) and PLLA (*) after ultrasonication processing. The arrow bar indicates the minimum sonication time indicating fully break-up (for PS and PMMA).

Figure 2 shows that as the sonication time increased, the same trend was observed for the concentration of short fibres in solution. Note that for the PMMA, a small fibre clump was present up to the 20 s sonication time point (removed prior to turbidity measurement). It was

completely fragmented after 40 s of sonication (when NTU was ca 250 units), whilst for PS complete fragmentation occurs after 60 seconds, by which time it also reached NTU of ca 250. From these observations, we can conclude that when the turbidity measurement reaches the ca. 250 NTU range, all PS and PMMA fibres had been broken up into short fibres, correlating to a minimum sonication time of 40 to 60 s (figure 2), similar to the minimum sonication time mentioned earlier. From visual inspection, short fibres begin to become present in supertant (as the supernatant color has turned slightly whitish) when the turbidity was greater than 50 NTU. This indicates that in the case of PAN, some limited scission commences after 40 sec of sonication, with the concentration of fibres gradually increasing for the full duration of the experiment. In contrast, the PLLA membranes essentially remain intact for the first 20 mins of sonication, with a limited amount of short fibres increasing at a slow, linear rate after 35 mins. This result indicates that the inherent polymer properties influence the scission events, suggesting the need for some pretreatment of those polymers we may wish to cut which intrinsically resisted such scissioning.

There are many factors that are likely to contribute to the difference in the sonication times required to reduce the membrane to discrete fibre lengths such as the electrospun fibre morphology (fibre diameter and alignment), as well as the mechanical properties of the electrospun polymers. Since all the electrospun fibres were of broadly similar diameter and randomly aligned, and given that the same ultrasonication experimental parameters were used for all materials (80 % amplitude and 2/2 lapsed time), it can be concluded that any differences in results from sonication are largely due to material properties of the initial electrospun membrane. In the case of the PMMA and PS nanofibres that did scission, we note that PMMA was slightly thinner, and it also appeared to sonicate slightly more rapidly.

In order to make further comparison, we examine the mechanical properties of the membranes that we obtained by tensile testing (figure 3), with the key mechanical properties from these curves shown in table 2, in order to elucidate which of these is most relevant to the results of sonication.

Table 2 Mechanical and size properties of electrospun PS, PMMA, PAN and PLLA membranes

Materials	PS	PMMA	PAN	PLLA
Tensile strength (MPa)	0.6 ± 0.2	1.6 ±0.4	2.5 ± 0.1	1.6 ± 0.2
Tensile modulus (MPa)	8.0 ± 0.8	0.4 ± 0.1	12.2 ± 7.7	11.1 ± 2.6
Ductility (%)	16.8 ±1.9	1.9 ± 0.8	86.3 ±22.1	79.2 ±17.9
Glass transition tenperature ($T_{g,}$ °C)	100	120	100	55
Electrospun fibre diameter (nm)	775 ± 160	550 ± 160	635 ± 165	771±240
Minimum sonication time (secs)	60	40	N/A	N/A
Final short fibre length (µm)	10.5 ± 6.2	10.3 ± 5.6	N/A	N/A

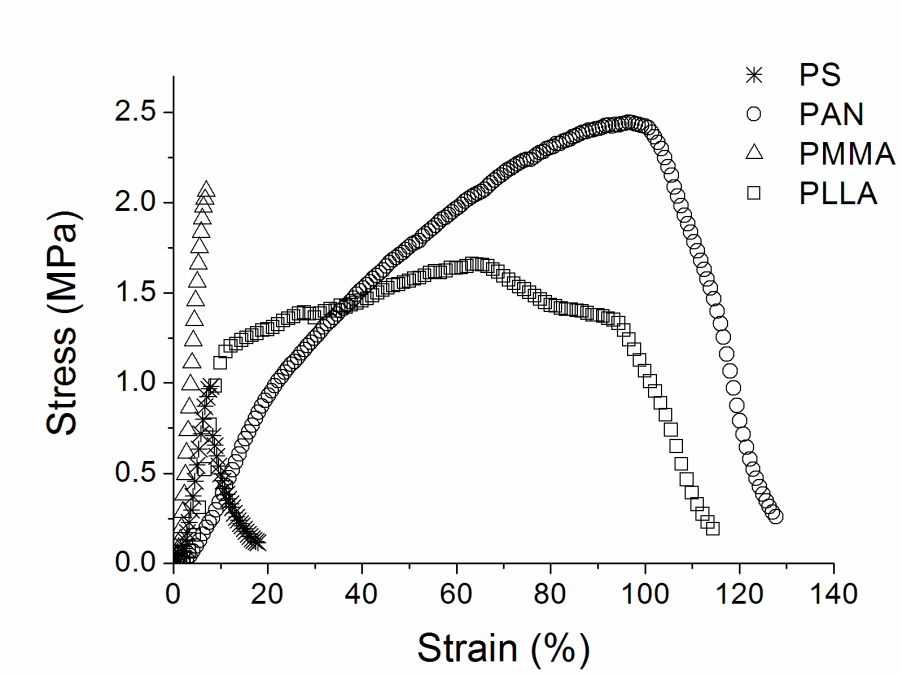

Figure 3 Stress-strain curves of the electrospun fibre membranes

What can be seen clearly from figure 3 and the data in table 2, is that whilst the modulus and strength appear of all membranes appears to be broadly similar, the PAN and PLLA membranes can be seen to be much more ductile than those of PS and PMMA. It should be noted that whilst the determination of modulus and strength of electrospun webs is relatively straightforward from an experimental perspective, the nature of how the fibres are folded and stacked within the tensile sample would influence their values. In contrast, in the case of measurement of ductility, the fibres are likely to be more elongated, and thus the ductility for the membrane is more likely to be related to that of the individual fibres. When considering the process of membrane breakup by sonication, there will likely be aspects of both stretching the web initially and/or deformation of the individual fibres. It can be seen from table 2 that for the nanofibres, membrane ductility shows the greatest correlation with the minimum sonication time (ease of fibre scission), with the more ductile PLLA and PAN not showing significant scission even for the longer sonication times. PMMA appears visually (and via turbidity measurements) more readily scissioned by sonication than PS and is also the less ductile. It should be noted that PAN fibres have the smallest fibre diameter and yet remain unbroken after a comparably long sonication time, and thus it appears that simple variations in diameter do not explain the different behaviours observed. In conclusion, materials that are sufficiently ductile and tough are able to resist the deformations imposed by the sonication process. We also note that although neither PAN nor PLLA were able to scission to any significant extent, PAN appeared to be able to produce some small fibres to a greater degree, as indicated by its turbidity curves. The ductility of PAN and PLLA are (within error) the same, and the PAN fibre has a slightly lower diameter, and could be a reason for its improved propensity to scission.

In order to further understand the mechanism of failure, high magnification SEM images of the electrospun fibres before and after sonication were examined (figure 4).

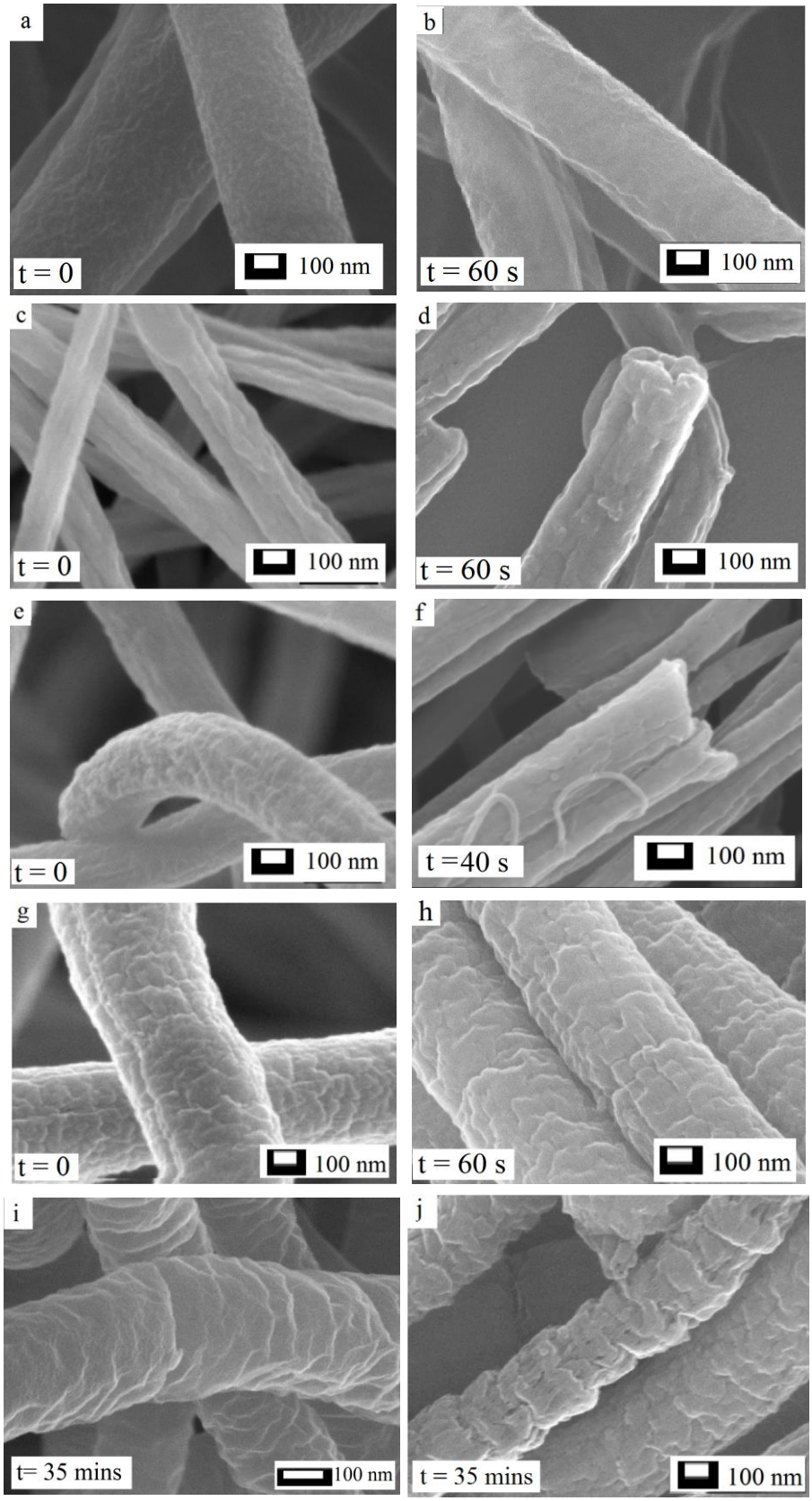

Figure 4 SEM images of the fibres before sonication, t = 0 and after sonication run time with the respective sonication run time shown a) presonicated PLLA , b) PLLA at t = 60 s, c) presonicated PS, d) PS at t=60s, e) presonicated PMMA f) PMMA at t = 40s, g) presonicated PAN, h) PAN at t = 60s, i) PLLA at t= 35mins and j) PAN at t = 35 mins.

The SEM images of the fibre surface before sonication shows some surface roughness. This degree of roughness is common on the surface of electrospun fibres, although it is little discussed due to the few images in the literature taken at such high magnifications. It has been reported that such roughness in electrospun fibres arises from solvent-polymer interaction and the rate of solvent removal, which depends on the types of solvent employed, polymer concentration and relative humidity [33-35], and indeed, controlling humidity during electrospinning can be used to manipulate nanofibre porosity. The sonicated samples, however, show an even greater degree of roughness, particularly the PLLA and PAN samples at a sonication time of 35 mins in figure 4i and j, respectively, indicating that the prolonged sonication managed to roughen the surface of the nanofibres of these two materials, without any scissioning effect.

The above observations allow us to make some general comments about the mechanism of the cutting procedure in these polymeric nanofibres. Much of the previous work in ultrasonic scission of nanofibres has related to either single- or multi-walled carbon nanotubes and a range of possible failure mechanisms have been discussed for those materials. It is likely that during sonication, nanofibres are exposed to a range of forces due to the expansion and collapse of bubbles, with the manner in which these forces interact, deform or cause ultimate failure of the nanofibres depending on aspects such as the nature of the material, as well as its dimensions. Pagani et al [24] presented simulations in which the fibre is drawn tangentially towards the collapsing bubble. What happens as the bubble ultimately collapses is related to nanofibre length, persistence length and diameter. If the nanofibre is sufficiently long, it becomes captured close to the bubble surface a torque imbalance subjects the nanofibres to a series of forces such as compression and rotation, resulting in buckling and curvature. The shortest nanofibres continue to rotate and become radially pulled in to the bubble, with the balance of forces being tensile extension, since the end closest to the bubble is pulled at a greater strain rate than the far end. The influence of these forces on the nanofibre will be very much controlled by the class of material. Chew et al [23] notes that single walled nanotubes can fail under the compressive force due to ejection of the atoms from the single wall, whereas failure in tension may occur due to flaws in the wall.Concievably in other materials buckling or tension may show a different mode of failure, such as in polymers where molecular flow and ductility is possible. Other researchers have stated that ejection of eroding microjets against a solid surface could be a key aspect of the breakage mechanism in reducing the micro to nano size particle, where the impact would produce a jagged circular indentation follows by fragmentation [28, 36, 37]. Likewise, it has been proposed that high temperatures may be likely due to compression as the bubble collapses and causing the nanotube to fail [25], although this mechanism seems unlikely in our case due to the lack of any electron microscopy evidence of melting of the nanofibres [21].

It is of interest, then, to consider the process of the intial breakdown of the nonwoven membrane when exposed to sonication. It would be expected that since the nanofibres are long and in a web, there would be some level of bending in the early stages of sonication (especially prior to the initial scissioning), although this may not lead to the breakage of the fibres. It can be seen in figure 1b and 1h, that although the PAN and PLLA fibres do not fail, that they are generally extended and bent, with significant amounts of U-shapes and curls.Even in the scissioned PS fibres (figure 1d), where cutting has been observed, there also appears to be curvature of the fibres, with a radius of curvature ranging from ca. 5 – 15 microns. This is seen to a lesser degree in scissioned PMMA nanofibres (figure 1f). It appears that bending alone, although able to cause curling and deformation, is not the only or indeed primary manner in which these samples are scissioned. At the start of the process when there is largely the non-woven membrane, the idea of short nanofibres being drawn into

the collapsing bubble and stretched to failure is not possible, and thus other mechanisms for the initial breakdown of the fibre must be considered.

The electron micrographs of the fibres after sonication do show that there is a greater degree of pitting and erosion on the surface of the fibres, and it may be that is an important part of the mechanism by which these submicron diameter fibres fail. Large scale melting is not seen on any of the fibres in figure 1 or figure 4 of the sonicated samples, and thus the mechanism of high temperatures at the point of collapsing bubbles does not appear to be likely, and this has also been discarded as an option by others [21, 23]. It thus seems likely that a mechanism such as microjetting and erosive wear of the surface can create a rougher surface, likely to fail by subsequent stresses on this weakened zone. Samples which are tougher (greater ductility) such as PAN and PLLA would thus presumably be a more resistive to erosive wear and/or to subsequent deformations of the fibres, which can be seen in the evolvement of the surface morphology of the post sonicated sample for 1 min (figure 4b and 4h)and 35 mins (figure 4i and 4j) sonication showing the increment of the surface roughness without scissioning effect. Certainly the features, although rough in the unsonicated samples, are further roughened after sonication. It can be seen from figure 4 that the post sonicated surfaces of the ductile materials (PLLA and PAN) are rougher, compared to PS and PMMA, where the increase of roughness is more marginal. Once the nanofibre membrane is broken, and shorter fibres achieved, other mechanisms may be possible – either further bending or tensile drawing, as well as further pitting and failure, depending on length. We do note that the ends of the fibres in figure 4 that have failed (PMMA and PS), are not particularly drawn to a a slender tip and the resultant cut fibres remain bent. It may be that the scissioned fibres, both prior to and after scissioning, may undergo bending/buckling, but that is not the cause of failure, with the degree of curvature stress being insufficient. As further evidence of ductility being the key property, we use calculation of maximum tensional force adapted from [19] to support our argument. This makes use of equations 1 and 2 below,

$$F_M = \frac{1}{2}\pi\mu\dot{\varepsilon}.L^2 \qquad (1)$$

$$F_c = \sigma_{break}.\pi\frac{D^2}{4} \qquad (2)$$

where F_M is the maximum tensional force at the center of the fibre and F_c is the fracture stress required to break the fibre, with μ, viscosity of water taken as 1 mPa s and strain rate of $10^9 s^{-1}$,σ_{break} is the tensile strength and the initial fibre diameter, D is taken from table 2. The fibre will fail when the maximum stress in tension is greater than the failure stress. The four types of electrospun materials we have investigated, showed that the tensile strength and the diameter of the fibre did not vary significantly and thus theoretically, we predict approximtely the same maximum tensile force is required to break the fibres, which would have resulted in the scission of all types of fibres membrane. However, since not all materials fail, this suggests other material properties (such as ductility) may be important with regards to scission.

To test the above hypothesis, and to seek a method by which we can induce scissioning in the sonication of ductile polymer fibres, we exposed the the PLLA non-woven membrane to a UV-ozone pretreatment , to induce potential points of weakness on the PLLA membrane by roughening the membrane nanofibres. UV ozone treatments have been widely used for removing organic contamination, such as from silicon wafers, and can also be used to counteract low wettability and hydrophobicity of organic materials through the introduction of polar groups [38, 39]. We irradiated the PLLA electrospun membrane for 12 mins, followed by sonication for 29 mins (during which full fibre break up was observed). The SEM images in figure 5 show the irradiated PLLA membrane before and after the minimum

sonication time of 29 mins. We note that even though break up was now possible, a significant length of sonication time was still required, further indicative of the ductility of the sample.

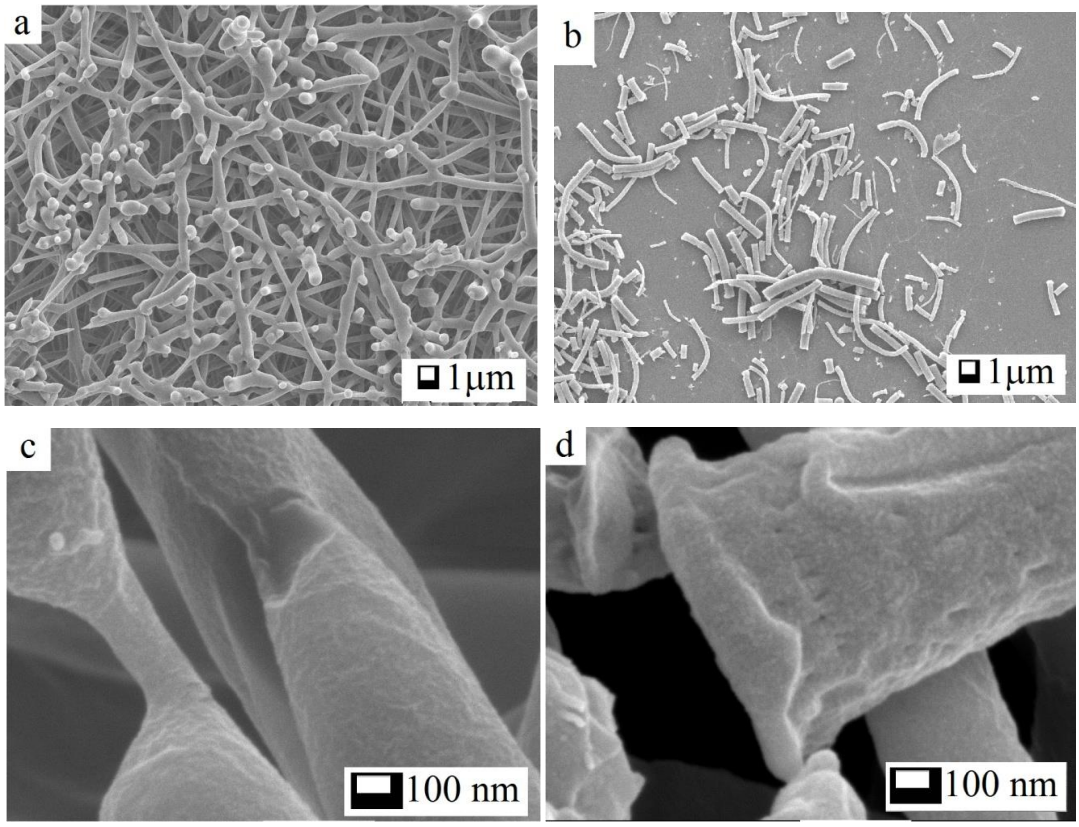

Figure 5 SEM images of UV irradiated PLLA sample before (a, c) and after sonication run time of 29 mins (b, d).

The PLLA membrane, which previously could not produce short fibres after sonication, was now able to be fragmented into short fibres of 5 ± 5 μm in length (figure 5b). SEM images of the irradiated sample (figure 5c) indicate that UV ozone irradiation leads to localised fibre etching, which has previously been observed [38]. The UV-ozone irradiation of PLLA may in part also degrade the PLLA macromolecules themselves, as well as pitting the nanofibre surface [39]. Although those samples exposed to UV-ozone treatment had a rougher, more pitted surface compared with the pre-sonicated sample (figure 5d), this change was not as significant as for the untreated sample which was exposed to sonication alone (figure 4b and 4i).

3.2 Ultrasonication of polystyrene nanofibres

In order to investigate the process in more depth, sonication of PS was carried out in water using different conditions. Factors investigated include: the initial fibre orientation, sonication time, the influence of the original nanofibre diameter, the influence of removing or introducing additional gas in the sonication medium to initiate/inhibit microbubble formation and the effect of the sonication medium temperature.

3.2.1 Effect of electrospun fibre orientation

The influence of fibre orientation on ultrasonication processing, random and aligned PS membranes (collected on a spinning mandrel with a surface velocity of 6.3 m/s) was fabricated. Figure 6 shows the images of electrospun fibres before and after sonication (8

mins), and quantification of the short fibre length at different sonication times. The visually-observed minimum sonication time for both membranes appeared the same, ca. 1 minute.

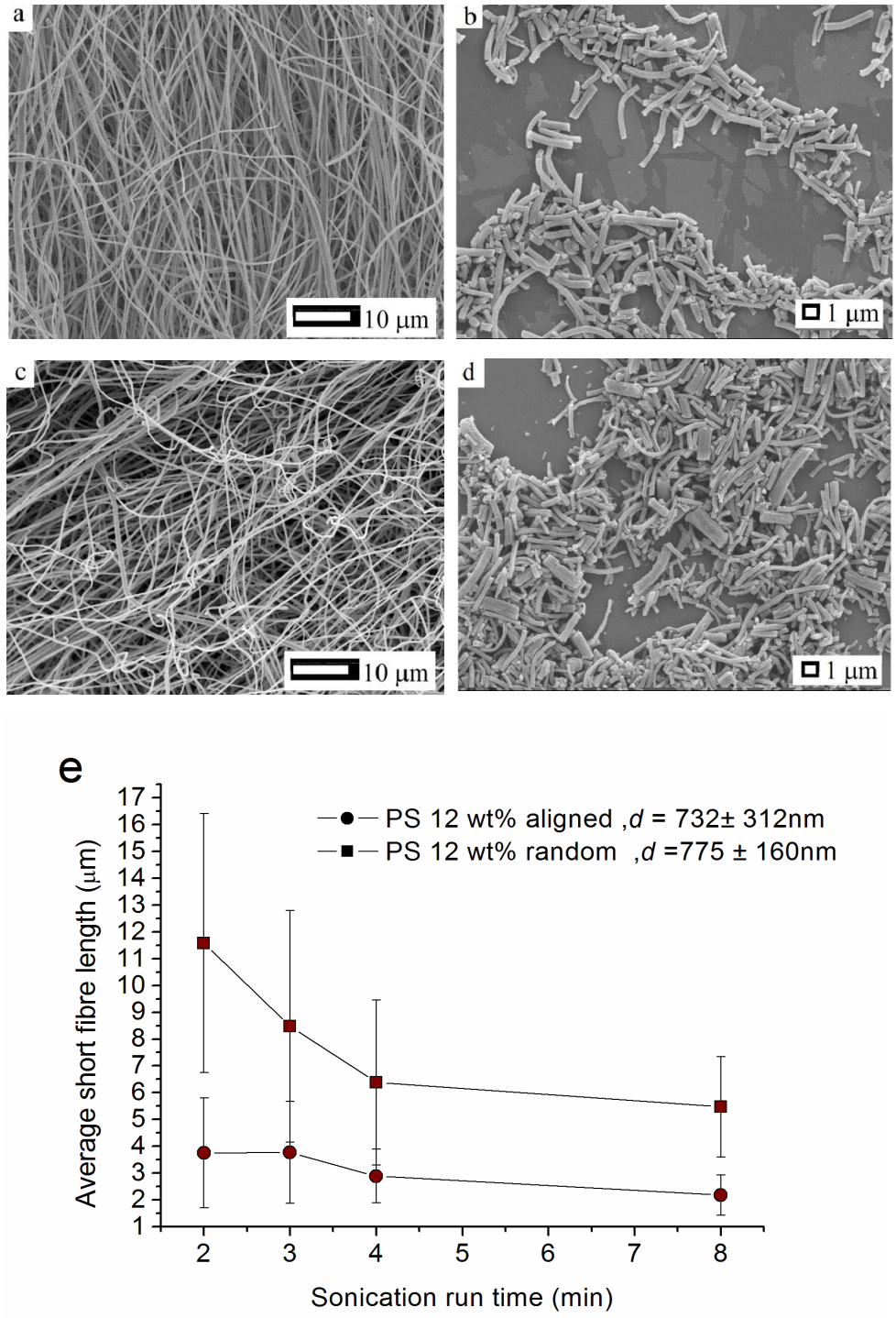

Figure 6 SEM images of the as spun fibres and after sonication run time of 8 mins respectively, a-b) aligned fibres, c-d) random fibres and e) average short fibre lengths of sonicated, electrospun fibres at different orientation.

The SEM images, figure 6a and 6c, show that, regardless of orientation, both initial electrospun nanofibre diameters were approximately the same. Sonication of fibres of both orientations for 1 min to 8 min resulted in the random, electrospun membranes being converted to discrete short fibres. The random webs led to a longer average fibre length and

higher standard deviation compared to those produced from the aligned membranes, with fibre lengths of 6 ± 2 µm and 3± 1 µm, respectively. Statistical analysis (Independent T-test) highlighted that there is a significant difference (p<0.05) in the fibre length between the aligned and random fibre webs for each sonication time (figure 6e). In addition to the overall macroscopic alignment of the fibres, it should be noted that aligning the fibres in an electrospun membranes also likely leads to a higher degree of molecular orientation of the polymer chains within those fibres, resulting in higher strength and reduced elongation at break and ductility [40], the latter particularly facilitating scission. In addition, scission of random fibres may be more difficult due to a denser, entangled fibre network having reduced possibilities for bubble infusion and less possibility for flexing of the fibres.

Since the aligned PS membrane produced a more uniform and shorter fibre length with a reduced lower standard deviation, all the results presented below were obtained using an electrospun PS membrane with an aligned orientation.

3.2.2 Effect of sonication run time

The effect of sonication time was examined for aligned PS nanofibre webs produced on the rapidly rotating mandrel. It was found that increasing the sonication run time resulted in shorter fibre lengths, as shown in figure 6e. Higher magnification images of the short fibre after sonication run time of 1, 2, 3, 4 and 8 mins are shown in figure 7.

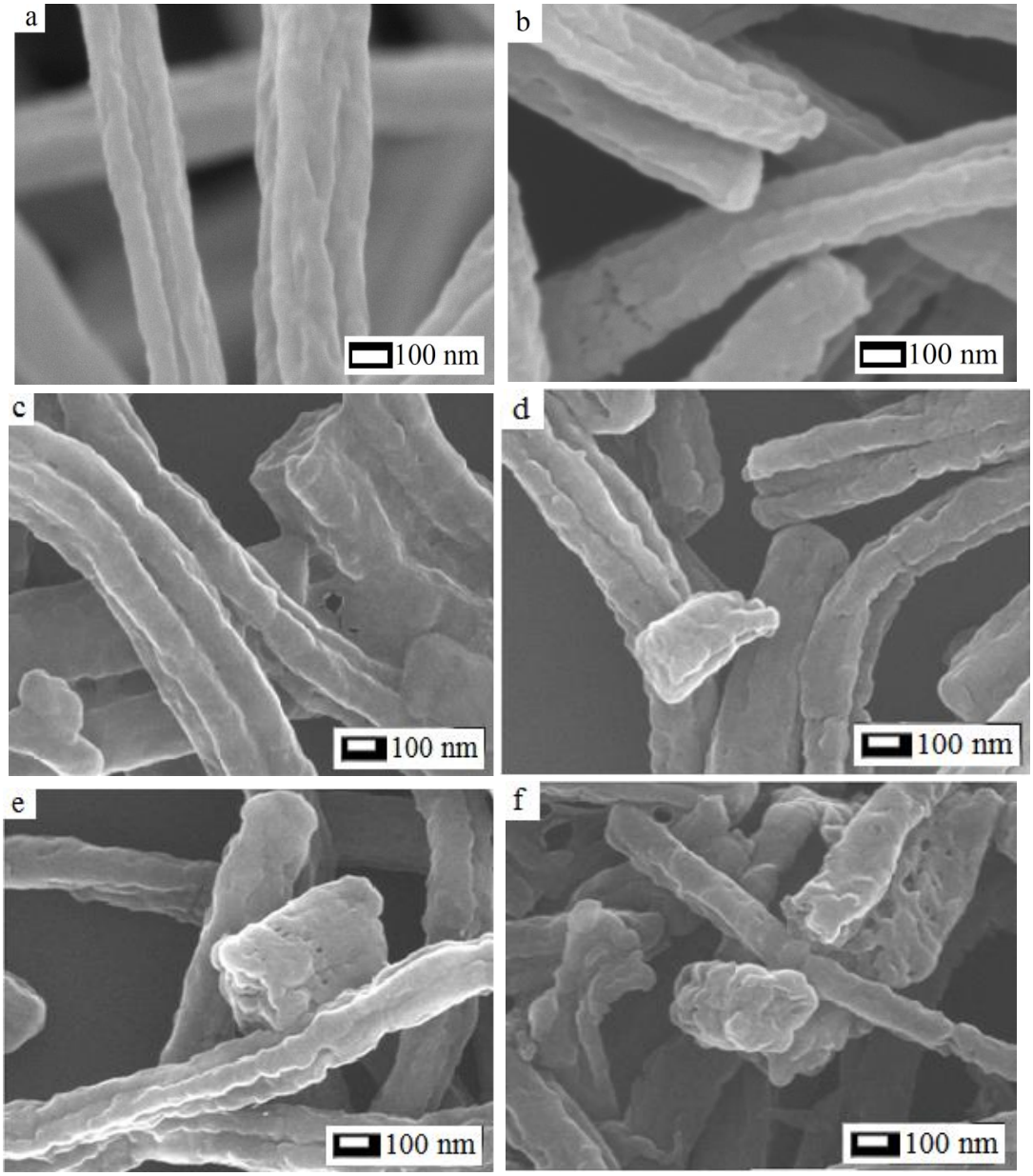

Figure 7 Greater magnification of PS short fibres pre (a) and post sonication in water, showing the eroded and pitted surface of the short fibre after time of 1, 2, 3, 4 and 8 mins of sonication run time (b-f, respectively)**.** A hole puncture on the fibre surface after a sonication run time of 2 mins is visible, even more obvious after 8 mins of sonication and is consistent with possible impact by high speed microjets.

The initial membrane of ca. 1 cm^2 was readily broken into smaller pieces after 1 min of sonication, with longer sonication times resulting in shorter fibre lengths, a significant decrease occurring after 3 mins, with longer processing times showing a reduced effect on fibre length. This is likely due the fact that the microjets formed are not as effective at causing failure in the scissioned fibres, as they are more dispersed and it is statistically less likely that microjets will impinge on the surface of a fibre (unless that surface itself particularly nucleates bubbles which then collapse). It is possible that the maximum tensile force resulting from the bubble implosion is less than the force required to cause the sample to fail.

Previous studies have shown that the size of suspended particles which are sonicated influences the degree of cavitation erosion due to microjetting [28, 41, 42]. It is necessary for

the solid surface to be larger than the bubble size [42, 43] in order for the bubble to attach and implode on the surface, and such bubbles can range from ca. 5 – 30 microns [18]. The implosion of attached bubble would likewise cause greater fibre damaged if they impacted directly on the fibre surface, as opposed to jet formation formed from a bubble which implodes at a distance the fibre surface [28].

In further support of a jetting mechanism as the mechanism for fibre scission, it is found that, increasing the sonication time also caused an increase in surface roughness, where the fibre morphology becomes rougher to a significant extent (figure 7). Erosion and pitting becomes more visible on the surface in the case of sonication run times of 8 mins (figure 7f), with some of the short fibres were severely eroded with multiple holes on its surface, due to impingement of high velocity microjets on the surface [44, 45]. This is also seen in TEM micrographs (figure 8) which shows extensive pitting and indentations on the fibre surface after 8 mins of sonication time. The indention evident in figure 8b indicates that the microjets do not always cause direct failure, but rather may be responsible for initiating failure and it may take several cavitation cycles to cause complete fibre scission.

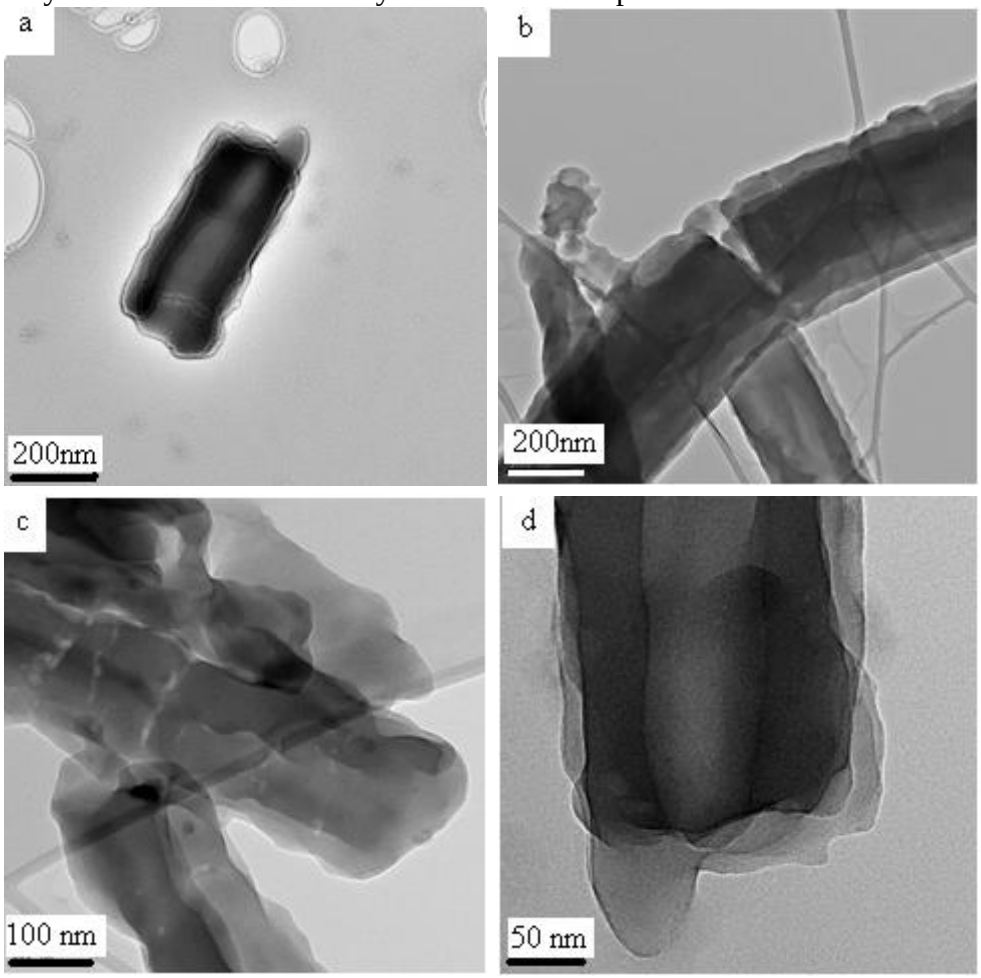

Figure 8 TEM images of PS sonicated in water for 8 mins a) short nanofibres at lower magnification, b) middle side of the short fibres showing the indentations which could act as the weak point to initiate total fracture of the short nanofibre, c) pitting and erosion visible along the surface d) the rough, cut end of the nanofibre.

3.2.3 Effect of initial fibre diameter

To investigate the influence of fibre diameter on scission events, aligned PS membranes with an average fibre diameter of 240 ±70 nm, 730 ±310 nm and 930 ± 290 nm, were electrospun. This was obtained by increasing the electrospining polymer concentrations from 8 wt% to 16

wt%, with the more concentrated polymer solution leading to fibres of greater thickness. The short fibres that result from these different initial diameters after a sonication time of 1 to 8 mins are shown in figure 9.

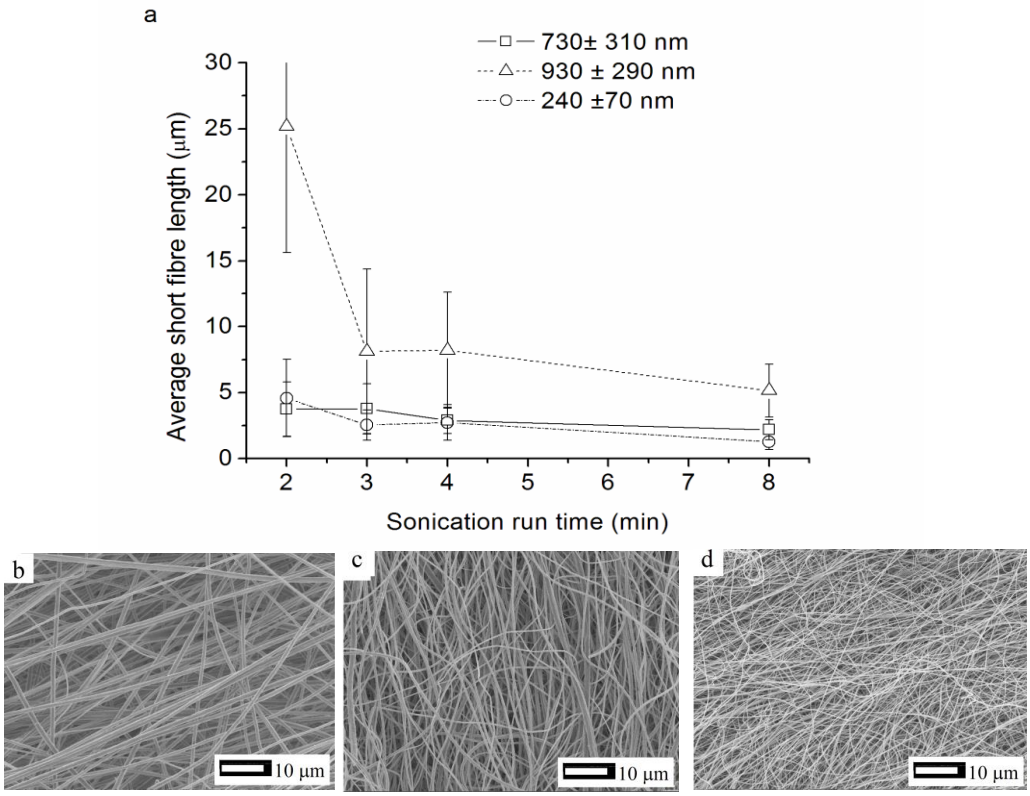

Figure 9 Effect of sonication on PS fibre at different initial fibre diameter (a) and SEM images of polystyrene before sonication at different concentration and diameter b) 16 wt%, c) 12 wt% and d) 8 wt %.

Figure 9 indicates that large fibre diameter samples were reduced in length to a lesser degree, for all sonication times. In particular, at very short sonication times (2 mins), the fibres with the greatest diameter were significantly greater in length (albeit with a greater size distribution). The membrane with the largest diameter fibres (930 ± 290 nm) resulted in longer scissioned fibres, compared to the other two membranes for each of the sonication times, as determined using ANOVA analysis, with $p<0.05$. No significant difference in terms of the short fibre length was observed between the 730±310 nm and 240 ±70 nm membranes ($p>0.05$).

Given that, in a broad sense, all of the PS fibres of different diameter have similar ductility and strength, the force required for failure during bubble collapse is greater for the thicker fibre. Equation 2 indicates that the force required to break the fibre would be proportional to the fibre diameter. Assuming the tensile strength for all the fibre membranes is the same, the tensile force required to break the fibre as a function of diameter (from the greatest to smallest diameter) should be greater than 300 nN, 200 nN and 30 nN, respectively (according to equation 2). However, as mentioned above, fibre scission is not due to tensile forces alone. Failure may arise due to other modes of deformation, including from the impact of jetting and, buckling. If it is assumed that the erosive depth caused by an impinging jet is the same for all fibres, this represents a reduced relative penetration of fibres with a larger diameter, and the strain generated by collapsing bubbles may be less likely to lead to sufficient stresses to take the impinged, thicker fibre to failure. Consequently, the length of scissioned, thicker fibres is slightly greater. This must be balanced with the larger diameter fibres presumably having a greater statistical likelihood of bubbles becoming attached to their surface. Note that

this discussion also makes the assumption that the molecular morphology, including chain orientation between different diameter fibre samples, is the same, which may not be the case. However, if molecular orientation was the important factor, one may expect that the chains in the thicker fibres to be less oriented and thus would show more ductile behaviour on deformation. This would also contribute to the outcome that fibres with greater diameter are more ductile, harder to scission, and result in longer, scissioned fibres. It is not clear which of the above possibilities is the most influential.

3.2.4 Effect of bubble nucleation via degassing and helium injection in water

Previous studies on carbon nanotubes have suggested that most sonication effects are due to the bubble cavitation behaviour [28, 46] and thus modifying the cavitation properties of the solution should also influence the scission events. One of factors that influence cavitation is the presence and/or concentration of dissolved gases in the solvent. The effect of degassing equilibrated water, and the incorporation of additional helium to the degassed sample for PS sonicated in water, is shown in figure 10.

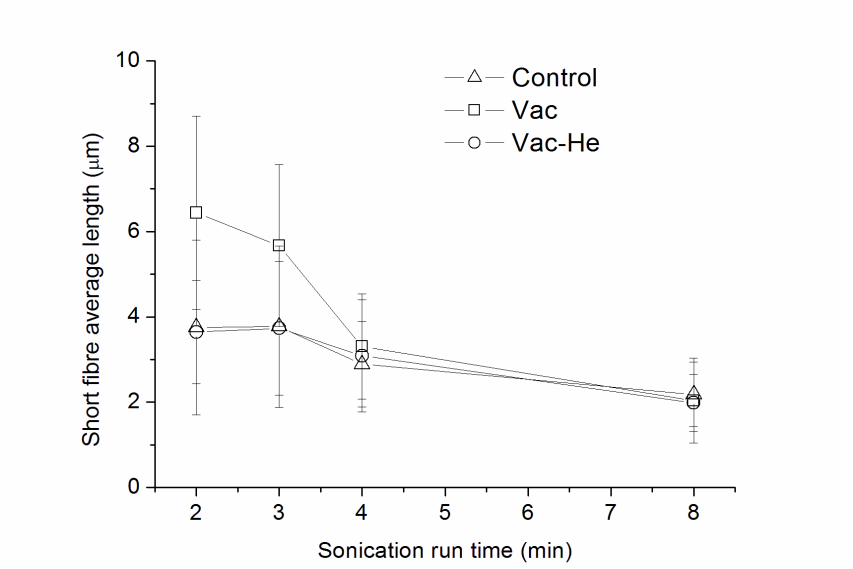

Figure 10 Effect of degassing (□) and the introduction of helium (○), on the nanofibre length after sonication. A controlled experiment (Δ) was carried out with water equilibrated at room temperature and pressure, whilst the degassing (Vac) experiment was achieved by degassing water in vacuum oven for 12 hrs. The Vac-He experiment involved first degassing under vacuum, followed by bubbling of helium for 30 mins .

For shorter sonication times (less than 3 mins) degassing of the water increased the resultant fibre length, compared to sonication in water with equilibrium concentrations of dissolved air (control) or water with additional helium added, the latter two showing no significant difference ($p>0.05$) in the final length of the scissioned fibres. Whilst dissolved gases can act as nucleating sites, they can also diffuse into the growing bubble and cushion bubble collapse [47], reducing its potential impact on the fibres. However, the use of helium, which is less soluble in water than air, would reduce this cushioning effect, and yet ensure availability of gas for nucleation. Conversely, degassing the water should theoretically reduce the bubble nucleating sites, resulting in less cavitation (and thus fibre scission). However, in this instance there would also be less gas that can diffuse into the bubbles and thus the severity of any collapse of bubbles formed would be greater, with the balance of these properties related to the gas type.

In previous work, the effects of sonication on single polymer chains in solution have been found to be enhanced for systems saturated with monatomic gas (such as Ar and He) where cavitation is easier, compared to diatomic gases (O_2, H_2, $N_2$and air) and polyatomic gases (eg CO_2) [47, 48] . The different behaviour is due to differences in specific heat capacity ratio of the monatomic gases, which are higher compared to diatomic and polyatomic gases. The specific heat ratio influences the maximum heat and maximum pressure of the bubble implosion sites, thereby affecting the sonochemical process. Equation 3 and 4 shows the relationship of the ratio of specific heat with the maximum pressure and temperature [49, 50].

$$T_{\max} = T_o\left[P_m(\gamma - 1)/P\right] \quad (3)$$

$$P_{\max} = P\left[P_m(\gamma - 1)/P\right]^{\gamma/(\gamma-1)} \quad (4)$$

where T_o is the temperature of the liquid/solvent, P_m is the pressure in the bubble after collapse, P is the pressure before collapse (usually assumed to the vapour pressure of the liquid and γ is the ratio of specific heats of dissolved gas or vapour. The greater the specific heat, the greater the pressure and thus the more energy released to the surrounding upon implosion, directly leading to a greater sonochemical effect. This indicates that sonication in water equilibrated with helium (monatomic gas) which has a lower solubility and higher specific heat ratio compared to air (diatomic gas) would produce a greater cavitation effect, due to greater bubble nucleation and subsequent bubble collapse, itself leading to a greater scission rate.

However, the findings in this work show that scission of the PS nanofibres is not greatly affected by the type of dissolved gas. The gas, regardless of type, appears to act as a nucleation site for bubbles leading to collapse and the formation of microjets, explaining the rapid shortening of fibres compared to the degassed sample. This effect appears to dominate the two possible mechanisms (nucleation vs. cushioning), and the role of gas in the cushioning effect of collapsing bubbles appears to be less. As sonication time increases (more than 3 min), the average fibre length for all conditions becomes statistically the same, attributable to equilibrium amounts of air becoming entrained in the initially-evacuated sample at longer sonication times.

3.2.5 Effect of temperature on scission of PS nanofibre by sonication in water

The effect of temperature was investigated by comparing low temperature sonication (initial temperature about 5^{o}C, achieved by cooling the vessel with ice-water slurry) to that of a comparatively high temperature condition (initial temperature at ambient, ice-pack only). The recorded temperature (not shown) for both samples after sonication for various times indicates that the maximum, final temperature of the low temperature processing were about 30^{o}C, whilst the high temperature processing (ice pack only) was in the range of 70^{o}C to 90^{o}C. Although the temperature of processing is different, the post sonication short fibre length remained statistically the same (data not shown). It has previously been found that when the temperature of the sonication media was lower, cavitation processes increase, leading to a greater degree of sonochemical reaction [51]. This phenomenon is related to solvent properties such as viscosity and vapour pressure. A lower temperature, and thus a higher viscosity, will lead to greater cohesive forces between solvent molecules which will increase the threshold of cavitation, thereby making scission more difficult [49]. If sufficient energy were delivered to overcome these forces and cause cavitation, upon the bubbles ultimate collapse, the hydrodynamic shear force exerted on the fibres would be greater [51, 52]. It has been reported that when sonication is used to scission individual polymer chains, the solvent viscosity must usually be optimised to ensure the shear force between the solvent

molecule is sufficient to cause the breakage of chemical bonds [53], showing that a viscosity that is too high or low is undesirable for effective cavitation (and thus scission).

In addition, an increase in temperature would lead to an increase in vapour pressure, hence encouraging more vapour entering the cavitation bubble and cushioning its implosion [51]. We did not observed such differences, probably because the range of the temperature differences we could achieve with our experimental set up was not sufficiently large enough to cause a significant effect on cavitation, as compared to other researchers who varied temperature from -10^{o}C to 61^{o}C[54].

3.3 Confocal microscopy imaging

All images presented this far were taken using electron microscopy, where a solution which contains short fibres was deposited onto a stub and the solvent allowed to evaporate, leaving the cluster of nanofibres. However, an artefact of the process was the agglomeration of fibres during drying, making it difficult for them to be imaged individually and to understand their dispersion in a solid or liquid medium. In the various applications for which such short nanofibres may be relevant, such as drug delivery and injectable tissue engineering scaffolds, good dispersion of short fibres with an aqueous-based matrix is required. To investigate their morphology in such a matrix, confocal microscopy was used to image the short nanofibres fluorescently labelled with Rhodamine B which were injected into an agar gel. Figure 11 shows the confocal image of the short fibres that had been sonicated for 4 mins before injection. The short nanofibres are well dispersed and did not become significantly entangled with one another. This highlights the potential for these short fibres to be used in applications that required them to be well dispersed in appropriate media, such as in tissue engineering or for composite reinforcement.

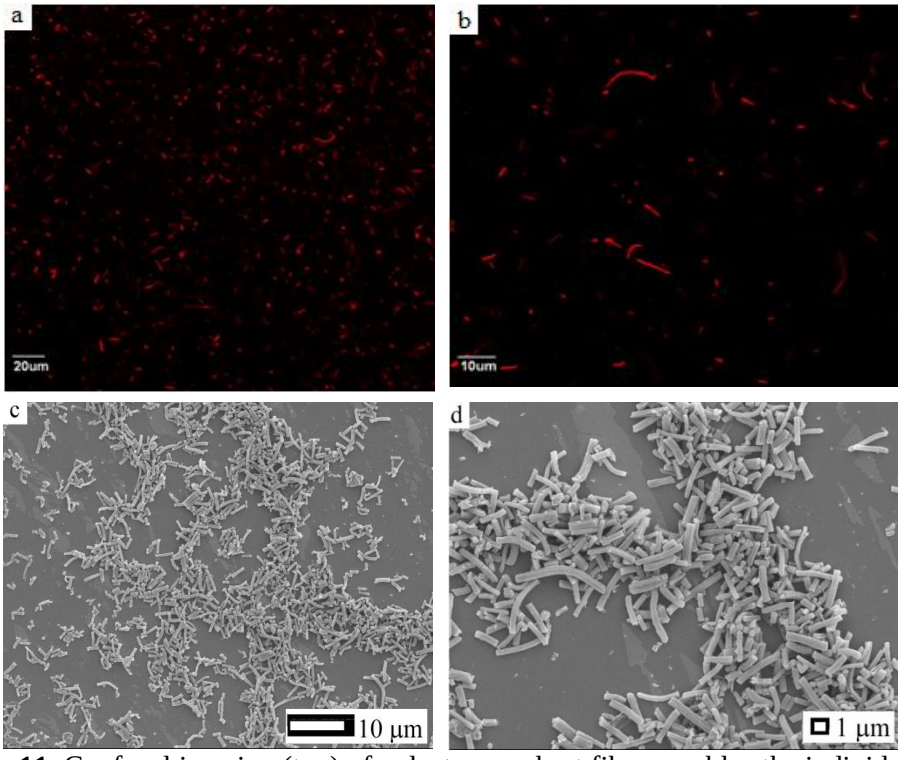

Figure 11 Confocal imaging (top) of polystyrene short fibres enables the individual short fibres to be readily, compared with SEM images (bottom) which densely agglomerate during the drying process. Note that all the shorts fibre images were from the same sample i.e. fluorescently-labelled PS at 12 wt% after 4 mins sonication run time.

3.4 Characterisation via Fourier Transform Infrared spectroscopy (FTIR) and Differential Scanning Calorimetry (DSC)

Both infrared spectroscopy and thermal scanning calorimetry were performed on the sonicated samples to determine if any changes to the polymers bulk and surface properties resulted from the sonication process. The FTIR spectra (not shown here) indicate that there is no chemical change of sonicated, electrospun PS fibres in water. Furthermore, there was no clear change observed in the glass transition temperature (approximately 100^{o}C) of sonicated samples, compared to virgin materials.

It appears then that the sonication process does not modify the chemical or physical structure of the electrospun polystyrene nanofibres. However, it should be noted that changing the types of sonicating medium (to those other than water) may produce a different result. This is due to the difference in solubility, vapour pressure and viscosity that would affect the surface morphology and properties of the resulted materials [55-57].

3.5 Cryogenic milling of electrospun polystyrene

Cryogenic milling (previously-reported in the literature as a method to fabricate short fibres[12]) was utilised to compare the morphology of short fibres produced from electrospun scaffolds using our sonication method. Visually, the cryogenically-milled electrospun fibre appears powder-like. The SEM micrographs (figure 12) show that the powder consists of a combination of fibres and chips/flakes. Energy dispersive spectrometry (EDS) spectrums (not shown here) were used on the fibres and flakes, confirming that the particles are of the same element i.e. PS. This result is different with the work by Verreck et al where 1 to 4 µm diameter of itraconazole/hydroxypropylmethylcellulose (HPMC) fibres were successfully cut into 27 µm length of fibres by cryomilling method [12]. Unfortunately, no images of their short fibres were provided, and their final morphology could not be confirmed.

The PS chips that resulted from our cryogenic milling probably arose due to the PS electrospun membrane used not being sufficiently brittle to fail, and becoming flattened when impacted. This is surprising since we found it a brittle material, as judged by tensile testing when in a membrane form, and in its ease of scissioning by sonication. These results nonetheless demonstrate that for the polymer nanofibres used in this work, cryogenic milling is not suitable for producing short nanofibres.

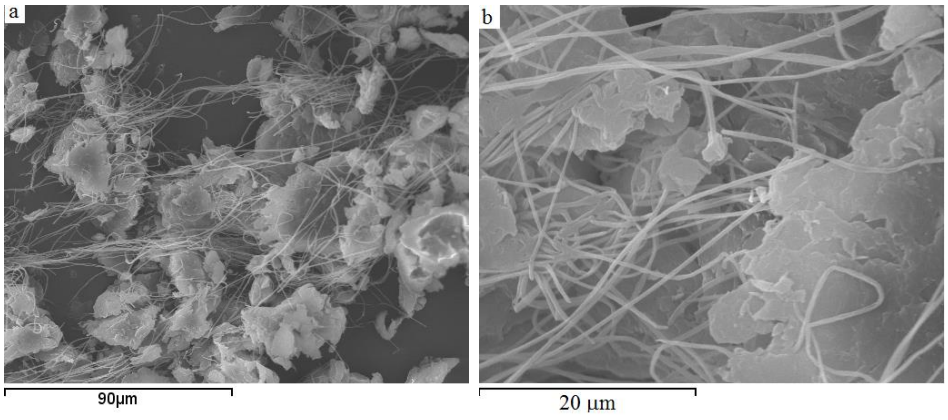

Figure 12 SEM images of cryogenically-milled (for total time of 10 mins) electrospun PS nanofibres at different magnification showing the fibre and flakes.

4 Conclusion

This work demonstrates that ultrasonication is a new and effective method to cause the scission of brittle submicron/nanometre-diameter electrospun polymers such as PS and

PMMA. In contrast, generating short fibres from more ductile electrospun polymers such as PAN and PLLA was more difficult. Pre-treatment of these ductile polymers, such as using UV-ozone treatment, was able to induce flaws and embrittle the material, and act as points of failure, facilitating the scissioning of these more ductile materials.

The mechanism of the scissioning relates to the formation of cavitation bubbles, which upon collapse can potentially lead to a range of deformations, including bending, fibre compression, and erosion and pitting of samples and, if the fibres are short enough, their extension is in a tensile manner. It is likely that there are various combinations of these at different times during the sonication process. In the initial catastrophic event, where a portion of the non-woven, electrospun membrane is reduced to fibres, both flexing and microjet erosion are likely the primary mechanisms acting on the fibres as they are likely drawn tangentially to the bubble edge. The attainment of curled fibres (whether the membrane are scissioned or not) and greater roughening, respectively, indicate bending and erosion mechanisms. Once the fibres are smaller than a certain length, they can potentially be drawn into the collapsing bubble, with the particles long axis oriented in a radial manner to the bubble surface, and thus can be subjected to a high rate of tensile deformation.

Based on these understandings of mechanism, other variables such as the morphology (diameter, orientation) of the initial electrospun fibres were investigated. It was found that smaller diameter membrane was broken into slightly smaller length fibres, likely due to the lower force being required to elongate the fibres to failure. Increased alignment of the fibres in the original web, achieved by increasing the rotation speed of the drum collector during electrospinning, also resulted in smaller fibres upon scissioning. This is probably because of the greater orientation of the polymer chains and reduced ductility due to greater molecular alignment within the fibres, as well as differences in the non-woven membrane morphology. Other processing variables such as temperature and dissolve gas did not appear to significantly change the cavitation/scission process, and thus did not greatly influence final length. It was found that the sonication process itself did not affect the chemical or physical structure of the fibres or their constituent polymers.

By taking advantage of various flexibilities in the electrospinning process itself such as composite fibres with nanoparticles or core-shell membranes, a wide range of short nanofibres can potentially be made using this method, which could enable their application in many applications such as coatings, composites and in the biomedical field. Further work is being undertaken to gain a better understanding of the nature of the scission process, and find ways to allow even greater control of the final fibre morphology.

Acknowledgments

MS acknowledge financial support from Ministry of Higher Education, Malaysia and the use of imaging facilities within the Monash Centre for Electron Microscopy (MCEM), Monash University.

References

1. Huang, Z.-M., et al., *A review on polymer nanofibers by electrospinning and their applications in nanocomposites.* Composites Science and Technology, 2003. **63**(15): p. 2223-2253.
2. Ramakrishna, S., et al., *An Introduction to Electrospinning and Nanofibers* 2005, Singapore: World Scientific Pub.
3. Bhardwaj, N. and S.C. Kundu, *Electrospinning: A fascinating fiber fabrication technique.* Biotechnology Advances. **28**(3): p. 325-347.
4. Nisbet, D.R., et al., *Neurite infiltration and cellular response to electrospun polycaprolactone scaffolds implanted into the brain.* Biomaterials, 2009. **30**(27): p. 4573-4580.
5. Nisbet, D.R., et al., *Review Paper: A Review of the Cellular Response on Electrospun Nanofibers for Tissue Engineering.* Journal of Biomaterials Applications, 2009. **24**(1): p. 7-29.
6. Nisbet, D.R. and et al., *Interaction of embryonic cortical neurons on nanofibrous scaffolds for neural tissue engineering.* Journal of Neural Engineering, 2007. **4**(2): p. 35.
7. Li, D., Y. Wang, and Y. Xia, *Electrospinning of polymeric and ceramic nanofibers as uniaxially aligned arrays.* Nano Lett., 2003 (3): p. 1167.
8. Jalili, R., M. Morshed, and S.A.H. Ravandi, *Fundamental parameters affecting electrospinning of PAN nanofibers as uniaxially aligned fibers.* Journal of Applied Polymer Science, 2006. **101**(6): p. 4350-4357.
9. Sancaktar, E. and D. Aussawasathien, *Nanocomposites of Epoxy with Electrospun Carbon Nanofibers: Mechanical Behavior.* The Journal of Adhesion, 2009. **85**(4-5): p. 160-179.
10. Deniz, A.E., et al., *Electrospun polymeric nanofibrous composites containing TiO2 short nanofibers.* Materials Chemistry and Physics, 2011. **129**(3): p. 701-704.
11. Kim, J.S. and D.H. Reneker, *Mechanical properties of composites using ultrafine electrospun fibers.* Polymer Composites, 1999. **20**(1): p. 124-131.
12. Verreck, G., et al., *Preparation and Characterization of Nanofibers Containing Amorphous Drug Dispersions Generated by Electrostatic Spinning.* Pharmaceutical Research, 2003. **20**(5): p. 810-817.
13. Kriha, O., et al., *Connection of Hippocampal Neurons by Magnetically Controlled Movement of Short Electrospun Polymer Fibers—A Route to Magnetic Micromanipulators.* Advanced Materials, 2007. **19**(18): p. 2483-2485.
14. Mark, S.S., et al., *Bioconjugation of Alkaline Phosphatase to Mechanically Processed, Aqueous Suspendible Electrospun Polymer Nanofibers for Use in Chemiluminescent Detection Assays.* Macromolecular Bioscience, 2008. **8**(6): p. 484-498.
15. Stoiljkovic, A. and S. Agarwal, *Short Electrospun Fibers by UV Cutting Method.* Macromolecular Materials and Engineering, 2008. **293**(11): p. 895-899.
16. Watmough, D.J., *Role of ultrasonic cleaning in control of cross-infection in dentistry.* Ultrasonics, 1994. **32** (4): p. 315-317.
17. Suslick, K.S., ed. *Ultrasound : Its Chemical, Physical and Biological Effects*. 1988, VCH Publishers Inc: New york.
18. Brenner, M.P., S. Hilgenfeldt, and D. Lohse, *Single-bubble sonoluminescence.* Reviews of Modern Physics, 2002. **74**(2): p. 425-484.
19. Hennrich, F., et al., *The Mechanism of Cavitation Induced scission of Single-Walled Carbon Nanotubes.* J.Physical Chemistry B, 2007. **111**: p. 1932-1937.

20. Chen, H., et al., *Effect of dispersion method on tribological properties of carbon nanotube reinforced epoxy resin composites.* Polymer Testing, 2007. **26**(3): p. 351-360.
21. Ahir, S.V., Y.Y. Huang, and E.M. Terentjev, *Polymers with aligned carbon nanotubes: Active composite materials.* Polymer, 2008. **49**(18): p. 3841-3854.
22. Lucas, A., et al., *Kinetics of Nanotube and Microfiber Scission under Sonication.* The Journal of Physical Chemistry C, 2009. **113**(48): p. 20599-20605.
23. Chew, H.B., et al., *Compressive dynamic scission of carbon nanotubes under sonication: fracture by atomic ejection.* Proceedings of the Royal Society A: Mathematical, Physical and Engineering Science, 2011. **467**(2129): p. 1270-1289.
24. Pagani, G., et al., *Competing mechanisms and scaling laws for carbon nanotube scission by ultrasonication.* Proceedings of the National Academy of Sciences, 2012.
25. Liu, J., et al., *Fullerene Pipe.* Science, 1998. **280**: p. 1253-1256.
26. Suslick, K.S. and G.J. Price, *Application of Ultrasound to Materials Chemistry.* Annual Review of Materials Science, 1999. **29**(1): p. 295-326.
27. Guo, Z., et al., *High-speed observation of the effects of ultrasound on liquid mixing and agglomerated crystal breakage processes.* Powder Technology, 2007. **171**(3): p. 146-153.
28. Wagterveld, R.M., et al., *Visualization of acoustic cavitation effects on suspended calcite crystals.* Ultrasonics Sonochemistry, 2011. **18**(1): p. 216-225.
29. Kim, T.G. and T.G. Park, *Biodegradable Polymer Nanocylinders Fabricated by Transverse Fragmentation of Electrospun Nanofibers through Aminolysis.* Macromolecular Rapid Communications, 2008. **29**(14): p. 1231-1236.
30. Kim, T.G., et al., *Hierarchically Assembled Mesenchymal Stem Cell Spheroids Using Biomimicking Nanofilaments and Microstructured Scaffolds for Vascularized Adipose Tissue Engineering.* Advanced Functional Materials, 2010. **20**(14): p. 2303-2309.
31. Hsieh, A., et al., *Hydrogel/electrospun fiber composites influence neural stem/progenitor cell.* Soft Matter, 2010. **6**: p. 2227-2237.
32. Lu, K.L., et al., *Mechanical damage of carbon nanotubes by ultrasound.* Carbon, 1996. **34**(6): p. 814-816.
33. Casper, C.L., et al., *Controlling surface morphology of electrospun polystyrene fibers: Effect of humidity and molecular weight in the electrospinning process.* Macromolecules, 2004. **37**(2): p. 573-578.
34. Megelski, S., et al., *Micro- and Nanostructured Surface Morphology on Electrospun Polymer Fibers.* Macromolecules, 2002. **35**(22): p. 8456-8466.
35. Pai, C.-L., M.C. Boyce, and G.C. Rutledge, *Morphology of Porous and Wrinkled Fibers of Polystyrene Electrospun from Dimethylformamide.* Macromolecules, 2009. **42**(6): p. 2102-2114.
36. Haosheng, C., W. Jiadao, and C. Darong, *Cavitation damages on solid surfaces in suspensions containing spherical and irregular microparticles.* Wear, 2009. **266**(1–2): p. 345-348.
37. Price, G.J., A.J. White, and A.A. Clifton, *The effect of high-intensity ultrasound on solid polymers.* Polymer, 1995. **36**(26): p. 4919-4925.
38. Sakai, W. and N. Tsutsumi, *Photodegradation and Radiation Degradation*, in *Poly(Lactic Acid)*2010, John Wiley & Sons, Inc. p. 413-421.
39. Yixiang, D., et al., *Degradation of electrospun nanofiber scaffold by short wave length ultraviolet radiation treatment and its potential applications in tissue engineering.* Tissue Engineering - Part A., 2008. **14**(8): p. 1321-1329.
40. Inai, R., M. Kotaki, and S. Ramakrishna, *Structure and properties of electrospun PLLA single nanofibres.* Nanotechnology, 2005. **16**(2): p. 208-213.

41. Chen, H., et al., *Study on effect of microparticle's size on cavitation erosion in solid-liquid system.* Journal of Applied Physics, 2007. **101**(10).
42. Suslick, K.S., S.J. Doktycz, and E.B. Flint, *On the origin of sonoluminescence and sonochemistry.* Ultrasonics, 1990. **28**(5): p. 280-290.
43. Suslick, K.S., *Sonoluminescence and Sonochemistry*, in *Encyclopedia of Physical Science and Technology*, A.M. Robert, Editor 2001, Academic Press: New York. p. 363-376.
44. Philipp, A. and W. Lauterborn, *Cavitation erosion by single laser-produced bubbles.* Journal of Fluid Mechanics. **361**: p. pp 75-116
45. Shima, A., *Studies on bubble dynamics.* Shock Waves, 1997. **7**(1): p. 33-42.
46. Jambrak, A.R., et al., *Ultrasound effect on physical properties of corn starch.* Carbohydrate Polymers, 2010. **79**(1): p. 91-100.
47. Price, G.J., ed. *Current Trends in Sonochemistry*. 1992, The Royal Society of Chemistry: Cambridge.
48. Mason, T.J., ed. *Chemistry with Ultrasound*. 1990, Elsevier Applied Science: New York. 195.
49. J.Mason, T. and J.P. Lorimer, *Applied Sonochemistry*2002, Verlag GmbH, Weinheim Wiley-Vch
50. Luche, J.-L., *Synthetic Organic Sonochemistry*1998, New York: Plenum Press.
51. Vijayalakshmi, S.P. and G. Madras, *Effect of temperature on the ultrasonic degradation of polyacrylamide and poly(ethylene oxide).* Polymer Degradation and Stability, 2004. **84**(2): p. 341-344.
52. Grönroos, A., P. Pirkonen, and O. Ruppert, *Ultrasonic depolymerization of aqueous carboxymethylcellulose.* Ultrasonics Sonochemistry, 2004. **11**(1): p. 9-12.
53. Vijayalakshmi, S.P. and G. Madras, *Effects of the pH, concentration, and solvents on the ultrasonic degradation of poly(vinyl alcohol).* Journal of Applied Polymer Science, 2006. **100**(6): p. 4888-4892.
54. Price, G.J. and P.F. Smith, *Ultrasonic degradation of polymer solutions: 2. The effect of temperature, ultrasound intensity and dissolved gases on polystyrene in toluene.* Polymer, 1993. **34**(19): p. 4111-4117.
55. Dang, F., et al., *Sonochemical synthesis of monodispersed magnetite nanoparticles by using an ethanol–water mixed solvent.* Ultrasonics Sonochemistry, 2009. **16**(5): p. 649-654.
56. Vijayalakshmi, S.P. and G. Madras, *Effect of initial molecular weight and solvents on the ultrasonic degradation of poly(ethylene oxide).* Polymer Degradation and Stability, 2005. **90**(1): p. 116-122.
57. Starczewska, A., et al., *Influence of the solvent on ultrasonically produced SbSI nanowires.* Ultrasonics Sonochemistry, 2009. **16**(4): p. 537-545.